The Mineral-Electrogens-Electrodes System in Paddy Soils and their impacts on Trace Elements Behavior

Thesis submitted in accordance with the requirements of the University of Liverpool for the degree of Doctor in Philosophy

by

Williamson Gustave

Department of Environmental Science

University of Liverpool

March 2019

Dedicated to my wife and child

高伶慧 & 高礼安

Thank you for your unwavering support and unending love.

Declaration

I, **Williamson Gustave**, wish to declare that this thesis is my own independent work/investigation. It is being submitted in partial fulfillment of the requirement for the award of the requirements for the degree of PhD. I further declare that this work has never been submitted for any degree at this or any other University, and that the thesis is presented with the consent of my supervisor. Works by other authors, which served as a source of information, have been duly acknowledged by references to the authors. The views expressed are my own. I hereby give consent for my thesis, if accepted, to be available for photocopying and for inter-library loan, and for the title and summary to be made available to outside organizations.

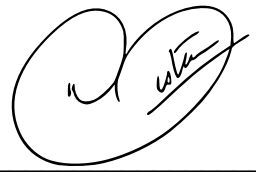

Signed: _____

Williamson Gustave (Candidate)

5th March 2019

Abstract

Soil trace heavy metal and metalloid contamination is a serious problem that threatens humans and other organisms' well-being. Trace metal heavy contaminated rice paddy fields have become of worldwide concern since an increasing amount of paddy soils are contaminated with trace heavy metals. Rice has a high capacity to accumulate trace heavy metals and metalloids, especially arsenic, into its grains which has potential adverse effects on public health. Hence, it is essential to regulate the bioavailability of these pollutants in paddy soil if the aim is to reduce their concentration in rice grains and subsequent exposure to humans. The ability to control soil-to-solution partitioning of these trace heavy metals and metalloid from the reductive dissolution process of iron oxides has been identified as the key to limiting heavy metal uptake by rice plants. Compared to other remediation technologies, bioelectrochemical systems (BES) appear to be a promising solution to this problem. BES are able to provide an inexhaustible electrode for oxidation and the energy needed for the extraction of heavy metal to less toxic species and from the soils, respectively. In this context, the application of the sediment microbial fuel cell (sMFC) in soil remediation was investigated in this thesis. The mechanisms involved and the way the sMFC anode changes soil properties to enable heavy metal remediation were examined.

The effect of the sMFC on the soil biotic and abiotic components were observed. The microbial community analysis revealed that the sMFC deployment can significantly influence the community composition within the soil profile. The results also indicate that the relic DNA generated by operating the sMFC has minimum effect on the culture independent estimates of microbial community composition. Moreover the effects of the sMFC's bioanode at different external resistance were examined. The results indicate that external resistance has a significant

effects on sMFC power production, organic matter removal efficiency and microbial beta diversity.

Moreover, the sMFC bioanode can significantly influence the behavior of trace element in soil. Our results showed that the sMFC was able to limit arsenic and iron reduction by creating a competition for organic substrate between sMFC bioanode and the iron- and arsenic-reducing bacteria in the soils. However, we observed an increase in iron and arsenic release into the soil porewater when the sMFC was deployed in soil with high dissolve organic matter content. This was ascribed to the acidification effect of sMFC bioanode and the increase of iron reducing bacteria in the sMFC bioanode vicinity and associated bulk soil. Nevertheless, when the sMFC was coupled with wet-dry cycles to decrease dissolve organic matter, we observed a decrease in the release of iron and arsenic into the soil porewater. These results indicated that sMFC can be used to limit arsenic bioavailability in soil porewater. In addition to soil pore water iron and arsenic, the behavior of cadmium, copper, chromium and nickel was also influenced by the bioanode.

Furthermore, we used the sMFC to limit the accumulation of trace metals in the rice plant parts. The results demonstrate that the sMFC can significantly reduce the total arsenic concentrations in the stems, leaves, husks, and rice grains. The total arsenic concentrations in the stems, leaves, husks, and rice grains were significantly decreased by 53.4%, 44.7%, 62.6%, and 67.9%, respectively in the plants with sMFC compared to the control. Similarly the effect of the sMFC on the accumulation of cadmium, copper, chromium and nickel in the rice plant parts were also investigated. The results showed that the sMFC can significantly limit the accumulation of cadmium, copper, chromium and nickel. The concentration of cadmium, copper, chromium and nickel in rice grains were 35.1%, 32.8%, 56.9% and 21.3% lower in the sMFC, respectively, than the control. Our work showed for the first time that operating the sMFC can significantly influence the behavior of paddy soil trace elements in soil. We also

showed for the first time that the sMFC can be used as a promising technique to limit toxic trace metal bioavailability and translocation in the rice plants while simultaneously producing electricity.

This page intentionally left blank

Acknowledgments

First and foremost, I would like to thank **God** Almighty for giving me the strength, knowledge, ability and opportunity to undertake my PhD studies and to successfully complete it. Without his blessings, this achievement would not have been possible.

I would like to express my deepest appreciation to my supervisor, **Dr. Zheng Chen** for his constant guidance, support and encouragement throughout my PhD studies and my personal life. I really appreciated the freedom I had too, thanks **Dr. Chen**! I would also like to extend my gratitude to **Dr. Sekar Raju** and **Salaun Pascal**, for being amazing mentors and for their constant guidance and support to bringing this thesis to fruition. I also wish to thank **Dr. Sujie Qin** and **Prof. George Wolf** for their valuable criticism and suggestion during the yearly progression meets.

I would like to thank all the members of the **Dr. Chen's eBiogeochemistry** Group for their valuable insights and constant motivation. Especially **Yuan Zhaofeng** and **Ren Yuxiang**, for without them I would have been lost. I also want to express special thanks to **Prof. Elmer Villanueva**, **Chang Hucheng, Dr. Kiran Kumar Vadde** and **Liu Jinjingyuan**, for their countless assistance both technically and intellectually and useful discussions. I want to acknowledge the kind help of **Xiao Zhou**, **Yili Cheng, Dr. Zhang Xiaoyan** and **Long Ping** for their technical support in the sample analysis. I also wish to express my immense gratitude to my brother **Jacqueline St. Jean** and my mother **Malthide Gustave** for their patience and support.

Finally, I would want to express my profound thankfulness to XJTLU for the PhD scholarship and the National Science Foundation of China (41571305) and Jiangsu Science and Technology Program (BK20161251) for the financial support of my PhD research. Without this I would not have accomplished this lifetime achievement.

Table of Contents

Acknowledgments..... VIII

List of Figures..... XVIII

List of Tables..... XXIII

List of Abbreviations..... XXIV

List of Publications..... XXV

List of Conferences..... XXVI

Chapter 1 : General Introduction to the application of the soil microbial fuel cell in soil heavy metal remediation..... 28

1.1. Introduction..... 28

1.2. Bioelectrochemical systems..... 31

1.2.1. Microbial Fuel Cells..... 31

1.2.2. Sediment Microbial Fuel Cell..... 32

1.3. Mechanism of sediment microbial fuel cells in soil remediation..... 34

1.3.1. Changes in soil Chemistry..... 36

1.3.2. Substrate competition..... 39

1.3.3. Electromigration..... 40

1.3.4. Changes in the soil microbial community composition..... 40

1.4. Application of microbial fuel cell in soil heavy metal remediation..... 42

1.4.1. Chromium..... 42

1.4.2. Uranium..... 43

1.4.3. Other metals 45

1.5. Research Aims and Objectives 47

1.6. References 50

Chapter 2 : General Materials and Methods 62

2.1. Soil Microbial Fuel Cells 62

2.1.1. Paddy soils collection and preparation 62

2.1.2. Anode and cathode preparation 62

2.1.3. Soil Microbial Fuel Cell assembly 62

2.1.4. Electrochemistry analysis 63

2.2. Soil Microbial Fuel Cells with Rice Plants 64

2.3. Chemical Analysis 65

2.4. Plant Samples Analysis 66

2.5. Microbial Community Analysis 66

2.6. Quantitative PCR (qPCR) of *arsC*, *aioA*, and *arsM* genes 69

2.7. Statistical Analysis 69

2.8. References 71

Chapter 3 : The effect of the soil microbial fuel cell on paddy soil microbial community profile 74

3.1. Abstract 74

3.2. Introduction 75

3.3. Materials and Methods 77

3.3.1. Paddy Soil Sample 77

3.3.2. Soil Microbial Fuel Cell assembly 77

3.3.3. Chemical Analysis 77

3.3.4. Microbial Community Analysis 78

3.3.5. Nucleotide sequence accession numbers 79

3.4. Results and Discussion 79

3.4.1. Voltage generation in MFCs 79

3.4.2. Influences of the sMFC and relic DNA on microbial community diversity 80

3.4.3. The effect of the MFCs and relic DNA on microbial community structure 82

3.4.4. Influences of sMFC on the microbial community composition 84

3.4.5. Influences of relic DNA on microbial community composition at phylum and class levels 90

3.5. Conclusion 91

3.6. References 93

3.7. Supplementary data 101

Chapter 4 : The effect of the sMFC on paddy soil components at different external resistance 108

4.1. Abstract 108

4.2. Introduction 109

4.3. Materials and Methods 113

4.3.1. Paddy Soil Sample 113

4.3.2. Soil Microbial Fuel Cell Assembly 113

4.3.3. Chemical Analysis 114

4.3.4. Microbial Community Analysis 114

4.3.5. Nucleotide sequence accession numbers 114

4.4. Results 114

4.4.1. Electricity generation from soil MFCs with different external resistors 114

4.4.2. Polarization properties of the sMFC 115

4.4.3. Microbial community structure 117

4.4.4. Organic matter removal and Change in soil pH 119

4.4.5. Changes of porewater As, Fe and Ni 121

4.5. Discussion 122

4.6. Conclusions 125

4.7. References 127

4.8. Supplementary data 134

Chapter 5 : The effect of the sMFC on arsenic in soil with low organic matter content 141

5.1. Abstract 141

5.2. Introduction 142

5.3. Materials and Methods 144

5.3.1. Paddy Soil Sample 144

5.3.2. Soil Microbial Fuel Cell Assembly 144

5.3.3. Chemical Analysis 145

5.3.4. Microbial Community Analysis 145

5.3.5. Nucleotide sequence accession number 146

5.4. Results and Discussion.....146

5.4.1. Power output of sMFC in As contaminated soil.....146

5.4.2. Effects of the sMFC on soil OM, pH and *E*h.....148

5.4.3. Change in total Fe and As concentration.....150

5.4.4. The interaction between anodes and Fe oxides: role of organic substrate, *E*h, pH and functional bacterial organisms.....152

5.4.5. Bacterial community structure.....156

5.5. Conclusions.....160

5.6. References.....162

5.7. Supplementary data.....173

Chapter 6 : The effect of the sMFC on arsenic in soil with high organic matter content.....180

6.1 Abstract.....180

6.2. Introduction.....181

6.3. Materials and Methods.....184

6.3.1. Paddy Soil Sample.....184

6.3.2 Soil Microbial Fuel Cell Assembly.....184

6.3.3. Dry-wet Cycles.....185

6.3.4. Chemical Analysis.....185

6.3.5. Microbial Community Analysis.....185

6.3.6. Nucleotide sequence accession number.....186

6.4. Results.....186

6.4.1. sMFC performance 186

6.4.2. Effect of sMFC on the soil physiochemical properties 187

6.4.3. The impacts of sMFC on Fe and As behavior in the paddy soil porewater 190

6.4.4. The impacts of sMFC on Bacterial community structure 193

6.5. Discussion 196

6.5.1 Current generation in the sMFC and sMFC-WM 196

6.5.2. sMFC enhances porewater Fe and As when soil OM is abundant 196

6.5.3. sMFC decreases porewater Fe and As when soil DOC is limited 199

6.6. Conclusions 201

6.7. Reference 202

6.8. Supplementary data 210

Chapter 7 : The effect of the sMFC on the accumulation of arsenic in rice plant parts 221

7.1. Abstract 221

7.2. Introduction 222

7.3. Materials and Methods 222

7.3.1. Paddy Soil Sample 224

7.3.2. Soil Microbial Fuel Cell Assembly 225

7.3.3. Preparation of Rice Seedlings 225

7.3.4. Chemical Analysis 226

7.3.5. Plant Samples Analysis 227

7.3.6. Microbial Community Analysis 227

7.3.7. Quantitative PCR (qPCR) of *arsC, aioA* and *arsM* genes 227

7.3.8. Nucleotide sequence accession number 228

7.4. Results 228

7.4.1. Voltage generation 228

7.4.2. Effects of sMFC on soil pH, Eh, DOC and plant growth. 229

7.4.3. Effect of sMFC on porewater As and Fe concentration 230

7.4.4. Effects of sMFC on As accumulation in rice 232

7.4.5. *arsC*, *aioA* and *arsM* genes abundance 233

7.4.6. Functional bacterial community 234

7.5. Discussion 238

7.5.1. Voltage output 238

7.5.2. The effect of the sMFC on the As and Fe mobility in the soil porewater 239

7.5.3. The sMFC significantly reduce total As accumulation in the rice grains 243

7.6. Conclusions 243

7.7. References 245

7.8. Supplementary data 251

Chapter 8 : The effect of the sMFC on the accumulation of other trace heavy metal in rice plant parts 253

8.1. Abstract 253

8.2. Introduction 254

8.3. Materials and Methods 256

8.3.1. Paddy Soil Sample 256

8.3.2. Soil Microbial Fuel Cell Assembly....256

8.3.3. Preparation of Rice Seedlings....257

8.3.4. Chemical Analysis....257

8.3.5. Plant Samples Analysis....257

8.3.6. Microbial Community Analysis....257

8.3.7. Nucleotide sequence accession number....258

8.4. Results and Discussion....258

8.4.1. Current generation and power output....258

8.4.2. Change is soil porewater metal concentrations....260

8.4.3. Decrease in Cd, Cu, Cr and Ni accumulation in rice plant tissue....264

8.5. Conclusions....265

8.6. References....266

8.7. Supplementary data....274

Chapter 9 : General Discussion, Conclusions and Future Directions....276

9.1. General Discussion and Conclusions....276

9.2. Future Directions....281

9.3. References....283

This page intentionally left blank

List of Figures

Figure 1.1 Schematic detail of a typical soil bioelectrochemical systems (BES) 31

Figure 1.2 The possible coupling behavior of extracellular microbes, mineral oxides and metals in soil without the sMFC (a) and in the presence of the sMFC (b). 35

Figure 2.1 Schematic of the sMFC reactor. 64

Figure 3.1 The mean voltage variation of four sMFC as a function of time (a). The polarization curve of the sMFC (b).. 80

Figure 3.2 Principal Coordinates Analysis (PCoA) of the sMFC and controls bacterial community (a) and the sMFC and controls archaeal community (b) 83

Figure 3.3 Relative abundance of bacterial community composition at phylum (a) and class (b) levels. 85

Figure 3.4 Heat map distribution of bacterial phylotypes classified to the genus level 88

Figure 3.5 Relative abundance of archaeal community composition at phylum (a) and genus (b) level 90

Figure 4.1 Current production from sMFC fixed with different external resistances during a 90-day operation. The insert represent the change in the control's voltage with time. 115

Figure 4.2 Polarization curves of the sMFC at various external resistance. The filled and open symbols represent power and voltage respectively. The insert represent the polarization curve of the sMFC set at 50Ω. 116

Figure 4.3 Principal Coordinates Analysis (PCoA) of the sMFC and controls bacterial community composition. 118

Figure 4.4 Relative abundance of bacterial community composition at genus level (a) anode vicinity and (b) bulk soil. 119

Figure 4.5 Removal efficiencies of lost on ignition carbon. 120

Figure 4.6 a-d Fe and As variation in soil porewater along with incubation time. Panels a and b represent Fe concentration in the bulk soil and anode vicinity respectively.....121
Figure 5.1 Relationship between current output (a), porewater DOC concentration (b), anode and cathode potential (c) over time.....147
Figure 5.2 Removal efficiencies of LOI carbon (a) and total organic carbon (b) in three layers of soil (Top, Middle, and Bottom) for the sMFC and the control 149
Figure 5.3 Iron (Fe) and Arsenic (As) variation in soil porewater as a function of incubation time.. 151
Figure 5.4 DOC variation in soil porewater as a function of incubation time. 154
Figure 5.5 Principal Coordinates Analysis (PCoA) of the sMFC and controls bacterial community composition.....158
Figure 6.1 The variations of current output, organic matter concentration (DOC), anode and cathode potential over time 187
Figure 6.2 DOC variation in the sMFC-WM and Control-WM soil porewater as a function of incubation time 190
Figure 6.3 Iron and As variation in the sMFC and control soil porewater as a function of incubation time 192
Figure 6.4 Iron and As variation in soil porewater as a function of incubation time. 193
Figure 6.5 Relative abundance of microbial community composition at genus level for the sMFC without (a) and with water management (b).....195
Figure 7.1 Voltage variation over time (a) and polarization curve (b). 228
Figure 7.2 Variations in DOC in the sMFC and control treatment. 230
Figure 7.3 Variations in As and Fe concentration in the sMFC and control treatment.....232
Figure 7.4 The concentration of As in the rice parts at maturation. 233

Figure 7.5 Absolute abundance of the (a) *arsC*, (b) *aioA* and (c) *arsM* genes in the sMFC and control rhizosphere soil at the end of the incubation period 234
Figure 7.6 Principal Coordinates Analysis (PCoA) of the sMFC and controls bacterial community composition.....236
Figure 7.7 Relative abundance of bacterial community composition at class (a) and genus (b) levels 238
Figure 8.1 Current variation overtime. 259
Figure 8.2 Variations in Cu and Cr concentration in the sMFC and control treatment.....260
Figure 8.3 Relative abundance of bacterial community composition at the phylum level....263
Figure 8.4 The concentrations of Cd (a), Cr (b), Cu (c) and Ni (d) in the rice parts at maturation. 265
Figure S 3.1 The voltage variation of the MFCs over time……. 107
Figure S 4.1 Anode (filled symbols) and cathode (open symbols) polarization curves. 136
Figure S 4.2 Rarefaction curves showing the diversity of OTUs (similarity cut off of 97%) 137
Figure S 4.3 Non-metric multidimensional scaling (NMDS) ordination diagrams of the variations in bacterial community structures for the sMFC with different external resistance and controls. 138
Figure S 4.4 Relative abundance of bacterial community composition at phylum and class levels ((a) = anode vicinity; (b) =bulk soil).....139
Figure S 4.5 Variations in Nickel in soil porewater along with incubation time. a and b represent nickel concentration in the bulk soil and anode vicinity, respectively. 140
Figure S 5.1 Polarization and power density curves for the sMFC after 15 days of operation. 176
Figure S 5.2 Correlation between iron and arsenic release in the sMFC.....177

Figure S 5.3 Rarefaction curves showing the diversity of OTUs (similarity cut off of 97%) 178
Figure S 5.4 Relative abundance of bacterial community composition at phylum level 178
Figure S 5.5 Heat map of the relative abundance of bacterial community composition at genus level.....179
Figure S 6.1 Current variation of the sMFC-WM over time. The red and blue arrows indicates the start of dry and wet periods respectively. 213
Figure S 6.2 Dissolved organic carbon (DOC) variation in soil porewater as a function of incubation time 214
Figure S 6.3 EEM fluorescence spectra of DOC in soil porewater. Panels a, c, e and g show DOC spectra in sMFC-WM. Panels b, d, f, and h show DOC spectra in the control-WM. P is tryptohan-like, H ultraviolet C (UVC) humic acid-like, F is fulvic acid-like and TH is terrestrial humic acid-like. 215
Figure S 6.4 EEM fluorescence spectra of DOC in soil porewater. Panels a, c, e and g show DOC spectra in sMFC. Panels b, d, f, and h show DOC spectra in the control. 216
Figure S 6.5 Correlation between Fe and As release in the sMFC.....217
Figure S 6.6 Rarefaction curves showing the diversity of OTUs (similarity cut off of 97%). T, M, A and BS: represents samples collected from top layer, middle layer, anode vicinity and bulk soil respectively. 218
Figure S 6.7 Relative abundance of bacterial community composition at class level for the sMFC without (a) and with water management (b). T, M, A and BS: represents samples collected from top layer, middle layer, anode vicinity and bulk soil respectively. 219
Figure S 7.1 Schematic diagram of soil microbial fuel cells 252
Figure S 8.1 Variations in Ni concentration in the sMFC and control treatment. Panels a, b and c show Ni concentrations in the top, middle and bottom layers, respectively. 274

Figure S 8.2 Relative abundance of bacterial community composition at the phylum level. 275

List of Tables

Table 1.1 Summary of previous studies where the MFC was used in soil heavy metal remediation.....46

Table 2.1 Details of primer pairs used in this study. 68

Table 6.1 Changes of pH and redox potential in soil samples of reactors at the end of the experiment.....188

Table S 3.1 Selected chemical properties of the fresh soils used in this study. 101

Table S 3.2 Concentration of DNA in each sample as measured immediately after the extraction. 102

Table S 3.3 Similarity-based microbial OTUs and species richness and diversity estimates 104

Table S 3.4 Similarity-based archaeal OTUs and species richness and diversity estimates. 106

Table S 3.5 Results of selected chemical analysis of soil at the end of the experiment. 106

Table S 4.1Similarity-based OTUs and species richness and diversity estimates.....134

Table S 4.2 Changes of pH in soil samples of sMFC set at different external resistance at the end of the experiment.....136

Table S 5.1 Selected properties of the fresh soils.....173

Table S 5.2 Changes of pH and redox potential in soil samples of sMFC and control at the end of the experiment. 174

Table S 5.3 Similarity-based OTUs and species richness and diversity estimates.....175

Table S 6.1 Selected properties of the fresh soils.....210

Table S 6.2 Similarity-based OTUs and species richness and diversity estimates.....211

Table S 7.1 Selected properties of the fresh soils.....251

Table S 7.2 As and Fe speciation in the soil porewater on day 110. 251

Table S 7.3 Similarity-based OTUs and species richness and diversity estimates.....252

List of Abbreviations

BES	Bioelectrochemical systems
cDNA	Complementary DNA
DNA	Deoxyribonucleic acid
DOC	Dissolved organic carbon
EEM	Excitation emission matrix
Eh	Redox potential
IC	Ion chromatography
ICPMS	Inductively coupled plasma mass spectrometry
IRB	Iron reducing bacteria
LOI	Loss on ignition
MEC	Microbial electrolysis cell
MFC	Microbial fuel cell
OM	Organic matter
PCR	Polymerase chain reaction
PMA	Propidium monoazide
QIIME	Quantitative insights into microbial ecology
qPCR	Quantitative polymerase chain reaction
RNA	Ribonucleic acid
sMFC	soil microbial fuel cell
sMFC-WM	soil microbial fuel cell with water management
TOC	Total organic carbon
16S rRNA	16S ribosomal RNA

List of Publications

[1] **Gustave, et al.** "Arsenic mitigation in paddy soils by using microbial fuel cells." Environmental Pollution 238 (2018): 647-655.

[2] **Gustave, et al**. "The change in biotic and abiotic soil components influenced by paddy soil microbial fuel cells loaded with various resistances." Journal of Soils and Sediments (2018): 1-10.

[3] **Gustave, et al. "**Relic DNA does not obscure the microbial community of paddy soil microbial fuel cells." Research in Microbiology, (2018)

[4] **Gustave, et al.** "Modulation of Porewater Arsenic by Microbial Fuel Cells and Water Management" (Under review)

[5] **Gustave, et al.** "Arsenic alleviation in rice grains by using microbial fuel cells" Plant and Soil (2019):1-17

[6] **Gustave, et al.** "Mitigation effects of the microbial fuel cells on trace heavy metal accumulation in rice (Oryza sativa L.)" (In preparation)

[7] Zhaofeng and **Gustave, et al.** "Tracing the dynamic changes of element profiles by novel soil porewater samplers with ultralow disturbance to soil water interface" Environmental Science & Technology (2019)

[8] Zhaofeng and **Gustave, et al.** "Simultaneous and rapid measurement of redox sensitive elements in saturated soil pore water" (Under review)

[9] **Gustave, et al.** "The application of sediment microbial fuel cells in heavy metal remediation" (In preparation)

List of Conferences

[1] **Gustave, et al.** "Simultaneous electricity production and arsenic mitigation in paddy soils by using microbial fuel cells" Xian Jiaotong-Liverpool University Graduate Students Poster Day, Suzhou, China (Poster). 'Most Popular Poster' award.

[2] **Gustave, et al.** "Simultaneous electricity production and arsenic mitigation in paddy soils by using microbial fuel cells" The 7th International Congress & Exhibition on Arsenic in the Environment, Environmental Arsenic in a Changing World (2018), Beijing, China (Oral).

[3] **Gustave, et al.** "The effects of the Bioanode on the Microbial Community and Element profile in Paddy soil" The 7th International Congress & Exhibition on Arsenic in the Environment, Environmental Arsenic in a Changing World (2018), Beijing, China (Poster).

[4] **Gustave, et al.** "The application of microbial fuel cells for arsenic mitigation in paddy soils" Jiangsu-UK Symposium on Meteorology and Environment (2018), Nanjing China (Oral).

[5] **Gustave, et al.** "Arsenic alleviation in rice by using paddy soil microbial fuel cells" 15th International Conference on the Biogeochemistry of Trace Elements (ICOBTE) (2019), Nanjing, China (Poster).

This page intentionally left blank

Chapter 1 : General Introduction to the application of the soil microbial fuel cell in soil heavy metal remediation

1.1. Introduction

Rapid industrialization, urbanization and the increasing use of pesticides and fertilizer in today's society have introduced many environmental challenges; such as air, water and soil pollution by numerous heavy metals pollutants from several anthropogenic sources (Li et al., 2014). Due to the excessive application of heavy metal containing agrochemicals, fossil fuel consumption, non-point source metal pollutants from mining and smelting operations, the improper disposal of industrial waste and irrigation of farmlands with contaminated water, most of the agricultural soils around the world are contaminated with heavy metals (Bolan et al., 2014; Facchinelli et al., 2001; Liu et al., 2018). It was estimated that over 100 million ha of land are contaminated by different heavy metal in China alone (He et al., 2015). These heavy metal pollutants impair food quality. Furthermore heavy metal pollutants are consumed by way of the food chain since they accumulate in living organisms (Jaishankar et al., 2014; Liu et al., 2018). The accumulation of these metals threatens the well-being of living organisms, resulting in detrimental effects such as biomembrane deterioration in plants (Marques et al., 2009) and carcinogenic symptoms in animals (Sajana et al., 2016). For example, chronic exposure to arsenic has left thousands in Bangladesh and India with dermal lesions, peripheral vascular disease and skin cancer (Chowdhury et al., 2000). Similarly, the accumulation of cadmium has also been linked to organ failure and lung cancer (Järup and Åkesson, 2009; Zukowska and Biziuk, 2008).

Bringing such activities associated with heavy metal production to a complete halt will negatively influence the socio-economic development of a nation. Hence, research has focused on developing a range of in-situ and ex-situ remediation techniques such as physical, chemical

and biological treatments to control and remediate heavy metal contaminated soil. Physical and chemical techniques such as the replacement of contaminated soil, the electrokinetic' methods (application of an electric current to extract metal pollutants) and the addition of chemical reagents to immobilize heavy metals or to mobilize as in the case of soil leaching has been explored (Liu et al., 2018; Yao et al., 2012). Moreover, biological methods including phytoremediation (Marques et al., 2009) and microbial remediation has also been utilized to alleviate soil of heavy metal contaminates (Gadd, 2004; Khan et al., 2000).

For example, microbial secretions and other metabolites have been used for the absorption, precipitation, oxidation or reduction of heavy metals (Yao et al., 2012). However, most of the methods that are available are not practiced on a large scale because they are expensive and in some cases will lead to the production of secondary pollutants and ecological destruction or simply just re-enter the environment as in the case of phytoremediation. Therefore the metals that were are stored in the leaves and stem of the plants are return to the environment when the leaves shed and when the wood is burnt (Marques et al., 2009). Nonetheless, compared to the chemical and other physical remediation techniques, bioremediation is considered to be the most environmentally friendly and cost-effective (Li and Yu, 2015; Pandey and Fulekar, 2012). Bioremediation employs the soil functional microbial community that are able to utilize many diverse metabolic routes to be immobilized or transform soil heavy metals pollutants into less toxic forms (Li and Yu, 2015) . However bioremediation still faces many challenges such as the limited electron acceptors/donor, low efficiency and poor controllability (Li and Yu, 2015; Pandey and Fulekar, 2012). Therefore, the search for more simple and effective ways for heavy metals bioremediation in soil are essential.

Bioelectrochemical systems (BES) appear to be a promising solution to this problem, since BES are able to overcome the limitations of other bioremediation techniques (Li and Yu,

2015; Thrash J. and D, 2008). BES are able to provide an inexhaustible electrode that is noninvasive and can easily be deploy to tune the soil microenvironment and promote bioremediation (Lovley, 2008). BES which are special types of bioreactors that can be used to enhance and accelerate bioremediation by providing an electron acceptor and/or donor for simultaneous production of value added products and heavy metal remediation (Abourached et al., 2014; Gregory and Lovley, 2005). A typical BES consist of an anode and a cathode that are connected via an external circuit (Fig.1.1). The anode and the cathode of the BES can served as non-exhaustible electron acceptors and donors during microbial degradation and respiration processes, thereby eliminating the need for the addition of electron donors and acceptors. The anode of the BEC is located in the anoxic conditions and can accept electrons from the microbial oxidized of substrates. These electrons can then flow to the cathode (oxic environment) through an external electric-circuit, where they can be used to produce electricity and reduce toxic elements species to their less toxic forms (Logan et al., 2006).

Although many reviews have discuss the use of BES for remediation of wastewater and soil organic pollutants (Li and Yu, 2015; Wang et al., 2015b; Wang and Ren, 2014; Wu et al., 2018), very few have focused on the application of the BES in soil heavy metal remediation. In this review we discuss how BES, with special focus on microbial fuel cells (MFC), can be applied as soil bioremediation tool. Moreover, the mechanisms involved and the way the sMFC anode changes soil properties to enable heavy metal remediation are also discussed.

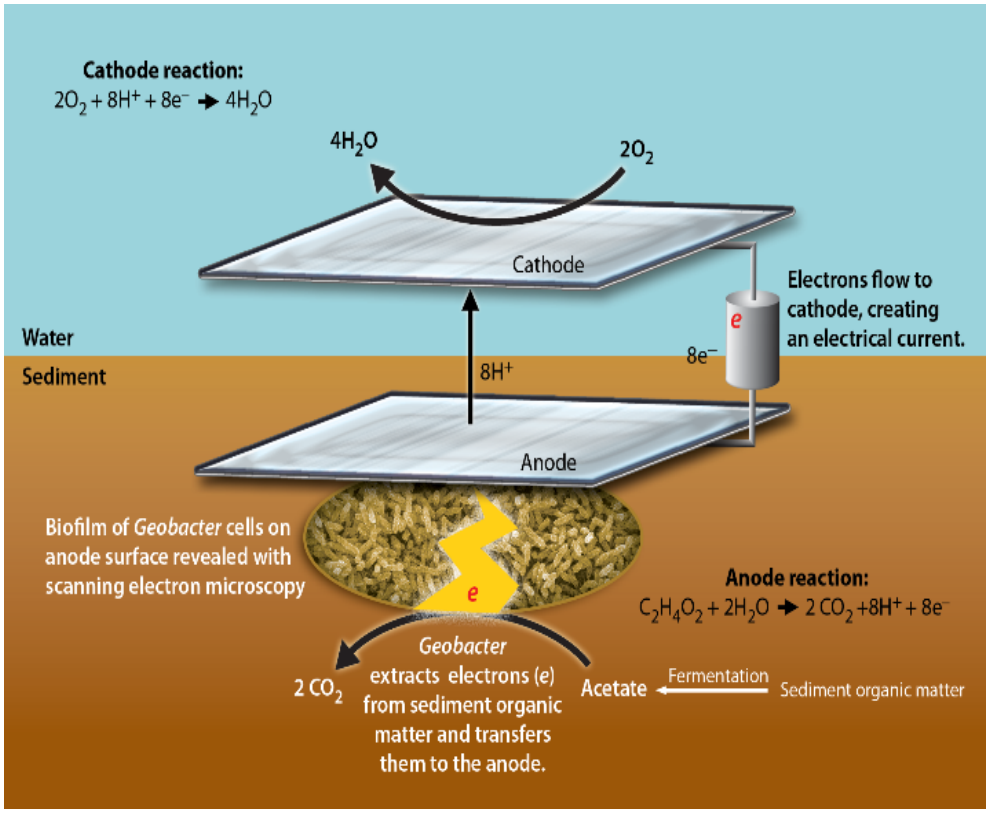

Figure 1.1 Schematic detail of a typical soil bioelectrochemical systems BES (US DOE., 2005)

1.2. Bioelectrochemical systems

1.2.1. Microbial Fuel Cells

Microbial Fuel Cells (MFC) are bioelectrochemical systems that capitalize on electrons produced by exoelectrogenic bacteria during metabolic activities to generate electricity (Liu et al., 2010; Min et al., 2005; Rozendal et al., 2007). MFC appears to be a promising green technology with prospective applications in green energy production and pollution remediation. Since the first report of MFC in 1911 by Potter when he observed electric current being generated by bacteria (Potter, 1911), MFC has under gone numerous modifications in its architecture, in its application (Logan, 2008) and numerous sources of organic matter have also been explored (De Schamphelaire et al., 2008). In the quest for higher electricity generation, columbic efficiency, stability, longevity and cost efficiency various materials have been used to construct the anode and cathode in MFC.

Previously, precious metals such as platinum and high energy catholytes such as ferricyanide and permanganate have been utilized, however, these materials are expensive and in some cases will lead to the production of secondary pollutants (eg. platinum may result in contaminating marine or freshwater environment) (Logan, 2008; Wang et al., 2011). More abundant and cheaper conductive metals like iron and copper were also employed, nonetheless due to their reactive properties these metals had fouled easily. Most recently, researchers have begun to use more cost effective carbon or graphite base materials to construct the electrodes due to their porosity which allows maximum surface area for electron transfer at the anode, biofilm formation and oxygen reduction in the cathodic chamber (Logan, 2008). In terms of a sustainable source of organic matter, wastewater, biomass, soil-sediment and many others have been identified (De Schamphelaire et al., 2008), however for the scope of this review, only the use of sediment are described in detailed. Sediment is a naturally occurring material with organic matter content ranging from 0.4 to 2.2 wt% (Rezaei et al., 2007). It is derived from the weathering and decaying of plants, animals and other sources of organic matter (Hong et al., 2010).

1.2.2. Sediment Microbial Fuel Cell

Sediment Microbial Fuel Cell (sMFC), is a special type of MFC that employs sediments from a large range of flooded environments and its microbial community to produce electricity (Bond D. R et al., 2002; Hong et al., 2009; Kaku et al., 2008; Schamphelaire et al., 2008; Song et al., 2010). Similar to traditional MFCs, sMFC generates electricity from the flow of electrons to the cathode from the anode. Sediment was first employed by Reimers et al. (2001) to produce a power density as high as 15mW/m^2 using platinum mesh as electron and since then have continued to evolve. One of the limiting factors in the sMFC is low oxygen concentration in the cathodic chamber (Reimers et al., 2001). Some studies have employed aeration pumps,

rotating cathodes (He et al., 2007) and the addition of particulate substrates, however these require the input of energy, thus increasing overhead cost.

To overcome this shortfall, some studies employ the use of photosynthetic algae or plants to provide in suit oxygen (del Campo et al., 2013; Wang et al., 2014). As an example, Wang et al. (2014), inoculated the cathode of their sMFC with *Chlorella vulgaris* to generate oxygen. The presence of the algae increased the power output of the sMFC by 2.4 folds compared with the unmodified cathode (Wang et al., 2014). In another study by Choi et al. (2010), a magnet was connected to the cathode in their setup and this increased the current output by 18%. They concluded that the increase of current production was due to the magnet inducing an increase in flux of oxidant into the cathode surface. Like these studies, other researchers focused on improving the sMFC configuration such as finding the optimum distance between the buried anode and the cathode to reduce ohmic resistance and produce maximum current output while keeping the anodic chamber anoxic (Chen et al., 2016a; Sajana et al., 2014; Wang et al., 2011). Further studies have varied the size of the anode and cathode (Ueoka et al., 2016) or have changed the design of the sMFC so that cathode is consistently exposed to the open air (He et al., 2007). Although a significant portion of research has focus on increasing the electrical performance sMFC, sMFC still faces many setbacks such as the relatively low power density and poor energy conversion. Also, scaling up does not increase voltage (Zabihallahpoor et al., 2015).

Alternatively sMFC research has shifted towards environmental remediation (Chen et al., 2015; Wu et al., 2018). The sMFC appears to be a promising in situ remediation approach for a number of reasons. The electrodes of sMFCs are pollutant-free, noninvasive, and inexhaustible substrates that can serve as an electron donor or acceptor for microbial metabolism and thus sustaining natural bioremediation (Huang et al., 2011; Logan, 2009; Yuan et al., 2010). Similarly sMFC can suppress the methanogenesis activities, thus leading to the

significant reduction in methane gas emission from marine environment while causing minimal disturbance to the surrounding aquatic environment. This occurs as a result of a decline in the archaeal community population around the polarized anode (Lin and Lu, 2015).

1.3. Mechanism of sediment microbial fuel cells in soil remediation

Many studies have demonstrated the feasibility of applying the sMFC in soil bioremediation (Chen et al., 2015; Hong et al., 2010; Hong and Gu, 2009; Wu et al., 2018). Based on these studies, the sMFC may influence soil the heavy metals in three main way and these mechanism are depicted in Fig.1.2a-b. The mechanisms include significant change in soil chemistry, organic matter contain, and microbial community structure. These changes in soil physiochemical and biological properties initiated by the sMFC can greatly influence the faith and transport of many redox sensitive heavy metal contaminates (Hong et al., 2009; Hong et al., 2010). In Fig. 1.2a-b the effect of the sMFC on the behavior of heavy metals co-precipitated with mineral oxides are used as an example. As shown in Fig. 1.2a, under anaerobic condition extracellular respiring electrogenic bacteria use mineral oxides as a final electron acceptor in the absent of the anode. This result in the dissolution of the mineral oxides and the release of the metals pollutant that were co-precipitated with it.

However, when the sMFC anode is present, as illustrated in Fig. 1.2b, it can compete with the mineral oxides for electrons thereby limiting their dissolution and increasing the concentration of mineral oxide in soil, since the anode is easy to be utilized by anode respiring bacteria (Logan, 2009). Hence, this increase the concentration of mineral oxide to fix metal pollutants. Moreover, the sMFC anode increases the abundance of mineral respiring microbes of the bulk soil in the immediate vicinity of the anode (Kouzuma et al., 2013; Lu et al., 2014). The mineral respiring microbes in the bulk soil may reduce the anode via long-rang and interspecies electron transfer. Species in the genus *Geobacter*, has been shown to transfer electrons to electron acceptor at distances in the micrometer length away from the biofilm.

Geobacter spp., produces proteinaceous filaments call pili that can facilitate the transfer of electrons to distance terminal electron acceptors (Bond D. R et al., 2002; Lovley, 2011). In addition to influencing soil heavy metal speciation and the sMFC also dictate soil heavy metal distribution through electrokinetic (Chen et al., 2015; Habibul et al., 2016a). Below we outline some possible mechanisms in detail on how the sMFC influences soil toxic heavy metal behavior.

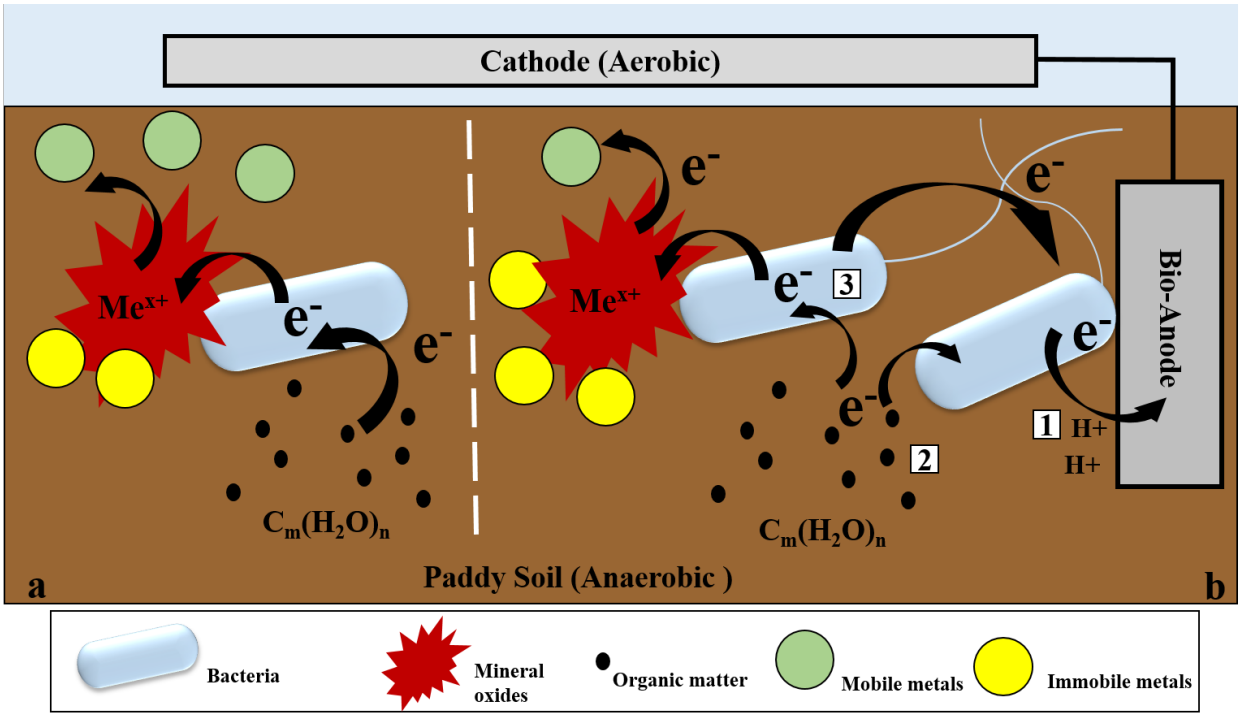

Figure 1.2 The possible coupling behavior of extracellular microbes, mineral oxides and metals in soil without the sMFC (a) and in the presence of the sMFC (b).

In (a) Mineral reduction results in the release of metal into the soil porewater. However in (b) the sMFC anode interact with mineral oxides in three different ways;

1) The organic matter at anode was oxidized to produce hydrogen ion and carbon dioxide. This anode half reaction lower the pH of the soil around the anode and promote dissolution of mineral oxide, subsequently raising the mineral ion concentration in the soil water.
2) There is a competition for organic matter in the porewater between microbes in anode and

mineral-reducing bacteria in the soil. This lead to limited reduction of mineral oxide by bacteria.

3) The anode can stabilize the insoluble mineral oxide in the soil. Since the anode can be used as an alternative electron acceptor for the bacteria in the distance soil via nanometer wire (pili) or conductive mineral. The high potential of the anode can compete with mineral in soil to alleviate the dissolution of mineral oxides. The embedding the anode into soil also changes the community structure of microbes.

1.3.1. Changes in soil Chemistry

1.3.1.1. Changes in soil Eh

When sMFCs are deployed, they can change some of the physiochemical properties of soil (Hong et al., 2009; Hong et al., 2010; Kouzuma et al., 2014; Lu et al., 2014). These changes in soil property has been shown to be beneficial in reducing soil contaminates (Wang et al., 2015b; Wu et al., 2018). As an illustration, under flooded conditions the redox potential (Eh) of the soil decreases rapidly because of the depletion of oxygen and other electron acceptors (Chen et al., 2012). However when an sMFC anode is embedded into the anaerobic soil, it functions as a permanent and high potential electron acceptor with low-cost and continuous sink for electrons produced from the oxidation of organic substances by the exoelectrogens (Huang et al., 2011; Logan, 2008; Yuan et al., 2010). This in turn may increase the soil Eh since the reason for the initial rapid decrease was the depletion of final electron acceptors.

The increase of soil Eh around the anode has been reported in numerous reports. Hong et al., (2009) found that the Eh in the vicinity of the anode increased to +246.3+/-67.7mV compared to that of the open-circuit soil which was -143.0 ± 7.18 mV (Hong et al., 2009). In another experiment, Hong et al. (2010) observed an increase in soil Eh around the vicinity of the anode under close circuit conditions when compared with that of the control (open Circuit). In their experiment the Eh of the control sample was -185mV+/- 20.5mV (vs. SHE) roughly

the same as that of the sampled lake soil (Hong et al., 2010). However, that of the sMFC under close circuit was +185+/-37.6 mV.

The increase in soil Eh is advantageous, because it can prevent the microbial reduction of metal oxides and limit the microbial mobilization of many redox sensitive heavy metals. The speciation and bioavailability of heavy metals have been closely linked to changes in soil Eh (Charlatchka and Cambier, 2000; Yamaguchi et al., 2011). Under oxidizing environments (positive Eh), cationic metals such as ferrous iron can react with sulfide and produce secondary insoluble mineral that can trap and immobilize to heavy metals (Burton et al., 2013; Lohmayer et al., 2014). For instances, Signespastor et al. (2007) observed that arsenic mobility and solubility is strong impeded under oxidizing condition. However under reducing conditions (negative Eh) microbes can reduce metal oxides and lead to the release of coprecipitated metals (Burton et al., 2013; Lohmayer et al., 2014).

Moreover, other studies have also reported that under high redox potential the bio-methylation of mercury is significantly reduce, thereby reducing methylated mercury release into the overlaying water from the sediment (DeLaune et al., 2004; Schamphelaire et al., 2008). Furthermore, the elevated Eh conditions can reduce the formation of hydrogen sulfide and increase overlaying water quality. Thus the sMFC anode can be used to prevent the release and transformation of soil toxic pollutants, through elevating soil Eh. Yuan et al. (2010) demonstrated that under close-circuit conditions the sMFC reduces the production of hydrogen sulfide. This occurs as a result of the increase of soil Eh, since the production of hydrogen sulfide requires the Eh to be below -100 mV (Yuan et al., 2010). Likewise, it has also been demonstrated that the sMFC could be successfully used to improve the color of the soil from black to brown by suppressing the rate of anaerobic microbial fermentation, methanogenesis and sulfate- reducing processes in soil (Jung and Regan, 2011; Ueno and Kitajima, 2012).

1.3.1.2. Changes in soil pH

Moreover, characteristically of anodic reaction, the metabolic breakdown of organic matter by the anodophillic bacteria cause the production of protons. The presence of the anode support the continuous oxidation of organic matter thus in turn allow for the increase in proton concentration which lead to the decrease of soil pH in the anode vicinity. Since the mass transfer of protons from the anoxic zone to the oxic zone is slow in soil (Hong et al., 2009). The movement of protons in soil is slow due to the poor permeability of the complex soil matrix (Huang et al., 2011). However the soil pH increases in the cathode vicinity because of the protons consumption. These changes in soil pH can in turn affect the biogeochemical cycling of many inorganic and organic compounds. For example, the change in soil pH can greatly affect the bioavailability of many redox active metals (Jiang et al., 2014; Signespastor et al., 2007).

Previous studies revealed that the increase in soil pH in the cathode region encourages the precipitation of iron and other metal oxides in the oxic soil that can then immobilize heavy metals pollutants and nutrients (Martins et al., 2014; Wu et al., 2017a; Yang et al., 2016). In a study by Martins et al. (2014), the sMFC was found to increase in the amounts of metal bound, calcium bound and refractory phosphorus. In another by Yang et al. (2016), similar results were obtained where the sMFC enhanced the microbial oxidation of ferrous iron that coprecipitated with liable phosphorous from the overlaying water. On the contrary, the decrease in soil pH in the anode vicinity can increase the solubility of many heavy metals and promote their migrations from the deep soil to the cathode chamber during electrokinesis. When in the cathode chamber these metals can precipitate on the cathode or precipitate with metal oxides (Wang et al., 2015a).

1.3.2. Substrate competition

Furthermore, the sMFC provides anodes as an electron acceptor that can stimulate continuous anaerobic oxidation of organic matter in soils (Huang et al., 2011; Logan, 2008). Hence, the sMFC can create a substrate competition between the microbes in the anode vicinity and that of the bulk soil. The simultaneous bioremediation of soil organic matter and electricity generation was observed in a study by Hong et al. (2009). Their results showed a direct relation between the current generation and the removal rate of organic matter (Hong et al., 2009). Hong et al. (2009) observed a significant decrease in organic matter after 160 days of operation under close-circuit conditions. Similarly, sludge collected from the riverbank of a tidal river had an organic carbon content biodegradation enhanced by 10-fold compared to the natural biodegradation, when sMFC technology was used (Touch et al., 2014).

From the above studies one can conclude that sMFC can effectively decrease organic matter bioavailability and create a substrate competition between the microbes in the anode vicinity and that of the bulk soil. This is of importance for heavy metal remediation because there is a direct relationship between the microbial mobilization of redox sensitive toxic metals and organic matter. Organic matter is essential in the microbial mediated reduction of iron oxide as it serves as both an electron donor and shuttle for extracellular electron transfer (Stuckey et al., 2015; Wang et al., 2016b). Therefore, if the organic matter in soil is limited the rate of microbial liberation of heavy metal will also be decreased. In a study done on evaluating the potential effects of biochar on the release of arsenic and iron, it was observed that biochar can increase the bioavailability of organic matter which enhances iron and arsenic reduction because the increase in organic matter can stimulate bacterial active (Chen et al., 2016b). Organic matter provides the electrons needed to reduce iron and at the same time organic matter can contain quinone-like substances that facilitate electron shuttling. These studies indicate that when organic matter concentration is high, an enhancement in iron

reduction and the release of iron co-precipitate metals should be expected and vice versa when organic is limited.

1.3.3. Electromigration

Another mechanism in which the sMFC can influence soil heavy metal remediation is through electromigration and electroosmotic flow (Chen et al., 2015; Habibul et al., 2016a). Electrokinetic remediation have been applied as a green remediation for soil heavy metal remediation (Chen et al., 2015; Habibul et al., 2016a; Yang et al., 2014). In electrokinetic remediation an electrical potential is applied to remove heavy metals via the electromigration and electroosmotic flow. This technique have been proven to be effective in removing desorbed metal pollutants from the soil and soil porewater (Yang et al., 2014). However, this technique is not widely practice because it is energy costly and requires the addition of electrolytes (Chen et al., 2015; Habibul et al., 2016a).

Recently the sMFC the have been used to generate the energy that is needed to drive the in situ electrokinetic remediation of the toxic metals without the addition of an external power source (Chen et al., 2015; Habibul et al., 2016a; Habibul et al., 2016b; Song et al., 2018). The current produce by the sMFC was used to accelerate the transfer of contaminants along with the pore fluid towards a charged electrode where it may be removed or treated. Furthermore, because the sMFC decreases the soil pH in the anode region, this can favor the solubilization of the toxic metals from soil particle surface and increase their removal efficiency.

1.3.4. Changes in the soil microbial community composition

Although naturally the soil microbial community can self-remediate the soil to some extent, however this is limited due to the depletion of suitable electron acceptors. To ease this problem, some research suggest the addition of external electron acceptors to improve the

remediation efficiency (Liu et al., 2018). However this is not widely practiced since many oxidants may lead to the generation of secondary pollutants and may incur extra cost (Li and Yu, 2015; Liu et al., 2018). The anode of the sMFC can sustain and enrich the growth of the functional microbial community that are needed for soil remediation. This in turn causes a redistribution of the microbial community structure in soils that employ sMFC. This change in microbial structure occurs because the in addition to serving as an electron acceptor, the anode can alter soil Eh, pH and nutrient bioavailability (Nicol et al., 2008; Pettridge and Firestone, 2005; Wu et al., 2017b).

Studies have shown that operating the sMFC can significantly enhance electrogenic microbes in the anode vicinity (Kouzuma et al., 2013; Lu et al., 2014). Xiao et al. (2015), examined the microbial community of several anode biofilms from various geographical locations in China and identified six core genera, (*Azospira, Azospirillum, Acinetobacter, Bacteroides, Geobacter, Pseudomonas*, and *Rhodopseudomonas*), of exoelectrogens. Their finding further supports the fact that the dominate members of the anodic community belong to the electrochemically active *Protobacteria* clans. Most members of the phylum *Proteobacteria* possess the ability to transfer electrons to extracellular insoluble-electron acceptors, such as iron oxides.

The directly transfer of electrons to the anode can prevent the reduction of metal oxides in the soil and prevent the liberation of toxic heavy metals. Eelectrogen, such as *Geobacter, Shewanella, Desulfuromonas,* and *Rhodopseudomonas*, has be shown to directly or indirectly respire the anode (Logan, 2009). Moreover, studies have also shown that sMFC microbial community can be used to transform toxic heavy metals to less toxic forms as in the case of chromium, uranium, cadmium, lead and copper. *Geobacter sulfurreducens* can extract electrons from the anode to transform reduces soluble U(VI) and Cr (VI) to insoluble U(IV)

less toxic Cr(III), respectively (Cologgi et al., 2011; Gregory and Lovley, 2005; Wang et al., 2015a).

1.4. Application of microbial fuel cell in soil heavy metal remediation

Different from the remediation of organic pollutants, soil heavy metals cannot be microbial degraded and thus are persistent in soil. MFC has already been shown to remove up to 100 percent of metal contaminates in the wastewater effluents and shows great potentials for the replacement of conventional wastewater treatment technologies such as anaerobic digesters (Wang and Ren, 2014). Although not completely transferable, due to design differences, the use of MFC in soil heavy metal remediation is highly possible though it has not been widely applied (Li and Yu, 2015).

The sMFC can immobilize and even extract metal species by changing their redox state and via electrokinetic processes (Gregory and Lovley, 2005; Li and Yu, 2015; Wang et al., 2015a) (Table 1.1). Researchers have demonstrated that sMFC can facilitate the reduction of numerous positively charged metal pollutants to less harmful species (Gregory and Lovley, 2005; Li and Yu, 2015; Wang et al., 2015a). In addition, the sMFC has also been used to fix some of these pollutants in the soil therefore limiting their bioavailability (Li and Yu, 2015; Wang et al., 2015a). This in turn, prevents the pollution of surface and ground water thereby limiting the uptake and consumption of these metals by plants and animals, respectively. However to date the sMFC have only been applied for the removal of a few heavy metals in the soil system.

1.4.1. Chromium

Chromium is a toxic heavy metal that enters the soil environment from the improper disposal of Cr(VI) and Cr(III) contaminated wastewater (Mathuriya and Yakhmi, 2014). The hexavalent form of chromium is more mobile than Cr(III) and possess a serious health risk for

cancer development (Kotaś and Stasicka, 2000). Cr(III) in it oxide form is highly insoluble in aqueous solution and is hardly bioavailable in the soil system. Thus, the reduction of Cr(VI) to Cr(III) has been identified as effective way to limiting chromium toxicity since Cr(III) is insoluble. The MFC has been shown to be able to effectively reduce Cr(VI) to Cr(III) by using Cr(VI) as a final electron acceptor in the cathode chamber. In a recent study, Wang et al., 2015a, showed that Cr(VI), can be successfully removed from soil with sMFC. In their study Cr(VI) was reduce to Cr(III) in the cathode chamber. The team observed a 99.1% maximum removal efficient in the fluvo-aquic soil when 100 ohm resistance was applied after 16 days. The removal rate in the fluvo-aquic soil at 100 ohm resistance was much high than that observed when 1000 ohm resistance (64.3%) was applied and also that of the red clay soil (62.7% with 100 ohm and 50.4% with 1000 ohm) (Wang et al., 2015a). This indicated that soil type and resistance applied had a significant influence on the efficiency Cr(VI).

Similarly, Habibul et al., 2016b, reported a 99% Cr(VI) removal efficiency using plant-microbial fuel cells (pMFC) and indicated that Cr(VI) removal rate depended on the initial Cr(VI) concentrations. This technology can be applied to both soil and wastewater remediation. It should be noted that this high efficient rate was a combination of both plant accumulation and reduction of Cr(VI), although the reduction of Cr(VI) played a big part (Habibul et al., 2016b). They indicated that the addition of nutrient medium could be eliminated when using pMFC since the plant root secretion can be used as an organic source for microbial metabolic activities.

1.4.2. Uranium

Uranium is a toxic heavy metal that enters the soil environment through mining, and the improper disposal of uranium containing weapons and wastewater (Li and Zhang, 2012). The toxicity of uranium is determined by its speciation and the more soluble forms of uranium compound are the most toxic (Newsome et al., 2014). Uranium is known to have many harmful

effect on the human health such as kidney and liver diseases (Craft et al., 2004). In the soil environment under oxidizing conditions, U(VI) is the dominate species and is relative mobile. However, under reducing conditions the poorly soluble U(IV) species dominate (Newsome et al., 2014). Many iron- and sulfate-reducing bacteria has been shown to be able to reduce U(VI) to the less mobile form U(IV) by using U(VI) as an alternative electron acceptor (Gavrilescu et al., 2009; Pous et al., 2018). Nevertheless, in the natural environment this process is limited due to lack of electron donors and the relatively low abundance of the functional microbial community.

To alleviate this problem, electron donors such as acetate and lactate were often added to the soil to promote iron- and sulfate-reducers abundance, stimulate anaerobic conditions and consequently the precipitation of U(IV) (Gavrilescu et al., 2009; Pous et al., 2018). However this process incur extra cost and may have some adverse ecological impacts. Given that the genus *Geobacter* was observed to be enrich in uranium contaminated soils (Anderson et al., 2003; Holmes et al., 2015) and was demonstrated to be able to extract electron from the electrode to reduce fumarate and nitrate (Gregory et al., 2004), the anode was propose to be used to supply the electrons needed to immobilize uranium (Gregory and Lovley, 2005). The use of the anode to supply the electron instead of acetate would not only decrease the cost, but also reduce the possible negative environmental effects.

The use of electrodes as an electron donor for soil microbes for the removal of uranium was first demonstrated by Gregory and Lovley (2005). Gregory and Lovley (2005) showed that by posing the electrodes at -500mV in the presence of microorganism, the electrode was able to remove uranium from the soil by changing its redox state. The microbial community of the electrode transformed the soluble U(VI) to its insoluble U(IV) form. The U(IV) precipitated onto carbon material and be remove from the soil by lifting the electrode from the soil (Gregory and Lovley, 2005).

1.4.3. Other metals

The power that is produced by the MFC have also been used to propel toxic heavy metals from soil. In a previous study, Chen et al. (2015), used the MFC to produce energy required to propel electrolytes and heavy metal ions from the soil and soil porewater via electrokinetic remediation. The authors concluded that MFC could successfully provide the energy needed to significantly remove zinc and cadmium from paddy soils at a very low cost compared to previous electrokinetic remediation systems that are known to be expensive (Chen et al., 2015).

Moreover, in another study Habibul et al. (2016a) obtained similar results where the sMFC was used to drive electrokinetic remediation of cadmium and lead from metal contaminated soil. They observed 31.0% and 44.1% removal efficiencies for cadmium and lead, respectively, in the anodic chamber (Habibul et al., 2016a). More recently, Wang et al. (2016a) investigated the ability of sMFC to enhance the electromigration of copper ions. Wang and coworkers' study concluded that sMFC can promote the migration of copper ions from the anodic area to the cathodic zone, where the copper ions can be recovered to alleviate the soil of the harmful copper pollutants. They also noted that the copper migration was significantly related to current production (Wang et al., 2016a).

In another study, Song et al. (2018) also showed that the sMFC can be used to reduce the risk of heavy metal leaching into groundwater from soil. The authors observed a 37.2% and 15.1% decrease in lead and zinc removal near the anode after 100 days of operating the sMFC. Other reports have shown where the sMFC can reduce toxic Cu(II), Hg(II), and Ag(I) species to the less toxic forms (Abbas et al., 2018; Wu et al., 2017a). In a recent study it was shown that the sMFC can be used to remove Hg(II), Cu(II) and Ag(I) from the overlaying water by 97.3%, 87.7% and 98.5 %, respectively, after 60 days of operation (Wu et al., 2017a).

Table 1.1 Summary of previous studies where the MFC was used in soil heavy metal remediation

Heavy metals	Removal mechanism	References
Chromium	The Cr(VI) migrates to the cathode chamber where it is reduce to Cr(III). The Cr(III) then reacts with hydroxides and precipitate out of solution.	(Abbas et al., 2018; Guan et al., 2019; Habibul et al., 2016b; Wang et al., 2015a)
Cadmium	The decrease in soil pH near the anode and the weak electric field generated produce by the MFC favor the migration of Cd to the cathode chamber. At the cathode chamber the higher soil pH resulted in the precipitation Cd with oxides	(Abbas et al., 2017; Chen et al., 2015; Habibul et al., 2016a)
Lead	The removal of Pb was similar to that of Cd.	(Abbas et al., 2017)
Zinc	The removal of Zn was similar to that of Cd.	(Chen et al., 2015)
Copper	The removal of Cu was similar to that of Cd.	(Abbas et al., 2018; Wang et al., 2016a; Wu et al., 2017a)
Sliver	The removal of Ag through reductive reaction and biosorption by the cathode microbial community.	(Wu et al., 2017a)
Mercury	The removal of Hg was similar to that of Ag.	(Wu et al., 2017a)
Uranium	Change in soil chemistry and microbial community encourages the transformation of soluble U(VI) to insoluble U(IV).	(Gregory and Lovley, 2005)

1.5. Research Aims and Objectives

Since it has been demonstrated that sMFC can directly or indirectly aid in the removal of heavy metals and other electrolytic pollutants, it is reasonable to assume that sMFC could have an effect on the behavior of paddy soil trace elements. Understanding the interaction between the anode and trace element in paddy soils is therefore crucial. The ability to control soil-to-solution partitioning of trace metals from the reductive dissolution process of metal oxides is identified as the key to remediation of metal polluted soils. Recent studies have also shown that sMFC implanted in paddy soil affects iron redox chemistry (Touch et al., 2017; Wang et al., 2015; Yang et al., 2016; Zhou et al., 2015). Thus, based on these studies it can be concluded that sMFC could play a crucial role in controlling porewater trace metal concentrations. Hence, sMFC can be commissioned in paddy fields to reduce trace metal contaminates in soil porewater. However, limited research has been conducted in this area and the mechanism of this process is still not fully understood. Therefore in this PhD work, we aim to understand the effect of the sMFC anode on the paddy soil microbial community and the effects on the fate of soil trace elements. To achieve this aim the following topics were addressed.

Chapter 3: The effect of the soil microbial fuel cell on paddy soil microbial community profile

The sMFC is known to shape the anode microbial community, however scarce data is available on its effect on the soil profile microbial community. Moreover, operation the sMFC is also known to generate a large amount of extra cellular (relic) DNA, nonetheless the effect of this relic DNA on the culture independent estimates of the sMFC microbial community have not been investigated. Therefore in this chapter we addressed the following questions. *What are the effect of the sMFC anode on the paddy soil microbial profile? How far can the sMFC*

influence the soil profile microbial community? Does the relic DNA that is generate effect the culture independent estimates of the microbial community?

Chapter 4: The effect of the sMFC on paddy soil components at different external resistance

External resistance is an important factor control the performance of the sMFC. However, studies examining the influence of the anode at different external resistance on soil biotic and abiotic constituents collectively are scarce. No studies has examined the effect of the sMFC at different external resistance on the soil and anode microbial community structure. Thus in this chapter we asked the following question. *Does different external resistance effect the microbial community that develop in the sMFC? How the different external resistance effect the sMFC abiotic components?*

Chapter 5: The effect of the sMFC on arsenic in soil with low organic matter content

The sMFC anode can be used as an alternative electron acceptor. Thus installing the sMFC may be able to reduce arsenic release into the soil porewater. Base on the aforementioned we asked the following question in this chapter. *Can the sMFC be used to manipulate the soil iron redox changes and prevent arsenic release? Which factor is the dominating factor that needs to be control in order to prevent arsenic liberation into the soil porewater?*

Chapter 6: The effect of the sMFC on arsenic in soil with high organic matter content

In chapter 5 we found that the sMFC was able to limit iron and arsenic release into the soil porewater by creating a substrate competition between the microbe in the anode and those of the bulk soil in a low organic matter soil. However, the following questions remain to be answered. *What happens when the sMFC is deployed in soil with high organic matter content? Can the sMFC be combine with water management to limit arsenic and iron dissolution?* Hence they were address in this chapter.

Chapter 7: The effect of the sMFC on the accumulation of arsenic in rice plant parts

We showed in chapters 5 and 6 that the sMFC can be used to limit the release of arsenic and iron into the soil porewater. Hence, in this chapter we ask the following questions. *Can the sMFC be used to limit the accumulation of arsenic in rice plant parts? What are the effect of the sMFC on the arsenic transformation genes in the rhizosphere?*

Chapter 8: The effect of the sMFC on the accumulation of other trace heavy metal in rice plant parts

In chapter 7 we showed that the sMFC can reduce the accumulation of arsenic. Thus in this chapter we ask the following question; *Can the sMFC be used to limit the accumulation of other heavy metals in rice plant parts?*

1.6. References

Abbas, S.Z., Rafatullah, M., Ismail, N., Nastro, R.A., 2017. Enhanced bioremediation of toxic metals and harvesting electricity through sediment microbial fuel cell. Int. J. Energ. Res. 41, 2345-2355.

Abbas, S.Z., Rafatullah, M., Ismail, N., Shakoori, F.R., 2018. Electrochemistry and microbiology of microbial fuel cells treating marine sediments polluted with heavy metals. Rsc Advances 8, 18800-18813.

Abourached, C., Catal, T., Liu, H., 2014. Efficacy of single-chamber microbial fuel cells for removal of cadmium and zinc with simultaneous electricity production. Water Res. 51, 228-233.

Anderson, R.T., Vrionis, H.A., Ortiz-Bernad, I., Resch, C.T., Long, P.E., Dayvault, R., Karp, K., Marutzky, S., Metzler, D.R., Peacock, A., 2003. Stimulating the in situ activity of Geobacter species to remove uranium from the groundwater of a uranium-contaminated aquifer. Appl. Environ. Microbiol. 69, 5884-5891.

Bolan, N., Kunhikrishnan, A., Thangarajan, R., Kumpiene, J., Park, J., Makino, T., Kirkham, M.B., Scheckel, K., 2014. Remediation of heavy metal (loid) s contaminated soils–to mobilize or to immobilize? J. Hazard. Mater. 266, 141-166.

Bond D. R, Holmes D. E, Tender L. M, R, L.D., 2002. Electrode reducing microorganisms that harvest energy from marine sediments. Science 295, 483–485.

Burton, E.D., Johnston, S.G., Planer-Friedrich, B., 2013. Coupling of arsenic mobility to sulfur transformations during microbial sulfate reduction in the presence and absence of humic acid. Chem. Geol. 343, 12-24.

Charlatchka, R., Cambier, P., 2000. Influence of reducing conditions on solubility of trace metals in contaminated soils. Water Air Soil Pollut. 118, 143-168.

Chen, S., Tang, J., Fu, L., Yuan, Y., Zhou, S., 2016a. Biochar improves sediment microbial fuel cell performance in low conductivity freshwater sediment. J. Soils Sediments 16, 2326-2334.

Chen, Z., Huang, Y.C., Liang, J.H., Zhao, F., Zhu, Y.G., 2012. A novel sediment microbial fuel cell with a biocathode in the rice rhizosphere. Bioresour. Technol. 108, 55-59.

Chen, Z., Wang, Y., Xia, D., Jiang, X., Fu, D., Shen, L., Wang, H., Li, Q.B., 2016b. Enhanced bioreduction of iron and arsenic in sediment by biochar amendment influencing microbial community composition and dissolved organic matter content and composition. J. Hazard. Mater. 311, 20-29.

Chen, Z., Zhu, B.K., Jia, W.F., Liang, J.H., Sun, G.X., 2015. Can electrokinetic removal of metals from contaminated paddy soils be powered by microbial fuel cells? Environ. Technol. Innov. 3, 63-67.

Choi, C.H., Kim, M.A., Hong, S.W., Choi, Y.S., Song, Y.I., Kim, S.H., Kim, H.J., 2010. Performance of a microbial fuel cell using a magnet attached cathode. Bull. Korean Chem. Soc. 31, 1729-1731.

Chowdhury, U.K., Biswas, B.K., Chowdhury, T.R., Samanta, G., Mandal, B.K., Basu, G.C., Chanda, C.R., Lodh, D., Saha, K.C., Mukherjee, S.K., 2000. Groundwater arsenic contamination in Bangladesh and West Bengal, India. Environ. Health Perspect. 108, 393.

Cologgi, D.L., Lampapastirk, S., Speers, A.M., Kelly, S.D., Reguera, G., 2011. Extracellular reduction of uranium via Geobacter conductive pili as a protective cellular mechanism. Proc. Natl. Acad. Sci. 108, 15248-15252.

Craft, E.S., Abu-Qare, A.W., Flaherty, M.M., Garofolo, M.C., Rincavage, H.L., Abou-Donia, M.B., 2004. Depleted and natural uranium: chemistry and toxicological effects. J. Toxicol. Environ. Health, Part B 7, 297-317.

De Schamphelaire, L., Rabaey, K., Boeckx, P., Boon, N., Verstraete, W., 2008. Outlook for benefits of sediment microbial fuel cells with two bio-electrodes. Microb. Biotechnol. 1, 446-462.

del Campo, A.G., Cañizares, P., Rodrigo, M.A., Fernández, F.J., Lobato, J., 2013. Microbial fuel cell with an algae-assisted cathode: a preliminary assessment. J. Power Sources 242, 638-645.

DeLaune, R., Jugsujinda, A., Devai, I., Patrick Jr, W., 2004. Relationship of sediment redox conditions to methyl mercury in surface sediment of Louisiana Lakes. J. Toxicol. Environ. Health, Part A 39, 1925-1933.

Facchinelli, A., Sacchi, E., Mallen, L., 2001. Multivariate statistical and GIS-based approach to identify heavy metal sources in soils. Environ. Pollut. 114, 313-324.

Gadd, G.M., 2004. Microbial influence on metal mobility and application for bioremediation. Geoderma 122, 109-119.

Gavrilescu, M., Pavel, L.V., Cretescu, I., 2009. Characterization and remediation of soils contaminated with uranium. J. Hazard. Mater. 163, 475-510.

Gregory, K.B., Bond, D.R., Lovley, D.R., 2004. Graphite electrodes as electron donors for anaerobic respiration. Environ. Microbiol. 6, 596-604.

Gregory, K.B., Lovley, D.R., 2005. Remediation and recovery of uranium from contaminated subsurface environments with electrodes. Environ. Sci. Technol. 39, 8943-8947.

Guan, C.-Y., Tseng, Y.-H., Tsang, D.C., Hu, A., Yu, C.-P., 2019. Wetland plant microbial fuel cells for remediation of hexavalent chromium contaminated soils and electricity production. J. Hazard. Mater. 365, 137-145.

Habibul, N., Hu, Y., Sheng, G.P., 2016a. Microbial fuel cell driving electrokinetic remediation of toxic metal contaminated soils. J. Hazard Mater. 318, 9-14.

Habibul, N., Hu, Y., Wang, Y.K., Chen, W., Yu, H.Q., Sheng, G.P., 2016b. Bioelectrochemical Chromium(VI) Removal in Plant-Microbial Fuel Cells. Environ. Sci. Technol. 50, 3882-3889.

He, Z., Shao, H., Angenent, L.T., 2007. Increased power production from a sediment microbial fuel cell with a rotating cathode. Biosens. Bioelectron. 22, 3252-3255.

He, Z., Shentu, J., Yang, X., Baligar, V.C., Zhang, T., Stoffella, P.J., 2015. Heavy metal contamination of soils: sources, indicators and assessment.

Holmes, D.E., Giloteaux, L., Chaurasia, A.K., Williams, K.H., Luef, B., Wilkins, M.J., Wrighton, K.C., Thompson, C.A., Comolli, L.R., Lovley, D.R., 2015. Evidence of Geobacter-associated phage in a uranium-contaminated aquifer. The ISME Journal 9, 333.

Hong, S.W., Chang, I.S., Choi, Y.S., Kim, B.H., Chung, T.H., 2009. Responses from freshwater sediment during electricity generation using microbial fuel cells. Bioprocess Biosyst. Eng. 32, 389-395.

Hong, S.W., Kim, H.S., Chung, T.H., 2010. Alteration of sediment organic matter in sediment microbial fuel cells. Environ. Pollut. 158, 185-191.

Hong, Y., Gu, J., 2009. Bacterial anaerobic respiration and electron transfer relevant to the biotransformation of pollutants. Int. Biodeterior. Biodegradation. 63, 973-980.

Huang, D.Y., Zhou, S.G., Chen, Q., Zhao, B., Yuan, Y., Zhuang, L., 2011. Enhanced anaerobic degradation of organic pollutants in a soil microbial fuel cell. Chem. Eng. J. 172, 647-653.

Jaishankar, M., Tseten, T., Anbalagan, N., Mathew, B.B., Beeregowda, K.N., 2014. Toxicity, mechanism and health effects of some heavy metals. Interdiscip. Toxicol. 7, 60-72.

Järup, L., Åkesson, A., 2009. Current status of cadmium as an environmental health problem. Toxicol. Appl. Pharmacol. 238, 201-208.

Jiang, W., Hou, Q., Yang, Z., Zhong, C., Zheng, G., Yang, Z., Li, J., 2014. Evaluation of potential effects of soil available phosphorus on soil arsenic availability and paddy rice inorganic arsenic content. Environ. Pollut. 188, 159-165.

Jung, S., Regan, J.M., 2011. Influence of External Resistance on Electrogenesis, Methanogenesis, and Anode Prokaryotic Communities in Microbial Fuel Cells. Appl. Environ. Microbiol. 77, 564-571.

Kaku, N., Yonezawa, N., Kodama, Y., Watanabe, K., 2008. Plant/microbe cooperation for electricity generation in a rice paddy field. Appl. Microbiol. Biotechnol. 79, 43-49.

Khan, A., Kuek, C., Chaudhry, T., Khoo, C., Hayes, W., 2000. Role of plants, mycorrhizae and phytochelators in heavy metal contaminated land remediation. Chemosphere 41, 197-207.

Kotaś, J., Stasicka, Z., 2000. Chromium occurrence in the environment and methods of its speciation. Environ. Pollut. 107, 263-283.

Kouzuma, A., Kaku, N., Watanabe, K., 2014. Microbial electricity generation in rice paddy fields: recent advances and perspectives in rhizosphere microbial fuel cells. Appl. Microbiol. Biotechnol. 98, 9521-9526.

Kouzuma, A., Kasai, T., Nakagawa, G., Yamamuro, A., Abe, T., Watanabe, K., 2013. Comparative metagenomics of anode-associated microbiomes developed in rice paddy-field microbial fuel cells. PLoS One 8, e77443.

Li, J., Zhang, Y., 2012. Remediation technology for the uranium contaminated environment: a review. Procedia Environ. Sci. 13, 1609-1615.

Li, W., Yu, H., 2015. Stimulating sediment bioremediation with benthic microbial fuel cells. Biotechnol. Adv. 33, 1-12.

Li, Z., Ma, Z., van der Kuijp, T.J., Yuan, Z., Huang, L., 2014. A review of soil heavy metal pollution from mines in China: pollution and health risk assessment. Sci. Total Environ. 468-469, 843-853.

Lin, B., Lu, Y., 2015. Bacterial and archaeal guilds associated with electrogenesis and methanogenesis in paddy field soil. Geoderma 259-260, 362-369.

Liu, L., Li, W., Song, W., Guo, M., 2018. Remediation techniques for heavy metal-contaminated soils: principles and applicability. Sci. Total Environ. 633, 206-219.

Liu, X.W., Sun, X.F., Huang, Y.X., Sheng, G.P., Zhou, K., Zeng, R.J., Dong, F., Wang, S.G., Xu, A.W., Tong, Z.H., Yu, H.Q., 2010. Nano-structured manganese oxide as a cathodic catalyst for enhanced oxygen reduction in a microbial fuel cell fed with a synthetic wastewater. Water Res. 44, 5298-5305.

Logan, B.E., 2008. Microbial Fuel Cells. A John Wiley & Sons, Inc.

Logan, B.E., 2009. Exoelectrogenic bacteria that power microbial fuel cells. Nat. Rev. Microbiol. 7, 375–381.

Logan, B.E., Hamelers, B., Rozendal, R.A., Schroder, U., Keller, J., Freguia, S., Aelterman, P., Verstraete, W., Rabaey, K., 2006. Microbial Fuel Cells: Methodology and Technology. Environ. Sci. Technol. 40, 5181-5192.

Lohmayer, R., Kappler, A., Lösekann-Behrens, T., Planer-Friedrich, B., 2014. Role of sulfur species as redox partners and electron shuttles for ferrihydrite reduction by Sulfurospirillum deleyianum. Appl. Environ. Microbiol. 04220-04213.

Lovley, D.R., 2008. The microbe electric: conversion of organic matter to electricity. Curr. Opin. Biotechnol. 19, 564-571.

Lovley, D.R., 2011. Live wires: direct extracellular electron exchange for bioenergy and the bioremediation of energy-related contamination. Energy Environ. Sci. 4, 4896-4906.

Lu, L., Huggins, T., Jin, S., Zuo, Y., Ren, Z.J., 2014. Microbial metabolism and community structure in response to bioelectrochemically enhanced remediation of petroleum hydrocarbon-contaminated soil. Environ. Sci. Technol. 48, 4021.

Marques, A.P.G.C., Rangel, A.O.S.S., Castro, P.M.L., 2009. Remediation of Heavy Metal Contaminated Soils: Phytoremediation as a Potentially Promising Clean-Up Technology. Crit. Rev. Environ. Sci. Technol. 39, 622-654.

Martins, G., Peixoto, L., Teodorescu, S., Parpot, P., Nogueira, R., Brito, A.G., 2014. Impact of an external electron acceptor on phosphorus mobility between water and sediments. Bioresour. Technol. 151, 419-423.

Mathuriya, A.S., Yakhmi, J.V., 2014. Microbial fuel cells to recover heavy metals. Environ. Chem. Lett. 12, 483-494.

Min, B., Cheng, S., Logan, B.E., 2005. Electricity generation using membrane and salt bridge microbial fuel cells. Water Res. 39, 1675-1686.

Newsome, L., Morris, K., Lloyd, J.R., 2014. The biogeochemistry and bioremediation of uranium and other priority radionuclides. Chem. Geol. 363, 164-184.

Nicol, G.W., Leininger, S., Schleper, C., Prosser, J.I., 2008. The influence of soil pH on the diversity, abundance and transcriptional activity of ammonia oxidizing archaea and bacteria. Environ. Microbiol. 10, 2966-2978.

Pandey, B., Fulekar, M., 2012. Bioremediation technology: a new horizon for environmental clean-up. Biol. Med. 4, 51.

Pettridge, J., Firestone, M.K., 2005. Redox fluctuation structures microbial communities in a wet tropical soil. Appl. Environ. Microbiol. 71, 6998-7007.

Potter, M.C., 1911. Electrical effects accompanying the decomposition of organic compounds. Proc. R. Soc. Lond. B 84, 260-276.

Pous, N., Balaguer, M.D., Colprim, J., Puig, S., 2018. Opportunities for groundwater microbial electro-remediation. Microb. Biotechnol. 11, 119-135.

Reimers, C.E., Tender, L.M., Fertig, S., Wang, W., 2001. Harvesting energy from themarine sediment–water interface. Environ. Sci. Technol. 35, 192–195.

Rezaei, F., Richard, T.L., A., B.R., E., L., 2007. Substrate-Enhanced Microbial Fuel Cells for Improved Remote Power Generation from Sediment-Based Systems. Environ. Sci. Technol. 41, 4053–4058.

Rozendal, R.A., Hamelers, H.V., Molenkamp, R.J., Buisman, C.J., 2007. Performance of single chamber biocatalyzed electrolysis with different types of ion exchange membranes. Water Res. 41, 1984-1994.

Sajana, T.K., Ghangrekar, M.M., Mitra, A., 2014. Effect of operating parameters on the performance of sediment microbial fuel cell treating aquaculture water. Aquacult. Eng." 61, 17-26.

Sajana, T.K., Ghangrekar, M.M., Mitra, A., 2016. In Situ Bioremediation Using Sediment Microbial Fuel Cell. J. Hazard Toxic Radioact. Waste, 21(2), 04016022.

Schamphelaire, L.D., Bossche, L.V.d., Dang, H.S., Höfte, M., Boon, N., Rabaey, K., Verstraete, W., 2008. Microbial Fuel Cells Generating Electricity from Rhizodeposits of Rice Plants. Environ. Sci. Technol. 42, 3053-3058.

Signespastor, A.J., Burlo, F., Mitra, K., Carbonellbarrachina, A.A., 2007. Arsenic biogeochemistry as affected by phosphorus fertilizer addition, redox potential and pH in a west Bengal (India) soil. Geoderma 137, 504-510.

Song, T.S., Yan, Z.-S., Zhao, Z.-W., Jiang, H.L., 2010. Removal of organic matter in freshwater sediment by microbial fuel cells at various external resistances. Journal of Chemical Technology & Biotechnology, 85(11), 1489-1493

Song, T.S., Zhang, J., Hou, S., Wang, H., Zhang, D., Li, S., Xie, J., 2018. In situ electrokinetic remediation of toxic metal-contaminated soil driven by solid phase microbial fuel cells with a wheat straw addition. J. Chem. Technol. Biotechnol. 93, 2860-2867.

Stuckey, Jason W., Schaefer, Michael V., Kocar, Benjamin D., Benner, Shawn G., Fendorf, S., 2015. Arsenic release metabolically limited to permanently water-saturated soil in Mekong Delta. Nat. Geosci. 9, 70-76.

Thrash J., D, C.J., 2008. Review: Direct and indirect electrical stimulation of microbial metabolism. Environ. Sci. Technol. 42, 3921–3931.

Touch, N., Hibino, T., Nagatsu, Y., Tachiuchi, K., 2014. Characteristics of electricity generation and biodegradation in tidal river sludge-used microbial fuel cells. Bioresour. Technol. 158, 225-230.

Ueno, Y., Kitajima, Y., 2012. Suppression of methane gas emission from sediment using a bioelectrochemical system. Environ. Eng. Manag. J. 11.

Ueoka, N., Sese, N., Sue, M., Kouzuma, A., Watanabe, K., 2016. Sizes of Anode and Cathode Affect Electricity Generation in Rice Paddy-Field Microbial Fuel Cells. J. Sustain. Bioener. Syst. 06, 10-15.

Wang, A., Cheng, H., Ren, N., Cui, D., Lin, N., Wu, W., 2011. Sediment microbial fuel cell with floating biocathode for organic removal and energy recovery. Front. Environ. Sci. Eng. 6, 569-574.

Wang, C., Deng, H., Zhao, F., 2015a. The Remediation of Chromium (VI)-Contaminated Soils Using Microbial Fuel Cells. Soil Sediment Contam. 25, 1-12.

Wang, D.-B., Song, T.-S., Guo, T., Zeng, Q., Xie, J., 2014. Electricity generation from sediment microbial fuel cells with algae-assisted cathodes. Int. J. Hydrog. Energy 39, 13224-13230.

Wang, H., Luo, H., Fallgren, P.H., Jin, S., Ren, Z.J., 2015b. Bioelectrochemical system platform for sustainable environmental remediation and energy generation. Biotechnol. Adv. 33, 317-334.

Wang, H., Ren, Z.J., 2014. Bioelectrochemical metal recovery from wastewater: a review. Water Res. 66, 219-232.

Wang, H., Song, H., Yu, R., Cao, X., Fang, Z., Li, X., 2016a. New process for copper migration by bioelectricity generation in soil microbial fuel cells. Environ. Sci. Pollut. Res. Int. 23, 13147-13154.

Wang, Y., Chen, Z., Liu, P., Sun, G., Ding, L., Zhu, Y., 2016b. Arsenic modulates the composition of anode-respiring bacterial community during dry-wet cycles in paddy soils. J. Soils Sediments 16, 1745-1753.

Wu, M., Xu, X., Zhao, Q., Wang, Z., 2017a. Simultaneous removal of heavy metals and biodegradation of organic matter with sediment microbial fuel cells. Rsc Advances 7, 53433-53438.

Wu, Y., Jing, X., Gao, C., Huang, Q., Cai, P., 2018. Recent advances in microbial electrochemical system for soil bioremediation. Chemosphere.

Wu, Y., Zeng, J., Zhu, Q., Zhang, Z., Lin, X., 2017b. pH is the primary determinant of the bacterial community structure in agricultural soils impacted by polycyclic aromatic hydrocarbon pollution. Sci. Rep. 7, 40093.

Xiao, Y., Zheng, Y., Wu, S., Zhang, E.H., Chen, Z., Liang, P., Huang, X., Yang, Z.H., Ng, I.S., Chen, B.Y., Zhao, F., 2015. Pyrosequencing Reveals a Core Community of Anodic Bacterial Biofilms in Bioelectrochemical Systems from China. Front. Microbiol. 6, 1410.

Yamaguchi, N., Nakamura, T., Dong, D., Takahashi, Y., Amachi, S., Makino, T., 2011. Arsenic release from flooded paddy soils is influenced by speciation, Eh, pH, and iron dissolution. Chemosphere 83, 925-932.

Yang, J.S., Kwon, M.J., Choi, J., Baek, K., O'Loughlin, E.J., 2014. The transport behavior of As, Cu, Pb, and Zn during electrokinetic remediation of a contaminated soil using electrolyte conditioning. Chemosphere 117, 79-86.

Yang, Q., Zhao, H., Zhao, N., Ni, J., Gu, X., 2016. Enhanced phosphorus flux from overlying water to sediment in a bioelectrochemical system. Bioresour. Technol. 216, 182.

Yao, Z., Li, J., Xie, H., Yu, C., 2012. Review on Remediation Technologies of Soil Contaminated by Heavy Metals. Procedia Environ. Sci 16, 722-729.

Yuan, Y., Zhou, S., Zhuang, L., 2010. A new approach to in situ sediment remediation based on air-cathode microbial fuel cells. J. Soils Sediments. 10, 1427-1433.

Zabihallahpoor, A., Rahimnejad, M., Talebnia, F., 2015. Sediment microbial fuel cells as a new source of renewable and sustainable energy: present status and future prospects. RSC Adv. 5, 94171-94183.

Zukowska, J., Biziuk, M., 2008. Methodological evaluation of method for dietary heavy metal intake. J. Food Sci. 73, R21-29.

Chapter 2 : General Materials and Methods

2.1. Soil Microbial Fuel Cells

2.1.1. Paddy soils collection and preparation

All of the soil used in this thesis to construct the sMFCs were collected from various contaminated paddy soil in south China. The soil was consider contaminated if the trace metal concentration exceed the permissible limited outline in the Chinese Standard (GB15618-1995) for agricultural soils. The soil used in chapters 3, 4 and 6 were from a paddy field in Qiyang Hunan, Southern China (GPS N26.760 E111.86). The soil used in chapter 5 was collected from a paddy field in Shangyu, Zhejiang, China (N29.159 E119.957) and that used in chapter 7 and 8 were sample from a paddy field in Shaoguan, Guandong Province (N25.638. E113.3841). The soils were sampled from 0–20 cm below the soil–water interface. All of the soils were air dried and stored at room temperature until time to use. Prior to being used the soil samples were ground and sieved to less than 2 mm.

2.1.2. Anode and cathode preparation

Carbon felt (Sanye Carbon Co., Ltd, Beijing, China) interwoven with titanium wire was used as the anode and cathode of all the sMFC. Before use the cathode and anode were heat-treated in a muffle furnace at 450 °C for 30 min to remove the impurities (Feng et al., 2010). Carbon felts were used as electrodes because they are sponge-like conductive material with many holes and holes increase the surface area on the cathode and anode, hence providing more oxygen reduction reaction sites on cathode, or habitats for anode-respiring bacteria.

2.1.3. Soil Microbial Fuel Cell assembly

The sMFCs used in chapters 3-6 were built in 1000 ml polyethylene terephthalate container (10 cm diameter × 15 cm depth) as previously described by Wang et al. (2016) with minor modifications. In general, the anode of each sMFC was buried in the anaerobic soil and

the cathode was placed in the overlaying water (Fig. 2.1). Deionized water was used to flood all of the sMFC (18.2 MΩ cm, Millipore Corp., Bedford, USA). For details of the size, shape and exact location of each electrode please see the method section of chapters 3-6. All the sMFC reactors used in this this thesis were equipped with soil porewater samplers at various location (see chapters 3-6 materials and methods for exact location). All of the treatment sMFC replicates were connected with an external resistor (close circuit) and no resistor was applied to the control sMFC replicates (open circuit) (see chapters 3-6 materials and methods section for external resister details).

2.1.4. Electrochemistry analysis

The voltage output of all of the sMFCs were recorded with a datalogger unless otherwise stated. The current and power density were calculated according to Ohm's law (equation 1):

$$I=V/R \quad (1)$$

Where I is the current (A), V the voltage between the cathode and the anode (V) and R the resistance (Ω). The current (A/m^2) and power density (W/m^2) were obtained by dividing both the current and power by the total anode geometric area (m^2). The sMFCs used in chapters 3-6 were incubated in a dark incubator (Yisheng, DHP-9902, Shanghai China) and maintained at 30 ºC. Additional deionized water was added daily to each sMFC to compensate for water lost due to evaporation.

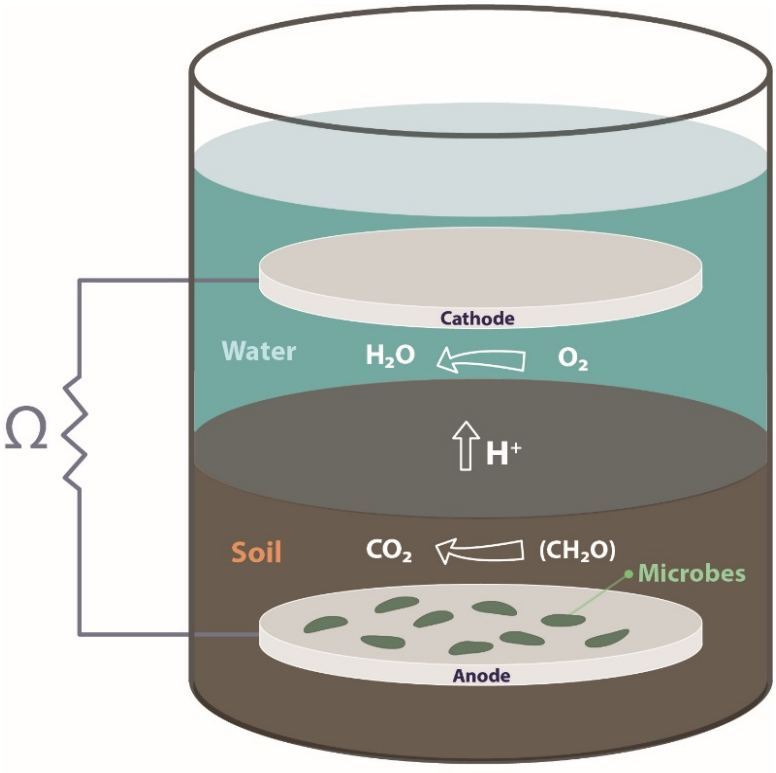

Figure 2.1 Schematic of the sMFC reactor.

2.2. Soil Microbial Fuel Cells with Rice Plants

The sMFC with rice plants configuration and electrode size are detailed in chapters 7-8. Each sMFC was constructed in a cylindrical polyvinylchloride pots (16 cm diameter × 30 cm depth) that were filled with 3 kg of soil amended with basal fertilizers NH_4NO_3 (120 mg N kg^{-1} soil) and K_2HPO_4 (30 mg Pkg^{-1} soil and 75.7 mg K kg^{-1} soil). Each sMFC was equipped with three anodes and 1 cathode. The anodes were cut into two halves and were connected with a titanium wire. The two half anodes were placed 1 cm a part to leave space for the rice roots to grow and their exact location in the sMFCs are detailed in chapters 7-8. All the sMFC reactors were equipped with soil porewater samplers at various location (see chapters 7-8 materials and methods section for exact the locations). The cathode was vertically installed in the overlaying water in aerobic conditions. Rice seedlings of *Oryza sativa* (Yliangyou, YLY) were germinated on cleaned moist perlite and three uniform rice seedlings were planted in each sMFC. The sMFC were first incubated in a plant cultivating room and then transferred to a

greenhouse at ambient temperature and natural photoperiod. Water loss via evaporation and plant respiration during operation was routinely replenished with deionized water to maintain a constant water level of ca. 6 cm. The filamentous algae and duckweed were removed from the overlaying water layer regularly. We removed the duckweed and filamentous algae to limit the effects of external factors, since the duckweed may change the overlying water chemistry and compete with the rice plants for nutrients. A data logger and Digital Multimeters (UNI-T UT71E) were used to record the voltage between the anode and cathode. Current and power densities were calculated using the same method described in the sMFC section.

2.3. Chemical Analysis

Five milliliters (5ml) of porewater sampled under negative pressure using syringe. Prior to sampling, 100 µl of 2M hydrochloric acid was added in each syringe to acidify the sample and prevent iron precipitation.

Trace metals and total Fe concentrations in soil porewater were determined by inductively coupled plasma mass spectrometry (ICPMS, NexlON^{TM} 350x, Pekin Elmer, USA) and atomic absorption spectrometry (AAS, PinAAcle™ 900,PerkinElmer, USA). Arsenic species and Fe speciation in soil porewater were analyzed by ion chromatography with inductively coupled plasma mass spectrometry detection (IC-ICPMS) as describe by (Suzuki et al., 2009) and the colorimetric reagent 1, 10-phenanthroline (Wang et al., 2016), respectively.

The soil samples collected from both the sMFC and the control were homogenized and the content of total organic carbon (TOC) and loss on ignition (LOI) carbon were determined. LOI carbon refers to the organic matter estimated based on the weight loss on ignition method (Santisteban et al., 2004). TOC and DOC (porewater) content were determined with a TOC analyzer (Shimadzu TOC-VCPH, Japan). LOI carbon content was determined by heating 10 g of soil at 550 ºC for 4hrs in a muffle furnace. Prior to heating at 550 ºC samples were dried at 105 ºC for 12 h and weighed. The decrease in mass after ignition of soil at 550 ºC from mass

obtained at 105 ºC was assumed as LOI carbon (Santisteban et al., 2004). LOI was calculated according to the following equation 2:

$$LOI\ (\%) = ((D105 - D550)/D105) * 100 \quad (2)$$

where D105 is the dry mass of the sample heated 105 ºC for 12 hours and D550 is the dry mass of the sample after 4 hours of incubation at 550 ºC. Samples were allowed to cool to room temperature in a desiccator before determining D550 (Jia-Ping et al. 2013; Touch et al. 2017).

Soil pH and redox potentials (*E*h) were measured using a HACH 440d Multi-Meter (Hach, USA) and a combined Pt and Ag/AgCl electrode, respectively. The *E*h of the soil was allowed to stabilize for 1 h before recording. The pH was determined from a soil slurry made by mixing dry soil with deionized water at a ratio of 1:2.5.

The fluorescence excitation emission matrix (EEM) analysis was conducted by using a fluorescence spectrophotometer (Cary Eclipse Fluorescence Spectrophotometer, Agilent Technologies, USA). The EEM analysis was used to characterize the DOC composition in the soil porewater. All the soil porewater samples were filtered and then adjusted to pH 7.0 with NaOH solution before fluorescence EEM spectra analysis (Spencer et al., 2007; Xiao et al., 2016). The fluorescence EEM were scanned at excitation and emission wavelength ranges set from 200 to 475nm and 300-600nm, respectively. Excitation and emission scanning intervals were set at 5 nm and 2 nm, respectively. Scan speed was set at 1200 nm min^{-1}, and excitation and emission slit widths were fixed at 10 nm. Photomultiplier detector voltage was fixed at 640 V.

2.4. Plant Samples Analysis

At the maturation (day 120), the rice plants were harvested and washed with ultrapure water. The washed plants were placed in an oven at 105°C for 2 h and then dried at 60 °C for 72 h. Prior to drying, the plant materials were divided into grains, husks, leaves, stems and roots. After drying, the samples were ground to powder and 0.5 g of each rice plant sample was

weighed and taken in 50 ml polypropylene digestion tube to which 10 ml 1:1 ratio of HNO_3 and H_2O_2 were added. The samples were then subjected to microwave digestion using a MARS 6™ Microwave Digestion System (CEM, USA). The digested samples were filtered through a 0.45 μm pore size filter and diluted with ultrapure water. The total As was then measured using the ICP-MS. Duplicate spike standards sample were measured after every ten sample as a quality control check.

2.5. Microbial Community Analysis

At the end of all the incubation samples were collected from all the sMFCs for microbial community analysis. Please see the materials and methods section of chapters 3-8 for details in regards to the sampling plan, DNA extraction procedure and treatments before amplification. The V4-V5 or the V3-V5 regions of the bacterial and V4-V5 region of the archaeal 16S rRNA genes were amplified using the primers listed in Table 2.1. The exact primer used in each experiment are detailed in the method section of chapters 3-8. Illumina sequencing adapters were also added to the ends of the 16S rRNA amplicons to generate indexed libraries ready for downstream NGS sequencing on Illumina Miseq. The PCR products were validated using an Agilent 2100 Bioanalyzer (Agilent Technologies, Palo Alto, CA, USA). The concentrations were quantified using a Qubit and real-time PCR (Applied Biosystems, Carlsbad, CA, USA). The purified amplicons were sequenced on an Illumina Miseq sequencing platform (Illumina Inc., San Diego,CA, USA) at GENEWIZ, Inc. (Suzhou, China).

Table 2.1 Details of primer pairs used in this study.

Primer name	Primer sequences	Gene target	Reference
347F 802R	5'-CCTACGGRRBGCASCAGKVRVGAAT-3' 5'-GGACTACNVGGGTWTCTAATCC-3'	16S rRNA (V4-V5)	(Li et al., 2017)
515 F 907 R	5'-GTGCCAGCMGCCGCGG-3' 5'-CCGTCAATTCMTTTRAGTTT-3'	16S rRNA (V3-V5)	(Sun et al. 2016; Xiao et al. 2016)
Arch519F Arch915R	5'-CAGCCGCCGCGGTAA-3' 5'-GTGCTCCCCCGC CAATTCCT-3'	16S rRNA (V4-V5)	(Yang et al., 2016)
amLt-42-F amLt-376-R	5'-TCGCGTAATACGCTGGAGAT-3' 5'-ACTTTCTCGCCGTCTTCCTT-3'	Arsenate reductase (*arsC*)	(Sun et al., 2004)
AroAdeg2F AroAdeg2R	5'-GTCGGYTGYGGMTAYCAYGYYTA-3' 5'-YTCDGARTTGTAGGCYGGBCG-3'	Arsenite oxidase (*aioA*)	(Inskeep et al., 2007)
arsMF1 arsMR2	5'-TCYCTCGGCTGCGGCAAYCCVAC-3' 5'-CGWCCGCCWGGCTTWAGYACCCG-3'	Arsenite Methylation (*arsM*)	(Wang et al., 2017)

Sequences were processed and analyzed using Quantitative Insights Into Microbial Ecology (QIIME 1.8.0) toolkit for 16S rRNA data analysis (Caporaso et al., 2010). The forward and reverse reads were joined and assigned to samples based on barcode and truncated by cutting off the barcode and primer sequence. Quality filtering on joined sequences was performed and sequence which did not fulfill the following criteria were discarded: sequence

length <200bp, no ambiguous bases, mean quality score >=0.2 (Range 0-1). Then the sequences were compared with the reference database (RDP Gold database) (Wang et al., 2007) using UCHIME algorithm (Edgar et al., 2011) to detect and removed chimeric sequences (Li et al., 2017b). The average length of the remaining sequences after the removal of the chimeric sequences was 450bp. The filtered sequences were used in the final analysis. Sequences were grouped into operational taxonomic units (OTUs) using the clustering program VSEARCH （1.9.6） against the Silva 119 database pre-clustered at 97% sequence identity. The Ribosomal Database Project (RDP) classifier was used to assign taxonomic category to all OTUs at confidence threshold of 0.8 (Lin et al., 2017). The RDP classifier uses the Silva_128 16S rRNA database (http://www.arb-silva.de/), which has taxonomic categories predicted down to the genus level. Sequences were rarefied prior to downstream analyses.

The alpha diversity indices (observed OTUs, Shannon diversity index and Chao 1 richness estimator) were calculated in QIIME1.8.0 (Vasileiadis et al., 2012). Beta diversity was calculated using weighted principal coordinate analysis (PCoA).

2.6. Quantitative PCR (qPCR) of *arsC*, *aioA*, and *arsM* genes

The abundance of the *arsC*, *aioA*, and *arsM* genes in the rice rhizosphere at the ending of the maturation stage (day 120) was determined by quantitative PCR (qPCR) performed on a real-time qPCR Instrument (LightCycler 480II, Switzerland). Primer pairs of amLt-42-F / amLt-376-R (Sun et al. 2004), AroAdeg2F / AroAdeg2R (Inskeep et al. 2007) and arsMF1 / arsMR2 (Yang et al. 2018) were used to amplify and quantify *arsC*, *aioA*, and the *arsM* genes, respectively. The As transformation genes were quantified according to a previously reported method (Wang et al. 2017) with some modifications. Specifically, in each individual PCR, 2 μL of DNA, 10 μL of 2 × SYBR Premix Ex Taq™ II (Takara, Japan), 0.4 μL of each primer, 0.2 μL of 0.1% BSA (Takara, Japan) was added. The PCR conditions for the *arsC* gene were 95 °C denaturation for 5 min, followed by 40 cycles of 95 °C for 30 s, 56 °C for 35 s, and 72 °C

for 1 min. For the *aioA* gene the conditions were 95 °C denaturation for 5 min, followed by 45 cycles at 95 °C for 30 s, 60 °C for 30 s, 72 °C for 1 min and then 72 °C for 10 min. The PCR conditions used for *arsM* gene was 95 °C denaturation for 5 min, followed by 35 cycles at 95 °C for 30 s, 64 °C for 35 s, 72 °C for 1 min and then 72 °C for 10 min. Each sample was quantified in triplicate as a quality control measure to ensure the correct amplification. A standard curve was constructed using standard plasmids containing known copy numbers of the *arsC*, *aioA* and *arsM* genes. The reaction efficiencies were all between 90% and 110%. The quantification of the As transformation were determined from the standard curves and are presented as the average copy number/μL DNA.

2.7. Statistical Analysis

One-way analysis of variance (ANOVA) followed by the Student–Newman–Keuls test were used to determine differences between samples in SPSS Statistical software package (IBM, SPSS Statistics 22). A $p < 0.05$ was considered to be statistically significant. ANOSIM was used to determine if the differences among samples was statistically significant using Bray–Curtis measure of similarity (QIIME), where the R-value ranges between 0 (complete similarity) to 1 (complete separation) (Hari et al., 2017; Li et al., 2017).

2.8. References

Caporaso, J.G., Kuczynski, J., Stombaugh, J., Bittinger, K., Bushman, F.D., Costello, E.K., Fierer, N., Pena, A.G., Goodrich, J.K., Gordon, J.I., 2010. QIIME allows analysis of high-throughput community sequencing data. Nature Methods 7, 335-336.

Edgar, R.C., Haas, B.J., Clemente, J.C., Quince, C., Knight, R., 2011. UCHIME improves sensitivity and speed of chimera detection. Bioinformatics 27, 2194-2200.

Feng Y, Yang Q, Wang X, Logan BE. Treatment of carbon fiber brush anodes for improving power generation in air–cathode microbial fuel cells. J. Power Sources 2010;195:1841-4.

Hari AR, Venkidusamy K, Katuri KP, Bagchi S, Saikaly PE. Temporal microbial community dynamics in microbial electrolysis cells–influence of acetate and propionate concentration. Front. Microbiol. 2017;8:1371.

Inskeep, W.P., Macur, R.E., Hamamura, N., Warelow, T.P., Ward, S.A., Santini, J.M., 2007. Detection, diversity and expression of aerobic bacterial arsenite oxidase genes. Environ. Microbiol. 9, 934-943.

Jia P W, Xiu J W, Zhang J., 2013. Evaluating loss-on-ignition method for determinations of soil organic and inorganic carbon in arid soils of northwestern china. Pedosphere 23:593-599

Li H, Tian Y, Qu Y, Qiu Y, Liu J, Feng Y, 2017. A Pilot-scale Benthic Microbial Electrochemical System (BMES) for Enhanced Organic Removal in Sediment Restoration. Sci. Rep.7:39802.

Li Y, Hu X, Yang S, Zhou J, Zhang T, Qi L, 2017. Comparative Analysis of the Gut Microbiota Composition between Captive and Wild Forest Musk Deer. Front. Microbiol. 8:1705.

Santisteban, J.I., Mediavilla, R., Lopezpamo, E., Dabrio, C.J., Zapata, M.B.R., Garcia, M.J.G., Castano, S.C., Martinezalfaro, P.E., 2004. Loss on ignition: a qualitative or quantitative method for organic matter and carbonate mineral content in sediments? J. Paleolimnol. 32, 287-299.

Spencer, R.G.M., Bolton, L., Baker, A., 2007. Freeze/thaw and pH effects on freshwater dissolved organic matter fluorescence and absorbance properties from a number of UK locations. Water Res. 41, 2941.

Sun W, Xiao E, Dong Y, Tang S, Krumins V, Ning Z, Sun M, Zhao Y, Wu S, Xiao T (2016) Profiling microbial community in a watershed heavily contaminated by an active antimony (Sb) mine in Southwest China. Sci. Total. Environ. 550:297-308

Suzuki, Y., Shimoda, Y., Endo, Y., Hata, A., Yamanaka, K., Endo, G., 2009. Rapid and effective speciation analysis of arsenic compounds in human urine using anion-exchange columns in HPLC-ICP-MS. J. Occup. Health 51, 380-385.

Touch N, Hibino T, Takata H, Yamaji S 2017. Loss on ignition-based indices for evaluating organic matter characteristics of littoral sediments. Pedosphere 27:978-984

Vasileiadis S, Coppolecchia D, Puglisi E, Balloi A, Mapelli F, Hamon RE, 2012. Response of ammonia oxidizing bacteria and archaea to acute zinc stress and different moisture regimes in soil. Microb. Ecol. 64:1028-37.

Wang, N., Xue, X., Juhasz, A.L., Chang, Z., Li, H., 2017. Biochar increases arsenic release from an anaerobic paddy soil due to enhanced microbial reduction of iron and arsenic. Environ. Pollut. 220, 514-522.

Wang, Q., Garrity, G.M., Tiedje, J.M., Cole, J.R., 2007. Naïve Bayesian classifier for rapid assignment of rRNA sequences into the new bacterial taxonomy. Appl. Environ. Microbiol. 73, 5261-5267.

Wang, Y., Chen, Z., Liu, P., Sun, G., Ding, L., Zhu, Y., 2016. Arsenic modulates the composition of anode-respiring bacterial community during dry-wet cycles in paddy soils. J. Soil Sediment. 16, 1745-1753.

Xiao E, Krumins V, Xiao T, Dong Y, Song T, Ning Z, Huang Z, Sun W., 2016. Depth-resolved microbial community analyses in two contrasting soil cores contaminated by antimony and arsenic. Environ. Pollut. 221:244

Xiao, K., Sun, J.Y., Shen, Y.X., Liang, S., Liang, P., Wang, X.M., Huang, X., 2016. Fluorescence properties of dissolved organic matter as a function of hydrophobicity and molecular weight: case studies from two membrane bioreactors and an oxidation ditch. RSC Adv. 6, 24050-24059.

Yang Y, Dai Y, Wu Z, Xie S, Liu Y., 2016. Temporal and spatial dynamics of archaeal communities in two freshwater lakes at different trophic status. Front. Microbiol. 7:451.

Chapter 3 : The effect of the soil microbial fuel cell on paddy soil microbial community profile

3.1. Abstract

Soil Microbial Fuel Cells (sMFC) are devices that can generate electricity by using the flooded soil's anode respiring microbial consortium. When the sMFC starts to work, the microbial community in the anode vicinity rapidly changes. This shift in the microbial community results in many dead cells that may release their DNA (relic DNA) and obscure culture independent estimates of microbial community composition. Although relic DNA is expected to increase in sMFC, the effect of relic DNA has not been investigated in the soil sMFC system. In this study the effect of the sMFC on the soil microbial community composition within the soil profile and the influence of relic DNA were investigated. Microbial community analysis revealed that the sMFC deployment significantly influenced the community composition within the soil profile. The phylum *Proteobacteria* (34.4% vs 23.6%) and the class *Deltaproteobacteria* (16.8% vs 5.9%) significantly increased in the sMFC compared to the control, while the phylum *Firmicutes* (24.0% vs 28.7%) and the class *Sphingobacteria* (5.3% vs 7.0%) were more abundant in the control. Furthermore, the archaeal phyla *Euryarchaeota* (40.7% vs 52.3%) and *Bathyarchaeota* (10.1% vs 17.3%) were significantly lower in the sMFCs, whereas the phylum *Woesearchaeota (DHVEG6)* (24.4% vs 19.4%) was slightly enhanced. Moreover, the results showed that relic DNA can affect the relative abundance of *Geobacter* and *Candidatus Methanoperedens*, however, it has no significant effects on the microbial community structure. These results indicate that sMFC can influence the soil microbial community profile, nevertheless the relic DNA generated has a minimum effect on the culture independent estimates of microbial community composition.

3.2. Introduction

Soil Microbial fuel cells (sMFC) are a type of bioelectrical system that can facilitate direct biotransformation of organic matter (OM) to electrical energy. In sMFC, the microbial community catalyzes the breakdown of OM and extracellularly transfer electrons to the anode to produce electricity (Huang et al., 2011). Recently, sMFC have been introduced in paddy fields for energy production and as a bioremediation tool (Chen et al., 2012; Gustave et al., 2018a; Kaku et al., 2008; Schamphelaire et al., 2008). During rice-cropping season, paddy fields are flooded and soil redox potential falls rapidly and becomes reduced. Under these reducing environments the natural microbial consortium in paddy soils, may respire the sMFC anode in the same manner as what occurs with iron and manganese oxides (Downie et al., 2018; Gustave et al., 2018a; Logan and Regan, 2006).

The distribution of anode respiring bacteria (ARB) in paddy soil has already been studied in sMFC. In previous studies, metal reducing microbes were usually enriched at the anode (Wang et al., 2015; Yuan et al., 2018). By contrast, other functional microbial groups such as methanogens were decreased during this enrichment process (Jung and Regan, 2011; Kouzuma et al., 2014). Hence, these changes in the microbial community may result in an increase in soil extracellular DNA (relic DNA). After soil microbes die, their genetic material may leak into the surroundings and persist in soil from days to years depending on the environmental conditions (Dellanno and Corinaldesi, 2004; Morrissey et al., 2015; Pietramellara et al., 2009).

The relic DNA that remains in the soil can be problematic and has the potential to create bias in culture independent estimates of microbial diversity, because the current high-throughput sequencing techniques does not differentiate between intact and lysed cells (Carini et al., 2016; Kapoor et al., 2015; Lennon et al., 2018). Carini et al. (2016) and Lennon et al. (2018) used propidium monoazide (PMA) and DNase, respectively, to remove relic DNA from

soil samples and revealed that relic DNA represents a significant portion of soil DNA. Carini et al. (2016) estimated that relic DNA comprises about 40% of the prokaryotic and fungal soil DNA. Similarly, Lennon et al. (2018) estimated that relic DNA was normally distributed and contributed anywhere between 0 to 83% (mean ± standard deviation [SD], 33± 21.8) of the total soil DNA by quantitative PCR (qPCR). However, whether or not this relic DNA can obscure and result in misrepresentation of the soil microbial community structure remains controversial (Carini et al., 2016; Lennon et al., 2018).

Moreover, the presence of relic DNA in the sMFC biofilm has received limited attention. Recently in Fed-batch microbial fuel cells (MFC) (Dessì et al., 2018) and microbial electrolysis cells (MEC) (Cerrillo et al., 2017), complementary DNA (cDNA) was used to distinguish between dead and metabolically active bacterial cells. The results showed that higher bacterial diversity was observed from the 16S rRNA gene based methods compared to cDNA based high throughput sequencing and high degree of variation in community composition between the two methods were observed. This suggests that relic DNA could hamper the true structure of the anode bacterial community and may result in the misrepresentation of the composition. Although, the bacterial community of sMFC anode has been extensively studied, to date, no studies have attempted to remove the influence of relic DNA on bacterial community estimates of the sMFC.

Therefore, the aims of this study were to evaluate the effect of the sMFC on the soil microbial community composition and the influence of relic DNA within the soil profile. In this regard, samples were taken at various locations away from the sMFC anode and a subset of the samples were treated with PMA to remove the relic DNA. Both sets of samples were then used for bacterial and archaeal community analysis and comparisons were made between PMA treated and non-PMA samples.

3.3. Materials and Methods

3.3.1. Paddy Soil Sample

Paddy soil was sampled from a field located in Qiyang Hunan, Southern China (GPS N26.760 E111.86). The main physio-chemical properties of four replicate soil samples were determined and are presented in Table S1. We chose to used four replicated based on our preliminary experiments and power analysis results.

3.3.2. Soil Microbial Fuel Cell assembly

Eight sMFC were assembled as previously described in chapter 2 with minor modifications. Four replicate sMFC were assigned as treatment and four replicates were used as control. The treatment replicates were connected with 500 Ω external resistor (close circuit) and no resistor was applied to the control replicates (open circuit). The anode, made of carbon felts (geometric surface area of 50.2 cm^2), was buried in the soil 1 cm above the bottom of reactor containing 1kg (dry weight) of soil. A carbon felt with the same dimension as the anode was used as the cathode electrode. After installing the cathode the remaining space in the reactor was filled with deionized water to simulate natural paddy soil conditions. A data logger (USB-7660B, ZTIC, China) was used to record the voltage between the anode and cathode.

3.3.3. Chemical Analysis

Soil porewater was sampled through 3 valve ports located in the anode vicinity, 2 cm above the anode (middle layer) and 1 cm below the soil-water interface (top layer) at the end of the incubation period on day 60. Total organic carbon (TOC) was determined from 2 g of soil. The soil TOC was measured from the top, middle and anode vicinity of each sMFC at the end of the incubation period. The trace metals and the TOC concentrations were determined as described in chapter 2.

3.3.4. Microbial Community Analysis

Soil samples were collected from the anode vicinity, 2 cm above the anode (middle layer) and 1 cm below the soil-water interface (top layer) at the end of the incubation period on day 60. The anode vicinity consists of loosely attached soil and biofilm from the anode. A sterile razor was used to scrap the loosely attached soil and biofilm from the anode. PMA and non-PMA treatment of soil were carried out following the method used by Carini et al. (2016) with minor modification. In an earlier study by Carini et al. (2016) 650 W halogen lamp was used to activate the PMA, however in our study we used a PMA-Lite™ LED photolysis device. Moreover, Carini et al. (2016) subjected their samples to four 30 s/30 s light/dark cycles for PMA activation, in our study we subjected the samples to 15 minutes of light (LED output wavelength 465-475 nm) as recommended by the manufacturer of our PMA-Lite™ LED photolysis device. Briefly, 0.30g of soil in duplicates from each sampling location was re-suspended in 3ml of sterile PBS (pH 7.4) solution in transparent centrifuge tubes. In total, there were 48 samples, 24 from the control replicates and 24 from the treatment replicates. Half of the control and half of treatment replicates were treated with PMA to a concentration of 40µM in the dark (PMA) and the other samples were not treated with PMA (non-PMA). A PMA concentration of 40µM was used because previous studies have shown that this concentration range was sufficient to remove relic from a variety of soil types (Carini et al., 2016; Nocker et al., 2006; Nocker et al., 2007). All samples were vortexed in the dark for 4 minutes. At the end of the vortexing cycle, 1.5 ml of each sample was transferred to a sterile 2 ml tube. Then, all of the samples were loaded on to a PMA-Lite™ LED photolysis device and were subjected to 15 minutes of light for PMA activation. Immediately following the light exposure, DNA was extracted from 960 µl of each sample using Powersoil DNA isolation Kit (MoBio Laboratories Inc., Carlsbad, CA, USA) according to the manufacturer's instructions. The extracted DNA were quantified using Qubit (Table S2) The V4-V5 region of the bacterial 16S rRNA genes

were amplified using the forward primers 347F (5'-CCTACGGRRBGCASCAGKVRVGAAT-3') and reverse primers 802R (5'-GGACTACNVGGGTWTCTAATCC-3') (Li et al., 2017b). The archaeal primers Arch519F (5′-CAGCCGCCGCGGTAA-3′)/Arch915R (5′-GTGCTCCCCCGC CAATTCCT-3′) (Yang et al., 2016) were used for the amplification of 16S rRNA genes in the sMFC anode archaeal community. The sequencing, community classification and statistical analysis were done as described in chapter 2.

3.3.5. Nucleotide sequence accession numbers

The dataset of 16S rRNA gene sequences was deposited in NCBI's GeneBank with accession numbers MG814044 - MG815131 and MF988366 - MF988678.

3.4. Results and Discussion

3.4.1. Voltage generation in MFCs

The voltage production over time was recorded from the sMFC with an external loading of 500 Ω. The sMFC voltage increased to 565 mV after 13 days (Fig. 3.1a and Fig. S 3.1) and then gradually decreased to 321 mV on day 15. Another peak in the MFCs voltage (445 mV) was observed on day 19 and then a steady decrease until day 60. The voltage in the control gradually increased to 887 mV until day 60. The rapid increase in the sMFC voltage indicated the high substrate content of the soil facilitated the enrichment of electroactive bacteria on the anode (Hong et al., 2009; Hong et al., 2010). The maximum power density was 123 ±2.2 mW/m^2 and the internal resistance was 834 ±19.5 Ω (Fig. 3.1b). The high power density obtained here was comparable to the values reported in the previous studies (Li et al., 2017a; Türker and Yakar, 2017; Xun et al., 2016).

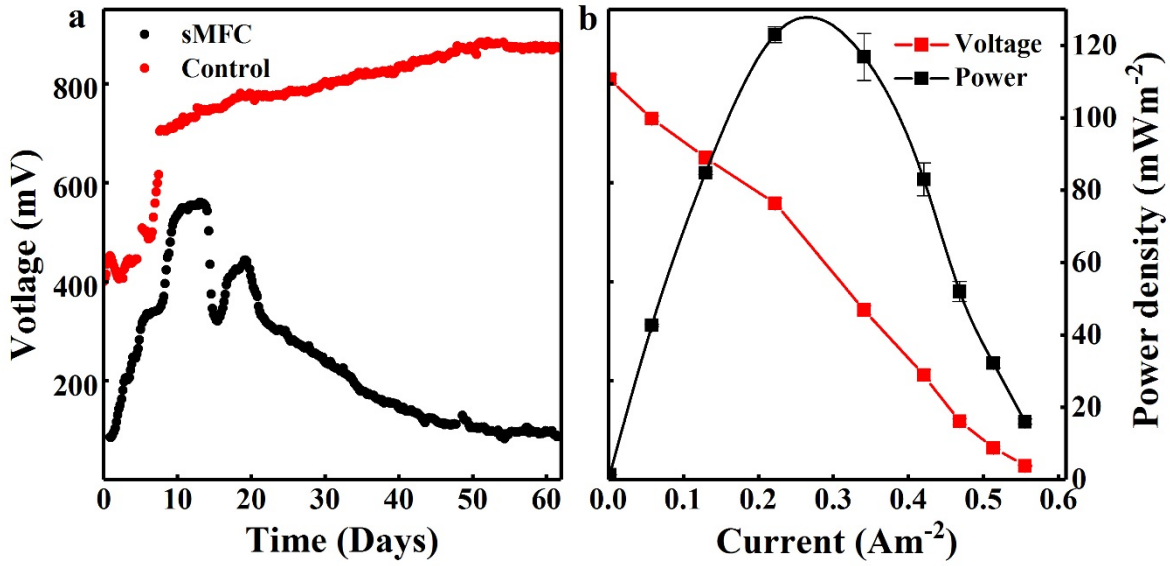

Figure 3.1 The mean voltage variation of four sMFC as a function of time (a). The polarization curve of the sMFC (b). The values represent the mean ±standard error of four replicate samples.

3.4.2. Influences of the sMFC and relic DNA on microbial community diversity

The microbial community of the sMFC from the anode vicinity and the bulk soil were analyzed by next generation Illumina Miseq sequencing. As shown in Table S 3.3 and S 3.4, the Goods coverages (99.2-99.8%) confirmed that most microbes were covered in this sequencing analysis. The number of bacterial OTUs around the sMFC anode vicinity (1216 ±15 - 1222 ±27) were less than that of the bulk soil regardless of treatment (1359 ±25 - 1532 ±20) (Table S 3.3). Moreover, the OTU numbers in the archaeal community were lower in the control anode vicinity (297 ±8 - 303 ±5) as compared to the community in sMFC anode vicinity (371 ±3 - 371 ±11) (Table S 3.4). Similar to the bacterial OTUs distribution, the ACE, Chao1 and Shannon indices were lower in the sMFC anode vicinity as compared to the control and bulk soil samples (Table S 3.4). The ACE, Chao1 and Shannon indices ranged from 1428.5 ±24.8 -1432.6 ±21.2, 1434.3 ±27.4 - 1444.3 ±21.6 and 6.7 ±0.02 - 6.94 ±0.09 respectively, for the MFCs. While the ACE, Chao1 and Shannon indices ranged from 1499.9 ±22.3 - 1736.4 ± 28.5, 1520.3 ± 23.8 - 1761.0 ±25.2 and 8.0 ±0.04 - 8.6 ±0.03 respectively, for the control and

bulk soil samples (Table S 3.3). These results indicated that the sMFC can significantly enhance specific groups in its anode vicinity while suppressing other functional groups. Previous studies have shown that the sMFC can significantly enrich the electrogenic bacterial community and suppress other functional microbial groups (Lu et al., 2014; Song et al., 2015; Yu et al., 2017). For the archaeal community, the ACE (400.6 ±2.5 - 401.7 ±10.5 vs 338.2 ±5.4 - 353.8 ±12.2), Chao1 (402.5 ±3.1 - 404.1 ±8.6 vs 338.2 ±7.5 - 358.8 ±18.8) and Shannon indices (5.8 ±0.1 - 6.0 ±0.07 vs 5.0 ±0.10 - 5.1 ±0.06) were significantly higher in the sMFC anode vicinity compared to that of the control (Table S 3.4).

However, with regards to microbial community richness and diversity, the ACE, Chao1 and Shannon indices showed no significant distinction between the PMA and non-PMA treated samples. Therefore, the relic DNA in our samples had minimal influence on the microbial community richness and diversity estimates. A possible explanation for this was that relic DNA from dead cells and that of bacterial community composition were at a state of equilibrium (Lennon et al., 2018). Lennon et al. (2018) found that relic DNA will have minimal effect on the microbial diversity, even if abandoned, when DNA from intact cells and extracellular DNA are at an equilibrium state. In our study we collected samples for microbial community analysis after day 60 when the voltage was stable (Fig.3.1a). This means that the microbial community may have also reached a state of equilibrium and was stable. Previous studies have shown that microbial community of the sMFC, regardless of carbon source will converge to a similar community, which was comprised of mostly electrogens, after continuous operation (Kouzuma et al., 2013a; Yates et al., 2012). Therefore, we hypothesize that in our sMFC system the relic DNA represented a similar microbial community composition to that of the intact cells. However, further studies are needed to confirm this hypothesis, since in this study the temporal variation of the microbial community was not examined.

3.4.3. The effect of the MFCs and relic DNA on microbial community structure

Principal Coordinate Analysis (PCoA) was used to demonstrate a visual representation influence of the sMFC and relic DNA on the microbial community (Fig. 3.2a and 3.2b). PCoA-PC1 vs PC2 analysis explaining 73.42% of the variance indicated three distinct bacterial groups among the samples (Fig. 3.2a). The sMFC anode vicinity formed one group, all the middle layer samples (both control and sMFC) and that of the control anode vicinity formed another. Whereas, the bacterial community in samples from the top layers clustered together to form a third group regardless of the treatment. These results agree with the study of Lu et al. (2014) on the distribution of microbial community in sMFC. The microbial community near the anode, although from the same paddy soil origin and microbial consortia, differed greatly from that of the bulk sediment and the anode community of the control. PCoA analysis was also used to assess the anode vicinity archaeal community structure (Fig.3.2b). The PC1 vs PC2 explaining 67.4% of the variance results showed two separate clusters, the sMFC anode biofilms was separated from the controls anode biofilms.

However, Analysis of Similarity (ANOSIM) revealed that microbial community of the sMFCs and the control significantly differed from one another in all locations although PCoA analysis did not yield this result. The microbial community structure of the top, middle and bottom layer of the sMFC were significantly different from that of the control (p = 0.031, R= 0.48), (p = 0.022, R=0.77) and (p = 0.018, R= 1), respectively. This indicated that the sMFC can significantly alter the microbial community structure in distances of centimeters away from the anode and this could be due to the sMFC ability to change the major driver of soil microbial community such as pH, redox potential and nutrient availability (Nicol et al., 2008; Pettridge and Firestone, 2005; Song et al., 2010; Wu et al., 2017; Zhang et al., 2005; Zhao et al., 2016). Gustave et al. (2018a), reported that the sMFC cathode and anode reactions can shape soil microbial community by altering soil pH, redox potential and organic carbon. Furthermore,

both PCoA and ANOSIM analysis revealed no significant difference between the PMA and non-PMA treated samples for both bacteria and archaeal community.

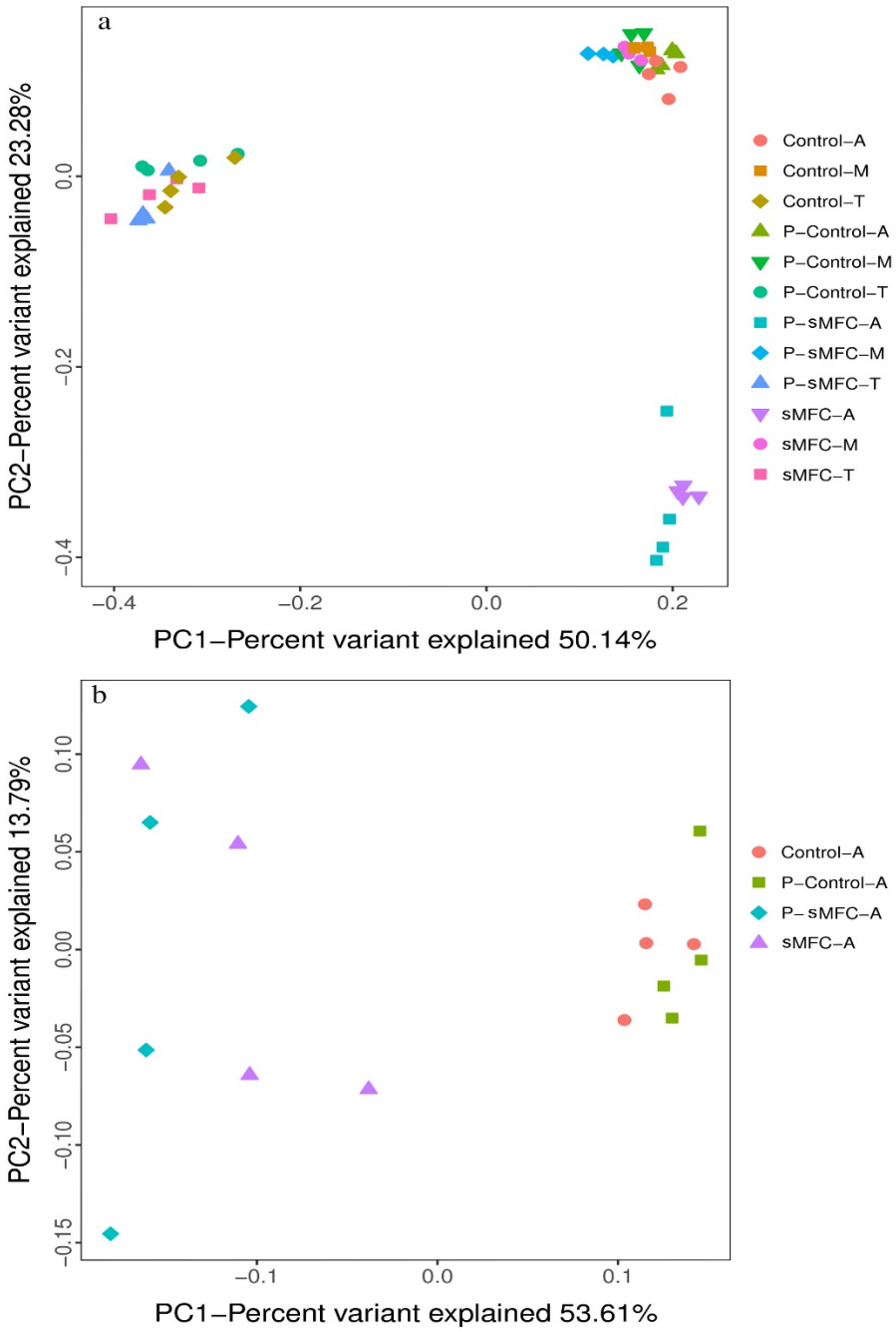

Figure 3.2 Principal Coordinates Analysis (PCoA) of the sMFC and controls bacterial community (a) and the sMFC and controls archaeal community (b) composition based on Bray-Curtis distance. The x- and y-axes are indicated by the first and second coordinates, respectively.

3.4.4. Influences of sMFC on the microbial community composition

Fig. 3.3a-b shows the relative abundance in bacterial community at the phylum and class levels for each sample. At the phylum level, *Proteobacteria* was the most predominant phylum with sequence percentages ranging from 11.30% to 48.50%, which was consistent with previous studies (Gustave et al., 2018a; Lu et al., 2014). *Firmicutes, Bacteroidetes, Ignavibacteriae* and *Acidobacteria* were the subdominant groups, comprising 12.10%-39.20%, 10.10%-20.60%, 3.1%-8.90% and 2.50%-8.50% of the community, respectively. At the class level, *Clostridia* (10.40%-35.50%), *Deltaproteobacteria* (3.90%-27.10%) and *Betaproteobacteria* (0.52%-27.10%) were the dominant groups.

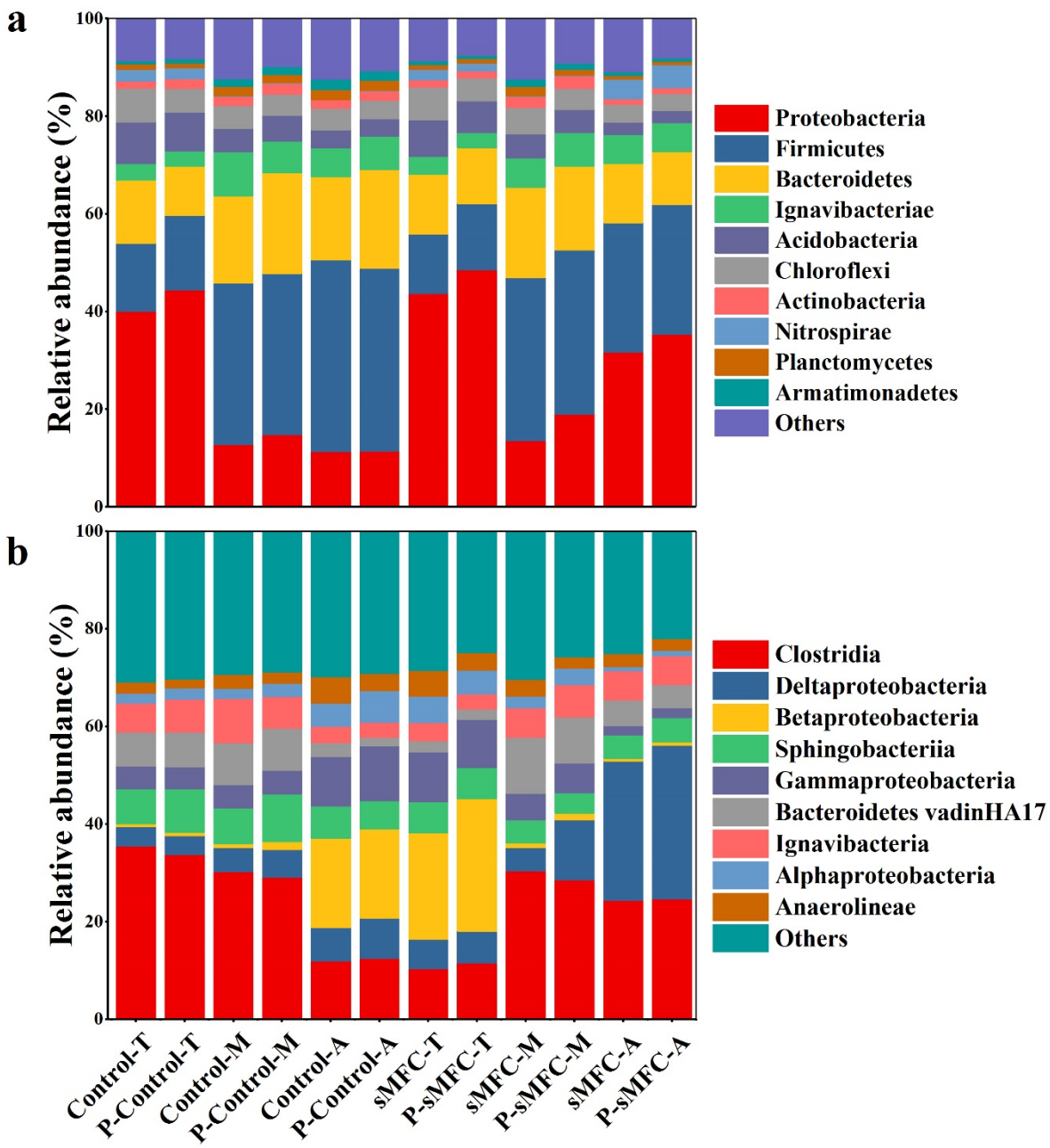

Figure 3.3 Relative abundance of bacterial community composition at phylum (a) and class (b) levels. The relative abundance values represent the mean of four replicates.

The microbial community structure at the phylum and class level manifested variation between the sampling site in the sMFC and the control. In the top layer, the phylum *Proteobacteria* was more abundant in the sMFC, while phyla *Firmicutes* and *Acidobacteria* were relatively less compared to the control in all layers. The increase in *Proteobacteria* in the

top layer may be due to the increase in the iron content (18.0 ±5.1 mg/l vs 10.0 ±5.0 mg/l) in that layer compared to the control (Table S 3.5). The increase in dissolved iron in the top layer of the sMFC has been observed to occur as a result of iron migration due to cathode reactions (Gustave et al., 2018a). This increase of iron can be inferred to be responsible for the increase in *Proteobacteria* since most of the many iron oxidizing and reducing bacteria falls within one or more classes of the phylum *Proteobacteria* (Hedrich et al., 2011; Peng et al., 2016). However more studies in the metabolic pathways at lower levels are needed to confirm the effect of iron on the phylum *Proteobacteria*. Similarly, iron has also been shown to influence microbial community structure of the sMFC (Liu et al., 2017; Liu et al., 2018; Yuan et al., 2018). The supplements of both ferric and ferrous iron were demonstrated to increase the relative abundance of exoelectrogenic bacteria (Liu et al., 2017; Liu et al., 2018). In our study, *Deltaproteobacteria* (6.5% vs 3.9%), *Betaproteobacteria* (27.1% vs 0.63%), *Alphaproteobacteria* (4.9% vs 2.0%) and *Anaerolineae* (5.3% vs 1.8%) (Kouzuma et al., 2013b; Wang et al., 2015; Yuan et al., 2018) were enhanced in the sMFC top layer top layer as known exoelectrogenic classes. Moreover, a reduction in *Firmicutes* (12.1% vs 15.2%) and *Acidobacteria* (6.5% vs 8.5%) was observed in the sMFC top layer compared to the control. Furthermore, at the class level, *Clostridia* (11.5% vs 35.5%) also decreased in the sMFC top layer compared to that of the control. This decrease in *Firmicutes Acidobacteria* and *Clostridia* was probably due to the decrease in organic matter and increase of pH in that layer (Table S5) (Liu et al., 2015; Naether et al., 2012). Previous studies have suggested that marginal increases in soil pH can significantly reduce the relative abundance of *Acidobacteria* (Jones et al., 2009), while others have shown a direct relationship between *Firmicutes, Clostridia* and organic matter (Dunaj et al., 2012; Wang et al., 2015). However, it should be noted that *Clostridia* contains some electrogens such the genera *Thermacola* and *Clostridium sensu stricto 10 (*Koch

and Harnisch, 2016; Rago et al., 2018). Nonetheless, no significant differences were observed between the sMFCs and control for these genera in the top layer.

Moreover, *Proteobacteria* (19.1% vs 14.8%) and *Chloroflexi* (5.5% vs 4.4%) were all significantly enhanced in the middle layer and anode vicinity of the sMFC. Furthermore, at the class level *Bacteroidetes vadinHA17* (9.5% vs 8.6%), *Alphaproteobacteria* (3.5% vs 2.9%) and *Anaerolineae,* were enhanced in the middle layer sMFC compared to the control. These results obtained here are in agreement with previous studies suggesting that the sMFC enhance the relative abundance of exoelectrogens near the anode and associated bulk soils (Dunaj et al., 2012; Wang et al., 2015; Yuan et al., 2018). The phyla *Proteobacteria* and *Chloroflexi* have all been reported to be enriched in the anode vicinity and to be comprised of wide distribution of electroactive bacteria (Liu et al., 2017; Yuan et al., 2018; Zhao et al., 2016; Zheng et al., 2017). Additionally, *Deltaproteobacteria*, *Bacteroidetes vadinHA17* and *Anaerolineae* are known electrogenic classes and have all been reported to be directly involved in electricity production (Gustave et al., 2018a; Wang et al., 2015; Yuan et al., 2018). However, it should be noted that *Gammaproteobacteria* (11.4% vs 1.8%) and *Betaproteobacteria* (18.3 vs 0.63) were found to be more abundant in the control anode vicinity compared to that of the sMFC, although these classes are known to contain some exoelectrogens (Kim et al., 2006). The predominant genera in the MFCs were affiliated with *Geobacter* (0.98%-25.9%), *Lentimicrobium* (1.2%-4.8%), *Clostridium sensu stricto10* (1.4%-2.15%) and *Thermincola* (0.07%-5.84%). However, in control, *Lentimicrobium* (1.68%-7.17%) and *Clostridium sensu stricto10* (1.60%-3.01%) were more abundant (Fig. 3.4). The species *Geobacter* (0.67% vs 26.0%) and *Thermincola* (0.47% vs 5.80%) were selectively enhanced in the sMFC anode vicinity compared to the control because both genera are able to use the electrodes as final electron acceptors (Wang et al., 2015; Wrighton et al., 2008). The relative abundance of known fermentative bacteria *Lentimicrobium* and *Clostridium sensu stricto10* decreased in the sMFC compared to the control, probably due

to the decrease of organic matter (Rago et al., 2018; Sun et al., 2016) (Table S 3.5). However it should be noted that the genus *Clostridium sensu stricto* contains some electroactive bacteria (Koch and Harnisch, 2016; Rago et al., 2018), although their relative abundance in this study was lower in the MFCs.

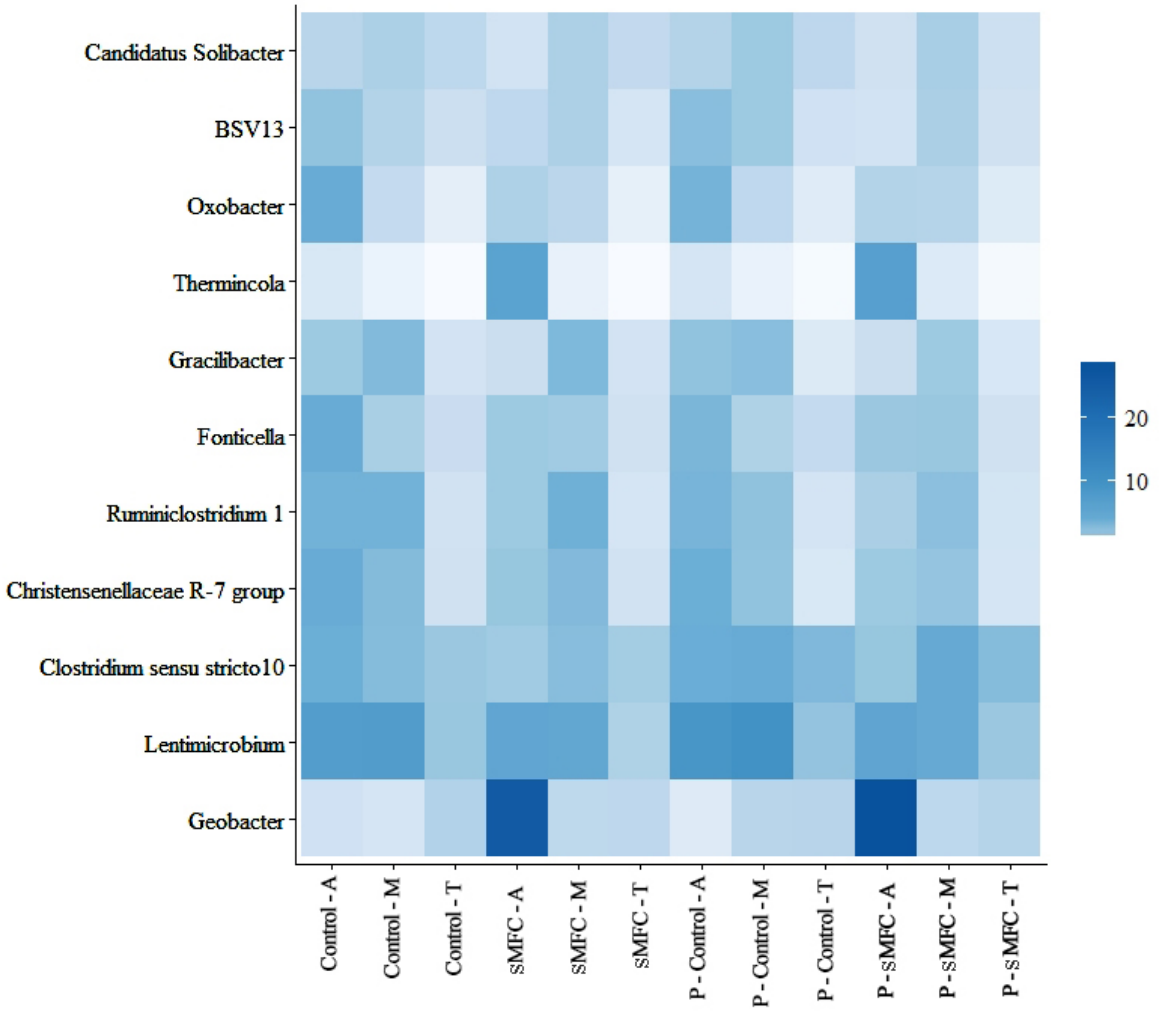

Figure 3.4 Heat map distribution of bacterial phylotypes classified to the genus level. The relative abundance values represent the mean of four replicates.

Additionally, the archaeal community was also significantly affected by the sMFC anode (Fig. 3.5a-b). At phylum level, *Euryarchaeota* (40.7% vs 52.3%) and *Bathyarchaeota* (10.1% vs 17.3%) were significantly decreased at the sMFC anode compared to the control. However, the phylum *Woesearchaeota (DHVEG 6)* (24.0% vs 19.5%) was slightly enhanced

(Fig.3.5a). Further analysis at genus level showed that the genera *Methanomassiliicoccus* (12.3% vs 17.9%) *Methanosarcina* (10.8% vs 14.6%) and *Methanosaeta* (0.9% vs 3.9%) were also significantly decreased in the sMFC anode vicinity compared to the control (Fig. 3.5b). These results further demonstrated that the sMFC played a significant role in the selection and enrichment of electrogenic microbes and decreases methanogens (Jung and Regan, 2011; Kouzuma et al., 2014; Ni et al., 2016). However, the genus *Candidatus Methanoperedens* (0.98% vs 0.15%) was slightly enhanced in the sMFC compared to the control. Members of the genus *Candidatus Methanoperedens* has been shown to be capable of performing nitrate-dependent anaerobic oxidation of methane. *Candidatus Methanoperedens* reduces nitrate anaerobically and use methane as the electron donor (Vaksmaa et al., 2017; Welte et al., 2016), therefore the marginal increase in their relative abundance in the anode vicinity suggest they could possibly be able to use the anode as an electron donor to reduce nitrate.

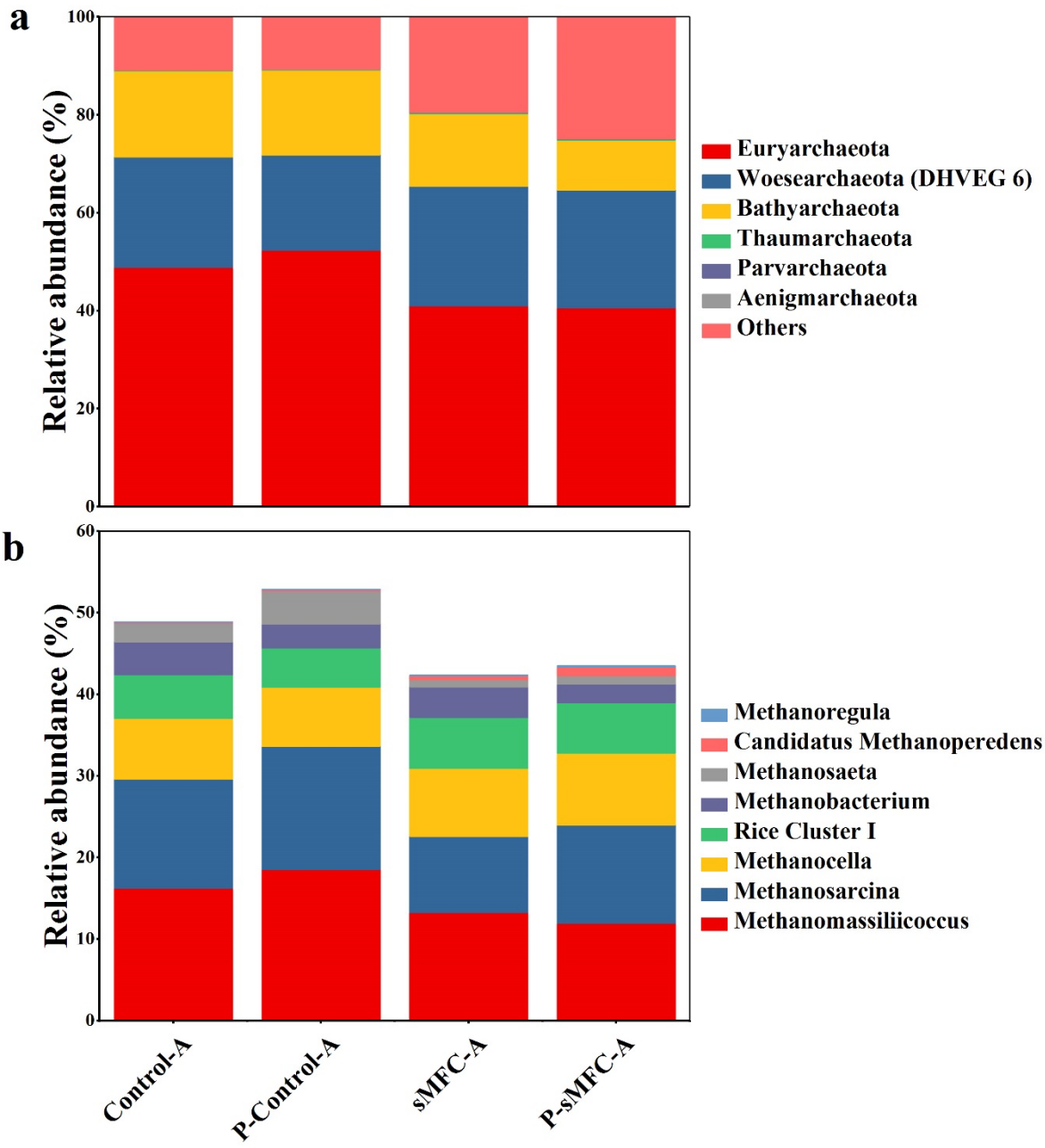

Figure 3.5 Relative abundance of archaeal community composition at phylum (a) and genus (b) level. The relative abundance values represent the mean of four replicates.

3.4.5. Influences of relic DNA on microbial community composition at phylum and class levels

Additionally, a comparison of the microbial community of PMA and non-PMA treated samples showed similar taxonomic distributions. However, it should be noted that the relative

abundance of the phylum *Proteobacteria*, although not significant, was slightly higher in the PMA treated samples compared to the non-PMA treaded samples in the sMFC irrespective of sample location. Moreover, the phyla *Bacteroidetes* and *Chloroflexi* were slightly lower in the MFCs samples treated with PMA (Fig. 3.3a). In contrast, a significant difference was observed at the genus level for the following groups; *Geobacter* ($p < 0.001$), *Fonticella* ($p = 0.015$), *Gracilibacter* ($p = 0.005$), *Thermincola* ($p = 0.002$), *Oxobacter* ($p = 0.008$), BSV13 ($p = 0.020$), *Candidatus_Solibacter* ($p = 0.011$) and *Mobilitalea* ($p = 0.013$). Also, the relative abundance of *Candidatus Methanoperedens* and *Methanosaeta* were relatively higher in the PMA treated samples, while that of *Methanobacterium* was slightly higher in the non-PMA treated samples (Fig. 3.5). These results suggest that although the sMFC altered the microbial community structure, relic DNA from the lysed cells were at a state of equilibrium with that of the intact cells. Therefore, in our system, relic DNA only had minimum effect on the culture independent estimates of microbial community composition. Numerous factors could be responsible for the lack of significant difference between the PMA and non-PMA treatment. For example, after cell death, some cells could be preserved by the soil and remain intact. This in turn rendering PMA ineffective because the concentration of PMA used in this study was insufficient to penetrate the intact cells (Carini et al., 2016). Another reason for the lack of dissimilarity may have occurred because the rate of cell death and the rate of extracellular removal may have been at a state of equilibrium (Lennon et al., 2018).

3.5. Conclusion

This study revealed that anodes of the soil sMFC can influence the microbial community structure of the bulk soil profile centimeters away. The phylum *Proteobacteria* and the class *Deltaproteobacteria* significantly increased in the sMFC compared to the control. Similarly, the archaeal community in the sMFC anode vicinity was strongly influenced by the anode. At the phylum level, the phyla *Euryarchaeota* and *Bathyarchaeota* were significant

decreased in the sMFC, while the phylum *Woesearchaeota (DHVEG 6)* was slightly enhanced. PCoA-PC1 vs PC2 analysis and ANOSIM analysis revealed that relic DNA had minimal effect on estimation of taxonomic and phylogenetic diversity in the sMFC system. This study shows for the first time that the removal rate of relic DNA may be at a state of equilibrium in the sMFC system after 60 days of operation and therefore will have minimum influence of culture independent estimates of the microbial community. However further studies are needed to determine the effect of relic DNA on the temporal microbial community of the soil sMFC.

3.6. References

Carini P, Marsden PJ, Leff JW, Morgan EE, Strickland MS, Fierer N. 2016. Relic DNA is abundant in soil and obscures estimates of soil microbial diversity. Nat. Microbiol. 2:16242.

Cerrillo M, Viñas M, Bonmatí A. 2017. Unravelling the active microbial community in a thermophilic anaerobic digester-microbial electrolysis cell coupled system under different conditions. Water Res. 110:192-201.

Chen Z, Huang YC, Liang J H, Zhao F, Zhu YG. 2012. A novel sediment microbial fuel cell with a biocathode in the rice rhizosphere. Bioresour. Technol. 108:55-9.

Dellanno A, Corinaldesi C. 2004. Degradation and Turnover of Extracellular DNA in Marine Sediments: Ecological and Methodological Considerations. Appl. Environ. Microbiol. 70:4384-6.

Dessì P, Porca E, Haavisto J, Lakaniemi A-M, Collins G, Lens PN. 2018. Composition and role of the attached and planktonic microbial communities in mesophilic and thermophilic xylose-fed microbial fuel cells. RSC Adv. 8:3069-80.

Downie HF, Standerwick JP, Burgess L, Natrajan LS, Lloyd JR. 2018. Imaging redox activity and Fe (II) at the microbe-mineral interface during Fe (III) reduction. Res Microbiol

Dunaj SJ, Vallino JJ, Hines ME, Gay M, Kobyljanec C, Rooney-Varga JN. 2012. Relationships between soil organic matter, nutrients, bacterial community structure, and the performance of microbial fuel cells. Environ. Sci. Technol. 46:1914-22.

Feng Y, Yang Q, Wang X, Logan BE. 2010. Treatment of carbon fiber brush anodes for improving power generation in air–cathode microbial fuel cells. J. Power Sources 195:1841-4.

Gustave W, Yuan ZF, Sekar R, Chang HC, Zhang J, Wells M, et al. 2018. Arsenic mitigation in paddy soils by using microbial fuel cells. Environ. Pollut. 238:647-55.

Gustave W, Yuan ZF, Sekar R, Ren YX, Chang H-C, Liu JY, et al. 2018. The change in biotic and abiotic soil components influenced by paddy soil microbial fuel cells loaded with various resistances. J. Soils Sediments 1-10.

Hedrich S, Schlömann M, Johnson DB. 2011. The iron-oxidizing proteobacteria. Microbiology 157:1551-64.

Hong SW, Chang IS, Choi YS, Kim BH, Chung TH. 2009. Responses from freshwater sediment during electricity generation using microbial fuel cells. Bioprocess. Biosyst. Eng. 32:389-95.

Hong SW, Kim HS, Chung TH. 2010. Alteration of sediment organic matter in sediment microbial fuel cells. Environ. Pollut. 158:185-91.

Huang DY, Zhou SG, Chen Q, Zhao B, Yuan Y, Zhuang L. 2011. Enhanced anaerobic degradation of organic pollutants in a soil microbial fuel cell. Chem. Eng. J. 172:647-53.

Jones RT, Robeson MS, Lauber CL, Hamady M, Knight R, Fierer N. 2009. A comprehensive survey of soil acidobacterial diversity using pyrosequencing and clone library analyses. The ISME journal 3:442.

Jung S, Regan JM. 2011. Influence of External Resistance on Electrogenesis, Methanogenesis, and Anode Prokaryotic Communities in Microbial Fuel Cells. Appl. Environ. Microbiol. 77:564-71.

Kaku N, Yonezawa N, Kodama Y, Watanabe K. 2008. Plant/microbe cooperation for electricity generation in a rice paddy field. Appl. Microbiol. Biotechnol. 79:43-9.

Kapoor V, Pitkänen T, Ryu H, Elk M, Wendell D, Santo Domingo JW. 2015. Distribution of human-specific bacteroidales and fecal indicator bacteria in an urban watershed impacted by sewage pollution, determined using RNA-and DNA-based quantitative PCR assays. Appl. Environ. Microbiol. 81:91-9.

Kim G, Webster G, Wimpenny J, Kim BH, Kim H, Weightman AJ. 2006. Bacterial community structure, compartmentalization and activity in a microbial fuel cell. J. Appl. Microbiol. 101:698-710.

Koch C, Harnisch F. 2016. Is there a specific ecological niche for electroactive microorganisms? Chem. Electro. Chem. 3:1282-95.

Kouzuma A, Kaku N, Watanabe K. 2014. Microbial electricity generation in rice paddy fields: recent advances and perspectives in rhizosphere microbial fuel cells. Appl. Microbiol. Biotechnol. 98:9521-6.

Kouzuma A, Kasai T, Nakagawa G, Yamamuro A, Abe T, Watanabe K. 2013. Comparative metagenomics of anode-associated microbiomes developed in rice paddy-field microbial fuel cells. PLoS One 8.

Lennon J, Muscarella M, Placella S, Lehmkuhl B. 2018. How, When, and Where Relic DNA Affects Microbial Diversity. mBio 9:e00637-18.

Li H, Tian Y, Qu Y, Qiu Y, Liu J, Feng Y. A Pilot-scale Benthic Microbial Electrochemical System (BMES) for Enhanced Organic Removal in Sediment Restoration. Sci. Rep. 2017;7:39802.

Liu B, Ji M, Zhai H. 2018. Anodic potentials, electricity generation and bacterial community as affected by plant roots in sediment microbial fuel cell: Effects of anode locations. Chemosphere.

Liu Q, Liu B, Li W, Zhao X, Zuo W, Xing D. 2017. Impact of Ferrous Iron on Microbial Community of the Biofilm in Microbial Fuel Cells. Front. Microbiol. 8:920.

Liu Q, Yang Y, Mei X, Liu B, Chen C, Xing D. 2018. Response of the microbial community structure of biofilms to ferric iron in microbial fuel cells. Sci. Total Environ. 631-632:695-701.

Liu S, Ren H, Shen L, Lou L, Tian G, Zheng P, et al. 2015. pH levels drive bacterial community structure in sediments of the Qiantang River as determined by 454 pyrosequencing. Front. Microbiol. 6:285.

Logan BE, Regan JM. 2006. Electricity-producing bacterial communities in microbial fuel cells. Trends Microbiol. 14:512-8.

Lu L, Huggins T, Jin S, Zuo Y, Ren ZJ. 2014. Microbial metabolism and community structure in response to bioelectrochemically enhanced remediation of petroleum hydrocarbon-contaminated soil. Environ. Sci. Technol. 48:4021.

Luo Z, Li S, Hou K, Ji G. 2018. Spatial and seasonal bacterioplankton community dynamics in the main channel of the Middle Route of South-to-North Water Diversion Project. Res. Microbiol.

Morrissey EM, Mchugh TA, Preteska L, Hayer M, Dijkstra P, Hungate BA, et al. 2015. Dynamics of extracellular DNA decomposition and bacterial community composition in soil. Soil Biol. Biochem. 86:42-9.

Naether A, Foesel BU, Naegele V, Wüst PK, Weinert J, Bonkowski M, et al. 2012. Environmental factors affect acidobacterial communities below the subgroup level in grassland and forest soils. Appl. Environ. Microbiol. 78:7398-406.

Ni G, Christel S, Roman P, Wong ZL, Bijmans MF, Dopson M. 2016. Electricity generation from an inorganic sulfur compound containing mining wastewater by acidophilic microorganisms. Res. Microbiol. 167:568-75.

Nicol GW, Leininger S, Schleper C, Prosser JI. 2008. The influence of soil pH on the diversity, abundance and transcriptional activity of ammonia oxidizing archaea and bacteria. Environ. Microbiol. 10:2966-78.

Nocker A, Cheung CY, Camper AK. 2006. Comparison of propidium monoazide with ethidium monoazide for differentiation of live vs. dead bacteria by selective removal of DNA from dead cells. J. Microbiol. Meth. 67:310-20.

Nocker A, Sossa-Fernandez P, Burr MD, Camper AK. 2007. Use of propidium monoazide for live/dead distinction in microbial ecology. Appl. Environ. Microbiol. 73:5111-7.

Peng QA, Shaaban M, Wu Y, Hu R, Wang B, Wang J. 2016. The diversity of iron reducing bacteria communities in subtropical paddy soils of China. Appl. Soil Ecol. 101:20-7.

Pettridge J, Firestone MK. 2005. Redox fluctuation structures microbial communities in a wet tropical soil. Appl. Environ. Microbiol. 71:6998-7007.

Pietramellara G, Ascher J, Borgogni F, Ceccherini M, Guerri G, Nannipieri P. 2009. Extracellular DNA in soil and sediment: fate and ecological relevance. Biol. Fertil. Soils 45:219-35.

Rago L, Zecchin S, Marzorati S, Goglio A, Cavalca L, Cristiani P, et al. 2018. A study of microbial communities on terracotta separator and on biocathode of air breathing microbial fuel cells. Bioelectrochemistry 120:18-26.

Schamphelaire LD, Bossche LVd, Dang HS, Höfte M, Boon N, Rabaey K, et al. 2008. Microbial Fuel Cells Generating Electricity from Rhizodeposits of Rice Plants. Environ. Sci. Technol. 42:3053-8.

Song TS, Yan ZS, Zhao ZW, Jiang HL. 2010. Removal of organic matter in freshwater sediment by microbial fuel cells at various external resistances. J. Chem. Technol. Biotechnol. 85(11), 1489-1493

Song Y, Xiao L, Jayamani I, He Z, Cupples AM. 2015. A novel method to characterize bacterial communities affected by carbon source and electricity generation in microbial fuel cells using stable isotope probing and Illumina sequencing. J. Microbiol. Methods 108:4-11.

Sun L, Toyonaga M, Ohashi A, Tourlousse DM, Matsuura N, Meng X-Y, et al. 2016. Lentimicrobium saccharophilum gen. nov., sp. nov., a strictly anaerobic bacterium representing a new family in the phylum Bacteroidetes, and proposal of Lentimicrobiaceae fam. nov. Int J Syst. Evol. Microbiol. 66:2635-42.

Türker OC, Yakar A. 2017. A hybrid constructed wetland combined with microbial fuel cell for boron (B) removal and bioelectric production. Ecol. Eng. 102:411-21.

Vaksmaa A, Guerrero-Cruz S, van Alen TA, Cremers G, Ettwig KF, Lüke C, et al. 2017. Enrichment of anaerobic nitrate-dependent methanotrophic 'Candidatus Methanoperedens nitroreducens' archaea from an Italian paddy field soil. Appl. Microbiol. Biotechnol. 101:7075-84.

Wang N, Chen Z, Li HB, Su JQ, Zhao F, Zhu YG. 2015. Bacterial community composition at anodes of microbial fuel cells for paddy soils: the effects of soil properties. J. Soils Sediments 15:926-36.

Wang Q, Garrity GM, Tiedje JM, Cole JR. 2007. Naïve Bayesian classifier for rapid assignment of rRNA sequences into the new bacterial taxonomy. Appl. Environ. Microbiol. 73:5261-7.

Wang Y, Chen Z, Liu P, Sun G, Ding L, Zhu Y. 2016. Arsenic modulates the composition of anode-respiring bacterial community during dry-wet cycles in paddy soils. J. Soils Sediments 16:1745-53.

Welte CU, Rasigraf O, Vaksmaa A, Versantvoort W, Arshad A, Op den Camp HJ, et al. 2016. Nitrate-and nitrite-dependent anaerobic oxidation of methane. Environ. Microbiol. Rep. 8:941-55.

Wrighton KC, Agbo P, Warnecke F, Weber KA, Brodie EL, DeSantis TZ, et al. 2008. A novel ecological role of the Firmicutes identified in thermophilic microbial fuel cells. The ISME Journal 2:1146.

Wu Y, Zeng J, Zhu Q, Zhang Z, Lin X. 2017. pH is the primary determinant of the bacterial community structure in agricultural soils impacted by polycyclic aromatic hydrocarbon pollution. Sci. Rep. 7:40093.

Xun X, Zhao Q, Wu M, Jing D, Zhang W. 2016. Biodegradation of Organic Matter and Anodic Microbial Communities Analysis in Sediment Microbial Fuel Cells with/without Fe(III) Oxide Addition. Bioresour. Technol.

Yang Y, Dai Y, Wu Z, Xie S, Liu Y. 2016. Temporal and spatial dynamics of archaeal communities in two freshwater lakes at different trophic status. Front. Microbiol. 7:451.

Yates MD, Kiely PD, Call DF, Rismani-Yazdi H, Bibby K, Peccia J, et al. 2012. Convergent development of anodic bacterial communities in microbial fuel cells. ISME J 6:2002-13.

Yu B, Tian J, Feng L. 2017. Remediation of PAH polluted soils using a soil microbial fuel cell: Influence of electrode interval and role of microbial community. J. Hazard Mater. 336:110.

Yuan HY, Liu PP, Wang N, Li XM, Zhu YG, Khan ST, et al. 2018. The influence of soil properties and geographical distance on the bacterial community compositions of paddy soils enriched on SMFC anodes. J. Soils Sediments 18:517-25.

Zhang LH, Jia JP, Ying DW, Zhu NW, Zhu YU. 2005. Electrochemical effect on denitrification in different microenvironments around anodes and cathodes. Res. Microbiol. 156:88-92.

Zhao Q, Li R, Ji M, Ren ZJ. 2016. Organic content influences sediment microbial fuel cell performance and community structure. Bioresour. Technol. 220:549-56.

Zheng W, Cai T, Huang M, Chen D. 2017. Comparison of electrochemical performances and microbial community structures of two photosynthetic microbial fuel cells. J. Biosci. Bioeng. 124:551-8.

3.7. Supplementary data

The effect of the soil microbial fuel cell on paddy soil microbial community profile

Table S 3.1 Selected chemical properties of the fresh soils used in this study.

Soils Texture	Fe(g/kg)	As (mg/kg)	pH	TOC (g/kg)
Loam Clay	53.7 ±1.8	73.7 ±5.9	6.2 ±0.1	23.2 ±0.9

Notes*:* Fe, soil total iron, As, soil total arsenic, TOC, total organic carbon. The values represent the mean ±standard error of four replicate samples.

Table S 3.2 Concentration of DNA in each sample as measured immediately after the extraction.

Sample ID	DNA (ng/µL)	Sample ID	DNA (ng/µL)
Control-T1	0.51	**sMFC-T1**	0.30
Control-T2	0.60	**sMFC-T2**	0.30
Control-T3	0.62	**sMFC-T3**	0.27
Control-T4	0.62	**sMFC-T4**	0.31
Control-M1	0.54	**sMFC-M1**	0.32
Control-M2	0.27	**sMFC-M2**	0.11
Control-M3	0.71	**sMFC-M3**	0.80
Control-M4	0.55	**sMFC-M4**	0.40
Control-A1	0.54	**sMFC-A1**	0.44
Control-A2	0.44	**sMFC-A2**	0.28
Control-A3	0.62	**sMFC-A3**	0.22
Control-A4	0.32	**sMFC-A4**	0.12
P-Control-T1	0.16	**P-sMFC-T1**	0.51
P-Control-T2	0.14	**P-sMFC-T2**	0.41
P-Control-T3	0.18	**P-sMFC-T3**	0.51
P-Control-T4	0.18	**P-sMFC-T4**	0.32
P-Control-M1	0.18	**P-sMFC-M1**	0.22
P-Control-M2	0.10	**P-sMFC-M2**	0.31
P-Control-M3	0.32	**P-sMFC-M3**	0.27
P-Control-M4	0.10	**P-sMFC-M4**	0.11
P-Control-A1	0.13	**P-sMFC-A1**	0.20

P-Control-A2	0.19	**P-sMFC-A2**	0.44
P-Control-A3	0.13	**P-sMFC-A3**	0.55
P-Control-A4	0.15	**P-sMFC-A4**	0.14

Note T, M and A: represents samples collected from top layer, middle layer and anode vicinity respectively.

Table S 3.3 Similarity-based microbial OTUs and species richness and diversity estimates (n=4).

Sample ID	Reads	Observed OTUs	ACE	Chao1	Shannon index	Good's Coverage (%)
Control-T	172320 ±22821	1512 ±12	1694.19 ±7.06	1725.26 ±11.02	8.57 ±0.03	99.20 ±0.00
Control-M	118892 ±8963	1396 ±8	1543.27 ±9.64	1570.27 ±8.09	8.14 ±0.06	99.30 ±0.00
Control-A	136342 ±7145	1359 ±25	1499.87 ±22.28	1520.87 ±23.77	8.22 ±0.08	99.40 ±0.00
P-Control-T	167132 ±24034	1494 ±23	1654.22 ±37.96	1674.55 ±37.88	8.68 ±0.08	99.30 ±0.00
P-Control-M	170169 ±26012	1372 ±10	1509.23 ±7.93	1535.48 ± 8.56	7.99 ±0.04	99.40 ±0.00
P-Control-A	136630 ±2479	1344 ±13	1470.42 ±17.46	1496.89 ±17.71	8.08 ±0.04	99.40 ±0.00
sMFC-T	138423 ±23067	1532 ±20	1736.43 ±28.50	1761.00 ±25.19	8.61 ±0.24	99.20 ±0.00
sMFC-M	131344 ±22816	1405 ±4	1536.76 ±24.50	1559.40 ±26.46	8.26 ±0.01	99.40 ±0.00
sMFC-A	133954 ±2479	1216 ±15	1428.48 ±24.83	1434.27 ±27.41	6.94 ±0.09	99.20 ±0.00

P-sMFC-T	179308 ±17954	1483 ±19	1655.92 ±28.44	1663.47 ±37.71	8.39 ±0.05	99.30 ±0.00
P-sMFC- M	142549 ±17060	1385 ±19	1540.01 ±5.22	1555.69 ±6.32	8.11 ±0.04	99.30 ±0.00
P-sMFC- A	130068 ±6956	1222 ±27	1432.61 ±21.16	1444.29 ±21.58	6.72 ±0.02	99.20 ±0.00

Notes: OTUs, The operational taxonomic units were defined with 3% dissimilarity. T, M and A: represents samples collected from top layer, middle layer and anode vicinity respectively. The values represent the mean ±standard error of four replicate samples.

Table S 3.4Similarity-based archaeal OTUs and species richness and diversity estimates.

Sample ID	Reads	Observed OTUs	ACE	Chao1	Shannon index	Good's Coverage (%)
Control-A	124632 ±6459	303 ±5	353.84 ±12.16	358.75 ±18.84	5.11 ±0.06	99.80 ±0.00
P-Control-A	143249 ±12512	297 ±8	338.20 ±5.36	338.19 ±7.50	5.04 ±0.10	99.80 ±0.00
sMFC-A	140226 ±7236	371 ±11	400.58 ±2.51	402.46 ±3.14	5.79 ±0.13	99.80 ±0.00
P-sMFC- A	116289 ±25229	371 ±3	401.72 ±10.52	404.12 ±8.62	6.04 ±0.07	99.80 ±0.00

Notes: OTUs, The operational taxonomic units were defined with 3% dissimilarity. A represents samples collected from vicinity respectively. The values represent the mean ±standard error of four replicate samples.

Table S 3.5 Results of selected chemical analysis of soil at the end of the experiment.

Sample ID	TOC (g/kg)	pH	*Fe (mg/l)
Control-T	20.12 ±0.10	5.85 ±0.10	9.96 ±5.00
Control-M	19.71 ±0.40	6.20 ±0.03	18.77 ±3.93
Control-A	19.35 ±0.13	6.20 ±0.06	18.32 ±2.31
sMFC-T	19.28 ±0.52	6.92 ±0.02	17.96 ±5.07
sMFC-M	18.33 ±0.27	5.85 ±0.03	35.30 ±5.57
sMFC-A	17.92 ±0.10	5.61 ±0.15	33.15 ±4.42

Notes: TOC indicates total organic carbon. T, M and A: represents samples collected from top layer, middle layer and anode vicinity respectively. * The iron presented here represent soil porewater total iron. The values represent the mean ±standard error of four replicate samples.

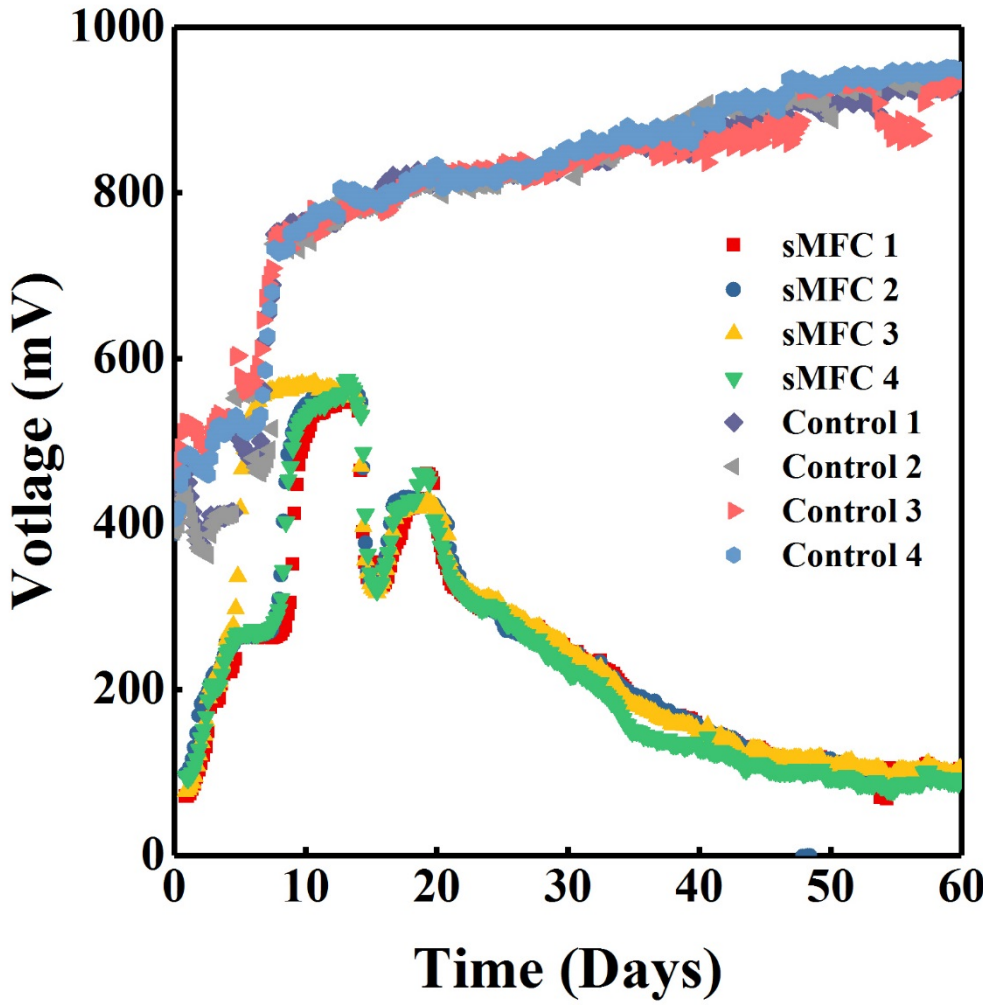

Figure S 3.1 The voltage variation of the MFCs over time.

Chapter 4 : The effect of the sMFC on paddy soil components at different external resistance

4.1. Abstract

The use of soil microbial fuel cells (sMFC) are a novel technique that uses organic matter in soils as an alternative energy source. External resistance (ER) is a key factor that influences sMFC performance and also alters the soil biological and chemical reactions. However, little information is available on how the microbial community and soil component changes in sMFC with different ER. Thus, the purpose of this study was to collectively examine the effects of different ER on paddy soil biotic and abiotic components. Eighteen paddy sMFC were constructed and operated at five different ER (2000 Ω, 1000 Ω, 200 Ω, 80 Ω and 50 Ω) in triplicates for 90 days. The effects of the sMFC anodes at different ER were examined by measuring organic matter (OM) removal efficiency, trace elements in porewater and bacterial community structure in contaminated paddy soil. The results indicate that ER has significant effects on sMFC power production, OM removal efficiency and bacterial beta diversity. Moreover, ER influences iron, arsenic and nickel concentration as well in soil porewater. In particular, greater current densities were observed at lower ER (2.6mA, 50Ω) as compared to a higher ER (0.3mA, 2000Ω). The removal efficiency of OM increased with decreasing ER whereas it decreased with soil distance away from the anode. Furthermore, principal coordinate analysis (PCoA) revealed that ER may shape the bacterial community that develop in the anode vicinity but have minimal effect on that of the bulk soil. The current study illustrates that lower ER can be used to selectively enhance the relative abundance of electrogenic bacteria and lead to high OM removal.

4.2. Introduction

Organic carbon in sediments or soils can be used as a new source of energy when employed in microbial fuel cells (MFC). Soil microbial fuel cells (sMFC) are special type of MFC that produce electricity by using organic chemicals present in the soils as an energy source (De Schamphelaire et al. 2008; Hong et al. 2009; Song et al. 2010; Chen et al. 2012). In sMFC, organic matter (OM) is anaerobically oxidized at the anode by the soil microorganisms, resulting in the production of electrons. The electrons produced during OM oxidation migrate toward the cathode, through an external circuit, where they combine with oxygen and protons to form water. sMFCs that employ paddy soil has gained considerable attention recently because the unique biological and chemical characteristics of paddy soil makes them ideal for power production (Kaku et al. 2008; Huijuan et al. 2012). In addition to power generation, sMFC have also found use in stimulating soil bioremediation. For instance, the anode of the sMFC can serve as an electron sink for anode respiring bacteria (ARB) and accelerate bioremediation of both polycyclic aromatic hydrocarbons and redox active heavy metals (Wang et al. 2015; Yu et al. 2017; Gustave et al. 2018).

However, sMFC deployment in paddy fields has been shown to alter both biotic components (e.g. soil bacterial community structure) and abiotic components (Kouzuma et al. 2014; Lu et al. 2014; Gustave et al. 2018). When an anode of sMFC is embedded into the anaerobic soils, it functions as a continuous sink for electrons therefore this alters soil chemistry (Logan, 2008; Huang et al. 2011). This in turn increases soil redox potential (E*h*), decreases soil pH and changes the bioavailability of soil nutrients such as phosphate, nitrogen and carbon (Hong et al. 2009a; Touch et al. 2017). Since soil Eh, pH and nutrient bioavailability are major drivers of bacterial community structure, the changes in soil chemistry may influence the soil bacterial community composition. (Pettridge and Firestone 2005; Nicol et al. 2008; Wu et al. 2017). Furthermore, sMFC have also been used to prevent the deterioration of overlying water

quality and for the removal or stabilization of toxic heavy metals (Chen et al. 2015; Wang et al. 2015; Zhou et al. 2015; Gustave et al. 2018). Previous studies have shown that sMFC can be used as a mitigation technology in soils contaminated with chromium, uranium, cadmium, lead, copper or organic pollutants (Zhang et al. 2012; Chen et al. 2015; Wang et al. 2015; Abbas et al. 2017). However, several factors such as dissolved oxygen, temperature, internal resistance, microbial activity and anode potential have been shown to impact the performance of sMFC (Jang et al. 2004; Min et al. 2008; Huan et al. 2014).

Among them the anode bacterial community is one of the most important factors that determine the capability of the sMFC to function effectively as a remediation technology. For example, when non-anode respiring bacteria are abundant in the anode chamber, these microbes may compete with ARB for resources, thereby limiting the performance of the sMFC (Jung and Regan 2011; Kouzuma et al. 2014). However, regulating the anode potential has been shown to effectively tailor the desired ARB consortium and suppress the growth of undesirable microbes, such as methanogens (Jung and Regan 2011; Kouzuma et al. 2014). This occurs because the anode potentials regulate the anode availability to accept electron from ARB and the energy ARB received for growth and development (Torres et al. 2009). Thus at certain anode potential, ARB are able to gain higher energy for growth from respiring the anode and out compete methanogens for OM (Jung and Regan 2011). Moreover, many studies have used a potentiostat to set the anode potential (Torres et al. 2009; Zhu et al. 2014). Although the electrode at a certain potential provides a controlled environment as the habitat of electrogens, it requires the input of external energy and is not feasible in field application. Furthermore, most of these studies have only been done in the double chamber MFC system but not in the soil MFC (Torres et al. 2009; Zhu et al. 2014). Therefore, the effect of the anode potential on the soil microbial community needs to be investigated, while using a simple method that does not incur additional cost.

Moreover, adjusting applied external resistance (ER) in sMFC has also been shown to affect the anode potential and the metabolic rate of ARB (Song et al. 2010; Rismani-Yazdi et al. 2011). Studies on the relation between anode potential and ER have reported that applying lower ER results in higher anode potentials (Song et al. 2010; Rismani-Yazdi et al. 2011; Del Campo et al. 2014). Del Campo et al. (2014), reported that lowering the applied ER increases anode potential because ER influences the transfer of electron from anode to cathode. Therefore, at lower ER the transfer of electron from the anode to the cathode is limited by internal resistance and this results in the increase of anode potential (Song et al. 2010; Rismani-Yazdi et al. 2011; Del Campo et al. 2014). Additionally, studies have demonstrated that lower ER increases the microbial degradation of OM and current output from the sMFC (Song et al. 2010). This occurs because different ER and anode potential can greatly impact the anode microbial community structure, morphology and sMFC performance (Aelterman et al. 2008; Torres et al. 2009; Rismani-Yazdi et al. 2011). Furthermore, the current produced by the sMFC can also stimulate microbial degradation of soil OM by anaerobic bacteria (Pitts et al. 2003; Yu et al. 2017). Hence studying the impact of ER in sMFC is important if the sMFC is to be applied in the field as a remediation technology. Because the applied ER regulate the bacterial activity on the anode which controls the maximum voltage, current, power output and OM removal efficiency of the sMFC (Menicucci et al. 2006; Song et al. 2010; Rismani-Yazdi et al. 2011; Del Campo et al. 2014).

Although the application of sMFC is increasing, studies examining the effect of anode potential on sMFC community have received limited to no attention. Many studies have reported changes in sMFC anode microbial community under close circuit conditions (Kouzuma et al. 2014; Lu et al. 2014; Wang et al. 2015; Gustave et al. 2018) however, as far as the authors are aware the effect of ER on the microbial community of sMFC has not been investigated thus far. Moreover, the influence of anode potentials on the biofilm community

composition in double chamber MFC have been investigated (Torres et al. 2009; Zhu et al. 2014), however, to date there is no universal consensus on the effect of anode potential on the anode community structure. Torres et al. (2009) observed selective enhancement of *Geobacter sulfurreducens* at lower anode potentials (−0.15V, −0.09V, and 0.02V vs Standard hydrogen electrode (SHE)) and an increase in bacterial diversity at higher anode potential (0.37V). On the contrary, Zhu et al. (2014), argues that anode community was unaffected by anode potential and that electrogenic communities acclimatize to different anode potentials. Nonetheless, to date, to the best of our knowledge, no studies have examined the influence of the anode at different ER on soil biotic and abiotic constituents collectively. Previous studies have examined the effects of ER on soil OM degradations (Song et al. 2010; Cao et al. 2015), nevertheless to date no studies have been done to assist the effect of ER on soil microbial community and soil porewater heavy metal behavior. Thus, the objectives of this study were, therefore, to collectively examine the effects of different ER on soil and anode bacterial community structure, OM removal efficiency and selective soil metal behavior at various resistances away from the anode. The results from this study suggest that lower ER can be used to enhance ARB abundance and increase OM removal.

4.3. Materials and Methods

4.3.1. Paddy Soil Sample

The paddy soil samples were collected from a rice paddy in Qiyang, Hunan located in Southern part of China (GPS N26.760 E111.86). The soil properties, including texture, pH, OM content, As and Iron (Fe) were measured to be clay, 6.0, 23.2g/kg, 73.7mg/kg and 53.69 g/kg, respectively.

4.3.2. Soil Microbial Fuel Cell Assembly

Eighteen sMFCs were constructed from the paddy soil and operated at different ER (2000 Ω, 1000 Ω, 200 Ω, 80 Ω and 50 Ω) in triplicates for 90 days incubation. Of the eighteen sMFC, three were controls, the anodes and cathodes were not connected (open circuit). All sMFC were constructed as previously described in chapter 2, with slight modifications. Briefly, a columnar polyethylene terephthalate container (10 cm diameter × 15 cm depth) with two valve ports (~2 cm above the anode and adjacent to the anode) was used to construct each sMFC. Circular carbon felts with geometric surface area of 50.2 cm^2 were used as anodes and cathodes. A data logger (USB-7660B, ZTIC, China) was used to record the voltage between the anode and cathode.

Using 700 g (dry weight) of soil sample, ~1 cm depth of soil was placed at the bottom of the sMFC container. Then, the anode was placed on the surface of the soil layer and then buried with additional soil to simulate anaerobic conditions. The cathode was placed above the soil in aerobic conditions (half submerged in water and the other half in the open air). Deionized water (1L) was added to flood the paddy soil. No external carbon source or electron acceptors were added during the entire operational period of the sMFC.

4.3.3. Chemical Analysis

Each constructed sMFC was equipped with two self-made soil porewater sampler. The sampler was made from a 0.45 μm hollow fiber membrane (modified polyethersulfone, Motimo Membrane Technology Co., Ltd, Tianjin, China), which was inserted into the soil through the valve port adjacent to the anode and 2 cm above the anode. The soil porewater was sampled and analyzed for As, Ni and Fe as described in chapter 2. Dissolved organic carbon (DOC) and loss on ignition (LOI) concentration was determined as outlined in chapter 2.

4.3.4. Microbial Community Analysis

Total Genomic DNA was extracted from the anode vicinity and bulk soil using the PowerSoil DNA isolation kit (Mo Bio Laboratories, Inc., Carlsbad, CA) from all of the treatments including the controls according to the manufacturer's protocol. The quantity of DNA in the extracts was measured at 260 and 280 nm using a Qubit 2.0 Fluorometer (Invitrogen, Carlsbad, CA) and the quality of the DNA was verified by agarose gel electrophoresis. The DNA extracts were stored at -80 °C until sequencing. The V3-V5 hypervariable regions of the 16S ribosomal RNA (rRNA) gene in bacteria were amplified using primer pair 515f/907R (Sun et al. 2016; Xiao et al. 2016). The procedure for the microbial community structure analysis has been previously described in chapter 2.

4.3.5. Nucleotide sequence accession numbers

Nucleotide sequences were deposited in the GeneBank database with accession numbers MG814044 - MG815131.

4.4. Results

4.4.1. Electricity generation from soil MFCs with different external resistors

In this study each sMFC was loaded with a fixed resistor for the duration of the experiment. Five different ER were tested ranging from 50 Ω to 2000 Ω and the current production from the sMFC for 90 days of operation is illustrated in Fig. 4.1. The current of all

the sMFC sharply increased during the initial stage regardless of ER and it reached a maximum current at around 10 days. The highest current produced was observed at an ER of 50 Ω (2.6mA), followed by those of 80 Ω (2.1 mA), 200 Ω (1.6 mA) and 1000 Ω (0.8 mA). An ER of 2000 Ω produced the lowest current (0.3mA). However after ca. 30 days all the current outputs irrespective of ER were approximately the same (0.15-0.2 mA). The insert in Fig. 4.1 shows change in the controls voltage with time. The voltage in the control reached approximately 0.92 V on day 52 and remained relatively stable until the end of the experiment.

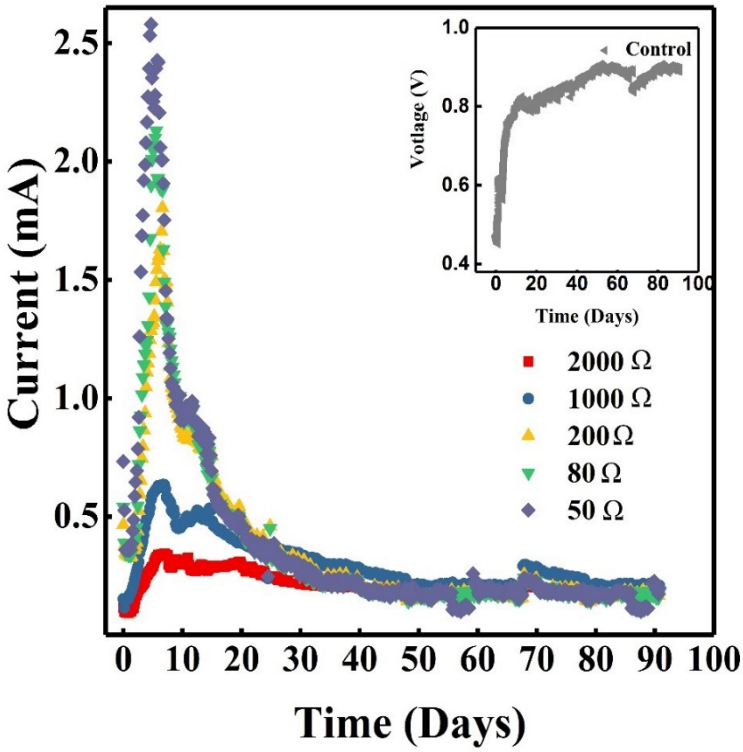

Figure 4.1 Current production from sMFC fixed with different external resistances during a 90-day operation. The insert represent the change in the control's voltage with time.

4.4.2. Polarization properties of the sMFC

The power current curve is an important attribute used to determine the performance of MFC. The power current curves in this study were obtained by varying ER from 10KΩ to 10Ω and are compared in Fig. 4.2. The power densities of the sMFC set at 1000 Ω and 2000 Ω ER were similar and those set at lower ER (50 Ω, 80 Ω and 200 Ω) mirrored each other. As shown

in Fig. 4.2, the maximum power density observed in the sMFC at different resistance were 22.2, 22.2, 24.1, 36.5 and 40.0 mW/m^2 for 50 Ω, 80 Ω, 200 Ω, 1000 Ω and 2000 Ω respectively. Similarly, the polarization slope method was used to determine the internal resistance for each sMFC. The results followed a similar trend to maximum power except for the case of 200 Ω. The 50 Ω ER had the lowest internal resistance and 2000 Ω had the highest internal resistance. The internal resistance increased in the following order 50 (389 Ω) < 80 (390 Ω) < 1000 (476 Ω) < 200 (556 Ω) < 2000 (572 Ω).

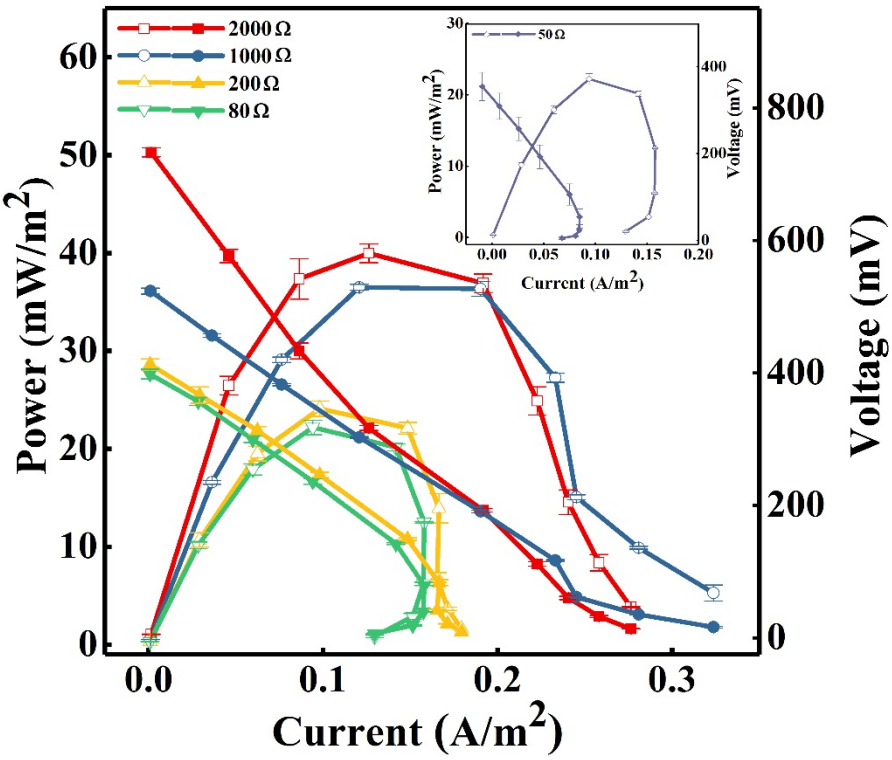

Figure 4.2 Polarization curves of the sMFC at various external resistance. The filled and open symbols represent power and voltage respectively. The error bars represent standard error of measured concentrations of triplicate samples. The insert represent the polarization curve of the sMFC set at 50Ω.

The anode and cathode potentials (versus Ag/AgCl reference electrode) for each sMFC at different ER are shown in Fig. S 4.1. In general, the anode potential became more positive with decreasing ER, however there was negligible difference between the potential of the anode

at 50 Ω, 80 Ω and 200 Ω. The working potential of the anode for the sMFC with an ER of 2000 Ω was much lower than those with other ER, approximately 345 mv lower than those with ER of 50 Ω, 80 Ω and 200 Ω. Moreover, the highest cathodic potential was observed in the sMFC with 200 Ω ER followed by that of 80 Ω and 1000 Ω. The cathodic potential of sMFC with ER of 50 Ω and 2000 Ω were approximately the same. These findings indicate that the cathode was responsible for the difference in sMFC performance with different ER, especially at ER of 200 Ω, 80 Ω and 50 Ω (Song et al. 2010). This was due to the sharp decrease in cathode potential with decreasing resistance compared to that of the anode.

4.4.3. Microbial community structure

The Illumina MiSeq sequencing of the 16S rRNA gene yielded a total of 2164539 bacterial sequences (average read length 450 bp). The valid reads clustered into 1162 OTUs at a 3% distance. The rarefaction analysis showed a clear saturation trend indicating that the sequencing depth of 30,000 was sufficient (Fig. S 4.2). The notion of sufficient depth being met was also supported by the high Good's Coverages (>0.99) (Table S 4.1). The observed alpha diversity indices showed that the bacterial communities in the vicinity of the anode were less diverse than that of the bulk soil and that applying different ER had a negligible influence on bacterial diversity (Table S 4.1).

Beta diversity indices, PCoA (Fig. 4.3) and NMDS (Fig. S 4.3) analyses of the bacterial community composition reveal three distinctive clusters. Where the bulk soils bacterial community clustered together regardless of applied ER, while the samples from anode vicinity posed at high ER (1000 Ω and 2000 Ω) clustered with the control and that of the lower resistances (50 Ω, 80 Ω and 200 Ω) formed another cluster. These findings demonstrate for the first time that the ER may shape the bacterial communities that develop in the anode vicinity of sMFC but have minimal effect on that of the bulk soil.

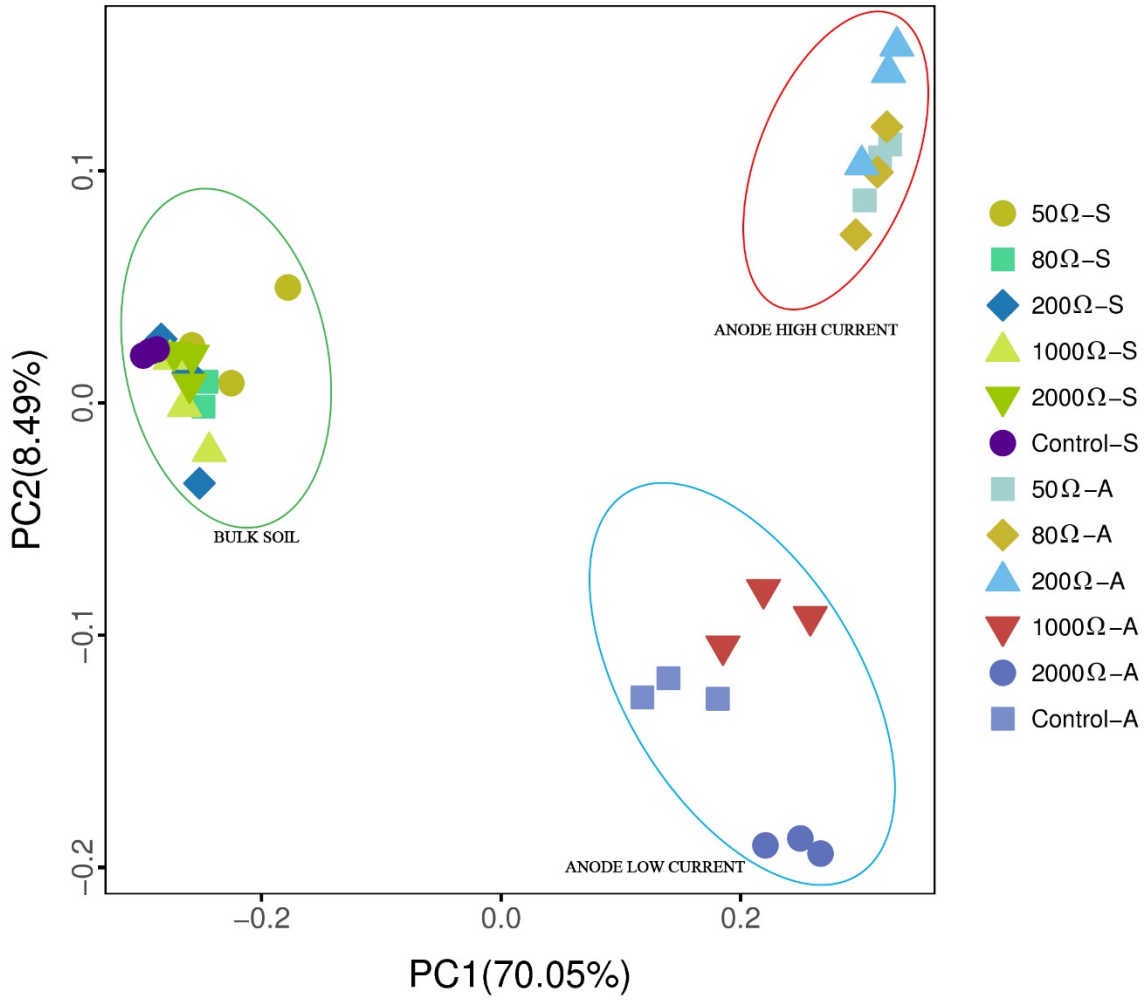

Figure 4.3 Principal Coordinates Analysis (PCoA) of the sMFC and controls bacterial community composition based on Bray-Curtis distance. The x- and y-axes are indicated by the first and second coordinates, respectively, and the values in parentheses show the percentages of the community variation explained.

Phylum and class level analysis reveal that fourteen bacterial phyla and fourteen bacterial classes, respectively made up the vast majority of total 16S rRNA gene sequences, accounting for 92% and 78% of total reads, respectively. Taxonomic classification at the phylum showed that the phyla *Proteobacteria, Chloroflexi, Nitrospirae* and *Chlorobi* were enhanced with decreasing ER and *Bacteroidetes, Acidobacteria* and *Euryarchaeota* were suppressed (Fig. S 4.5). The relative abundance of *Proteobacteria* in the anode biofilms were 29.7% (50 Ω), 26.5% (80 Ω), 27.2% (200 Ω), 23.2% (1000 Ω), 22.6% (2000 Ω) and 21.3%

(control) respectively, when *Chloroflexi* accounted for 10.8% (50 Ω), 11.7% (80 Ω), 11.5% (200 Ω), 10.3% (1000 Ω), 8.04% (2000 Ω) and 9.86% (control). The relative abundance of *Nitrospirae* and *Chlorobi* followed a similar trend 11.5 and 2.56 % (50 Ω), 14.1 and 2.36% (80 Ω), 13.9 and 1.64% (200 Ω), 8.01 and 1.06% (1000 Ω), 7.00 and 1.34% (2000 Ω) and 5.2 and 0.86% (control) respectively. Analysis on the class level showed that *Deltaproteobacteria*, *Bacteroidetes vadinHA17*, *Nitrospira* and *Subgroup18* were strongly influenced by ER. Further analysis at the genus level showed that the *Geobacter* and *Lentimicrobium* were the most sensitive genus to ER. *Geobacter* was enhanced with decreasing ER in both the bulk soil and the anode vicinity, while in the bulk soil *Lentimicrobium* was suppressed (Fig. 4.4).

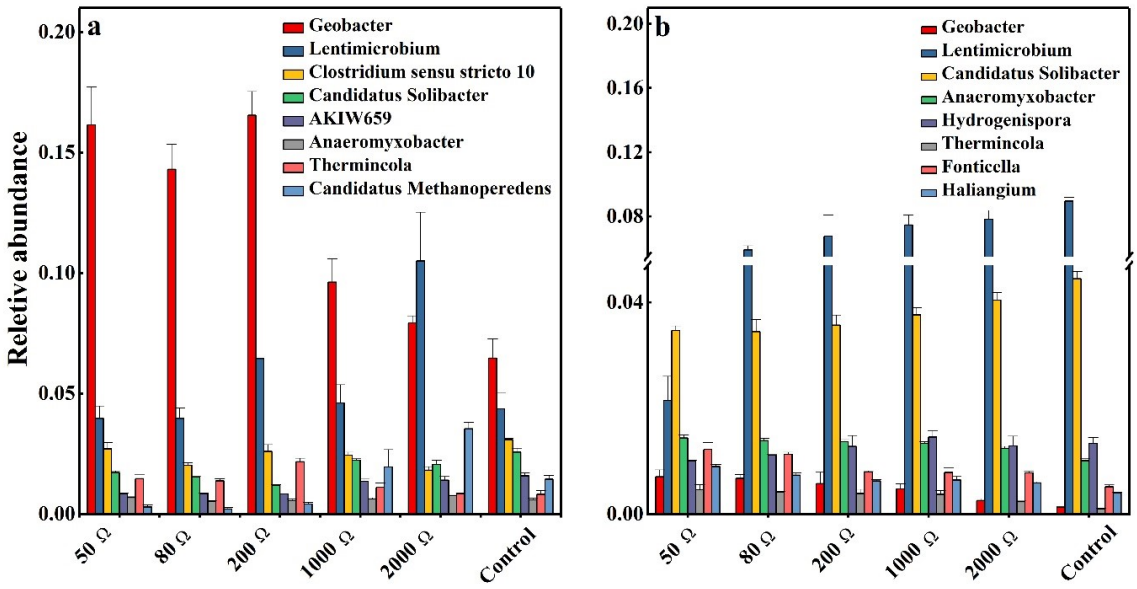

Figure 4.4 Relative abundance of bacterial community composition at genus level (a) anode vicinity and (b) bulk soil.

4.4.4. Organic matter removal and Change in soil pH

The loss on ignition (LOI) value was used as a proxy to estimate the OM content in the soil and its removal efficiency was used to analyze the effect of ER on degradation of organic carbon by the sMFC. Figure 4.5 illustrates the removal efficiency of LOI from the soil samples at two distances (~1cm and 2cm) away from the anode at different ER. The removal efficiency

of LOI increased with decreasing ER and distance away from the anode. The removal efficiency of LOI in the vicinity of the anode were 2.0%, 4.9%, 6.9%, 6.5% and 7.4% higher than the control, for sMFC loaded with 2000 Ω, 1000Ω, 200 Ω, 80 Ω and 50 Ω ER, respectively. A similar trend was observed in the removal efficiency of OM in the bulk soil. A significantly ($p < 0.05$) higher removal efficiency of LOI irrespective of location was observed between the control and all the treatments except for 2000 Ω (anode vicinity). The results obtained here demonstrate that the anode could enhance bacterial degradation of organics and decreasing ER can further promote this process. Moreover, ER also influences the sMFC soil pH (Table S 4.2). In general, the soil pH in the anode vicinity decreased with decreasing ER and the pH in of the bulk soil slightly increased with decreasing ER. The soil pH in the anode vicinity were 5.75, 5.84, 5.56, 5.60 and 5.67 for sMFC loaded with 2000 Ω, 1000Ω, 200 Ω, 80 Ω and 50 Ω ER, respectively. While the pH in the bulk soil were 5.88, 5.66, 5.77, 5.73 and 5.70 for sMFC loaded with 2000 Ω, 1000Ω, 200 Ω, 80 Ω and 50 Ω ER, respectively.

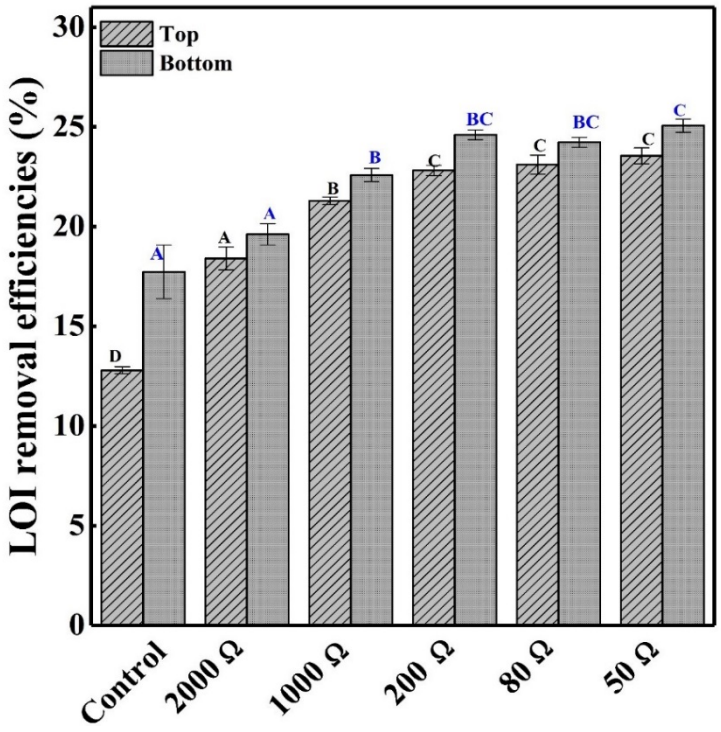

Figure 4.5 Removal efficiencies of lost on ignition carbon. The error bars represent standard error of measured concentrations of triplicate samples.

4.4.5. Changes of porewater As, Fe and Ni

The concentrations of As, Fe and Ni in the bulk soil porewater and in the anode vicinity were tested from day 0 to 60 at intervals of 10 days and then tested at the end of 90 days (Fig. 4.6a-d and Fig. S 4.5a-b). As shown in Fig. 4.6a-b and Fig. S 4.6a-b no significant (p >0.05) differences was observed in bulk soil porewater for As, Fe and Ni with time irrespective of ER, however the concentration of both Fe and As was slightly elevated in the treatments compared to the controls at the end of 90 days. In the vicinity of the anode the concentration of As, Fe and Ni were lower in the treatments compared to the control. In general, the concentration of these metals decrease with decreasing ER in the anode vicinity.

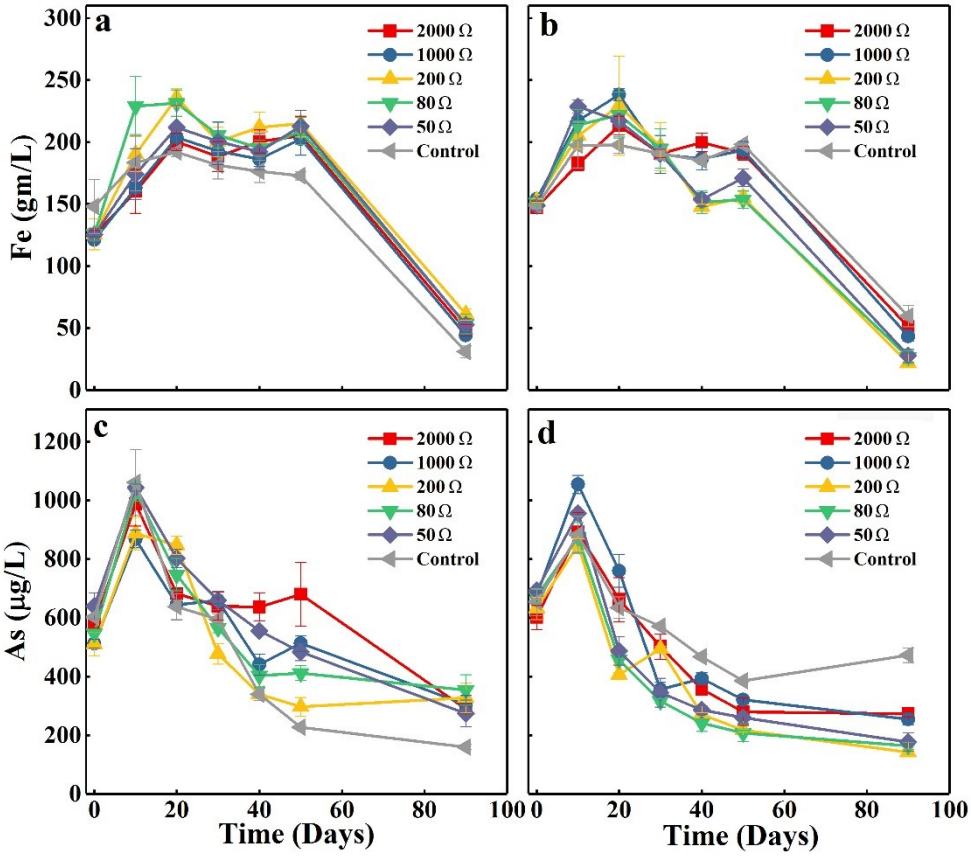

Figure 4.6 a-d Fe and As variation in soil porewater along with incubation time. Panels a and b represent Fe concentration in the bulk soil and anode vicinity respectively. Panels c and d represent As concentration in the bulk soil and anode vicinity respectively. The error bars represent standard error of measured concentrations of triplicate samples.

4.5. Discussion

Various studies have shown that the applied ER can greatly affect the current production, because ER plays an important role in the enrichment process of ARB on the anode (Mohan et al. 2008; Rismani-Yazdi et al. 2011). These studies revealed that low resistance stimulated ARB growth on the anode and thereby improved current production (Aelterman et al. 2008; Torres et al. 2009; Rismani-Yazdi et al. 2011). As illustrated in Fig. 4.1, the currents in sMFC increased with decreasing ER and were in agreement with previous reports (Song et al. 2010; Cao et al. 2015). The rapid initial increase in the sMFC current occurred as a result of the high readily oxidized organic content of the soil and the accumulation of the electrochemically active biofilm on the anode (i.e. *Geobacter*) (Logan et al. 2007; Quan et al 2013; Yu et al. 2017). The steady decrease in current observed after day 10 can be attributed to a number of factors such as reduction in the bioavailable DOC in the anode vicinity, cathode limitations and soil pH. Firstly, since no external DOC was supply to the sMFC and the mass transfer of DOC is limited in soil, a decline in DOC near the anode could have resulted in the current decrease (Holmes et al. 2004; Hong et al. 2009), because DOC is the main electron donor to ARB (Reimers et al.2001; Hong et al. 2009; Gustave et al. 2018). Furthermore, the cathode potential may have also contributed to the decrease in current as depicted in Fig. S 4.1 by the sharp decrease in cathode potential with decreasing resistance compared to that of the anode, which that the cathode became the limitation for the current generation (Song et al. 2010; Wang et al. 2012). Additional, the decrease in pH in the anode vicinity could have also contributed to the drop in current. Previous studies have shown that the ARB activity was slower in slightly acidic pH conditions (Ishii et al. 2008; Jadhav et al. 2009). The results obtained in this study were in accordance with that of Hong et al. (2009) and Holmes et al. (2004). In both studies, a maximum current was achieved within 10-20 days which was followed by a gradual decrease in current production with time.

The different intensity observed in current peak at different ER, was probably due to the increase in internal resistance with increasing ER (Fig. 4.2) (Song et al. 2010; Cao et al. 2015). Since lower ER can reduce the extracellular electron transfer resistance which results in the increase of electron transfer rate (Gill et al. 2003). Although the internal resistance of sMFC depends on the applied ER, it was not constant. A number of other limiting factors such as soil conductivity, organic matter availability, electrode resistance, and bacterial activity and soil pH can also affect the internal resistance (Logan 2008; Hong et al. 2009; Jadhav et al. 2009; Huan et al. 2014). In our study, we observed higher OM removal efficiencies and lower pH in the sMFC at 200 Ω compared to the sMFC at 1000 Ω. Thus, the lower pH and OM in the sMFC at 200 Ω could have been responsible for the higher internal resistance. Zhuang et al. (2010) observed that higher pH in the anode chamber improved MFC performance and lowered internal resistance. Moreover, because there is a direct relation between OM bioavailability and ARB activity, the lower OM in the sMFC at 200 Ω could have resulted in lower ARB activity. Further, the relatively high voltage observed in the control suggest that anode was under anaerobic conditions and the cathode was in aerobic conditions, since voltage is the difference in potential between that anode and the cathode (De Schamphelaire et al. 2008; Hong et al. 2010).

The increase in current with lower ER led to the higher removal efficiency of LOI in treatments fixed at low ER due to stimulated increase of anaerobe metabolic activities (Fig. 4.5). Previous studies have shown that current can accelerate the metabolic reaction rate in anaerobic bacteria by enhancing the release of enzymes and altering the permeability of anaerobes cell membrane (Pitts et al. 2003; Yu et al. 2017). Thus, increase in electron transfer rate from anode to cathode due to lower ohmic resistance improved bacterial metabolism of both the anaerobic bacteria in the anode vicinity and the bulk soil. This consequently led to the higher removal of OM by the sMFC with the 50 Ω, 80 Ω, and 200 Ω and 1000 Ω circuit load.

The relatively lower current at 2000 Ω circuit load results in minimal OM removal compared to the control. Many studies have reported that enhanced OM removal at lower ER attributes this phenomenon due to increase in bacterial activity (Song et al. 2010; Cao et al. 2015).

The increase in current and decrease in OM content in the treatment were probably responsible for the slightly lower concentration of As, Fe and Ni in the anode vicinity. Studies have shown that organic carbon is the main electron donor for anaerobic reduction of Fe oxide minerals bearing metals and metalloids. A positive correlation has also been observed between Fe and As mobilization and DOC bioavailability in paddy soil (Gustave et al. 2018). Gustave et al. (2018) observed a positive correlation between dissolved Fe and As in porewater and DOC concentration in sMFC. Moreover, the reduction of Ni in the anode vicinity of the treatment was probably due to electromigration and immobilization of Ni on the anode (Giannis et al. 2010).

The effect of different ER on bacterial community structure enriched in the bulk soil and the anode vicinity revealed differences in community profiles in the vicinity of the anode and minor changes in that of the bulk soils. As shown in the PCoA analysis (Fig. 4.3) and NMDS (Fig. S 4.3) the anode community can be divided into two groups. Samples taken from the anode vicinity with lower circuit loads (50 Ω, 80 Ω and 200 Ω i.e. high current) were similar and those from higher ER (1000 and 2000 Ω i.e. low current) were more comparable to the control. The results observed here suggest that distinct bacterial communities developed at different current densities.

The similarity in anode potential in groups with lower or higher ER could be the reason for the observed pattern. Numerous studies have shown that bacterial community varied depending on the anode potentials (Aelterman et al. 2008; Rismani-Yazdi et al. 2011). In addition, the anode has been shown to accelerate the metabolic rate and development of electroactive bacterial community in its vicinity (Aelterman et al. 2008; Rismani-Yazdi et al.

2011). In a study on the effects of ER on the anode Rismani-Yazdi et al. (2011), observed higher anode potential and columbic efficiency with lower ER. The authors concluded that lower ER produces higher current and that ER can be used to control anode potential and for the selection of ARB. Thus, it could be assumed that higher ER possibly limited ARB colonization and metabolic activities on the anode and vice versa when ER were reduced. Therefore, our results demonstrates for the first time that lower ER could be used to selectively enhance ARB in the anode vicinity and the associated bulk soil.

Moreover, taxonomical analysis of the anode community indicated that reducing ER enhances ARB such as *Deltaproteobacteria* and *Nitrospira*. This occurred because when ARB transfers electrons to the anode with higher electrochemical potentials, these ARB obtain more energy (Aelterman et al. 2008; Srikanth et al. 2010; Huan et al. 2014). Thus, at lower ER higher current generation and relative abundance of ARB were observed. Previous studies have demonstrated that *Geobacter* sp. current generation properties and growth were strongly affected by the anode potentials (Srikanth et al. 2008; Wei et al. 2010). Torres, et al. (2009) investigated the bacterial community at different anode potential and found that lower anode potential had a high selection of the *Geobacter* sp. since they are able to transfer electrons to the anode efficiently with minimal energy loss. These results were in line with our findings where *Geobacter* relative abundance increased with decreasing ER (Fig. 4.4). The results obtained here demonstrate that ER can significantly influence the composition of anode bacterial communities by selectively enhancing electrogenic bacteria.

4.6. Conclusions

In this study the effect of different ER on the sMFC performance, OM removal and bacterial community composition were collectively investigated. The results showed significant influences of ER on current production, OM removal efficiency and bacterial diversity. In particular, greater current densities, OM removal efficiencies and enhancement of

Geobacter were observed at lower ER (50 Ω, 80 Ω and 200 Ω). The current study illustrates that lower ER can be used to selectively enhance ARB relative abundance and increase OM removal efficiencies while decreasing metal concentration in soil porewater.

4.7. References

Abbas S Z, Rafatullah M, Ismail N, Syakir MI., 2017. A review on sediment microbial fuel cells as a new source of sustainable energy and heavy metal remediation: Mechanisms and future prospective. Int. J. Energy. Res. 41:1242-1264

Aelterman P, Freguia S, Keller J, Verstraete W, Rabaey K, 2008. The anode potential regulates bacterial activity in microbial fuel cells. Appl Microbiol Biotechnol 78:409-418

Cao X, Song H L, Yu C Y, Li X N, 2015. Simultaneous degradation of toxic refractory organic pesticide and bioelectricity generation using a soil microbial fuel cell. Bioresour. Technol. 189:87-93

Chen Z, Huang Y C, Liang J H, Zhao F, Zhu Y G, 2012. A novel sediment microbial fuel cell with a biocathode in the rice rhizosphere. Bioresour Technol 108:55-59

Chen Z, Zhu B K, Jia W F, Liang J H, Sun G X, 2015. Can electrokinetic removal of metals from contaminated paddy soils be powered by microbial fuel cells? Environ. Technol. Innov.3:63-67

De Schamphelaire L, Rabaey K, Boeckx P, Boon N, Verstraete W, 2008. Outlook for benefits of sediment microbial fuel cells with two bio-electrodes. Microb. Biotechnol. 1:446-462

Del Campo AG, Cañizares P, Lobato J, Rodrigo M, Morales FF, 2014. Effects of external resistance on microbial fuel cell's performance, Environment, energy and climate change II. Springer 175-197

Giannis A, Pentari D, Wang J Y, Gidarakos E, 2010. Application of sequential extraction analysis to electrokinetic remediation of cadmium, nickel and zinc from contaminated soils. J. Hazard. Mater. 184:547-554

Gil G C, Chang I S, Kim B H, Kim M, Jang J K, Park H S, Kim H J, 2003. Operational parameters affecting the performannce of a mediator-less microbial fuel cell. Biosens. Bioelectron. 18: 327-34

Gustave W, Yuan Z F, Sekar R, Chang H C, Zhang J, Wells M, Ren Y X, Chen Z, 2018. Arsenic mitigation in paddy soils by using microbial fuel cells. Environ. Pollut. 238:647-655

Holmes D E, Bond D R, O'Neil R A, Reimers C E, Tender L R, Lovley D R, 2004. Microbial communities associated with electrodes harvesting electricity from a variety of aquatic sediments. Microb. Ecol. 48:178-190

Hong S W, Chang I S, Choi Y S, Chung T H, 2009. Experimental evaluation of influential factors for electricity harvesting from sediment using microbial fuel cell. Bioresour. Technol. 100:3029-3035

Hong S W, Chang I S, Choi Y S, Kim B H, Chung T H. 2009a. Responses from freshwater sediment during electricity generation using microbial fuel cells. Bioprocess Biosyst. Eng. 32:389-395

Huan D, Yi C W, Zhang F, Huang Z C, Zheng C, Hui J X, Feng Z, 2014. Factors affecting the performance of single-chamber soil microbial fuel cells for power generation. Pedosphere 24:330-338

Huang D Y, Zhou S G, Chen Q, Zhao B, Yuan Y, Zhuang L, 2011. Enhanced anaerobic degradation of organic pollutants in a soil microbial fuel cell. Chem. Eng. J. 172:647-653

Huijuan L I, Jingjing P, Hongbo L I, 2012. Diversity and characterization of potential h2-dependent fe(iii)-reducing bacteria in paddy soils. Pedosphere 22:673-680

Ishii S I, Hotta Y, Watanabe K, 2008. Methanogenesis versus electrogenesis: morphological and phylogenetic comparisons of microbial communities. Biosci. Biotechnol. Biochem. 72:286-94

Jadhav G S, Ghangrekar M M, 2009. Performance of microbial fuel cell subjected to variation in pH, temperature, external load and substrate concentration. Bioresour. Technol. 100:717-23

Jang J K, Chang I S, Kang K H, Moon H, Cho K S, Kim B H, 2004. Construction and operation of a novel mediator- and membrane-less microbial fuel cell. Process. Biochem. 39:1007-12

Jung S, Regan J M, 2011. Influence of external resistance on electrogenesis, methanogenesis, and anode prokaryotic communities in microbial fuel cells. Appl. Environ. Microbiol. 77:564-571

Kaku N, Yonezawa N, Kodama Y, Watanabe K, 2008. Plant/microbe cooperation for electricity generation in a rice paddy field. Appl. Microbiol. Biotechnol. 79:43-49

Kouzuma A, Kaku N, Watanabe K, 2014. Microbial electricity generation in rice paddy fields: Recent advances and perspectives in rhizosphere microbial fuel cells. Appl. Microbiol. Biotechnol. 98:9521-9526

Logan B E 2008. Microbial fuel cells. A John Wiley & Sons, Inc.

Logan B, Cheng S, Watson V, Estadt G, 2007. Graphite fiber brush anodes for increased power production in air-cathode microbial fuel cells. Environ. Sci. Technol. 4:3341-6

Lu L, Huggins T, Jin S, Zuo Y, Ren Z J, 2014. Microbial metabolism and community structure in response to bioelectrochemically enhanced remediation of petroleum hydrocarbon-contaminated soil. Environ. Sci. Technol. 48:4021

Menicucci J, Beyenal H, Marsili E, Veluchamy RA, Demir G, Lewandowski Z, 2006. Procedure for determining maximum sustainable power generated by microbial fuel cells. Environ. Sci. Technol. 40:1062-8

Min B, Román ÓB, Angelidaki I, 2008. Importance of temperature and anodic medium composition on microbial fuel cell (MFC) performance. Biotechnol. Lett. 30:1213-8

Mohan S V, Mohanakrishna G, Reddy B P, Saravanan R, Sarma P, 2008. Bioelectricity generation from chemical wastewater treatment in mediatorless (anode) microbial fuel cell (mfc) using selectively enriched hydrogen producing mixed culture under acidophilic microenvironment. Biochem. Eng. J. 39:121-130

Nicol G W, Leininger S, Schleper C, Prosser J I, 2008. The influence of soil ph on the diversity, abundance and transcriptional activity of ammonia oxidizing archaea and bacteria. Environ. Microbiol. 10:2966-2978

Pettridge J, Firestone M K, 2005. Redox fluctuation structures microbial communities in a wet tropical soil. Appl. Environ. Microbiol. 71:6998-7007

Pitts K, Dobbin P S, Reyesramirez F, Thomson A J, Richardson D J, Seward H E, 2003. Characterization of the Shewanella oneidensis mr-1 decaheme cytochrome mtra expression in Escherichia coli confers the ability to reduce soluble Fe(III) chelates. J. Biol. Chem. 278:27758-27765

Quan X C, Quan Y P, Tao K, Jiang X M, 2013. Comparative investigation on microbial community and electricity generation in aerobic and anaerobic enriched MFCs. Bioresour. Technol. 128:259-65

Rismani-Yazdi H, Christy A D, Carver S M, Yu Z, Dehority B A, Tuovinen O H, 2011. Effect of external resistance on bacterial diversity and metabolism in cellulose-fed microbial fuel cells. Bioresour. Technol. 102:278-283

Song T S, Yan Z S, Zhao Z W, Jiang H L, 2010. Removal of organic matter in freshwater sediment by microbial fuel cells at various external resistances. J. Chem. Technol. Biotechnol. 85:1489-1493

Srikanth S, Marsili E, Flickinger M C, Bond D R, 2008. Electrochemical characterization of geobacter sulfurreducens cells immobilized on graphite paper electrodes. Biotechnol. Bioeng. 99:1065-1073

Srikanth S, Mohan S V, Sarma P N, 2010. Positive anodic poised potential regulates microbial fuel cell performance with the function of open and closed circuitry. Bioresour. Technol. 101:5337-5344

Sun W, Xiao E, Dong Y, Tang S, Krumins V, Ning Z, Sun M, Zhao Y, Wu S, Xiao T, 2016. Profiling microbial community in a watershed heavily contaminated by an active antimony (Sb) mine in Southwest China. Sci. Total Environ. 550:297-308

Torres C I, Krajmalnikbrown R, Parameswaran P, Marcus A K, Wanger G, Gorby Y A, Rittmann B E, 2009. Selecting anode-respiring bacteria based on anode potential: Phylogenetic, electrochemical, and microscopic characterization. Environ. Sci. Technol. 43:9519-9524

Touch N, Hibino T, Morimoto Y, Kinjo N, 2017. Relaxing the formation of hypoxic bottom water with sediment microbial fuel cells. Environ. Technol. 38: 3016-3025

Wang A, Cheng H, Ren N, Cui D, Lin N, Wu W, 2012. Sediment microbial fuel cell with floating biocathode for organic removal and energy recovery. Front. Environ. Sci. Eng. 6: 569-74

Wang C, Deng H, Zhao F, 2015. The remediation of chromium (VI)-contaminated soils using microbial fuel cells. Soil Sediment Contam. 25: 1-12

Wang N, Chen Z, Li H B, Su J Q, Zhao F, Zhu Y G, 2015. Bacterial community composition at anodes of microbial fuel cells for paddy soils: The effects of soil properties. J. Soils Sediments 15: 926-936

Wang N, Xue X, Juhasz A L, Chang Z, Li H, 2017. Biochar increases arsenic release from an anaerobic paddy soil due to enhanced microbial reduction of iron and arsenic. Environ. Pollut. 220:514-522

Wei J, Liang P, Cao X, Huang X, 2010. A new insight into potential regulation on growth and power generation of geobacter sulfurreducens in microbial fuel cells based on energy viewpoint. Environ. Sci. Technol. 44:3187-3191

Wu Y, Zeng J, Zhu Q, Zhang Z, Lin X, 2017. pH is the primary determinant of the bacterial community structure in agricultural soils impacted by polycyclic aromatic hydrocarbon pollution. Sci. Rep. 7:40093

Xiao E, Krumins V, Xiao T, Dong Y, Song T, Ning Z, Huang Z, Sun W, 2016. Depth-resolved microbial community analyses in two contrasting soil cores contaminated by antimony and arsenic. Environ. Pollut. 221:244

Yu B, Tian J, Feng L, 2017. Remediation of pah polluted soils using a soil microbial fuel cell: Influence of electrode interval and role of microbial community. J. Hazard. Mater. 336:110

Zhang C P, Shan-Shan C, Guang Li L, Zhang R D, Jian X, 2012. Characterization of strain pseudomonas sp. Q1 in microbial fuel cell for treatment of quinoline-contaminated water. Pedosphere 22:528-535

Zhou Y, Jiang H, Cai H, 2015. To prevent the occurrence of black water agglomerate through delaying decomposition of cyanobacterial bloom biomass by sediment microbial fuel cell. J. Hazard. Mater. 287:7-15

Zhu X, Yates M D, Hatzell M C, Rao H A, Saikaly P E, Logan B E, 2014. Microbial community composition is unaffected by anode potential. Environ. Sci. Technol. 48:1352-1358

Zhuang L, Zhou S, Li Y, Yuan Y, 2010. Enhanced performance of air-cathode two-chamber microbial fuel cells with high-pH anode and low-pH cathode. Bioresour. Technol. 101: 3514-9

4.8. Supplementary data

The effect of the sMFC on paddy soil components at different external resistance

Table S 4.1 Similarity-based OTUs and species richness and diversity estimates.

Sample ID	Reads	ACE	Chao1	Shannon index	Simpson	Good's Coverage
50Ω-S	65782 ±6751	1062 ±4.36	1079 ±3.50	8.28 ±0.13	0.991 ±0.00	0.997 ±0.00
80Ω-S	61413 ±10933	1058 ±4.64	1080 ±4.20	8.22 ±0.01	0.991 ±0.00	0.998 ±0.00
200Ω-S	61978 ±6980	1055 ±10.50	1064 ±14.03	7.99 ±0.04	0.988 ±0.00	0.997 ±0.00
1000Ω-S	64995 ±7878	1049 ±1.71	1057 ±5.57	8.08 ±0.05	0.989 ±0.00	0.998 ±0.00
2000Ω-S	60396 ±5919	1054 ±2.20	1069 ±6.58	8.16 ±0.05	0.990 ±0.00	0.997 ±0.00
Control-S	56614 ±2383	1003 ±6.52	1010 ±9.16	7.89 ±0.04	0.986 ±0.00	0.997 ±0.00
50Ω-A	52651 ±2032	1083 ±9.25	1097 ±9.28	7.81 ±0.06	0.987 ±0.00	0.996 ±0.00
80Ω-A	52177 ±5131	1061 ±13.44	1064 ±11.77	7.79 ±0.05	0.986 ±0.00	0.997 ±0.00
200Ω-A	50053 ±1202	1055 ±6.89	1067 ±8.51	7.52 ±0.03	0.982 ±0.00	0.996 ±0.00
1000Ω-A	75216 ±14811	1108 ±4.62	1123 ±17.53	8.10 ±0.02	0.989 ±0.00	0.997 ±0.00

2000Ω-A	59405 ±2795	1075 ±27.95	1086 ±3.44	7.77 ±0.01	0.986 ±0.00	0.997 ±0.00
Control-A	60832 ±822	1097 ±5.82	1104 ±8.05	8.24 ±0.04	0.991 ±0.00	0.997 ±0.00

Notes S and A: represents samples collected from bulk soil and anode vicinity respectively. The values represent the mean ±standard error of three replicate samples.

Table S 4.2 Changes of pH in soil samples of sMFC set at different external resistance at the end of the experiment.

	Sample ID					
Location	**2000 Ω**	**1000 Ω**	**200 Ω**	**80 Ω**	**50 Ω**	**Control**
Bulk soil	5.88±0.01	5.84±0.02	5.77±0.01	5.73±0.01	5.70±0.0	6.47±0.04
Anode Vicinity	5.75±0.03	5.66±0.02	5.56±0.02	5.60±0.01	5.67±0.01	6.81±0.01

Notes: Values represents mean ± SE (n = 3).

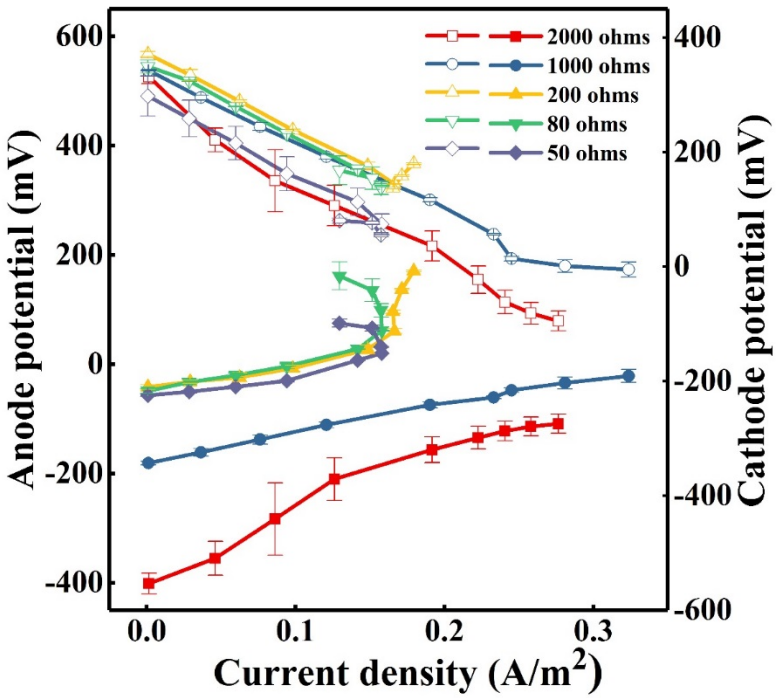

Figure S 4.1 Anode (filled symbols) and cathode (open symbols) polarization curves. The error bars represent standard error of measured potentials of triplicate samples.

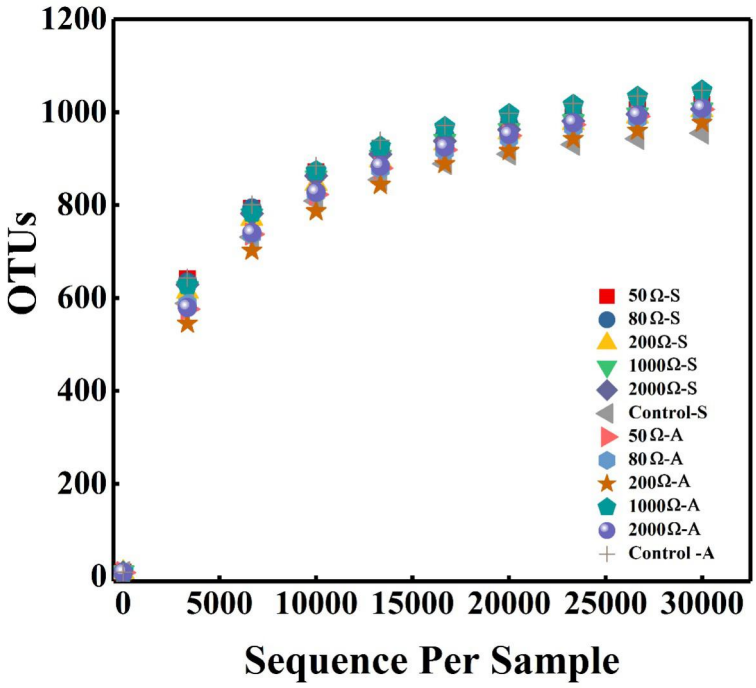

Figure S 4.2 Rarefaction curves showing the diversity of OTUs (similarity cut off of 97%). OTUs, Operational Taxonomic Units

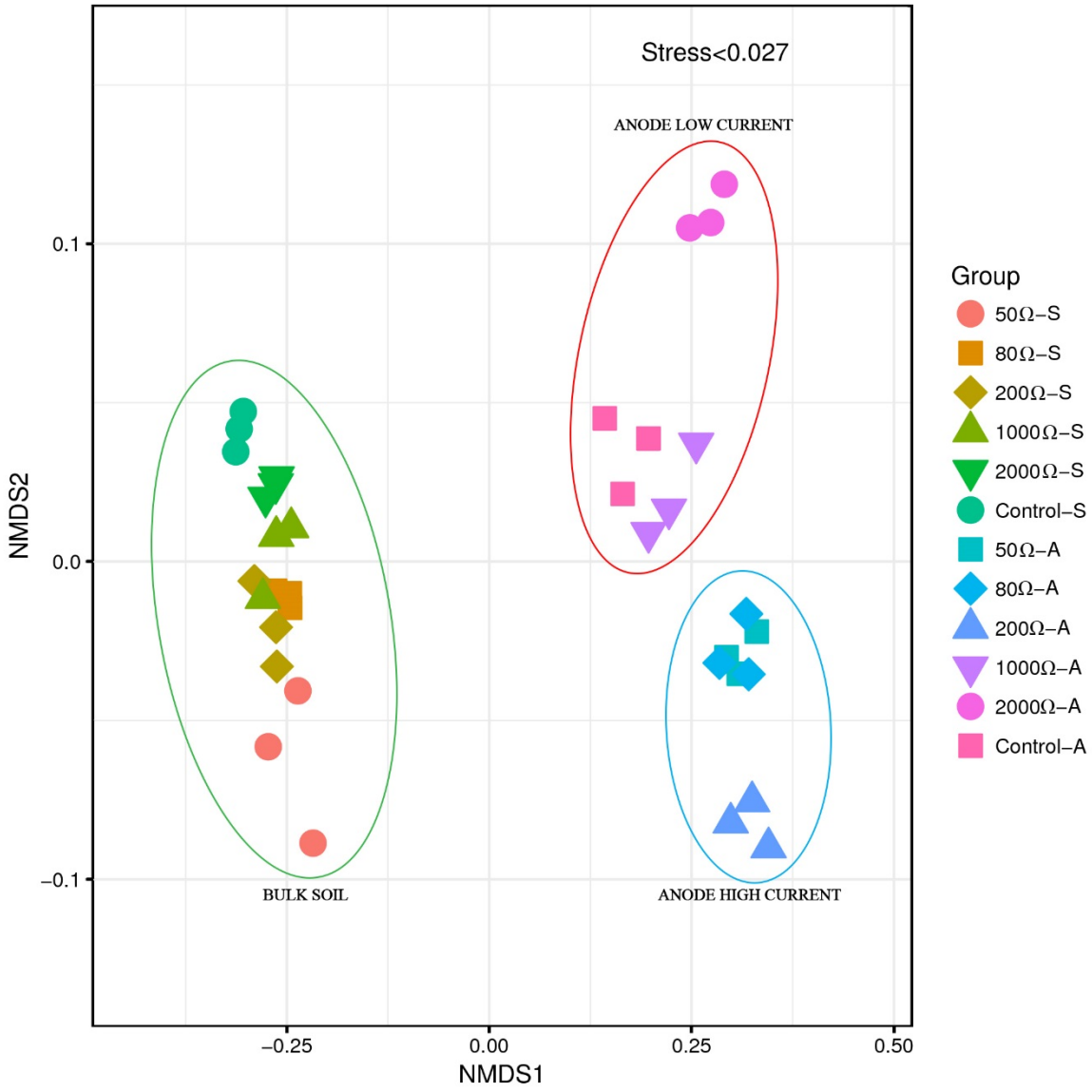

Figure S 4.3 Non-metric multidimensional scaling (NMDS) ordination diagrams of the variations in bacterial community structures for the sMFC with different external resistance and controls. The ordination is based on Bray–Curtis similarity matrices of the relative abundance data obtained from high-throughput amplicon sequencing for the bacterial community.

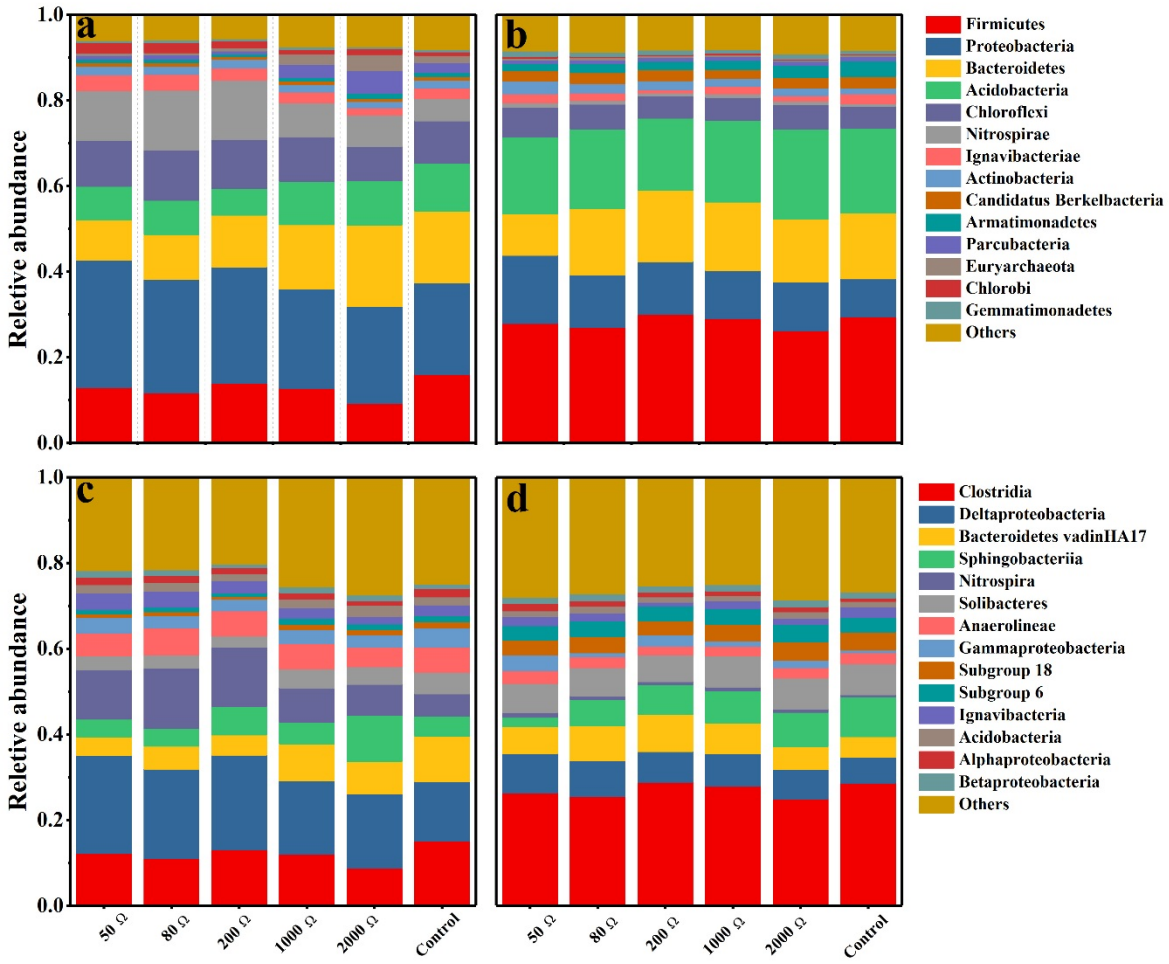

Figure S 4.4 Relative abundance of bacterial community composition at phylum and class levels ((a) = anode vicinity; (b) =bulk soil).

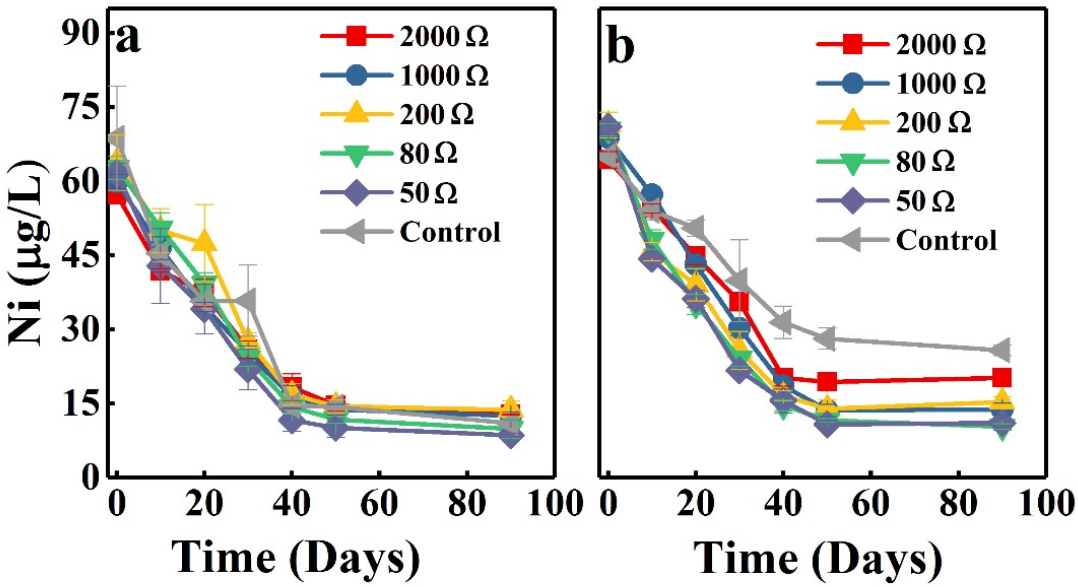

Figure S 4.5 Variations in Nickel in soil porewater along with incubation time. a and b represent nickel concentration in the bulk soil and anode vicinity, respectively. The error bars represent standard error of measured concentrations of triplicates samples.

Chapter 5 : The effect of the sMFC on arsenic in soil with low organic matter content

5.1. Abstract

Arsenic (As) behavior in paddy soils couples with the redox process of iron (Fe) minerals. When soil is flooded, Fe oxides are transformed to soluble ferrous ions by accepting the electrons from Fe reducers. This process can significantly affect the fate of As in paddy fields. In this study, we used a novel technique to manipulate the Fe redox processes in paddy soils by deploying soil microbial fuel cells (sMFC). The results showed that the sMFC bioanode can significantly decrease the release of Fe and As into soil porewater. Iron and As contents around sMFC anode were 65.0% and 47.0% of the control respectively at day 50. The observed phenomenon could be explained by a competition for organic substrate between sMFC bioanode and the iron- and arsenic-reducing bacteria in the soils. In the vicinity of bioanode, organic matter removal efficiencies were 10.3% and 14.0 % higher than the control for lost on ignition carbon (LOI) and total organic carbon (TOC), respectively. Sequencing of the 16S rRNA genes suggested that the influence of bioanodes on bulk soil bacterial community structure was minimal. Moreover, during the experiment a maximum current and power density of 0.31 mA and 12.0 mWm^{-2} were obtained, respectively. This study shows a novel way to limit the release of Fe and As in soils porewater and simultaneously generate electricity.

5.2. Introduction

Rice paddy soils are rich in iron (Fe) oxides, which serve as a potent repository for many soil contaminants, especially arsenic (As) (Li et al., 2011; Wang et al., 2009). When paddy soil becomes anoxic, bacteria oxidize organic matter (OM) to carbon dioxide (CO_2) and use soluble and insoluble electron acceptors such as sulfate, nitrate, arsenate (As(V)) and Fe (oxy)hydroxides as the final electron acceptors (Lovley et al., 2004; Lovley and Phillips, 1986; Qiao et al., 2017a; Qiao et al., 2017b). The transfer of electrons to Fe (oxy)hydroxide by iron reducing bacteria (IRB) is prevalent in flooded paddy soils and this results in the dissolution of Fe and consequent release of As(V), which can then be reduced to arsenite (As(III)) by As(V)-reducing and dissimilatory As(V)-reducing microorganisms (Qiao et al., 2017b; Roden et al., 2010; Shelobolina et al., 2003). In addition, the direct reduction of As(V) to As(III) from the surface of metal oxides can also enhance the release of As into the soil porewater (Qiao et al., 2017b; Takahashi et al., 2004). The reduction of Fe(III) and As(V) in turn increases As bioavailability and subsequent uptake of As by rice plants via the silicon pathway (Seyfferth et al., 2014; Seyfferth et al., 2017; Seyfferth et al., 2018; Williams et al., 2006; Zhu et al., 2008). The increased bioavailability of As in flooded paddy soil is a major concern because rice is consumed worldwide and the chronic consumption of As tainted rice expose individuals to this harmful carcinogen (Barragan et al., 2011; Chaney et al., 2016; Vithanage et al., 2017; Zhu et al., 2008). Hence there is an urgent need to develop ways to limit As bioavailability in paddy soil.

The redox cycles occurring in paddy fields give rise to electricity upon implantation of soil microbial fuel cells (sMFC) (Chen et al., 2012; De Schamphelaire et al., 2010; Kaku et al., 2008). A simultaneous outcome is that sMFCs are environmentally friendly bioelectrochemical systems that have the capacity to remove pollutants (Li and Yu, 2015). In sMFCs, exoelectrogens oxidize organic substrates and transfer electrons to the bioanode (Logan, 2008;

Rezaei et al., 2007). The electrons are then transferred to the cathode across an external circuit, where they reduce oxygen (Logan et al., 2006). Thus the bioanode of the sMFC is able to work as a continuous sink for electrons produced during the oxidation of organic substrates and in the same way influence soil redox chemistry and microbiology (Huang et al., 2011; Logan, 2009).

Previous studies have shown that the sMFC can immobilize and even extract metal ions by changing their redox state or via electrokinetic processes. It has been demonstrated that sMFC can facilitate the reduction of carcinogenic and mutagenic substance such Cr(VI) and U(VI) to the less harmful species (e.g. Cr(III) and U(IV)) in the cathode chamber (Wang et al., 2015a). Similarly, the bioanode has also been used to for the *in situ* bioremediation of U(VI) (Gregory and Lovley, 2005). Chen et al. (2015) demonstrated that the sMFC can be used to produce sufficient energy to extract zinc and cadmium removal from paddy soils via electrokinetic transport to the cathode chamber. In addition to metal remediation, sMFC have also been utilized in nutrient (Martins et al., 2014; Xu et al., 2017; Yang et al., 2016; Zhang and Angelidaki, 2012) and OM (Morris and Jin, 2012; Song et al., 2010; Xun et al., 2016; Zhu et al., 2016) removal. The sMFC favors phosphate and nitrogen removal from overlying waters by increasing soil redox potential, Fe(III) concentration and overlying water pH (Martins et al., 2014; Yang et al., 2016). However, few studies have investigated the influence of the bioanode on bulk soil Fe oxides and the elements coupled with Fe cycle in contaminated paddy soils.

When the sMFC operates in paddy soils, the bioanode may change the bacterial community (Lu et al., 2014), acidify soils (Hong et al., 2009; Jang et al., 2004) and deplete bioaccessible organic substrate (Morris and Jin, 2012; Song et al., 2010; Xun et al., 2016; Zhu et al., 2016). Recent studies have provided evidence that Fe containing mineral reduction in flooded soils might also be influenced by the buried bioanode (Touch et al., 2017; Yang et al., 2016). However, it is still unknown whether the bioanode can affect the behaviors of Fe and

soil trace elements, especially As bound with Fe mineral, in paddy soils, which have great significance in both plant nutrition and food safety. Given that the bioanode may affect Fe mineral behavior and can stimulate dissolved organic carbon (DOC) removal (Xu, 2015), we tried to manipulate redox processes in As-contaminated paddy soils by deploying sMFCs and observing changes in soil porewater total Fe and As concentration over time. Additionally, the effect of the bioanode on the bacterial community and paddy soil physiochemical properties at various distances away were also elucidated.

5.3. Materials and Methods

5.3.1. Paddy Soil Sample

Subsurface paddy soil was collected from an arsenic-contaminated paddy field in Shangyu, Zhejiang, China (N29.159 E119.957). The soil contained 140 mg total As kg^{-1} due to contamination from nearby mining activities. Selective soil properties were determined and are presented in Table S 5.1.

5.3.2. Soil Microbial Fuel Cell Assembly

Eight sMFCs, were assembled following the method previously described in chapter 2 with few modifications. Four were replicate treatments (close circuit) and four replicate controls (open circuit). Each sMFC contained 1 kg (dry weight) of paddy soil. A light-proof columnar polyethylene terephthalate container (10 cm diameter × 15 cm depth) was used to construct each sMFC. Soil porewater was sampled through 3 valve ports (Top: 1cm below the soil water inter phase, Middle: ~2 cm above the bioanode and Bottom: adjacent to the bioanode) by using a self-made sampler with 0.45 μm hollow fiber membrane (modified polyethersulfone, Motimo Membrane Technology Co., Ltd, Tianjin, China). Both the anode and cathode of the sMFC were prepared from circular carbon felt with a geometric surface area of 50.2 cm^2. A data logger (USB-6225, National Instrument, Austin, USA) was used to monitor the voltage between the anode and cathode continuously across a 500 Ohm resistor.

In each sMFC container, a 1 cm depth of soil was added and then the anode was placed on the surface of the soil layer. The remaining soil sample was then used to bury the anode. Then deionized water was used to flood the paddy soil to stimulate the natural conditions leaving 500 ml of overlying water. Additional water was added daily to each sMFC to compensate for water lost due to evaporation. The cathode was installed in the overlaying water in aerobic conditions. All of the cells were incubated in the dark for 60 days at 28 ºC.

5.3.3. Chemical Analysis

Total As and Fe concentrations in soil porewater were determined from day 0 to 50 at 10 days intervals. The soil from top, middle and bottom layers were collected on day 60 from both the sMFC and the control. The samples were homogenized and the content of total organic carbon (TOC) and loss on ignition (LOI) carbon was determined. Soil pH and redox potentials (*E*h) were measured. The Eh of the soil was measured approximately 0.5 cm above the bioanode and was allowed to stabilize for 1 h before recording. The pH was determined from a soil slurry made by mixing dry soil with deionized water at a ratio of 1:2.5. All of the above were determine according to the methods describe in chapter 2.

5.3.4. Microbial Community Analysis

The bacterial communities of all the sMFC were characterized at the end of the experiment by 16S rRNA gene targeted Illumina sequencing. Briefly, 0.25 g of soil was carefully sampled from the top and middle location within each replicates sMFC. Whereas in the anode location, 0.25 g of attached soil and biofilm were carefully scraped from the anode with a sterile razor and the genomic DNA was immediately extracted from the samples using Powersoil DNA isolation Kit (MoBio Laboratories, Carlsbad, CA, USA) according to the manufacturer's instructions. The DNA concentration was quantified by a spectrophotometer (Qubit 2.0 Fluorometer, Thermo Scientific, USA) and was stored at - 80 °C until sequencing. The V4-V5 region of the bacterial 16S rRNA genes were amplified using the forward primers

347F (5'-CCTACGGRRBGCASCAGKVRVGAAT-3') and reverse primers 802R (5'-GGACTACNVGGGTWTCTAATCC-3'). Details for Illumina sequencing, experimental steps and data analyses are described in chapter 2.

5.3.5. Nucleotide sequence accession number

Nucleotide sequences were all deposited in the GeneBank database with accession numbers MG100883-MG101815.

5.4. Results and Discussion

5.4.1. Power output of sMFC in As contaminated soil

Current from the sMFC during the experiment is shown in Fig.5.1a. The produced current increased sharply after connecting the 500 Ohm external resister, without any lag time and reached the first peak at around 0.2 mA on day 10. Afterwards, the current was quasi-steady, with slight fluctuations until the end of the experiment. The rapid increase in current production is indicative of the acclimatization of electrogenic bacteria on the bioanode and the oscillating current production that followed was probably due to the heterogeneous nature of DOC in soil (Hong et al., 2010).

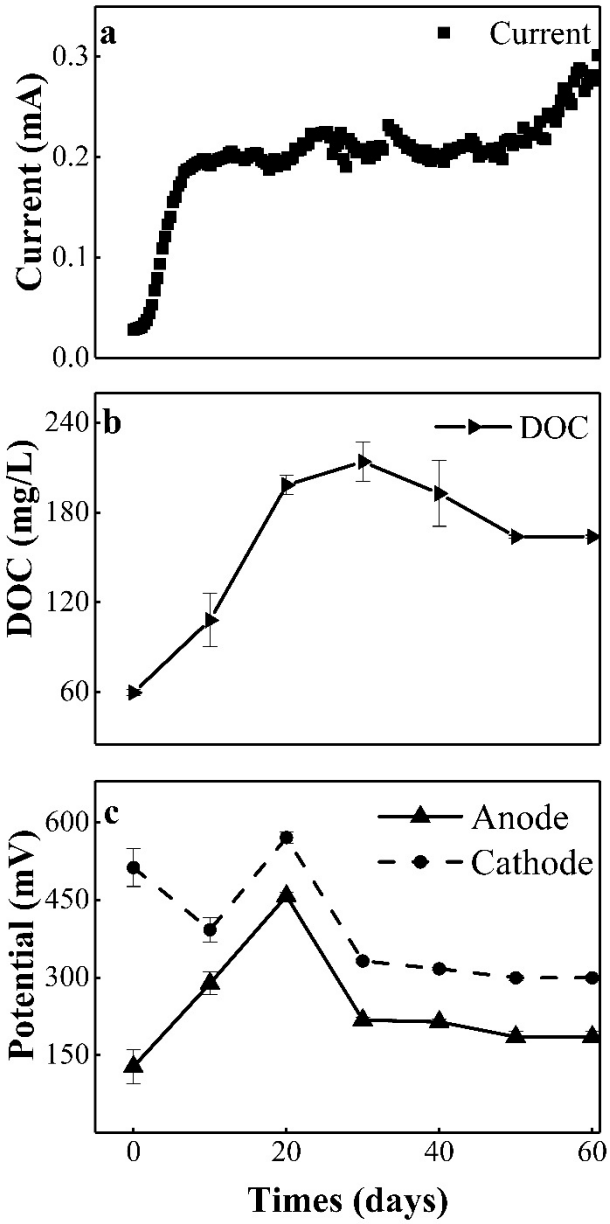

Figure 5.1 Relationship between current output (a), porewater DOC concentration (b), anode and cathode potential (c) over time. The error bars represent standard error of measured concentrations of four replicate samples.

In addition to current production, the change of porewater DOC concentration and the potential of both the anode and cathode are also shown in Fig. 5.1b-c. The DOC concentration increased rapidly within 30 days and then decreased slightly before stabilization at 163 mg L^{-1} on day 50. The anode potential rose sharply from 128 mV to 457 mV on day 20, then decreased

to 218 mV on day 30 where it remained relatively stable until the end of the experiment. The cathode potential fluctuated between 513 mV and 571 mV from day 0 to day 20. Afterwards the cathode potential decreased to 332 mV and varied slightly until day 60. These results indicate that the anode performance determined the current produced by the cell, which was dominated by the bioavailable DOC content of the soil porewater.

A polarization curve was obtained on day 15 when the power was quasi-stable. As illustrated in Fig. S 5.1, the maximum power density (normalized to the anode geometric surface area) was found to be 12.0 m Wm^{-2}, when the current density was 50.0 m Am^{-2} and the external resistance was 1000 Ohm. The power density obtained in this study was comparable to those observed in other studies (Kaku et al., 2008; Sajana et al., 2014; Takanezawa et al., 2010) and could be attributed to the DOC content, since DOC serves as the main substrate pool for bacterial extracellular respiration (Fig.5.1b).

5.4.2. Effects of the sMFC on soil OM, pH and *E*h

Both TOC and LOI carbon were measured and used to indicate the change in the amount of OM during the sMFC operation. The removal efficiencies of soil OM were calculated by comparing the soil OM content at the end of the experiment to the initial soil OM content. As shown in Fig. 5.2a and b, high OM removal was observed in the vicinity of the anodes, which were comparable to those obtained in previous studies (Song et al., 2010; Xu, 2015; Zhu et al., 2016). The removal efficiencies of TOC were 29.9%, 34.9% and 38.6% in the top, middle and bottom layers respectively in the sMFC. Meanwhile, the removal efficiencies of LOI carbon followed a similar pattern, which were 12.5%, 17.7% and 28.8% in the top, middle and bottom layers respectively in the sMFC. The overall removal efficiency of soil OM in sMFC treatment was higher than that of the control in all the layers. When comparing each layer, the difference in top layer between treatments and controls were insignificant ($p = 0.31$), but very significant in bottom layers ($p = 0.002$). Our findings suggest that the bioanode facilitates OM degradation.

This is reasonable because the bacterial community in the soil can use the bioanode as a final electron acceptor under anaerobic conditions to oxidize OM when other electron acceptors such as oxygen, nitrates and sulfates are depleted (Morris and Jin, 2012; Song et al., 2010; Xun et al., 2016; Zhu et al., 2016).

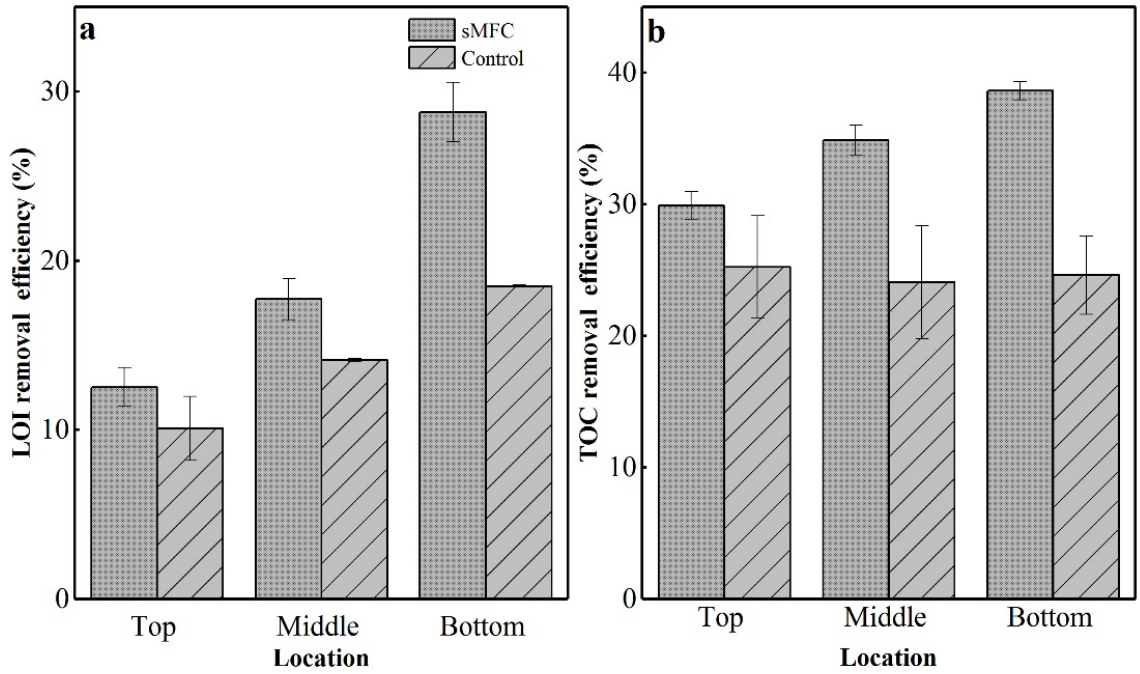

Figure 5.2 Removal efficiencies of LOI carbon (a) and total organic carbon (b) in three layers of soil (Top, Middle, and Bottom) for the sMFC and the control. The error bars represent standard error of measured concentrations of four replicate samples.

In addition to decreasing soil OM content, the sMFC also influenced the soil pH and soil potential (*E*h) and the results are presented in Table S 5.2. The soil pH in the top layer increased approximately 0.4 in the sMFC (6.09) versus the control (5.61), while the pH became more acidic with distances closer to the anode. The pH in the middle (5.39 vs 5.86) and bottom (5.21 vs 5.88) layer were significantly lower in the sMFC compared to the control. The oxidation of OM in the sMFC results in the production of protons in the vicinity of the bioanode and the reduction of oxygen on cathode consumed protons (Hong et al., 2009; Jang et al., 2004).

This led to the decrease in pH in the middle and bottom layers since the mass transfer of protons is slow in soil (Liu et al., 2016). Moreover, the *E*h in the sMFC (-133 mV) was significantly higher than that of the control (-445 mV), which indicated the bioanode altered the redox processes in soils (Hong et al., 2009; Inseop et al., 2006).

5.4.3. Change in total Fe and As concentration

Iron is one of the major redox active elements in paddy soils and the reductive dissolution of Fe(III) plays a vital role in the release of metals. Significant differences in Fe behavior were noticed in the control versus sMFC. Figure 5.3a-c, shows the soluble Fe concentration in different layers increased with incubation time. In the controls Fe concentration dramatically increased in the soil porewater of the top, middle and bottom layers from 0.13 to 57.1 mg L^{-1}, 0.17 to 162 mg L^{-1} and 0.24 to 233 mg L^{-1}, respectively from day 0 to 50. A similar trend in Fe release from the soil to soil porewater was observed in the sMFC. The dissolved Fe concentration in the top, middle and bottom layers increased from 0.20 to 83.1 mg L^{-1}, 0.16 to 109 mg L^{-1}, and 0.19 to 144 mg L^{-1}, respectively from day 0 to 50. Furthermore, average Fe concentration in the soil porewater of the sMFC was lower than that of the control in the middle and bottom layer but not the top layer. In the top layer the concentration of Fe was higher in the sMFC. These results suggest that the bioanode significantly reduced Fe reduction in its vicinity with time. Since the dissolved Fe in the middle and bottom layer of the sMFC was significantly lower ($p = 0.008$ and 0.001, respectively) than that of the control treatment. On the contrary, the results also showed that in the top layer the concentration of Fe was significantly higher ($p = 0.021$) in the sMFC compared to the control.

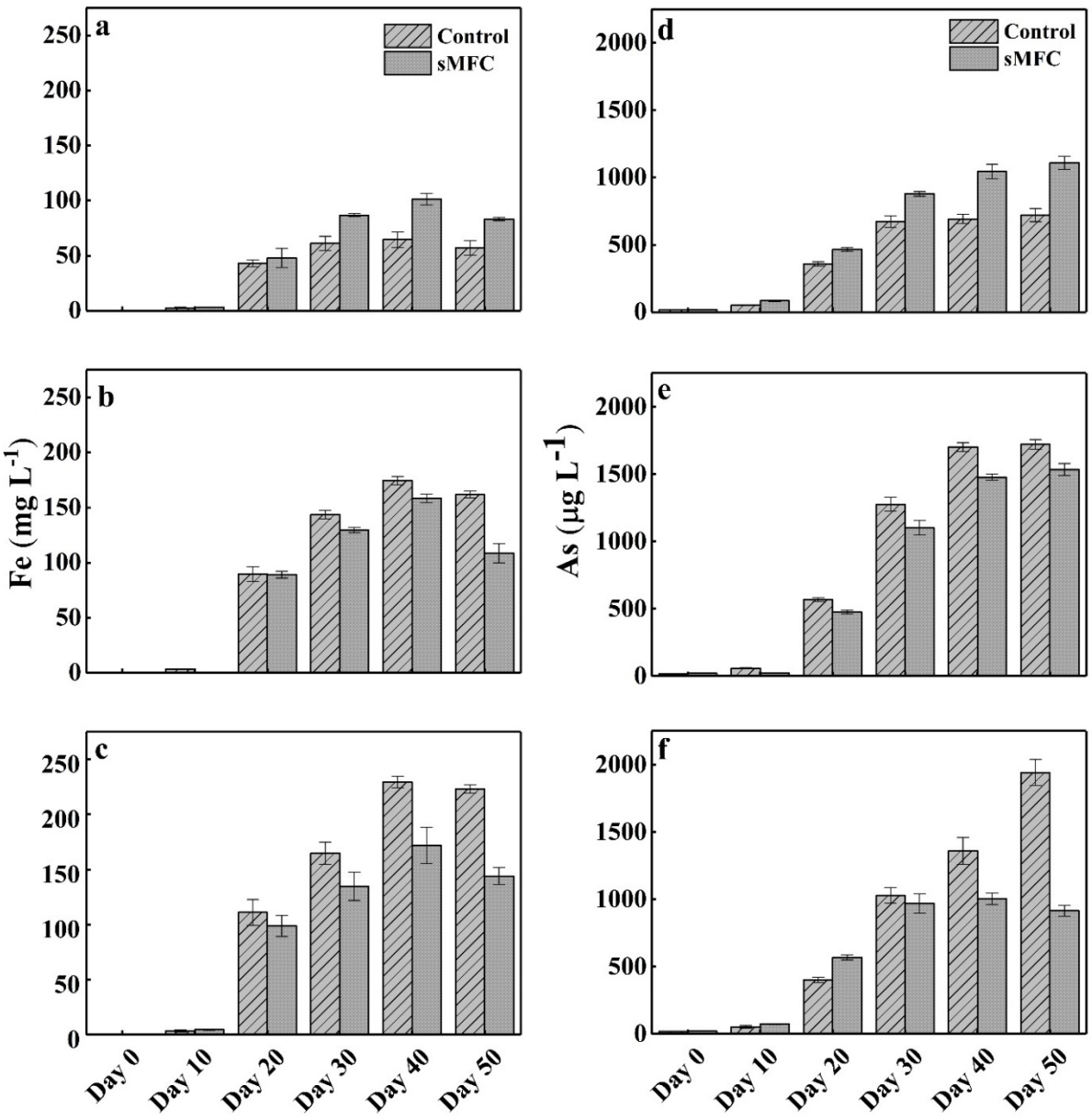

Figure 5.3 Iron (Fe) and Arsenic (As) variation in soil porewater as a function of incubation time. Panels a, b and c show Fe concentration in the top, middle and bottom layers, respectively. Panels d, e and f show As concentration in the top, middle and bottom layers, respectively. The error bars represent standard error of measured concentrations of four replicate samples.

In paddy fields As release usually occurs as a consequence of Fe(III) and As(V) reduction. Therefore, similar to Fe, the release of As in the sMFC was significantly ($p < 0.05$) reduced compared to that of the control in the middle and bottom layers (Fig.5.3d-f). The As

concentration increased sharply with increasing incubation time in both the control and the sMFC. However, the rate of As released in the sMFC was lower than that of the control on average from day 10 to 50 in the middle and day 30-50 in the bottom layer. In the bottom layer on day 0, 10 and 20 the As concentration was lower in the control (17.6 vs 19.5 μg L^{-1}, 51.8 vs 71.6 μg L^{-1} and 400 vs 567 μg L^{-1}, respectively), compared to the sMFC. In contrast, higher As concentrations were observed in the top layer of the sMFC compared to the control. A repeated measures ANOVA with a Greenhouse-Geisser correction revealed that applying the sMFC significantly ($p < 0.05$) impaired As mobility in the middle and bottom layers in long flooded paddy soils. However, in the top layer of the sMFC dissolved As was significantly higher ($p = 0.005$) than that of the control.

A correlation analysis was done to test whether As release in the sMFC was related to Fe reduction (Fig. S 5.2). The release of As in the top ($R^2 = 0.925$, $p < 0.05$), middle ($R^2 = 0.785$, $p < 0.05$) and bottom ($R^2 = 0.883$, $p < 0.05$) layers correlated positively with the increase in Fe concentration. Arsenic mobility in flooded soil is closely associated with Fe reduction and solubilization (Roden et al., 2010; Shelobolina et al., 2003).This observed correlation provides confirmatory evidence that the decrease in As concentration in the sMFC middle and bottom layer was probably due to a decrease in Fe reduction. While the increase in As concentration in the top layer may be due to Fe reduction and ion migration.

5.4.4. The interaction between anodes and Fe oxides: role of organic substrate, *E*h, pH and functional bacterial organisms

Fe and As releases into soil porewater after IRB or As(V)-reducers oxidize OM and transfer the electrons to As bearing Fe minerals or As(V) (Islam et al., 2004; Wang et al., 2017a). The rate at which Fe and As(V) reduction occurs strongly correlate with the bioavailability of DOC. Because IRB's and As(V)-reducer's catalyzing the dissolution of Fe minerals and As(V), respectively, by using DOC as an electron donor. Therefore, if the

bioavailability of DOC is high, more Fe oxide and As(V) reduction is expected to occur (Knorr, 2012; Stuckey et al., 2015).

In our study the application of the sMFC significantly reduced DOC content in the vicinity of the bioanode and limited Fe and As release into the aqueous solution of the sMFC middle and bottom layers (Fig.5.4a-c). These results suggests that significantly lower ($p < 0.05$) DOC concentration in the sMFC than the control might be responsible for the decrease Fe oxide and As(V) reduction in the sMFC middle and bottom layers. The Fe and As contents around sMFC anode were 65.0% and 47.0% of the control respectively at day 50. The reduction in As observed here were comparable to that of other remediation technologies use is soil porewater As mitigation (Cutler et al., 2014; Hartley et al., 2004; Yang et al., 2015; Zhou et al., 2017). The limited microbial reduction of Fe oxide in the sMFC middle and bottom layers compared to the control may be the mechanism responsible for the decrease of As release into the soil porewater of these layers. This rationale is feasible because Fe oxides are potent repositories of As (Li et al., 2011; Roden et al., 2010; Shelobolina et al., 2003; Wang et al., 2017a) and was support by the strong positive correlations observed between Fe and As release in this study (Fig. S 5.2). Several studies have suggested that a DOC is the main fuel for the microbial driven release of As into the soil solution from the surface of Fe oxides. In two separate studies done on evaluating the potential mechanism of As release in groundwater, Nickson et al. (2000) and Whaleymartin et al. (2016) reported that the reduction of arseniferous iron-oxyhydroxides under anaerobic conditions was responsible for the release of As into the groundwater. Moreover, the more negative Eh in the control may explain the higher As and Fe in the middle and bottom layers. In reductive environments an increase in the microbial dissolution of the Fe oxide and the release of As(V) occurs (Islam et al., 2004; Yamaguchi et al., 2011). The released As(V) can then be reduce to As(III) and this may have contributed to the higher dissolved As

in the control as As(III) has a lower affinity for Fe oxide compared to As(V) (Beiyuan et al., 2017; Frohne et al., 2011; Gorny et al., 2015; Qiao et al., 2017b; Seyfferth and Fendorf, 2012).

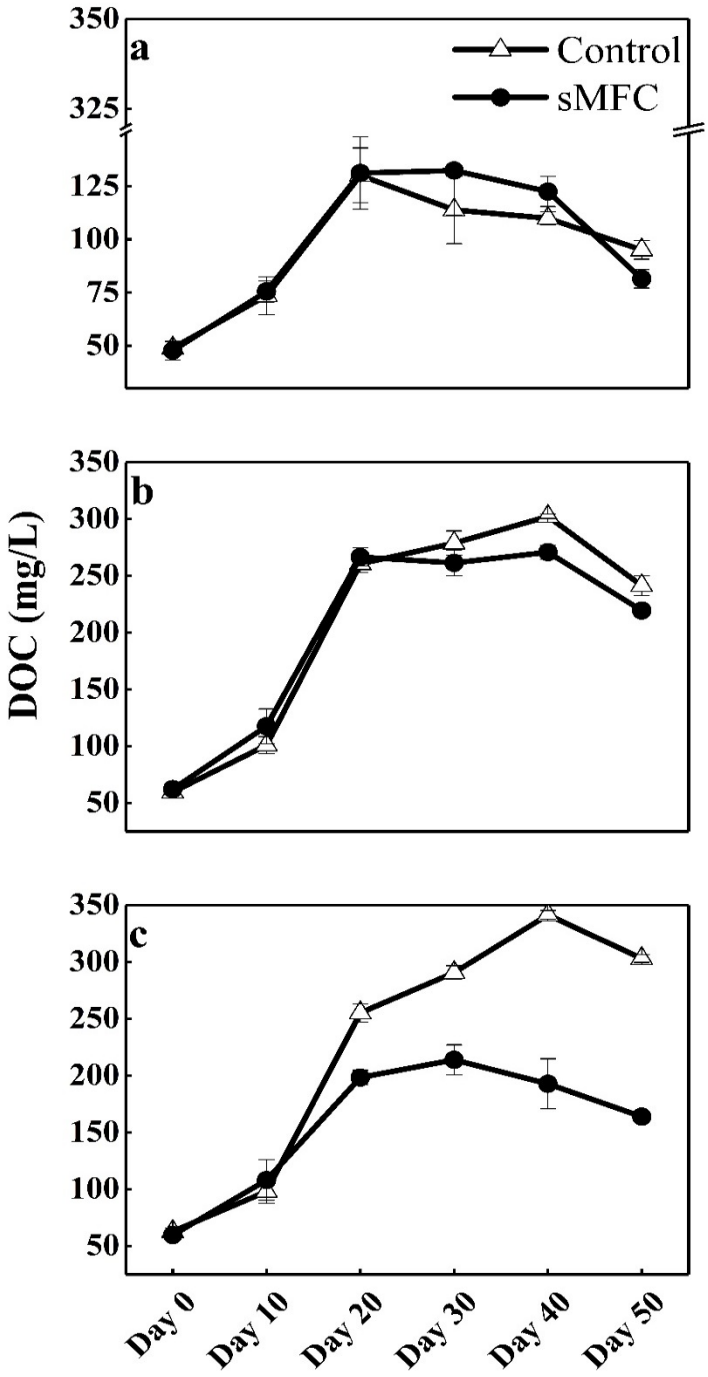

Figure 5.4 DOC variation in soil porewater as a function of incubation time. Panels a, b and c represent top, middle and bottom layers, respectively. The error bars represent standard error of measured concentrations of four replicate samples.

Furthermore, As(V) reduction to As(III) may be limited by the lower DOC in the treatment, then resulted in less As in the soil porewater of the sMFC in middle and bottom layer. Previous studies have shown that reduction of As(V) to As(III) is a major mechanism for the release of As into aqueous solution (Qiao et al., 2017b; Takahashi et al., 2004; Wang et al., 2017b). It was estimated that the reduction of As(V) reduction to As(III) contributes to roughly 50% of the total As release in anaerobic paddy soils (Takahashi et al., 2004). However, in this study As speciation was not directly examined to confirm As(V) to As(III) reduction. Nonetheless, studies has shown that As(III) is the predominant As speciation in soil porewater under anaerobic condition and that As(V) has strong tendency to precipitate with most mineral oxides (Goldberg, 2002; Takahashi et al., 2004; Yamaguchi et al., 2011). Therefore, we hypothesized that the majority of the total As in this study was As(III) and that limited As(V) reduction along with Fe oxide dissolution contributed to the decrease in total Fe and As in the sMFC middle and bottom layer soil porewater.

Conversely, the higher Fe and As concertation observed in the sMFC top layer may be due to cathodic reactions. Soil pH is an important factor for the mobility of Fe and As, because pH can influence the surface charge and solubility of Fe oxide (Antoniadis et al., 2017; Burstein, 1997; Jiang et al., 2014). When the sMFC runs, cations (e.g. ferrous ions) move from anode to cathode and precipitate at the soil-water interface, forming an Fe-oxidizing layer. Because in the cathode zone, protons are consumed (Logan, 2008), thus leading to an increase in soil pH which facilitates the Fe oxide precipitation (Weber et al., 2006). Consequently the dissolved Fe in the deeper soil layer migrates upward because of the diffusive and electrical forces that are created by operating sMFC. Therefore the higher Fe and As concentration observed in the top layer of the sMFC (1 cm below the Fe oxide layer) was probably due to the ferrous ions migration driven by the electric field generated between cathode and anode and the diffusive force created by the Fe oxide layer.

Furthermore, the inconsistency that is observed in the bottom layer on day 10 and 20, where the Fe reduction rate was lower in the sMFC compared to the control (Fig 3b), but more As was present in the sMFC (Fig. 5.3d) during that period, was probably due to the lower pH observed in the vicinity of the anode and the direct reduction of As(V) to As(III) by As(V) reducing bacteria (Tufano et al., 2008; Wang et al., 2017b). This occurred because low pH environments influence the desorption behavior of As and Fe oxide through altering Fe oxide surface charge thereby leading to a reduction in As sorption sites (Ascar et al., 2008; Gorny et al., 2015; Houben et al., 2013; Masscheleyn et al., 1991).

5.4.5. Bacterial community structure

The bacterial community of the bioanode and the bulk soil were investigated by Illumina high-throughput sequencing. As shown in Fig. S 5.3 and Table S 5.3, both rarefaction curves and Good's coverage indicated that sufficient sequencing depths were achieved. This is evident by the observed saturated trend in the rarefaction curves with increasing sequence and the high Good's coverage (99.6 - 99.7) obtained in all of the samples. High quality sequences reads ranging from 132409 – 198845 were achieved from the samples after removing chimeric sequences and classified into operational taxonomic units (OTUs) at a 97% similarity threshold. As shown in Table S 5.2, alpha diversity measures revealed that in general samples taken from the control cells were more diversified than those obtained from the sMFC. This was not unusual since sMFCs' bioanodes have been shown to enhance specific groups of microbes (Wang et al., 2015b; Zhou et al., 2015) on the anode and associated bulk soil. However, it is worth noting that the sMFC top layer surprisingly had the lowest alpha index as opposed to the sMFC bioanode. The lower diversity seen in the sMFC top layer was probably due to the thick Fe oxide layer and the increase in soil pH due to cathodic reactions. Soil pH has been identified as a key determinant of bacterial community structure (Nicol et al., 2008; Wu et al., 2017).

In addition, beta diversity and Anosim analysis were conducted to further assess the influence of the sMFC on bacterial community structure distribution. Principal Coordinates Analysis (PCoA)-PC1 vs PC2 (explaining 55.0%) showed that sMFC strongly altered the bacterial community on the anode and the top layer compartments compared to the control (Fig. 5.5). The results revealed the formation of three distinctive clusters. Where samples from sMFC anode and the top layer formed two separate groups, samples from the control (all layers) and sMFC middle layers comprised the third cluster. Anosim analysis further confirmed that bacterial community on the sMFC anode (p= 0.026) and the top layer (p= 0.035) were significantly different from that of the control, while no significant difference was observed in the middle layer between the two. The results showed sMFC had minimal influence on the bacterial community in middle layer of the bulk soil, but significantly altered the bacterial on top layers and anodes.

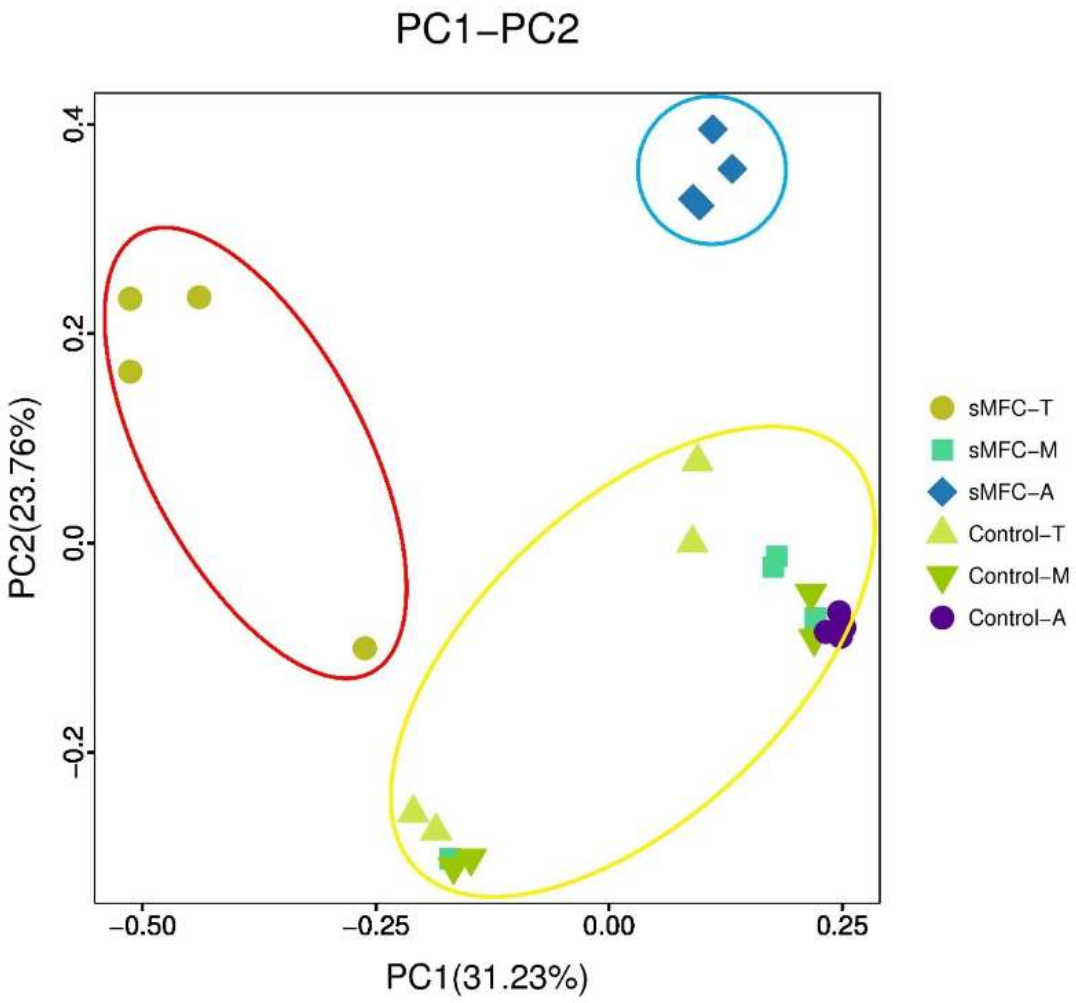

Figure 5.5 Principal Coordinate Analysis (PCoA) of the sMFC and controls bacterial community composition based on Bray-Curtis distance. The x- and y-axes are indicated by the first and second coordinates, respectively, and the values in parentheses show the percentages of the community variation explained.

The relative abundance of the sequences obtained from the sMFC and the control at the phylum level are shown in Fig. S 5.4. The top 5 dominant phyla in all samples were *Acidobacteria* (30.0-54.3%), *Proteobacteria* (7.45-43.6%), *Firmicutes* (1.10-27.8%), *Bacteroidetes* (3.58-8.18%) and *Chloroflexi* (2.79-5.64%). However, in the sMFC *Parcubacteria* (10.5% vs 0.438%), *Nirtospirae* (2.79% vs 0.580%) and *Chlorobi* (3.59 vs 0.580%) were more abundant compared to that of the control. Affiliates of the phylum *Parcubacteria* have been shown to be actively involved in anaerobic methane oxidation,

hydrogen production and sulfur and Fe cycling (Borrel et al., 2010; Peura et al., 2012; Reis et al., 2016; Wrighton et al., 2012). The phyla *Nirtospirae* (Xu et al., 2017) and *Chlorobi* (Thompson et al., 2017) contains members that are actively involved in denitrification. *Nirtospirae* and *Chlorobi*, may have encouraged the precipitation of Fe (III) from the soil porewater and consequently As during denitrification. Since nitrate-reducing bacteria could influence the fate of As under anaerobic conditions, via the nitrite-driven oxidation of Fe(II) and As(III) (Gnanaprakasam et al., 2017; Hohmann et al., 2009; Omoregie et al., 2013).

On the contrary the phylum *Firmicutes* was more abundant in the control, accounting for 27.5% of the controls anode bacterial community. *Firmicutes* contains known classes of Fe(III) and As(V) reducing bacteria and they may have played a role in the increase of Fe and As concentration in the control cells (Hohmann et al., 2009; Oremland and Stolz, 2005; Song et al., 2009). At the class level *Clostridia* (25.0%) was higher in the control's anode. The class *Clostridia* contains both dissimilatory Fe(III) and As(V)-reducing lineages (i.e. *Clostridium sp. OhiLAs* and *C. beijerinckii*) (Dobbin et al., 1999; Langner and Inskeep, 2000; Stolz et al., 2007; Wang et al., 2017a; Wang et al., 2017b). In a recent study, Qiao et al. (2017a) observed a significantly strong positive correlation between the number of *Clostridium* with Fe(III) reduction. This suggests that *Clostridia* could have facilitated the reduction of Fe oxide and As(V) in the control and resulted in the higher Fe and As in the control middle and bottom layers. Furthermore at the genus level *Anaeromyxobacter* and *Geobacter* were statistically enhanced ($p < 0.05$) in control's bulk soil compared to the sMFC (Fig. S 5.5). Both *Anaeromyxobacter* and *Geobacter* have been shown to have the capability to reduce Fe minerals and As(V) during the catabolism of OM leading to an increase in the solubility of the metals in soil porewater (Chen et al., 2016; Lovley and Phillips, 1988; Qiao et al., 2017a). In addition the relative abundance of *Bacillus* was slightly higher in the control bulk soil compared to the sMFC. *Bacillus* abundance has been observed to positively correlate with

dissolve As is soil porewater (Yang et al., 2018). Studies have demonstrates that *Bacillus* stains can reduce Fe oxides and As(V) to facilitate the release of As into paddy soil porewater (Qiao et al., 2017a; Qiao et al., 2017b; Wang et al., 2017a). These findings demonstrate that the bacterial community within control bulk soil probably contributed to the relatively higher Fe and As concentration in the soil porewater, while the bacterial community on sMFC bioanode may have favored Fe (III) and As (V) precipitation.

5.5. Conclusions

In summary, this study demonstrates that the sMFC can generate electricity in As-contaminated paddy soils and at the same time decrease the release of Fe and As in paddy soil porewater. Although still under development, sMFC might be used as a novel tool in limiting As mobilization for management of contaminated soil. Since the bioanode can potentially be used as a mitigation strategy to limit As mobility in paddy soil, which consequently may reduce As accumulation in rice grains. This is of importance, because rice has high As accumulation potential and consumption of contaminated rice poses a major health concern due to increasing the dietary intake of As in the human body. In addition, long-term exposure of As, poses a significant risk of chronic disease to the Asian populations. Nonetheless, this study is still in its infancy and the direct transfer of this technology to the field warrant further research in terms of application and cost. New sMFC design is highly required to overcome the challenges associated with laying two pieces of carbon felts into the paddy fields. The production cost and benefits maybe be balanced by using cheap and inexhaustible electrode materials. Moreover, we acknowledge that the power out of the sMFC was low in this study. It should be noted that the soil used here contained low OM. Further, chemical reagents that are known to also encourage As precipitation such as hematite and goethite can also be used to modifying the electrodes and improve soil conductivity to increase the power output of the sMFC in order of

magnitudes. Thus, we conclude that the sMFC can be used to limit As and Fe release into the soil porewater, however the transfer of this technology into the field warrant further research.

5.6. References

Antoniadis, V., Levizou, E., Shaheen, S.M., Yong, S.O., Sebastian, A., Baum, C., Prasad, M.N.V., Wenzel, W.W., Rinklebe, J., 2017. Trace elements in the soil-plant interface: Phytoavailability, translocation, and phytoremediation–A review. Earth Sci. Rev. 171, 621-645.

Ascar, L., Ahumada, I., Richter, P., 2008. Influence of redox potential (Eh) on the availability of arsenic species in soils and soils amended with biosolid. Chemosphere 72, 1548-1552.

Barragan, L., Seyfferth, A., Fendorf, S., 2011. Arsenic Concentrations in Rice and Associated Health Risks Along the Upper Mekong Delta, Cambodia, AGU Fall Meeting.

Beiyuan, J., Awad, Y.M., Beckers, F., Tsang, D.C., Ok, Y.S., Rinklebe, J., 2017. Mobility and phytoavailability of As and Pb in a contaminated soil using pine sawdust biochar under systematic change of redox conditions. Chemosphere 178, 110.

Borrel, G., Lehours, A., Bardot, C., Bailly, X., Fonty, G., 2010. Members of candidate divisions OP11, OD1 and SR1 are widespread along the water column of the meromictic Lake Pavin (France). Arch. Microbiol. 192, 559-567.

Burstein, G., 1997. The iron oxides: Structure, properties, reactions, occurrence and uses: RM Cornell and U. Schwertmann. 573 pp. VCH, Weinheim and New York, 1996. ISBN: 3-527-28576-8. Pergamon.

Chaney, R.L., Kim, W.I., Kunhikrishnan, A., Yang, J.E., Yong, S.O., 2016. Integrated management strategies for arsenic and cadmium in rice paddy environments. Geoderma 270, 1-2.

Chen, Z., Huang, Y.-c., Liang, J.-h., Zhao, F., Zhu, Y.-g., 2012. A novel sediment microbial fuel cell with a biocathode in the rice rhizosphere. Bioresour. Technol. 108, 55-59.

Chen, Z., Wang, Y., Xia, D., Jiang, X., Fu, D., Shen, L., Wang, H., Li, Q.B., 2016. Enhanced bioreduction of iron and arsenic in sediment by biochar amendment influencing microbial community composition and dissolved organic matter content and composition. J. Hazard. Mater. 311, 20-29.

Chen, Z., Zhu, B. K., Jia, W. F., Liang, J. H., Sun, G. X., 2015. Can electrokinetic removal of metals from contaminated paddy soils be powered by microbial fuel cells? Environ. Technol. Innov. 3, 63-67.

Cutler, W.G., Elkadi, A., Hue, N.V., Peard, J., Scheckel, K., Ray, C., 2014. Iron amendments to reduce bioaccessible arsenic. J. Hazard. Mater. 279, 554-561.

De Schamphelaire, L., Cabezas, A., Marzorati, M., Friedrich, M.W., Boon, N., Verstraete, W., 2010. Microbial community analysis of anodes from sediment microbial fuel cells powered by rhizodeposits of living rice plants. Appl. Environ. Microbiol. 76, 2002-2008.

Dobbin, P.S., Carter, J.P., Garcia-Salamanca, S.J.C., Von, H.M., Powell, A.K., Richardson, D.J., 1999. Dissimilatory Fe(III) reduction by *Clostridium beijerinckii* isolated from freshwater sediment using Fe(III) maltol enrichment. Fems Microbiol. Lett. 176, 131–138.

Frohne, T., Rinklebe, J., Diaz-Bone, R.A., Laing, G.D., 2011. Controlled variation of redox conditions in a floodplain soil: Impact on metal mobilization and biomethylation of arsenic and antimony. Geoderma 160, 414-424.

Ganz, H.H., Doroud, L., Firl, A.J., Hird, S.M., Eisen, J.A., Boyce, W.M., 2017. Community-Level Differences in the Microbiome of Healthy Wild Mallards and Those Infected by Influenza A Viruses. Msystems 2, e00188-00116.

Gnanaprakasam, E.T., Lloyd, J.R., Boothman, C., Ahmed, K.M., Choudhury, I., Bostick, B.C., van Geen, A., Mailloux, B.J., 2017. Microbial Community Structure and Arsenic

Biogeochemistry in Two Arsenic-Impacted Aquifers in Bangladesh. Mbio 8, e01326-01317.

Goldberg, S., 2002. Competitive adsorption of arsenate and arsenite on oxides and clay minerals. Soil Sci. Soc. Am. J. 66, 413-421.

Gorny, J., Billon, G., Lesven, L., Dumoulin, D., Madé, B., Noiriel, C., 2015. Arsenic behavior in river sediments under redox gradient: A review. Sci. Total Environ. 505, 423-434.

Gregory, K.B., Lovley, D.R., 2005. Remediation and recovery of uranium from contaminated subsurface environments with electrodes. Environ. Sci. Technol. 39, 8943-8947.

Hartley, W., Edwards, R., Lepp, N.W., 2004. Arsenic and heavy metal mobility in iron oxide-amended contaminated soils as evaluated by short- and long-term leaching tests. Environ. Pollut. n 131, 495-504.

Hohmann, C., Winkler, E., Morin, G., Kappler, A., 2009. Anaerobic Fe (II)-oxidizing bacteria show As resistance and immobilize As during Fe (III) mineral precipitation. Environ. Sci. Technol. 44, 94-101.

Hong, S.W., Chang, I.S., Choi, Y.S., Kim, B.H., Chung, T.H., 2009. Responses from freshwater sediment during electricity generation using microbial fuel cells. Bioprocess Biosyst. Eng. 32, 389-395.

Hong, S.W., Kim, H.S., Chung, T.H., 2010. Alteration of sediment organic matter in sediment microbial fuel cells. Environ. Pollut. 158, 185-191.

Houben, D., Evrard, L., Sonnet, P., 2013. Mobility, bioavailability and pH-dependent leaching of cadmium, zinc and lead in a contaminated soil amended with biochar. Chemosphere 92, 1450-1457.

Huang, D.Y., Zhou, S.G., Chen, Q., Zhao, B., Yuan, Y., Zhuang, L., 2011. Enhanced anaerobic degradation of organic pollutants in a soil microbial fuel cell. Chem. Eng. J. 172, 647-653.

Inseop, C., Hyunsoo, M., Orianna, B., Jaekyung, J., Hoil, P., Kenneth, H.N., Byunghong, K., 2006. Electrochemically active bacteria (EAB) and mediator-less microbial fuel cells. J. Mol. Microbiol. Biotechnol. 16, 163-177.

Islam, F.S., Gault, A.G., Boothman, C., Polya, D.A., Charnock, J.M., Chatterjee, D., Lloyd, J.R., 2004. Role of metal-reducing bacteria in arsenic release from Bengal delta sediments. Nature 430, 68-71.

Jang, J.K., Chang, I.S., Kang, K.H., Moon, H., Cho, K.S., Kim, B.H., 2004. Construction and operation of a novel mediator and membrane-less microbial fuel cell. Process Biochem. 39, 1007-1012.

Jiang, W., Hou, Q., Yang, Z., Zhong, C., Zheng, G., Yang, Z., Li, J., 2014. Evaluation of potential effects of soil available phosphorus on soil arsenic availability and paddy rice inorganic arsenic content. Environ. Pollut. 188, 159-165.

Kaku, N., Yonezawa, N., Kodama, Y., Watanabe, K., 2008. Plant/microbe cooperation for electricity generation in a rice paddy field. Appl. Microbiol. Biotechnol. 79, 43-49.

Knorr, K., 2012. DOC-dynamics in a small headwater catchment as driven by redox fluctuations and hydrological flow paths – are DOC exports mediated by iron reduction/oxidation cycles? Biogeosciences 10, 891-904.

Langner, H.W., Inskeep, W.P., 2000. Microbial reduction of arsenate in the presence of ferrihydrite. Environ. Sci. Technol. 34, 3131-3136.

Li, H., Peng, J., Weber, K.A., Zhu, Y., 2011. Phylogenetic diversity of Fe(III)-reducing microorganisms in rice paddy soil: enrichment cultures with different short-chain fatty acids as electron donors. J. Soils Sediments. 11, 1234-1242.

Li, W., Yu, H., 2015. Stimulating sediment bioremediation with benthic microbial fuel cells. Biotechnol. Adv. 33, 1-12.

Liu, L., Chou, T.Y., Lee, C.Y., Lee, D.J., Su, A., Lai, J.Y., 2016. Performance of freshwater sediment microbial fuel cells: Consistency. Int. J. Hydrogen Energy 41, 4504-4508.

Logan, B.E., 2008. Microbial Fuel Cells. A John Wiley & Sons, Inc.

Logan, B.E., 2009. Exoelectrogenic bacteria that power microbial fuel cells. Nat. Rev. Microbiol. 7, 375–381.

Logan, B.E., Hamelers, B., Rozendal, R.A., Schroder, U., Keller, J., Freguia, S., Aelterman, P., Verstraete, W., Rabaey, K., 2006. Microbial Fuel Cells: Methodology and Technology Environ. Sci. Technol. 40, 5181-5192.

Lovley, D.R., Holmes, D.E., Nevin, K.P., 2004. Dissimilatory Fe(III) and Mn(IV) reduction. Adv. Microb. Physiol. 49, 219-286.

Lovley, D.R., Phillips, E.J., 1986. Organic matter mineralization with reduction of ferric iron in anaerobic sediments. Appl. Environ. Microbiol. 51, 683-689.

Lovley, D.R., Phillips, E.J.P., 1988. Novel Mode of Microbial Energy Metabolism: Organic Carbon Oxidation Coupled to Dissimilatory Reduction of Iron or Manganese. Appl. Environ. Microbiol. 54, 1472-1480.

Lu, L., Huggins, T., Jin, S., Zuo, Y., Ren, Z.J., 2014. Microbial metabolism and community structure in response to bioelectrochemically enhanced remediation of petroleum hydrocarbon-contaminated soil. Environ. Sci. Technol. 48, 4021.

Martins, G., Peixoto, L., Teodorescu, S., Parpot, P., Nogueira, R., Brito, A.G., 2014. Impact of an external electron acceptor on phosphorus mobility between water and sediments. Bioresour. Technol. 151, 419-423.

Masscheleyn, P.H., Delaune, R.D., Jr, W.H.P., 1991. Effect of redox potential and pH on arsenic speciation and solubility in a contaminated soil. Environ. Sci. Technol. 25, 1414-1419.

Morris, J.M., Jin, S., 2012. Enhanced biodegradation of hydrocarbon-contaminated sediments using microbial fuel cells. J. Hazard. Mater. 213-214, 474-477.

Nickson, R.T., Mcarthur, J.M., Ravenscroft, P., Burgess, W.G., Ahmed, K.M., 2000. Mechanism of arsenic release to groundwater, Bangladesh and West Bengal. Appl. Geochem. 15, 403-413.

Nicol, G.W., Leininger, S., Schleper, C., Prosser, J.I., 2008. The influence of soil pH on the diversity, abundance and transcriptional activity of ammonia oxidizing archaea and bacteria. Environ. Microbiol. 10, 2966-2978.

Omoregie, E.O., Couture, R.M., Van Cappellen, P., Corkhill, C.L., Charnock, J.M., Polya, D.A., Vaughan, D.J., Vanbroekhoven, K., Lloyd, J.R., 2013. Arsenic Bioremediation by Biogenic Iron Oxides and Sulfides. Appl. Environ. Microbiol. 79, 4325-4335.

Oremland, R.S., Stolz, J.F., 2005. Arsenic, microbes and contaminated aquifers. Trends Microbiol. 13, 45-49.

Peura, S., Eiler, A., Bertilsson, S., Nykanen, H., Tiirola, M., Jones, R., 2012. Distinct and diverse anaerobic bacterial communities in boreal lakes dominated by candidate division OD1. ISME J. 6, 1640-1652.

Qiao, J.-t., Li, X.-m., Li, F.-b., 2017a. Roles of different active metal-reducing bacteria in arsenic release from arsenic-contaminated paddy soil amended with biochar. J. Hazard. Mater.

Qiao, J., Li, X., Hu, M., Li, F., Young, L.Y., Sun, W., Huang, W., Cui, J., 2017b. Transcriptional activity of arsenic-reducing bacteria and genes regulated by lactate and biochar during arsenic transformation in flooded paddy soil. Environ. Sci. Technol. 52(1), 61-70.

Reis, M.P., Dias, M.F., Costa, P.S., Avila, M.P., Leite, L.H.R., Araujo, F.M.G., Salim, A., Bucciarellirodriguez, M., Oliveira, G., Chartonesouza, E., 2016. Metagenomic

signatures of a tropical mining-impacted stream reveal complex microbial and metabolic networks. Chemosphere 161, 266-273.

Rezaei, F., Richard, T.L., A., B.R., E., L., 2007. Substrate-Enhanced Microbial Fuel Cells for Improved Remote Power Generation from Sediment-Based Systems. Environ. Sci. Technol. 41, 4053–4058.

Roden, E.E., Kappler, A., Bauer, I., Jiang, J., Paul, A., Stoesser, R., Konishi, H., Xu, H., 2010. Extracellular electron transfer through microbial reduction of solid-phase humic substances. Nat. Geosci. 3, 417-421.

Sajana, T.K., Ghangrekar, M.M., Mitra, A., 2014. Effect of presence of cellulose in the freshwater sediment on the performance of sediment microbial fuel cell. Bioresour. Technol. 155, 84-90.

Seyfferth, A.L., Fendorf, S., 2012. Silicate Mineral Impacts on the Uptake and Storage of Arsenic and Plant Nutrients in Rice (Oryza sativa L.). Environ. Sci. Technol. 46, 13176-13183.

Seyfferth, A.L., Mccurdy, S., Schaefer, M.V., Fendorf, S., 2014. Arsenic concentrations in paddy soil and rice and health implications for major rice-growing regions of Cambodia. Environ. Sci. Technol. 48, 4699-4706.

Seyfferth, A., Ross, J., Webb, S., 2017. Evidence for the Root-Uptake of Arsenite at Lateral Root Junctions and Root Apices in Rice (Oryza sativa L.). Soils 1, 3.

Seyfferth, A.L., Limmer, M.A., Dykes, G.E., 2018. On the Use of Silicon as an Agronomic Mitigation Strategy to Decrease Arsenic Uptake by Rice. Adv. Agron.

Shelobolina, E.S., Vanpraagh, C.G., Lovley, D.R., 2003. Use of Ferric and Ferrous Iron Containing Minerals for Respiration by *Desulfitobacterium Frappieri*. Geomicrobiol. J. 20, 143-156.

Song, B., Chyun, E., Jaffe, P.R., Ward, B.B., 2009. Molecular methods to detect and monitor dissimilatory arsenate-respiring bacteria (DARB) in sediments. FEMS Microbiol. Ecol. 68, 108-117.

Song, T.S., Yan, Z.S., Zhao, Z.W., Jiang, H.L., 2010. Removal of organic matter in freshwater sediment by microbial fuel cells at various external resistances. J. Chem. Technol. Biotechnol. 85, 1489-1493.

Stolz, J.F., Perera, E., Kilonzo, B., Kail, B., Crable, B., Fisher, E., Ranganathan, M., Wormer, L., Basu, P., 2007. Biotransformation of 3-nitro-4-hydroxybenzene arsonic acid (roxarsone) and release of inorganic arsenic by *Clostridium* species. Environ. Sci. Technol. 41, 818.

Stuckey, Jason W., Schaefer, Michael V., Kocar, Benjamin D., Benner, Shawn G., Fendorf, S., 2015. Arsenic release metabolically limited to permanently water-saturated soil in Mekong Delta. Nat. Geosci. 9, 70-76.

Takahashi, Y., Minamikawa, R., Hattori, K., Kurishima, K., Kihou, N., Yuita, K., 2004. Arsenic behavior in paddy fields during the cycle of flooded and non-flooded periods. Environ. Sci. Technol. 38, 1038-1044.

Takanezawa, K., Nishio, K., Kato, S., Hashimoto, K., Watanabe, K., 2010. Factors affecting electric output from rice-paddy microbial fuel cells. Biosci. Biotechnol. Biochem. 74, 1271-1273.

Thompson, K.J., Simister, R.L., Hahn, A.S., Hallam, S.J., Crowe, S.A., 2017. Nutrient Acquisition and the Metabolic Potential of *Photoferrotrophic Chlorobi.* Front. Microbiol. 8.

Touch, N., Hibino, T., Morimoto, Y., Kinjo, N., 2017. Relaxing the formation of hypoxic bottom water with sediment microbial fuel cells. Environ. Technol. 1-25.

Tufano, K.J., Reyes, C., Saltikov, C.W., Fendorf, S., 2008. Reductive processes controlling arsenic retention: revealing the relative importance of iron and arsenic reduction. Environ. Sci. Technol. 42, 8283-8289.

Vithanage, M., Herath, I., Joseph, S., Bundschuh, J., Bolan, N., Yong, S.O., Kirkham, M.B., Rinklebe, J., 2017. Interaction of arsenic with biochar in soil and water: A critical review. Carbon 113.

Wang, C., Deng, H., Zhao, F., 2015a. The Remediation of Chromium (VI)-Contaminated Soils Using Microbial Fuel Cells. Soil Sediment Contam. 25, 1-12.

Wang, N., Chen, Z., Li, H.B., Su, J.Q., Zhao, F., Zhu, Y.G., 2015b. Bacterial community composition at anodes of microbial fuel cells for paddy soils: the effects of soil properties. J. Soils Sediments 15, 926-936.

Wang, N., Xue, X., Juhasz, A.L., Chang, Z., Li, H., 2017a. Biochar increases arsenic release from an anaerobic paddy soil due to enhanced microbial reduction of iron and arsenic. Environ. Pollut. 220, 514-522.

Wang, X., Liu, T., Li, F., Li, B., Liu, C., 2017b. Effects of simultaneous application of ferrous iron and nitrate on arsenic accumulation in rice grown in contaminated paddy soil. ACS Earth Space Chem.

Wang, X.J., Yang, J., Chen, X.P., Sun, G.X., Zhu, Y.G., 2009. Phylogenetic diversity of dissimilatory ferric iron reducers in paddy soil of Hunan, South China. J. Soils Sediments 9, 568-577.

Weber, K.A., Achenbach, L.A., Coates, J.D., 2006. Microorganisms pumping iron: anaerobic microbial iron oxidation and reduction. Nat. Rev. Microbiol. 4, 752-764.

Whaleymartin, K.J., Mailloux, B.J., Van, G.A., Bostick, B.C., Silvern, R.F., Kim, C., Ahmed, K.M., Choudhury, I., Slater, G.F., 2016. Stimulation of Microbially-Mediated Arsenic

Release in Bangladesh Aquifers by Young Carbon Indicated by Radiocarbon Analysis of Sedimentary Bacterial Lipids Environ. Sci. Technol. 50.

Williams, P.N., Islam, M.R., Adomako, E.E., Raab, A., Hossain, S.A., Zhu, Y.G., Feldmann, J., Meharg, A.A., 2006. Increase in Rice Grain Arsenic for Regions of Bangladesh Irrigating Paddies with Elevated Arsenic in Groundwaters. Environ. Sci. Technol. 40, 4903-4908.

Wrighton, K.C., Thomas, B.C., Sharon, I., Miller, C.S., Castelle, C.J., Verberkmoes, N.C., Wilkins, M.J., Hettich, R.L., Lipton, M.S., Williams, K.H., 2012. Fermentation, Hydrogen, and Sulfur Metabolism in Multiple Uncultivated Bacterial Phyla. Science 337, 1661-1665.

Wu, Y., Zeng, J., Zhu, Q., Zhang, Z., Lin, X., 2017. pH is the primary determinant of the bacterial community structure in agricultural soils impacted by polycyclic aromatic hydrocarbon pollution. Sci. Rep. 7, 40093.

Xu, P., Xiao, E., Xu, D., Zhou, Y., He, F., Liu, B.Y., Zeng, L., Wu, Z.B., 2017. Internal nitrogen removal from sediments by the hybrid system of microbial fuel cells and submerged aquatic plants. PloS one, 12(2), e0172757

Xu, X., 2015. Removal and Changes of Sediment Organic Matter and Electricity Generation by Sediment Microbial Fuel Cells and Amorphous Ferric Hydroxide. Chem. Biochem. Eng. Q. 28, 561-566.

Xun, X., Zhao, Q., Wu, M., Jing, D., Zhang, W., 2016. Biodegradation of Organic Matter and Anodic Microbial Communities Analysis in Sediment Microbial Fuel Cells with/without Fe(III) Oxide Addition. Bioresour. Technol. 225, 402-408.

Yamaguchi, N., Nakamura, T., Dong, D., Takahashi, Y., Amachi, S., Makino, T., 2011. Arsenic release from flooded paddy soils is influenced by speciation, Eh, pH, and iron dissolution. Chemosphere 83, 925-932.

Yang, Q., Zhao, H., Zhao, N., Ni, J., Gu, X., 2016. Enhanced phosphorus flux from overlying water to sediment in a bioelectrochemical system. Bioresour. Technol. 216, 182.

Yang, Y., Zhang, H., Yuan, H., Duan, G., Jin, D., Zhao, F., Zhu, Y., 2018. Microbe mediated arsenic release from iron minerals and arsenic methylation in rhizosphere controls arsenic fate in soil-rice system after straw incorporation. Environ. Pollut. 236, 598-608.

Yang, Z., Liu, L., Chai, L., Liao, Y., Yao, W., Xiao, R., 2015. Arsenic immobilization in the contaminated soil using poorly crystalline Fe-oxyhydroxy sulfate. Environ. Sci. Pollut. Res. 22, 12624-12632.

You, J., Wu, G., Ren, F., Chang, Q., Yu, B., Xue, Y., Mu, B., 2016. Microbial community dynamics in Baolige oilfield during MEOR treatment, revealed by Illumina MiSeq sequencing. Appl. Microbiol. Biotechnol. 100, 1469-1478.

Zhang, Y., Angelidaki, I., 2012. Bioelectrode-based approach for enhancing nitrate and nitrite removal and electricity generation from eutrophic lakes. Water Res. 46, 6445-6453.

Zhou, J., Shu, W., Gao, Y., Cao, Z., Zhang, J., Hou, H., Zhao, J., Chen, X., Pan, Y., Qian, G., 2017. Enhanced arsenite immobilization via ternary layered double hydroxides and application to paddy soil remediation. Rsc. Advances 7, 20320-20326.

Zhou, Y., Jiang, H., Cai, H., 2015. To prevent the occurrence of black water agglomerate through delaying decomposition of cyanobacterial bloom biomass by sediment microbial fuel cell. J. Hazard. Mater. 287, 7-15.

Zhu, D.W., Wang, D.B., Song, T.S., Guo, T., Wei, P., Ouyang, P.K., Xie, J.J., 2016. Enhancement of cellulose degradation in freshwater sediments by a sediment microbial fuel cell. Biotechnol. Lett. 38, 271-277.

Zhu, Y., Williams, P., Meharg, A.A., 2008. Exposure to inorganic arsenic from rice: a global health issue? Environ. Pollut. 154, 169-171.

5.7. Supplementary data

The effect of the sMFC on arsenic in soil with low organic matter content

Table S 5.1 Selected properties of the fresh soils

Sample	Soil texture	pH	OM (g/Kg)	TN (g/Kg)	TS (g/Kg)	Fe (g/kg)	As (mg/kg)	Mn (mg/kg)	Mg (g/kg)
Zhejiang Shangyu	Sandy loam	5.88 ±0.14	14.4 ±1.14	1.30 ±0.2	0.31 ±0.01	39.7 ±3.9	140 ±2.67	977 ±13.0	2.10 ±2.5

Notes: OM: Organic matter content; TN: Total nitrogen and TS: Total sulfur. The values represent the mean ±standard error of four replicate samples.

Table S 5.2 Changes of pH and redox potential in soil samples of sMFC and control at the end of the experiment.

	Sample ID					
	sMFC-T	**sMFC-M**	**sMFC-B**	**Control-T**	**Control-M**	**Control-B**
pH	6.09 ±0.04	5.39 ±0.01	5.21 ±0.01	5.61 ±0.03	5.86 ±0.01	5.88 ±0.01
***E*h (mV vs Ag/AgCl)**	-	-	-133 ±10	-	-	-445±1

Notes: T, M and A: represents samples collected from top layer, middle layer and anode vicinity respectively. Mean ± SE (n = 4)

Table S 5.3 Similarity-based OTUs and species richness and diversity estimates.

Sample ID	Reads	ACE	Chao1	Shannon index	Simpson	Good's Coverage
sMFC-T	153048 ±11331	623 ±41.1	642 ±46.8	7.03 ±0.20	0.977 ±0.00	0.997 ±0.00
sMFC-M	132409 ±7106	748 ±9.17	762 ±7.47	7.39 ±0.06	0.986 ±0.00	0.997 ±0.00
sMFC-A	192839 ±3326	690 ±11.0	701 ±10.7	6.95 ±0.15	0.975 ±0.00	0.996 ±0.00
Control-T	151873 ±1026	766 ±29.6	772 ±33.8	7.33 ±0.13	0.981 ±0.00	0.997 ±0.00
Control-M	142537 ±8886	740 ±8.16	753 ±11.9	7.30 ±0.06	0.983 ±0.00	0.996 ±0.00
Control-A	198845 ±5177	722 ±10.3	735 ±11.3	7.73 ±0.03	0.989 ±0.00	0.997 ±0.00

Notes: T, M and A: represents samples collected from top layer, middle layer and anode vicinity respectively. The values represent the mean ±standard error of four replicate samples.

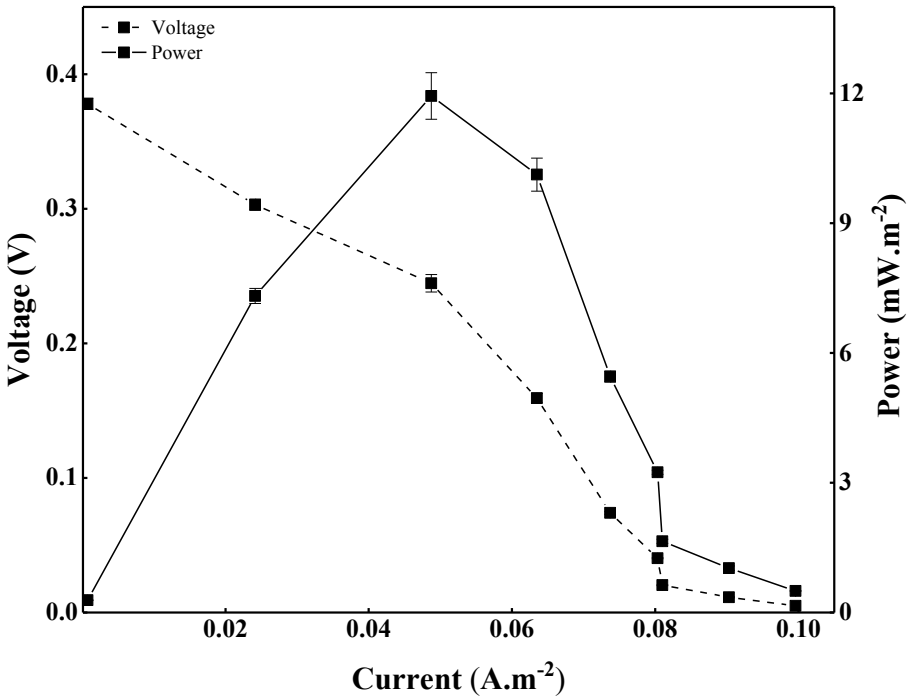

Figure S 5.1 Polarization and power density curves for the sMFC after 15 days of operation. The error bars represent standard error of measured concentrations of four replicate samples.

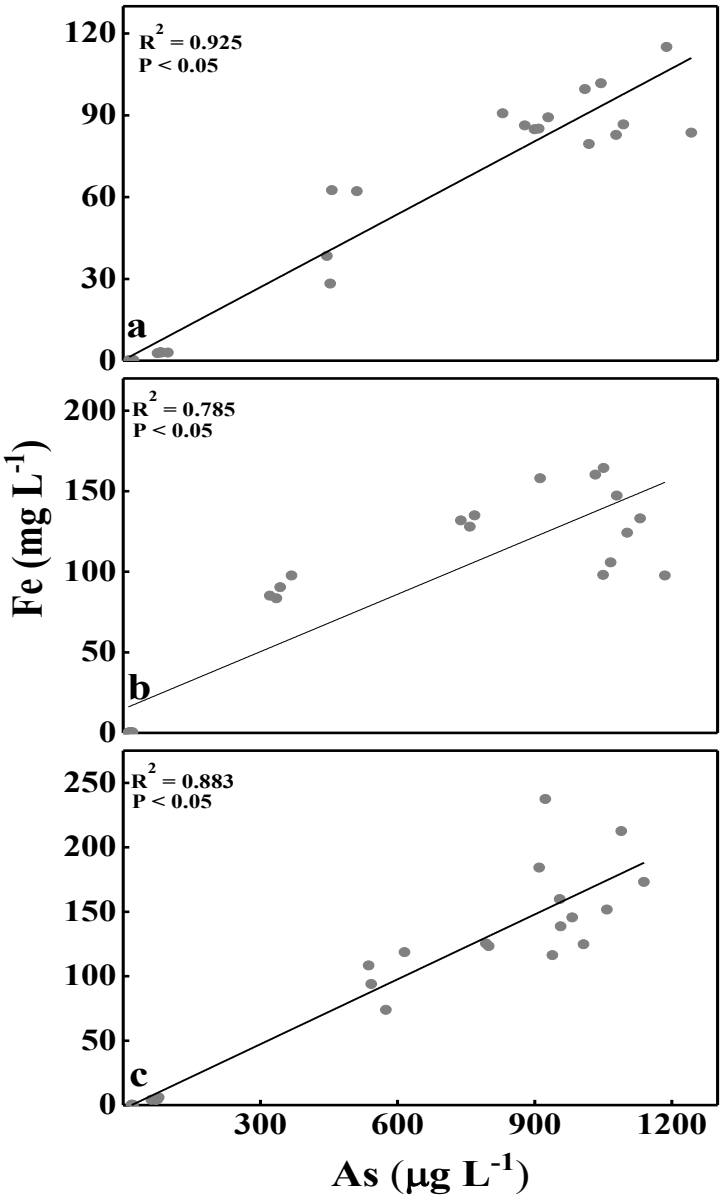

Figure S 5.2 Correlation between iron and arsenic release in the sMFC

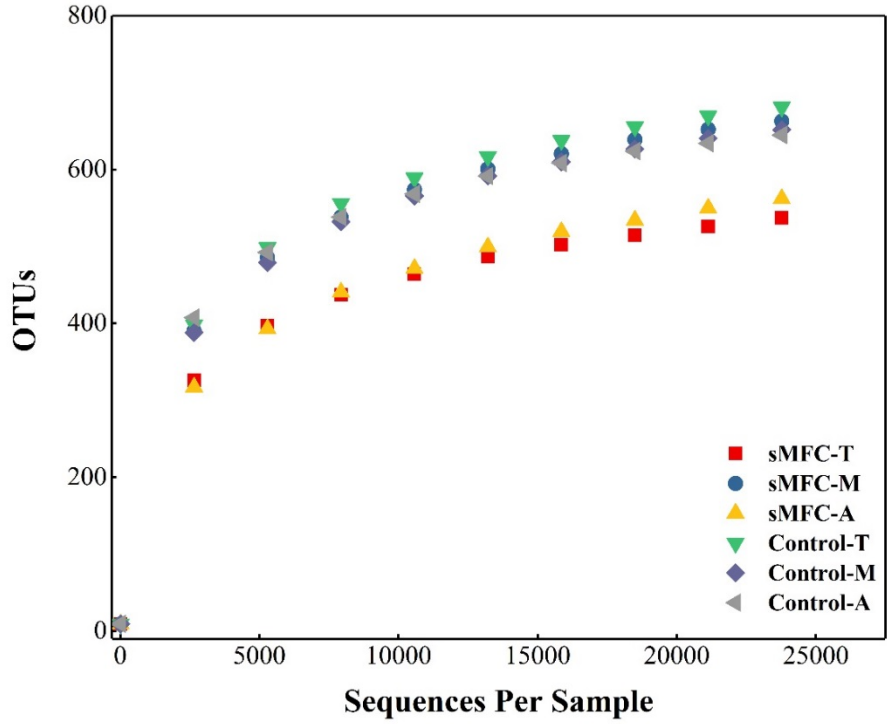

Figure S 5.3 Rarefaction curves showing the diversity of OTUs (similarity cut off of 97%)

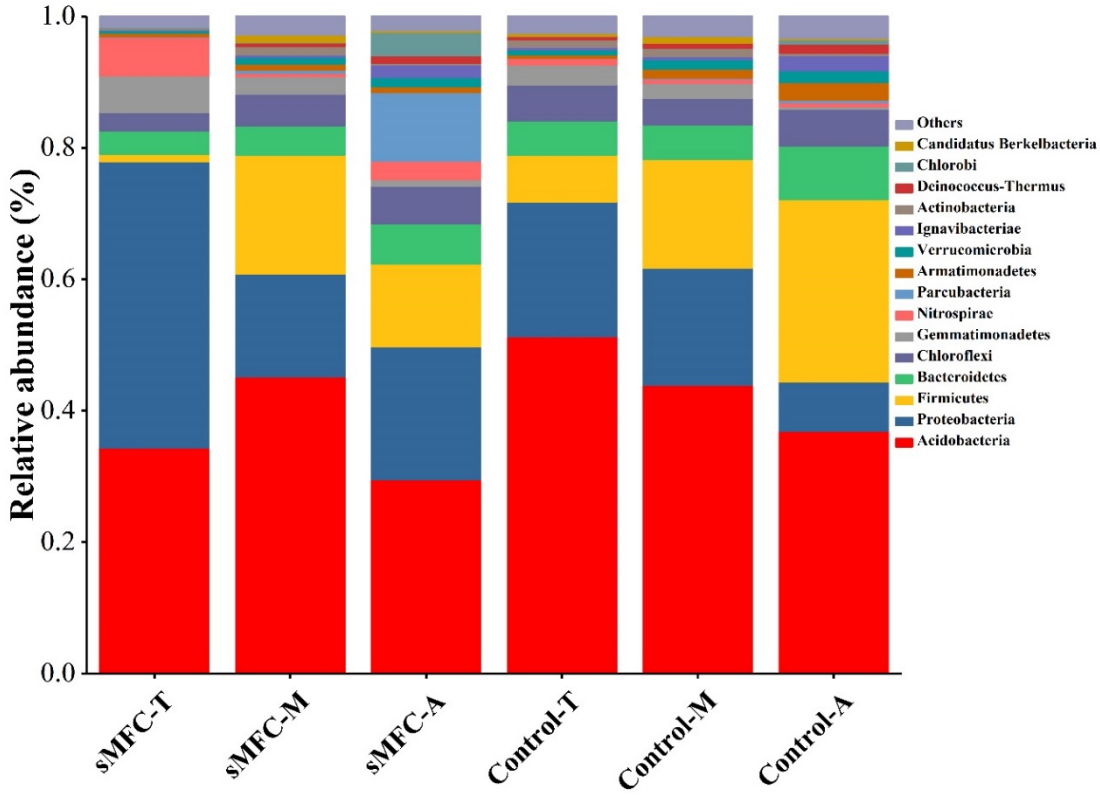

Figure S 5.4 Relative abundance of bacterial community composition at phylum level

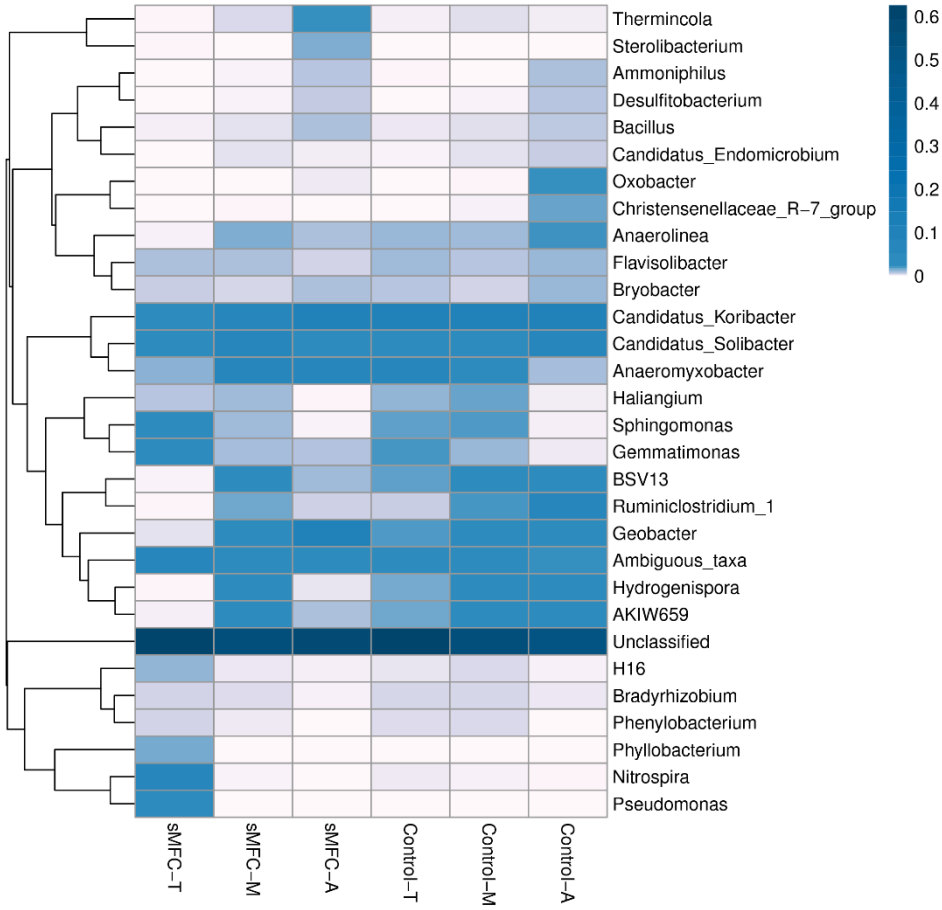

Figure S 5.5 Heat map of the relative abundance of bacterial community composition at genus level

Chapter 6 : The effect of the sMFC on arsenic in soil with high organic matter content

6.1 Abstract

Arsenic (As) mobility in paddy soils is mainly controlled by iron (Fe) oxides and Fe reducing bacteria. The Fe reducing bacteria are also considered to be enriched on the anode of soil microbial fuel cells (sMFC). Thus, the sMFC may have an impact on elements' behavior, especially Fe and As, mobilization and immobilization in paddy soils. In this study, we found dissolved organic matter (DOC) abundance was a major determinate for the sMFC impact on Fe and As. In the constructed sMFCs with and without water management, distinctive behaviors of Fe and As in paddy soil were observed, which can be explained by the low or high DOC content under different water management. When the sMFC was deployed without water management, i.e. DOC was abundant, the sMFC promoted Fe and As movement into the soil porewater. The As release into the porewater was associated with the enhanced Fe reduction by the sMFC. This was ascribed to the acidification effect of sMFC anode and the increase of Fe reducing bacteria in the sMFC anode vicinity and associated bulk soil. However when the sMFC was coupled with alternating dry-wet cycles, i.e. DOC was limited, the Fe and As concentration in the soil porewater dramatically decreased by up to 2.3 and 1.6 fold, respectively, compared to the controls under the same water management regime. This study implies an environmental risk for the *in-situ* application of sMFC in organic matter rich wetlands and also points out a new mitigation strategy for As management in paddy soils.

6.2. Introduction

Paddy fields are important farmlands that are used to cultivate rice; a crop that accounts for more than half of the global population's caloric and essential micronutrients intake (Chen et al., 2018; Fitzgerald et al., 2009). However rice consumption poses a health risk, because heavy metals are increasingly found in paddy soils worldwide, especially arsenic (As) (Islam et al., 2016; Sun et al., 2009). Arsenic is a highly toxic and carcinogenic metalloid element that exists mainly as arsenate (As(V)) and arsenite (As(III)) in natural environments with the latter being more toxic (Zhu et al., 2017). Arsenic contamination in soil decreases rice quality, threatens food safety and may lead to land abandonment. Moreover, the removal of heavy metals from the soil matrix is very difficult and costly, which farmers cannot afford (Khalid et al., 2016; Wan et al., 2016). As a consequence many heavily As-contaminated paddy fields have been abandoned, hence alternative methods are required to make good use of these contaminated lands.

Arsenic mobilization from in paddy soil has been linked to the complex processes in paddy soils. Several mechanisms have been proposed to explain As mobilization in paddy soils. The reduction of Fe oxide (Wang et al., 2009) and the direct reduction of As(V) to As(III) has been proposed as the primary mechanisms controlling the mobilization of As (Li et al., 2011; Zhu et al., 2017). In aerobic settings, As in paddy soil is mainly absorbed onto the surface of Fe oxides, consequently having restricted mobility. On the contrary, when rice fields are flooded during cultivation, the bulk soil becomes anaerobic favoring the growth of Fe-reducing bacteria which can transfer electron produced from the oxidation of organic matter (OM) to insoluble Fe oxides and/or As(V) in the soil. This results in the release of As(V) and/or the reduction of As(V) to As(III) by As(V)-reducing and dissimilatory As(V)-reducing microorganisms (Yamaguchi et al., 2011). This reduction of As(V), results in the increase of As (III) bioavailability in the soil environment, that can then be taken up by rice plants via the

silicon pathway and stored in their grains (Islam et al., 2016). This is a major health concern because consuming high quantities of As increases the risk of developing various terminal illnesses, such as skin and liver cancers (Minatel et al., 2018).

In addition to cultivating rice, paddy fields have been utilized as bioelectrochemical systems in the form of *in-situ* soil microbial fuel cells (sMFC) in small scale experiments and the results are promising (Kaku et al., 2008). In these systems the anode of sMFC was buried in the anaerobic soil and served as a terminal electron acceptor for electrons produced during the anaerobic microbial degradation of OM. The sMFC anode can sustain the growth and metabolic activity of exoelectrogens in its vicinity (Gustave et al., 2018b) enhances bioavailable dissolved organic matter (DOC) in soil porewater degradation. Besides influencing DOC concentration, the anode can also influence soil, nutrients availability, pH, redox potential (E*h*), methane emissions and microbial community structure (Gustave et al., 2018a; Hong et al., 2009; Kouzuma et al., 2013; Touch et al., 2017). Although, enhancement of exoelectrogens is beneficial for power output of the sMFC (Logan, 2009) and removal of organic pollutants (Huang et al., 2011), in As contaminated paddy soil this may be problematic, since the enhancement of Fe-reducing bacteria (IRB) and the decrease in soil pH favors Fe oxide reduction and As mobility (Gustave et al., 2018a; Yamamura et al., 2018).

However, the influence of sMFC on soil trace metal mobilization has not been well investigated. In some previous work, the impact of the sMFC on solubilization of Fe oxides has been described (Gustave et al., 2018a; Touch et al., 2017; Wang et al., 2015; Yang et al., 2016; Zhou et al., 2015). Nevertheless, the reports on the impact of sMFC on Fe dissolution in soil porewater are contradictory. Several studies observed that the anode immobilized Fe and prevented Fe release into the soil porewater (Gustave et al., 2018a; Touch et al., 2017; Wang et al., 2015; Yang et al., 2016). This phenomenon was explained by the oxidation of Fe(II) to Fe(III) during anode bacterial growth, changes in soil E*h* (Touch et al., 2017; Wang et al., 2015;

Yang et al., 2016) and decreased DOC availability in the soil porewater (Gustave et al., 2018a). On the contrary, it has also been reported that the sMFC enhances reduction and consequently increases soil porewater dissolved Fe in lake sediment (Zhou et al., 2015). The reasons claimed for the increase solubility of Fe was attributed to the enhanced Fe reduction by IRB and high DOC concentration (Zhou et al., 2015). All of the results above indicate, that the behaviors of Fe and elements (especially As) that was precipitated with Fe would change when sMFC is installed, followed by the change of DOC availability, soil Eh and pH changes, and/ or the soil microbial community that developed. However, the influence of those factors on Fe and As cycling in the sMFC remains unclear.

When sMFCs are proposed to be deployed in wetlands whether to produce electricity or decrease pollutants, it is important to understand how the sMFC will impact the biogeochemical behavior of Fe and the associated elements of environmental concern. Hence in this study, we aim to reveal the effects of the sMFC on Fe and As mobility in paddy fields, a typical artificial wetland in agriculture. We hypothesized that the impacts of sMFC on Fe and As behaviors are linked with DOC abundance, the acidification effect of sMFC bioanode, and the anode microbial community. To disentangle the mechanism, water management was applied as a moderate method to control soil DOC levels with small disturbance of other soil properties. Thus, we considered two scenarios, a simple paddy soils MFC system (sMFC) (high DOC) and paddy soils MFC coupled with water management (sMFC-WM) (limited DOC). We coupled the sMFC with water management because alternating wet-dry cycles has been shown to enhance DOC mineralization from paddy soil (Li et al., 2015; Saidpullicino et al., 2016).

6.3. Materials and Methods

6.3.1. Paddy Soil Sample

The paddy soil was collected from a rice paddy in Qiyang Hunan, southern China (GPS N26.760 E111.86). The total carbon, As and Fe concentration were measured to be 23.2±0.9 g/kg, 73.7±5.9 mg/kg and 53.7±1.8g/kg, respectively (Table S 6.1).

6.3.2 Soil Microbial Fuel Cell Assembly

Eight sMFC were constructed from the paddy soil and operated for 60 days to examine the effect of the anode on Fe and As movement in paddy soil. In this experiment, all cells were left at open circuit for ten days prior to adding the external resistor and only after adding the external resister was the voltage recorded. Of the eight sMFC four were control replicates, the anodes and cathodes were not connected to any resister (open circuit). The remaining four were treatment replicates and were connected to a 500Ω external resistance (close circuit). All sMFC were constructed according to a previously reported method in chapter 2. Briefly, a columnar polyethylene terephthalate container (10 cm diameter × 15 cm depth) with a three valve port was used to construct each sMFC. The valve ports were located 1 cm below the soil water interphase (top layer), 2cm above the anode (middle layer) and one adjacent to the anode (bottom layer). Circular carbon felts with geometric surface area of 50.2 cm^2 were used as anodes and cathodes. A data logger (NI-USB-6225, USA) was used to record the voltage between the anode and cathode every ten minutes.

Using the 1kg (dry weight) of soil sample, ~1 cm depth of soil was placed at the bottom of the sMFC container. Then the anode was placed on the surface of the soil layer and buried with the remaining soil. Deionized water was added to flood the paddy soil. The cathode was placed above the soil in aerobic conditions (half submerged in water and the other half in the open air).

6.3.3. Dry-wet Cycles

In this experiment sMFC were constructed as described above with slight modifications. Each cell was equipped with three soil porewater sampler and a draining valve to facilitate the drying cycles adjacent to the anode. The control sMFC (control-WM), were left at open circuit and treatment sMFC (sMFC-WM) were connected to a 500Ω external resistor immediately after construction. All cells (control-WM and sMFC-WM) were drained by opening the drain valve to allow the water to leak out of the cell during each draining cycle. The cells were subjected to drying phases to allow oxygen diffusion into the anaerobic soil to enhance DOC mineralization (Li et al., 2015; Saidpullicino et al., 2016). Water was refilled when the sMFC voltage dropped below 20 mV. Soil porewater was collected prior to each dry phase on day 7, 14, 21, 28 and 35. There were 4 replicates for each treatment.

6.3.4. Chemical Analysis

Soil porewater was analyzed for total As, total Fe and dissolved organic carbon (DOC) concentration. In this study DOC is a measurement of the amount of OM in soil porewater after filtration through a 0.45 μm filter. The fluorescence excitation emission matrix (EEM) analysis was to characterize the DOC composition in the soil porewater. Soil E*h* was determined with a platinum (Pt) and Ag/AgCl electrode. Both the Pt and the Ag/AgCl electrode were inserted in the soil ca. 0.5cm above the anode and the E*h* was allowed to stabilize for 1 hour before being recorded. Soil pH was measured with a soil pH meter by mixing soil with water at a ratio of 1:2.5. All of the analysis were conducted according to the methods descried in chapter 2.

6.3.5. Microbial Community Analysis

Soil samples were collected from the anode and associated soil, 2 cm above the anode and 1 cm below the soil water interphase in the sMFC. In the sMFC with water management soil samples were collected only from anode and associated soil and the bulk soil (BS) at the end of the incubation period for extraction of genomic DNA. The genomic DNA was extracted

immediately after collection from 0.25g of each sample using MoBio Laboratories Inc.'s Powersoil DNA isolation Kit (MoBio, Carlsbad, CA, USA) according to the manufacturer's instructions. The V4-V5 region of the bacterial 16S rRNA genes were amplified using the forward primers 347F (5'-CCTACGGRRBGCASCAGKVRVGAAT-3') and reverse primers 802R (5'-GGACTACNVGGGTWTCTAATCC-3'). Details for Illumina sequencing, experimental steps and data analyses are described in detail elsewhere (You et al., 2016) and Chapter 2.

6.3.6. Nucleotide sequence accession number

The nucleotide sequences can be found at NCBI GeneBank database with accession number MF949071-MF950889 and MH989602 - MH990255.

6.4. Results

6.4.1. sMFC performance

The sMFC's performance and DOC variation over 60 days are shown in Fig. 6.1. The current initially increased to a maximum of 1.15mA on day 13 then decreased gradually. The cathode potentials increased slightly and remained relatively stable during the whole operational period while the anode potential increased steadily. Additionally, the DOC concentration near the anode gradually decreased with time. These results suggest that the current changes were mainly controlled by the anode potential and DOC bioavailability. Furthermore, the variations in current from the sMFC-WM are shown in Fig. S 6.1. The maximum current output of the sMFC-WM (0.6mA) was observed during the second cycle. However the current decreased with dry-wet cycles. A maximum power density of 123.0 ±2.2 mWm^{-2} and 43.4 ±2.8 mWm^{-2} were observed in the sMFC and the sMFC-WM, respectively.

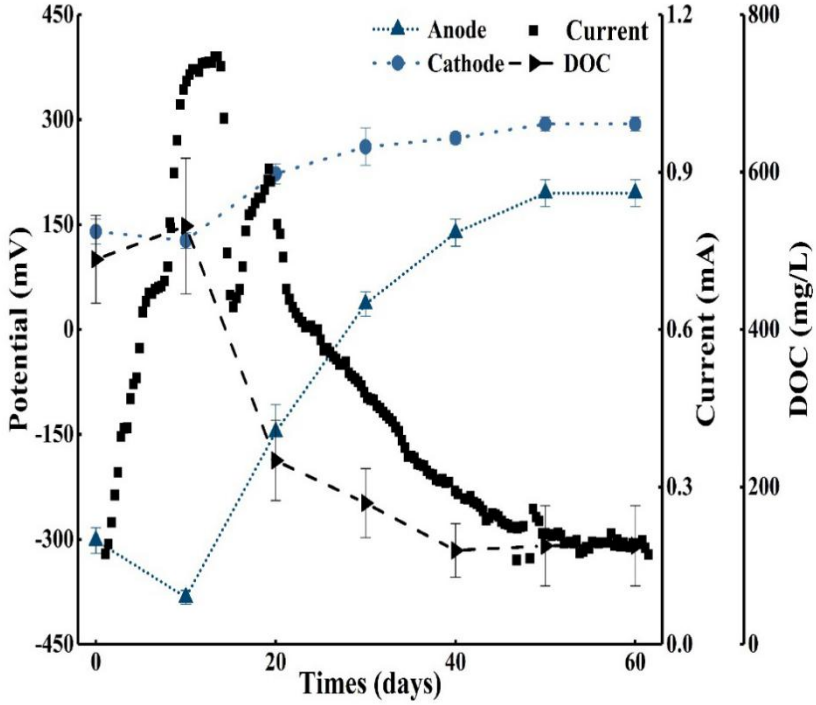

Figure 6.1 The variations of current output, organic matter concentration (DOC), anode and cathode potential over time. The error bars represent standard error of measured concentrations and potential of four replicate samples.

6.4.2. Effect of sMFC on the soil physiochemical properties

The change in soil E*h* and pH were examined in the sMFC and the sMFC-WM. In the control and control-WM, the soil E*h* sharply decreased to -460±3.3 mV and -314.8±28.5 mV (vs the Ag/Cl electrode). In contrast, the soil E*h* around the anode of the sMFC and sMFC-WM increased to -154.6±6.6 mV and 110.0±23.5 mV (Table 6.1). Furthermore, the soil pH at the bottom and middle layers were more acidic in the sMFC compared to the control (Table 6.1). While the pH in the top layer of the sMFC was more basic than that of the control. Similar pH patterns were observed in the sMFC-WM. The pH in the bottom and middle layer of the sMFC-WM were lower than that of the control-WM. Moreover, the pH in the top layer of the sMFC-WM was also higher than that of control-WM (Table 6.1). However it should be noted that the pH in the sMFC-WM were higher than that of sMFC in all layers.

Table 6.1 Changes of pH and redox potential in soil samples of reactors at the end of the experiment

	Sample ID											
	sMFC-T	sMFC-M	sMFC-A	Control-T	Control-M	Control-A	sMFC-WM-T	sMFC-WM-M	sMFC-WM-A	Control-WM-T	Control-WM-M	Control-WM-A
pH	6.9 ±0.02	5.9 ±0.03	5.6 ±0.2	5.9 ±0.1	6.2 ±0.03	6.2 ±0.1	7.7 ±0.1	6.7 ±0.04	6.5 ±0.03	6.9 ±0.1	7.1 ±0.1	7.3 ±0.1
Eh (mV vs Ag/AgCl)	-	-	-154.6 ±6.6	-	-	-460.0 ±3.3	-	-	111.0 ±23.5	-	-	-314.8 ±28.5

Notes: T, M and A: represents samples collected from top layer, middle layer and anode vicinity respectively. Mean ± SE (n = 4)

The DOC concentration gradually decreased with time in both the sMFC and the control (Fig. S 6.2). No significant differences were observed in the top, middle and bottom layers between the DOC in the sMFC and control treatment. However when the sMFC was combined with dry-wet cycles accelerated DOC degradation was observed in all layers of the sMFC-WM compared to control-WM (Fig. 6.2). The results showed that sMFC-WM, could significantly enhance DOC mineralization. The DOC concentration was 1.5 folds lower in sMFC-WM anode vicinity compared to the control-WM on day 35. Moreover, fluorescence spectroscopy was used to characterize the soil porewater DOC composition to understand the mechanism behind the enhanced DOC removal in sMFC-WM. Figure S3a-h and. Figure S4a-h shows the change in typical EEM feature of DOC with time in the sMFC-WM and sMFC respectively. In Fig. S 6.3 and S 6.4, peaks corresponding to tryptohan-like components (ex < 240 and em shorter than 360) (Fellman et al., 2010) decreased significantly after 30 days of incubation in all treatments. Furthermore, the concentration of ultraviolet C (UVC) humic acid-like component (ex 320-360 and em 420-460) (Fellman et al., 2010) significantly decreased in sMFC-WM with time compared to the control-WM. The components assigned to terrestrial humic acid-like (ex 220-235 and em 478) and fulvic acid-like (ex 220 and em 408) (Derrien et al., 2017) (Lapierre and Del Giorgio, 2014) significantly increased in sMFC-WM with time. In the control-WM the concentration of UVC humic-like component increased with time. These results suggest that the sMFC-WM favored the transformation of DOC components from UVC humic-like to more fulvic acid-like. However no substantial differences was observed in the sMFC and the control.

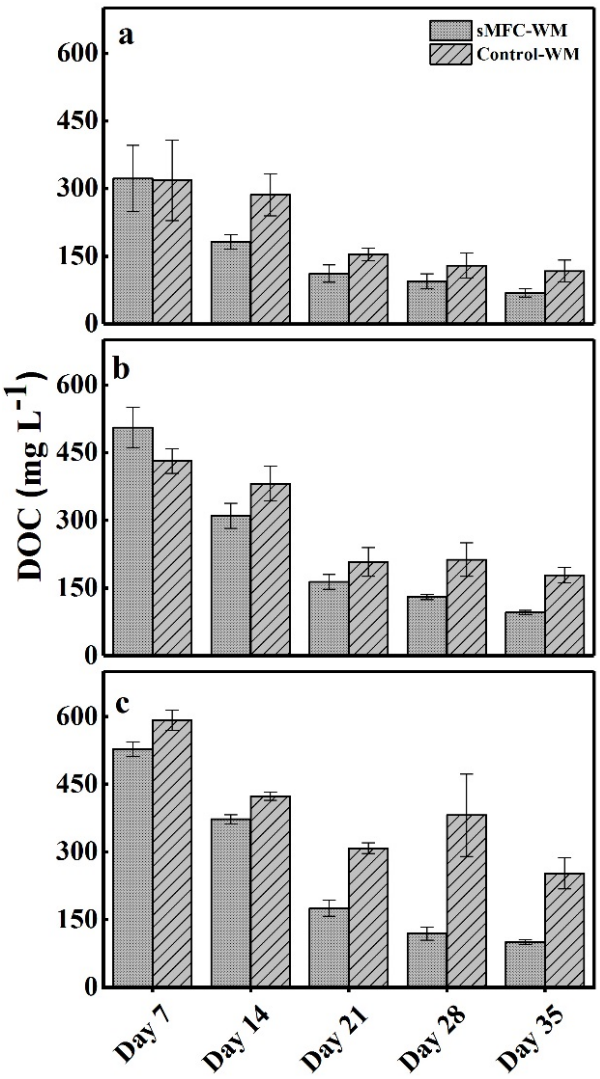

Figure 6.2 DOC variation in the sMFC-WM and Control-WM soil porewater as a function of incubation time. Panels a, b and c show DOC concentrations in the top, middle and bottom layers, respectively. The error bars represent standard error of measured concentrations of four replicate samples.

6.4.3. The impacts of sMFC on Fe and As behavior in the paddy soil porewater

The concentrations of porewater total Fe and As in different layers of the sMFCs are illustrated in Fig. 6.3a-f. The Fe concentration increased with time in both the sMFC and the control to a maximum and then decreased. The decrease in porewater Fe could be due to the formation of new insoluble Fe minerals. However significantly higher soil porewater Fe was

observed in the sMFC compared to the control in all layers. The biggest difference between the sMFC and the control was observed in the bottom layer (Fig. 6.3c, P = 0.014) compared to that of the middle layer (Fig. 6.3b, P = 0.040) and top layer (Fig. 6.3a, P = 0.031), indicating that the effects of the anode decrease with increasing distance away the anode. A similar trend was observed for As concentration in soil porewater (Fig.6.3d-f). The mean concentrations of As were elevated in the sMFC compared to those of the control in all layers. The increase of As irrespective of distance away from the anode highly correlated with the increase of Fe (R^2 = 0.61 $p < 0.005$, $R^2 = 0.45$ $p < 0.005$ and $R^2 = 0.80$ $p < 0.005$ in the top, middle and bottom layers respectively), suggesting that As release could be due to an increased reduction of Fe oxides (Fig. S 6.5a-c). Furthermore when dry-wet cycles were applied, the sMFC-WM significantly limited Fe reduction which consequently led to a decrease of As concentration in the soil porewater with time in all layers (Fig. 6.4a-c). After 35 days of operation the concentration of As in sMFC-WM anode vicinity (288.0±98.6 µg/L) was significantly lower than the control-WM (737.2±145.0 µg/L).

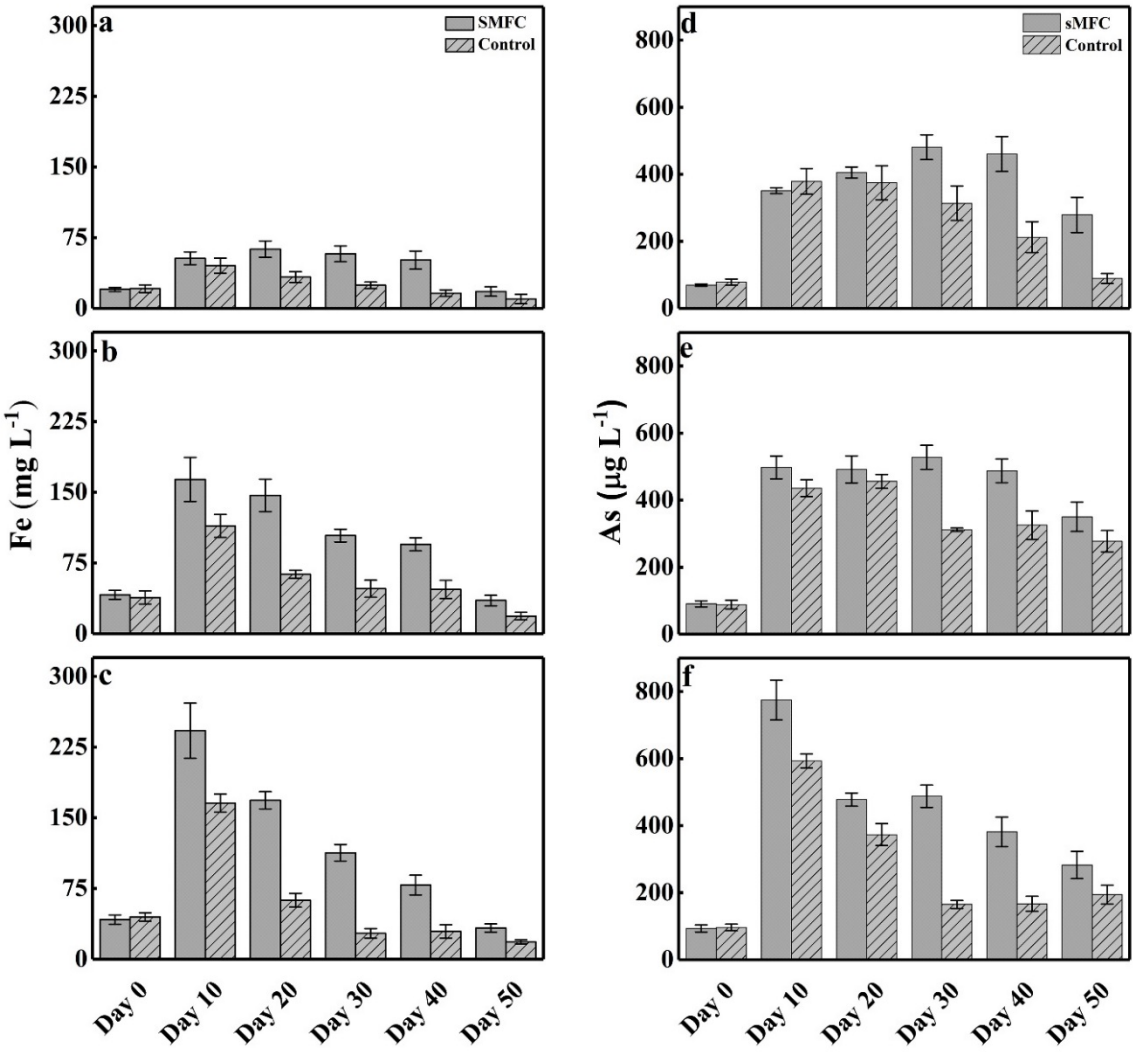

Figure 6.3 Iron and As variation in the sMFC and control soil porewater as a function of incubation time. Panels a, b and c show Fe concentrations in the top, middle and bottom layers, respectively. Panels d, e and f show As concentrations in the top, middle and bottom layers, respectively. The error bars represent standard error of measured concentrations of four replicate samples.

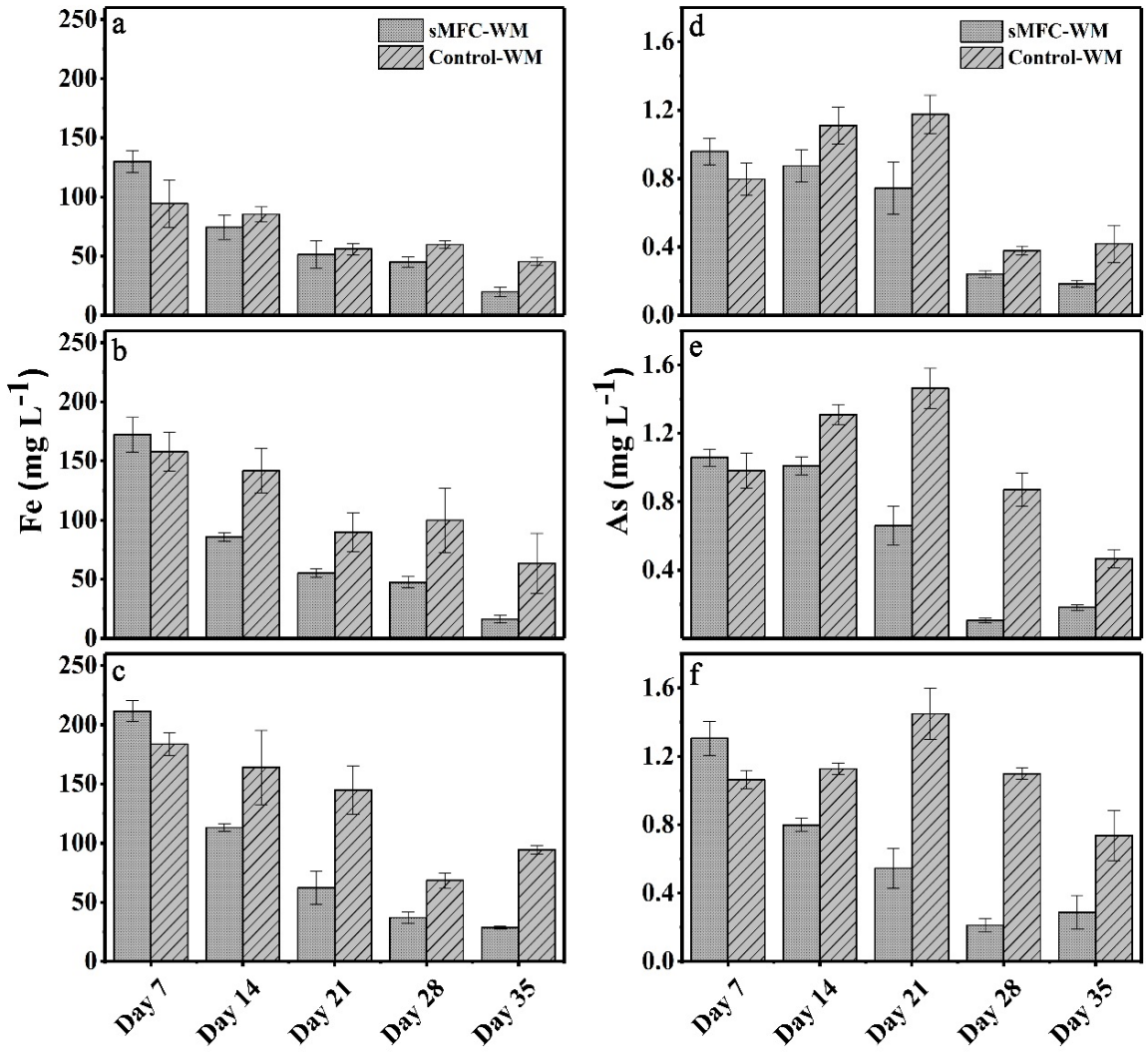

Figure 6.4 Iron and As variation in soil porewater as a function of incubation time. Panels a, b and c show Fe concentrations in the top, middle and bottom layers, respectively. Panels d, e and f show As concentrations in the top, middle and bottom layers, respectively. The error bars represent standard error of measured concentrations of four replicate samples.

6.4.4. The impacts of sMFC on Bacterial community structure

The bacterial community was investigated by the Illumina high through-put sequencing technique. Rarefaction curves displayed a saturated trend, indicating sufficient sequencing depths were achieved (Fig. S 6.6). Alpha diversity measures revealed the richest diversity in the bulk soil irrespective of treatment and lowest diversity in the anode vicinity of the sMFC

and sMFC-WM (Table S 6.2). It should also be noted that higher diversity was observed in the sMFC compared to the sMFC-WM. Furthermore, the bacterial community in the sMFC top layer (p =0.031), middle layer (p =0.022) and anode vicinity (p =0.018) were significantly different from that of the control. The bacterial community in the bulk soil (p =0.026) and anode vicinity (p =0.026) of the sMFC-WM was significantly different from that of the control-WM. Moreover the bacterial community that developed in the sMFC was significantly different from that of the sMFC-WM.

At the class level, the dominant class differed among different sample locations and treatments. The majority of the bacterial reads belonged to *Clostridia, Deltaproteobacteria, Betaproteobacteria, Sphingobacteriia, Gammaproteobacteria, Bacteroidetes vadinHA17, Ignavibacteria, Alphaproteobacteria, Acidobacteria, Actinobacteria, Bacilli* and *Anaerolineae* (Fig. S 6.7a-b). In the top layers of sMFC and the control, *Betaproteobacteria* was the most dominant group with a relative abundance of 21.8% and 18.24%, respectively. Whereas, in the middle layers and the anode vicinity of the control *Clostridia* was relatively higher than the others. The control middle layer and the control anode vicinity had 30.5% and 35.5% *Clostridia,* respectively. The middle of the sMFC contained 30.3% *Clostridia.* The relative abundance of *Deltaproteobacteria* in the anode vicinity of the sMFC was significantly (28.5%) ($p< 0.001$) higher than that from all other locations. Similar to the control, *Clostridia* (34.4%-38.9%) dominated the bulk soil and anode vicinity of the sMFC-WM. *Deltaproteobacteria* (13.6%-14.1%) in the bulk soil and anode vicinity of the control-WM was higher than that of sMFC-WM. The sequences were further classified to the genus level and the top 8 genus are illustrated in Fig. 6.5a-b. The genus *Geobacter* (0.98%-25.9%) and *Thermincola* (0.07%-5.84%) were the most dominant groups in sMFC. Moreover, in control *Lentimicrobium* (1.68%-7.17%) and *Clostridium sensu stricto10* (1.60%-3.01%) were more abundant. In the sMFC-WM *Clostridium sensu stricto10* (6.5%-6.9%) and *f family XVIII unclassified* (6.5%-11.4%) were

more abundant. *Anaeromyxobacter* (10.3%-11.3%) and *Flavisolibacter* (2.3%-2.9%) were the most dominant groups in control-WM.

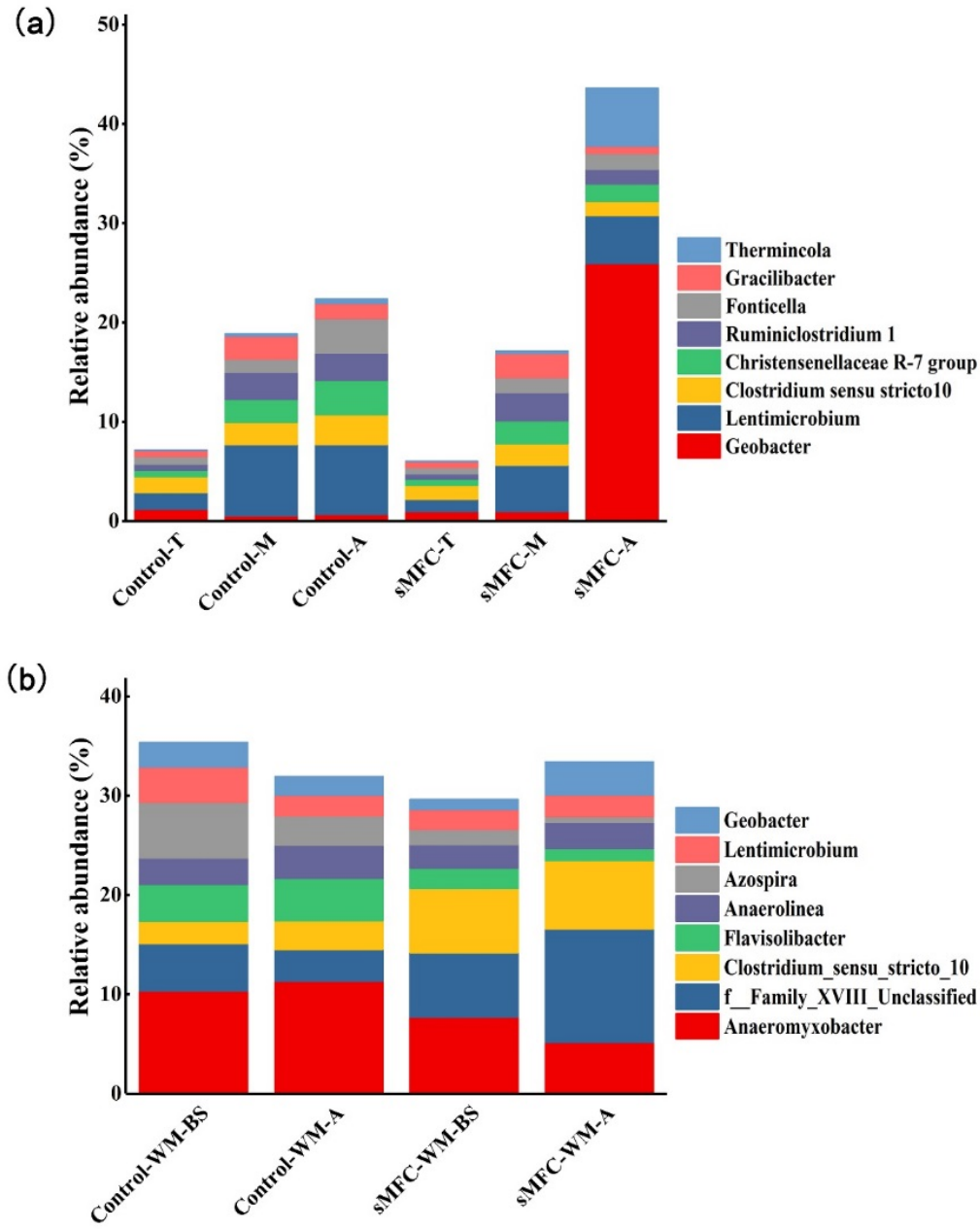

Figure 6.5 Relative abundance of microbial community composition at genus level for the sMFC without (a) and with water management (b).T, M, A and BS: represents samples collected from top layer, middle layer, anode vicinity and bulk soil respectively. The value represent the mean of four replicates

6.5. Discussion

6.5.1 Current generation in the sMFC and sMFC-WM

In all the cells assembled in this study, the current raised sharply in the beginning, and dropped when DOC concentration decreased (Fig.6.1 and Fig. S 6.1). This suggests that the current was most likely to be controlled by the availability of organic substrate, as indicated by the DOC and current production trends (Fig. 6.1). Furthermore, a simultaneous drop of sMFC-WM current and DOC was found when the cells were dried and re-wet (Fig. S 6.1). The observed results suggested that DOC became a limiting factor of current generation when DOC decreased. Although the DOC (ca 150 mg/l) was high in our study, the current decreased observed here was probably due to the DOC being mostly composed of biorefractory components such as humic acid (He et al., 2013). The fluorescence EEM spectra analysis showed that the DOC composed mostly of biorefractory ultraviolet C (UVC) humic acid-like components (He et al., 2013). The bioavailable DOC is considered to be important for production of electricity in sMFC and bioavailable DOC concentration has been shown to positively correlate with electricity generation and power output (Hong et al., 2010; Song and Jiang, 2018).

6.5.2. sMFC enhances porewater Fe and As when soil OM is abundant

In this study, higher dissolved Fe and As concentration were observed in the sMFC compared to the control. Our results were in agreement with Zhou et al. (2015) study, which applied the sMFC to prevent the occurrence of black water agglomerate (deterioration of water quality caused by cyanobacteria bloom). In both case, sMFC was operated under high DOC conditions and enhanced Fe reduction. When DOC was abundant, an accelerated degradation of DOC by sMFC cannot be observed (Fig. S 6.2), which suggests there was no clear competition for DOC between anode community and the bacteria in bulk soil. Thus, we hypothesized that the enhancement of total Fe and As in soil porewater can be explained by

two mechanisms: the acidification effect of anode reactions and functional bacteria re-distribution influenced by the anode bacteria community.

In the sMFC, the anode can sustain the growth and metabolic activates of IRB (Wang et al., 2015; Yuan et al., 2018) and enhance DOC degradation by serving as an electron sink (Gustave et al., 2018a; Song et al., 2010). The continuous degradation of DOC results in the production of protons and carbondioxide (Gustave et al., 2018a; Hong et al., 2009), which in turn may have led to the decrease in soil pH in sMFC middle layer and the anode vicinity (Table 6.1). Therefore, this decrease in paddy soil pH may have contributed to observed increase in porewater Fe and As concentrations in the sMFC, since acidic soil conditions favor the formation of soluble Fe phases (Gorny et al., 2015; Hutchins et al., 2007). Furthermore the lower soil pH could have also affected the surface charge of Fe oxides thus influencing the adsorption-desorption behavior of As on Fe oxides (Table 6.1). Jiang et al. (2014), observed a negative relation between the dissolved Fe and soil pH. A similar relationship for soil porewater As concentration was also reported in a study by Signespastor et al. (2007). Moreover, the gradual decrease in the amount of dissolved Fe and As in both the sMFC and the control could be due to the formation of insoluble iron minerals such as iron sulfide and iron carbonates minerals. Previous studies have shown that under anoxic conditions microbially-derived sulfide can react with Fe and As to produce Fe sulfide minerals (e.g., pyrite and mackinawite) and As-sulfide-like species (e.g., orpiment and realgar), respectively (Burton et al., 2011; Hashimoto and Kanke, 2018). Studies have shown that under reducing conditions that these newly form Fe and As sulfide species can induce As precipitation and insolubilization (Burton et al., 2011; Hashimoto and Kanke, 2018). Similarly, iron carbonate minerals have also shown remove As from water solutions under anoxic conditions (Guo et al., 2013). However, in this study we did not measure Fe mineralogy to confirm the above, thus further studies are needed. Nonetheless the paddy soil environment is suitable formation of secondary Fe minerals that

can reduce the aqueous concentration of Fe and As (Burton et al., 2011; Hashimoto and Kanke, 2018).

Furthermore, changes in the bacteria community could have also contributed to the increase of Fe and As solubility. The class *Deltaproteobacteria* was enriched in the vicinity of the sMFC anode and is known to contain many dissimilatory Fe and As reducing bacteria (Hori et al., 2010). Moreover, at the genera level two well-known Fe reducing genus, *Geobacter* and *Thermincola* (Logan, 2009; Marshall and May, 2009) were enriched on the anode and bulk soil of the sMFC (Fig. 6.5a). Species from the *Geobacter* clade demonstrates the ability to use DOC as an electron donor to reduce both Fe(III) and As(V) (Chen et al., 2016; Lovley and Phillips, 1988; Qiao et al., 2017). Similar to *Geobacter*, members of the genus *Thermincola* can utilize insoluble Fe oxide as an electron acceptor. The most prevalent *Thermincola* sequence found in the sMFC was closely related to *Thermincola ferriacetica*, a known metal-reducer (data not shown) (Zavarzina et al., 2007). *Thermincola ferriacetica* was found to reduce amorphous Fe oxide with acetate as an electron donors (Zavarzina et al., 2007). Additionally, members of the *Bacteroidetes* environmental groups *VadinHA17* was also significantly higher in the sMFC middle layer (Fig. S 6.7a). *Bacteroidetes* have been observed to degrade complex DOC while using nitrate or elemental sulfur to produce acetate with hydrogen and carbondioxide as byproducts (Baldwin et al., 2015; Grabowski et al., 2005; Krespi et al., 2006). The acetate that is produced by *Bacteroidetes*, could have been used by IRB as an electron source and the carbondioxide possibly contributed to the lower pH and the increase in soil porewater Fe and As in the bulk soil of the sMFC.

Diffusion and cathodic reactions might explain the elevated Fe and As levels in the sMFC top layer (Gustave et al., 2018a) (Fig. 6.5a). The concentrations of dissolved Fe and As in top levels were much lower than those in middle and bottom layers, thus Fe and As could continuously be diffused upward due to diffusive forces. At the same time, the overlaying water

and top soil layers were alkalized by the cathode of the sMFC, which consumed proton to reduce oxygen (Logan, 2008). The near neutral condition in surface water facilitated Fe(II) precipitation and the co-precipitation of As with Fe oxides (Weber et al., 2006).

6.5.3. sMFC decreases porewater Fe and As when soil DOC is limited

When sMFC was coupled with water management, the soil porewater Fe and As behaviors were distinct from the previous results obtained in sole sMFC experiment. We observed a significant decrease of total Fe and As in the sMFC-WM treatment compared to the control-WM (Fig. 6.4a-c). This could be due to the bacterial re-distribution and substrate competition. In the control-WM, known iron and arsenic reducing bacteria such as *Geobacter, Flavisolibacter, Anaeromyxobacter* and *Azospira* were significantly ($p< 0.001$) higher in the control-WM bulk soil than that of the sMFC-WM (Fig. 6.5b). *Geobacter, Flavisolibacter, Anaeromyxobacter* and *Azospira* have been reported to achieve dissimilatory Fe and/ or As - reduction and owing to their dominance in the control-WM bulk soil, these genera may have a role in Fe and As enrichment in the soil porewater control-WM through dissimilatory reduction processes (Kudo et al., 2013; Peng et al., 2016).

Moreover DOC was also dramatically decreased in the sMFC after implementing dry-wet cycles (Fig. 6.2). In sMFC-WM we verified that soil DOC was responsible for the enhance Fe and As mobility as was evident in sample Day 7, before commencing the dry-wet cycles (Fig. 6.4a-c). Even though the sMFC-WM was operational, under high DOC loads, similar to the sMFC an increase in total Fe and As concentration was observed in all layers (Fig.6.4 a c). This result supports our hypothesis that under high DOC content the sMFC enhances Fe and As release. Furthermore, EEM spectra results of DOC samples suggest that the increase in Fe and As may have occurred because the DOC contained a high abundance of UVC humic-like molecules (containing quinone-like structures) (Fellman et al., 2010) (Fig. S 6.3a). Since UVC humic-like molecules could have been used to facilitate electron shuttling to reduce Fe-oxide

and As(V) in the bulk soil (Chen et al., 2003; Kappler et al., 2016; Roden et al., 2010) and led to the higher As concentration in the soil porewater. Zhou et al. (2015), observed similar results when sMFC was applied in soil with high DOC concentrations. In their study higher dissolved Fe was observed in soil porewater of sMFC amend with cyanobacterial bloom biomass (CBB) compared to non-CBB sMFC and control sMFC. Likewise, higher dissolved Fe was observed in the non-CBB sMFC compared to the control sMFC (Zhou et al., 2015). Their results agreed with ours, suggesting that the sMFC will enhance Fe reduction under high DOC conditions.

The decrease in DOC in the sMFC-WM may have led to the significant decrease in soil porewater As concentration compared to the control-WM (Fig. 6.2a-c). Many studies have shown a positive relationship between Fe oxide and DOC with As mobility in soil porewater (Gustave et al., 2018a; Stuckey et al., 2015; Wang et al., 2016). The microbial As release was mainly due to the reduction of As bearing Fe oxides or As(V) and DOC was a limiting factor (Gustave et al., 2018a; Stuckey et al., 2015). Therefore, because the sMFC-WM made DOC a limiting factor this may have resulted in a shortage of electron donors to IRB in the bulk soil and consequently decrease As concentration in the soil porewater. In addition to the decrease in DOC, the change in DOC composition from UVC humic acid-like molecules to less aromatic like humic may have also resulted in the incidence of fewer redox active aromatic compounds to facilitate electron shuttle between bacteria to Fe oxide in the bulk soil. This thereby may have limited the activity of bacteria that uses electron shuttles during anaerobic reparation (Chen et al., 2003; Kappler et al., 2016; Roden et al., 2010). However, to the best of our knowledge, the exact mechanism in which the dry-wet cycles enhance DOC mineralization and transformation in the sMFC-WM is not fully understood yet. One putative pathway is that during the wet-dry cycles oxygen was introduced into anaerobic soil and reacted with Fe(II) and/or the reduction of aromatic components of DOC to produce •OH via Fenton reactions. The •OH then rapidly reacts with DOC and enhances the degradation of the reluctant DOC to

produce degraded aromatic and non-aromatic molecules (Trusiak et al., 2018). Nonetheless further studies are required to confirm this mechanism.

6.6. Conclusions

The results obtained here demonstrate for the first time that the sMFC may enhance the risk of As if operated in As-polluted paddy soils with high OM. This occurs because the sMFC can promote the mobilization of As through the decrease in soil pH and the increase in bulk soil Fe and As reducing bacteria. Therefore, the *in-situ* use of sMFC in high OM wetland environments should be carefully evaluated in respect to environmental risk. Furthermore, this study also shows that incorporating sMFC with water management practices in OM rich soil can reverse this negative effect by decreasing DOC and UVC humic acid-like molecules.

6.7. Reference

Baldwin, S.A., Khoshnoodi, M., Rezadehbashi, M., Taupp, M., Hallam, S., Mattes, A., Sanei, H., 2015. The microbial community of a passive biochemical reactor treating arsenic, zinc, and sulfate-rich seepage. Front. bioeng. biotechnol. 3, 27.

Burton, E.D., Johnston, S.G., Bush, R.T., 2011. Microbial sulfidogenesis in ferrihydrite-rich environments: effects on iron mineralogy and arsenic mobility. Geochim. Cosmochim. Ac. 75, 3072-3087.

Chen, H., Tang, Z., Wang, P., Zhao, F.J., 2018. Geographical variations of cadmium and arsenic concentrations and arsenic speciation in Chinese rice. Environ. Pollut. 238, 482-490.

Chen, J., Gu, B., Royer, R.A., Burgos, W.D., 2003. The roles of natural organic matter in chemical and microbial reduction of ferric iron. Sci. Total Environ. 307, 167-178.

Chen, Z., Wang, Y., Xia, D., Jiang, X., Fu, D., Shen, L., Wang, H., Li, Q.B., 2016. Enhanced bioreduction of iron and arsenic in sediment by biochar amendment influencing microbial community composition and dissolved organic matter content and composition. J. Hazard. Mater. 311, 20-29.

Derrien, M., Yun, K.L., Park, J.E., Li, P., Chen, M., Sang, H.L., Lee, S.H., Lee, J.B., Jin, H., 2017. Spectroscopic and molecular characterization of humic substances (HS) from soils and sediments in a watershed: comparative study of HS chemical fractions and the origins. Environ. Sci. Pollut. R. 24, 1-13.

Fellman, J.B., Hood, E., Spencer, R.G.M., 2010. Fluorescence spectroscopy opens new windows into dissolved organic matter dynamics in freshwater ecosystems: A review. Limnol. Oceanogr. 55, 2452-2462.

Fitzgerald, M.A., Mccouch, S.R., Hall, R.D., 2009. Not just a grain of rice: the quest for quality. Trends Plant Sci. 14, 133-139.

Gorny, J., Billon, G., Lesven, L., Dumoulin, D., Madé, B., Noiriel, C., 2015. Arsenic behavior in river sediments under redox gradient: A review. Sci. Total Environ. 505, 423-434.

Grabowski, A., Tindall, B.J., Bardin, V., Blanchet, D., Jeanthon, C., 2005. Petrimonas sulfuriphila gen. nov., sp. nov., a mesophilic fermentative bacterium isolated from a biodegraded oil reservoir. Int. J. Syst. Evol. Microbiol. 55, 1113-1121.

Guo, H., Ren, Y., Liu, Q., Zhao, K., Li, Y., 2013. Enhancement of arsenic adsorption during mineral transformation from siderite to goethite: mechanism and application. Environ. Sci. Technol. 47, 1009-1016.

Gustave, W., Yuan, Z. F., Sekar, R., Chang, H.C., Zhang, J., Wells, M., Ren, Y.X., Chen, Z., 2018a. Arsenic mitigation in paddy soils by using microbial fuel cells. Environ. Pollut. 238, 647-655.

Gustave, W., Yuan, Z.-F., Sekar, R., Ren, Y.-X., Chang, H.-C., Liu, J.-Y., Chen, Z., 2018b. The change in biotic and abiotic soil components influenced by paddy soil microbial fuel cells loaded with various resistances. J. Soil Sediment 1-10.

Hashimoto, Y., Kanke, Y., 2018. Redox changes in speciation and solubility of arsenic in paddy soils as affected by sulfur concentrations. Environ. Pollut. 238, 617-623.

He, Y.R., Xiao, X., Li, W.W., Cai, P.J., Yuan, S.J., Yan, F.-F., He, M.X., Sheng, G.P., Tong, Z.H., Yu, H.Q., 2013. Electricity generation from dissolved organic matter in polluted lake water using a microbial fuel cell (MFC). Biochem. Eng. J. 71, 57-61.

Hong, S.W., Chang, I.S., Choi, Y.S., Kim, B.H., Chung, T.H., 2009. Responses from freshwater sediment during electricity generation using microbial fuel cells. Bioprocess Biosyst. Eng. 32, 389-395.

Hong, S.W., Kim, H.S., Chung, T.H., 2010. Alteration of sediment organic matter in sediment microbial fuel cells. Environ. Pollut.158, 185-191.

Hori, T., Muller, A., Igarashi, Y., Conrad, R., Friedrich, M.W., 2010. Identification of iron-reducing microorganisms in anoxic rice paddy soil by 13C-acetate probing. The ISME J. 4, 267-278.

Huang, D.Y., Zhou, S.G., Chen, Q., Zhao, B., Yuan, Y., Zhuang, L., 2011. Enhanced anaerobic degradation of organic pollutants in a soil microbial fuel cell. Chem. Eng. J. 172, 647-653.

Hutchins, C.M., Teasdale, P.R., Lee, J., Simpson, S.L., 2007. The effect of manipulating sediment pH on the porewater chemistry of copper- and zinc-spiked sediments. Chemosphere 69, 1089-1099.

Islam, S., Rahman, M.M., Islam, M., Naidu, R., 2016. Arsenic accumulation in rice: Consequences of rice genotypes and management practices to reduce human health risk. Environ. Int. 96, 139-155.

Jiang, W., Hou, Q., Yang, Z., Zhong, C., Zheng, G., Yang, Z., Li, J., 2014. Evaluation of potential effects of soil available phosphorus on soil arsenic availability and paddy rice inorganic arsenic content. Environ. Pollut. 188, 159-165.

Kaku, N., Yonezawa, N., Kodama, Y., Watanabe, K., 2008. Plant/microbe cooperation for electricity generation in a rice paddy field. Appl. Microbiol. Biotechnol. 79, 43-49.

Kappler, A., Wuestner, M.L., Ruecker, A., Harter, J., Halama, M., Behrens, S., 2016. Biochar as an Electron Shuttle between Bacteria and Fe(III) Minerals. Environ. Sci. Technol. Lett. 1, 339-344.

Khalid, S., Shahid, M., Niazi, N.K., Murtaza, B., Bibi, I., Dumat, C., 2016. A comparison of technologies for remediation of heavy metal contaminated soils. J. Geochem. Explor. 182.

Kouzuma, A., Kasai, T., Nakagawa, G., Yamamuro, A., Abe, T., Watanabe, K., 2013. Comparative metagenomics of anode-associated microbiomes developed in rice paddy-field microbial fuel cells. PLoS One 8, e77443.

Krespi, Y.P., Shrime, M.G., Kacker, A., 2006. The relationship between oral malodor and volatile sulfur compound–producing bacteria. Otolaryngology—Head and Neck Surgery 135, 671-676.

Kudo, K., Yamaguchi, N., Makino, T., Ohtsuka, T., Kimura, K., Dong, D.T., Amachi, S., 2013. Release of arsenic from soil by a novel dissimilatory arsenate-reducing bacterium, Anaeromyxobacter sp. strain PSR-1. Appl. Environ. Microbiol. 79, 4635-4642.

Lapierre, J.F., Del Giorgio, P.A., 2014. Partial coupling and differential regulation of biologically and photo-chemically labile dissolved organic carbon across boreal aquatic networks. Biogeosciences 11, 5969-5985.

Li, H., Peng, J., Weber, K.A., Zhu, Y., 2011. Phylogenetic diversity of Fe(III)-reducing microorganisms in rice paddy soil: enrichment cultures with different short-chain fatty acids as electron donors. J. Soil Sediment.11, 1234-1242.

Li, Z., Wu, L., Zhang, H., Luo, Y., Christie, P., 2015. Effects of soil drying and wetting-drying cycles on the availability of heavy metals and their relationship to dissolved organic matter. J. Soil Sediment. 15, 1510-1519.

Logan, B.E., 2008. Microbial Fuel Cells. A John Wiley & Sons, Inc.

Logan, B.E., 2009. Exoelectrogenic bacteria that power microbial fuel cells. Nat. Rev. Microbiol. 7, 375–381.

Lovley, D.R., Phillips, E.J.P., 1988. Novel Mode of Microbial Energy Metabolism: Organic Carbon Oxidation Coupled to Dissimilatory Reduction of Iron or Manganese. Appl. Environ. Microbiol. 54, 1472-1480.

Marshall, C.W., May, H.D., 2009. Electrochemical evidence of direct electrode reduction by a thermophilic Gram-positive bacterium, Thermincola ferriacetica. Energ. Envin. Sci. 2, 699-705.

Minatel, B.C., Sage, A.P., Anderson, C., Hubaux, R., Marshall, E.A., Lam, W.L., Martinez, V.D., 2018. Environmental arsenic exposure: from genetic susceptibility to pathogenesis. Environ. Int. 112, 183-197.

Peng, Q.A., Shaaban, M., Wu, Y., Hu, R., Wang, B., Wang, J., 2016. The diversity of iron reducing bacteria communities in subtropical paddy soils of China. Appl. Soil Ecol. 101, 20-27.

Qiao, J.T., Li, X.M., Li, F.B., 2017. Roles of different active metal-reducing bacteria in arsenic release from arsenic-contaminated paddy soil amended with biochar. J. Hazard. Mater. 344, 958-967.

Roden, E.E., Kappler, A., Bauer, I., Jiang, J., Paul, A., Stoesser, R., Konishi, H., Xu, H., 2010. Extracellular electron transfer through microbial reduction of solid-phase humic substances. Nat. Geoscience 3, 417-421.

Saidpullicino, D., Miniotti, E., Sodano, M., Bertora, C., Lerda, C., Chiaradia, E.A., Romani, M., De Maria, S.C., Sacco, D., Celi, L., 2016. Linking dissolved organic carbon cycling to organic carbon fluxes in rice paddies under different water management practices. Plant and Soil 401, 273-290.

Signespastor, A.J., Burlo, F., Mitra, K., Carbonellbarrachina, A.A., 2007. Arsenic biogeochemistry as affected by phosphorus fertilizer addition, redox potential and pH in a west Bengal (India) soil. Geoderma 137, 504-510.

Song, N., Jiang, H. L., 2018. Effects of initial sediment properties on start-up times for sediment microbial fuel cells. Int. J. Hydrog. Energy 10082-10093.

Song, T.S., Yan, Z.-S., Zhao, Z.W., Jiang, H.L., 2010. Removal of organic matter in freshwater sediment by microbial fuel cells at various external resistances. J. Chem. Technol. Biot. 85, 1489-1493.

Stuckey, Jason W., Schaefer, Michael V., Kocar, Benjamin D., Benner, Shawn G., Fendorf, S., 2015. Arsenic release metabolically limited to permanently water-saturated soil in Mekong Delta. Nat. Geoscience 9, 70-76.

Sun, G.X., Williams, P.N., Zhu, Y.G., Deacon, C., Carey, A.-M., Raab, A., Feldmann, J., Meharg, A.A., 2009. Survey of arsenic and its speciation in rice products such as breakfast cereals, rice crackers and Japanese rice condiments. Env. Int. 35, 473-475.

Touch, N., Hibino, T., Morimoto, Y., Kinjo, N., 2017. Relaxing the formation of hypoxic bottom water with sediment microbial fuel cells. Environ. Technol. 1-25.

Trusiak, A., Treibergs, L.A., Kling, G.W., Cory, R.M., 2018. The role of iron and reactive oxygen species in the production of CO 2 in arctic soil waters. Geochim. Cosmochim. Ac. 224, 80-95.

Wan, X., Lei, M., Chen, T., 2016. Cost–benefit calculation of phytoremediation technology for heavy-metal-contaminated soil. Sci. Total Environ. 563-564, 796-802.

Wang, N., Chen, Z., Li, H.B., Su, J.Q., Zhao, F., Zhu, Y.G., 2015. Bacterial community composition at anodes of microbial fuel cells for paddy soils: the effects of soil properties. J. Soil Sediment. 15, 926-936.

Wang, X., Xueping, C., Jing, Y., Zhaosu, W., Guoxin, S., 2009. Effect of microbial mediated iron plaque reduction on arsenic mobility in paddy soil. J. Environ. Sci. (China) 21, 1562-1568.

Wang, Y., Chen, Z., Liu, P., Sun, G., Ding, L., Zhu, Y., 2016. Arsenic modulates the composition of anode-respiring bacterial community during dry-wet cycles in paddy soils. J. Soil Sediment. 16, 1745-1753.

Weber, K.A., Urrutia, M.M., Churchill, P.F., Kukkadapu, R.K., Roden, E.E., 2006. Anaerobic redox cycling of iron by freshwater sediment microorganisms. Environ. Microbiol. 8, 100-113.

Yamaguchi, N., Nakamura, T., Dong, D., Takahashi, Y., Amachi, S., Makino, T., 2011. Arsenic release from flooded paddy soils is influenced by speciation, Eh, pH, and iron dissolution. Chemosphere 83, 925-932.

Yamamura, S., Sudo, T., Watanabe, M., Tsuboi, S., Soda, S., Ike, M., Amachi, S., 2018. Effect of extracellular electron shuttles on arsenic-mobilizing activities in soil microbial communities. J. Hazard. Mater. 342, 571-578.

Yang, Q., Zhao, H., Zhao, N., Ni, J., Gu, X., 2016. Enhanced phosphorus flux from overlying water to sediment in a bioelectrochemical system. Bioresour. Technol. 216, 182.

You, J., Wu, G., Ren, F., Chang, Q., Yu, B., Xue, Y., Mu, B., 2016. Microbial community dynamics in Baolige oilfield during MEOR treatment, revealed by Illumina MiSeq sequencing. Appl. Microbiol. Biotechnol. 100, 1469-1478.

Yuan, H.-Y., Liu, P.-P., Wang, N., Li, X.-M., Zhu, Y.-G., Khan, S.T., Alkhedhairy, A.A., Sun, G.-X., 2018. The influence of soil properties and geographical distance on the bacterial community compositions of paddy soils enriched on SMFC anodes. J. Soil Sediment. 18, 517-525.

Zavarzina, D.G., Sokolova, T.G., Tourova, T.P., Chernyh, N.A., Kostrikina, N.A., Bonchosmolovskaya, E.A., 2007. Thermincola ferriacetica sp. nov., a new anaerobic, thermophilic, facultatively chemolithoautotrophic bacterium capable of dissimilatory Fe(III) reduction. Extremophiles 11, 1-7.

Zhou, Y., Jiang, H., Cai, H., 2015. To prevent the occurrence of black water agglomerate through delaying decomposition of cyanobacterial bloom biomass by sediment microbial fuel cell. J. Hazard. Mater 287, 7-15.

Zhu, Y.G., Xue, X.M., Kappler, A., Rosen, B.P., Meharg, A.A., 2017. Linking genes to microbial biogeochemical cycling: lessons from arsenic. Environ. Sci. Technol. 51, 7326-7339.

6.8. Supplementary data

The effect of the sMFC on arsenic in soil with high organic matter content

Table S 6.1 Selected properties of the fresh soils.

Soils Texture	Fe(g/kg)	As (mg/kg)	pH	TC (g/kg)
Loam Clay	53.7±1.8	73.7±5.9	6.2±0.1	23.2±0.9

Notes: Fe, soil total iron, As, soil total arsenic, TC, soil organic carbon. The values represent the mean ±standard error of four replicate samples.

Table S 6.2 Similarity-based OTUs and species richness and diversity estimates.

Sample ID	ACE	Chao1	Shannon index	Simpson	Good's Coverage
Control-T	1694.2 ±7.06	1725.3 ±11.6	8.60 ±0.03	0.990 ±0.00	99.2 ±0.00
Control-M	1543.3 ±9.64	1570.3 ±8.09	8.10 ±0.06	0.990 ±0.00	99.3 ±0.00
Control-A	1499.9 ±22.3	1520.9 ±23.8	8.20 ±0.08	0.990 ±0.00	99.4 ±0.00
sMFC-T	1736.4 ±21.6	1761.1 ±21.6	8.60 ±0.02	0.990 ±0.00	99.2 ±0.00
sMFC-M	1536.8 ±5.22	1559.4 ±6.32	8.30 ±0.04	0.990 ±0.00	99.4 ±0.00
sMFC-A	1428.5 ±28.4	1434.3 ± 37.7	6.90 ±0.05	0.960 ±0.00	99.2 ±0.00
Control-WM-BS	631.0 ±3.18	632.9 ±4.28	7.30 ±0.18	0.980 ±0.00	99.9 ±0.00
Control-WM-A	628.2 ±6.06	635.6 ±8.25	7.40 ±0.15	0.980 ±0.00	99.9 ±0.00
sMFC-WM-BS	629.6 ±212	631.8 ±1.18	7.60 ±0.07	0.990 ±0.00	99.9 ±0.00
sMFC-WM-A	621.6 ±7.95	629.3 ±5.63	7.30 ±0..31	0.980 ±0.00	99.9 ±0.00

Notes: T, M, A and BS: represents samples collected from top layer, middle layer, anode vicinity and bulk soil respectively. The values represent the mean ±standard error of four replicate sample

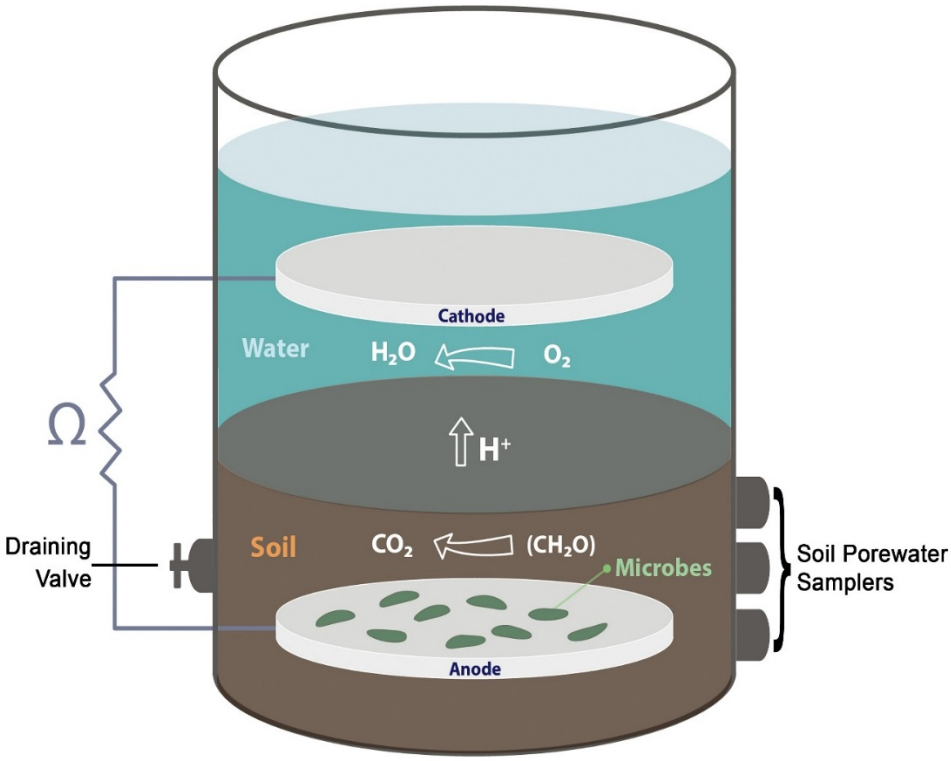

Schem. 1 Schematic diagram of the sMFC retractor

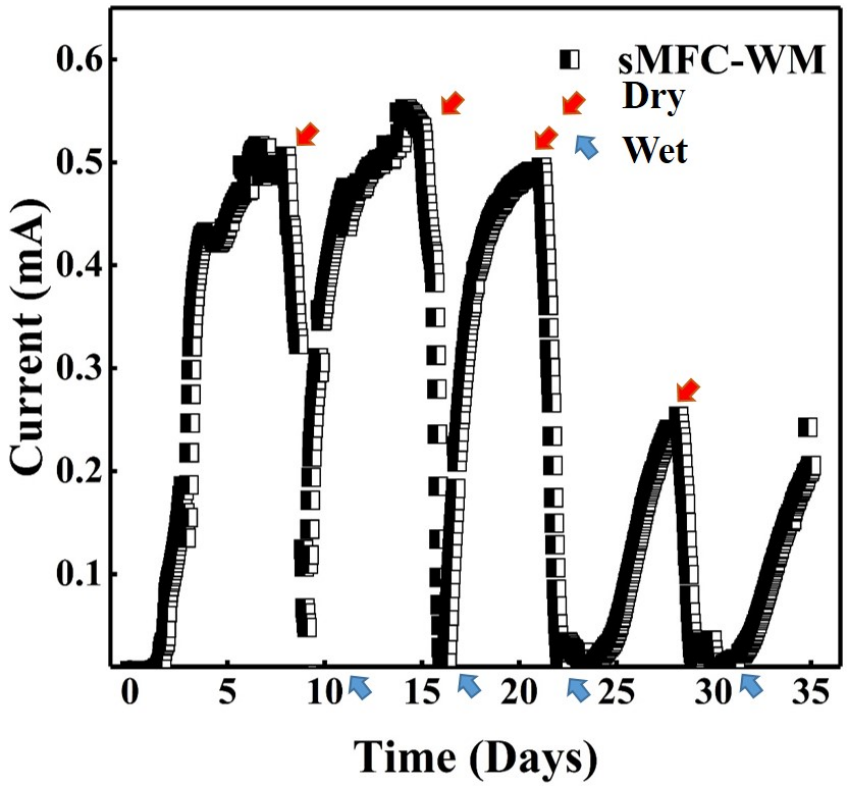

Figure S 6.1 Current variation of the sMFC-WM over time. The red and blue arrows indicates the start of dry and wet periods respectively.

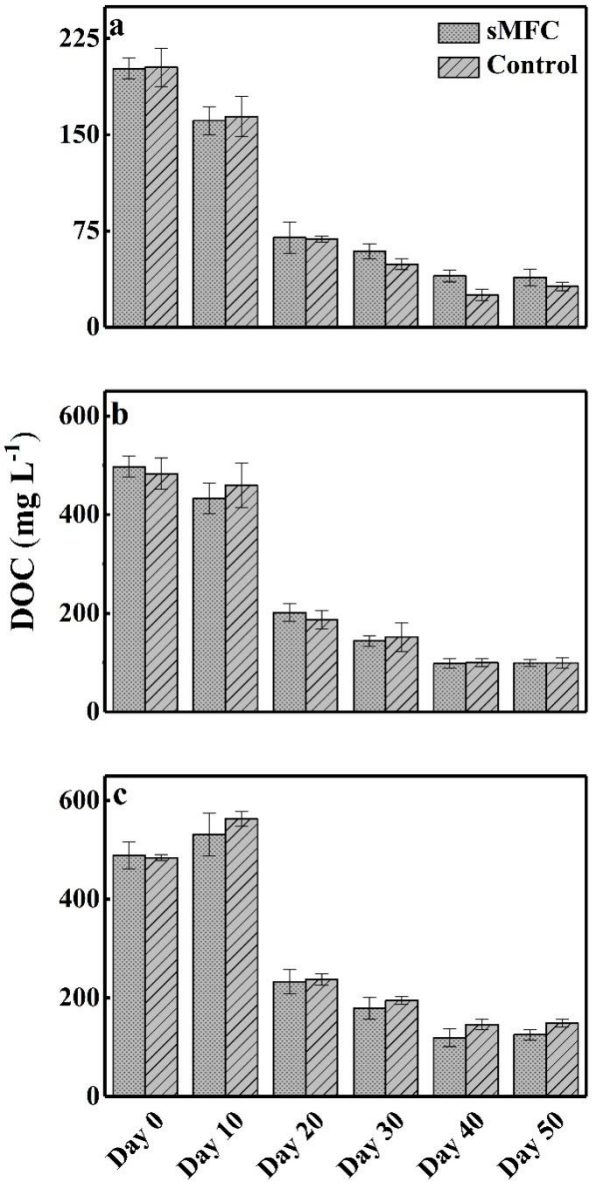

Figure S 6.2 Dissolved organic carbon (DOC) variation in soil porewater as a function of incubation time. Panels a, b and c show DOC concentration in the top, middle and bottom layers, respectively. The error bars represent standard error of measured concentrations of four replicate samples

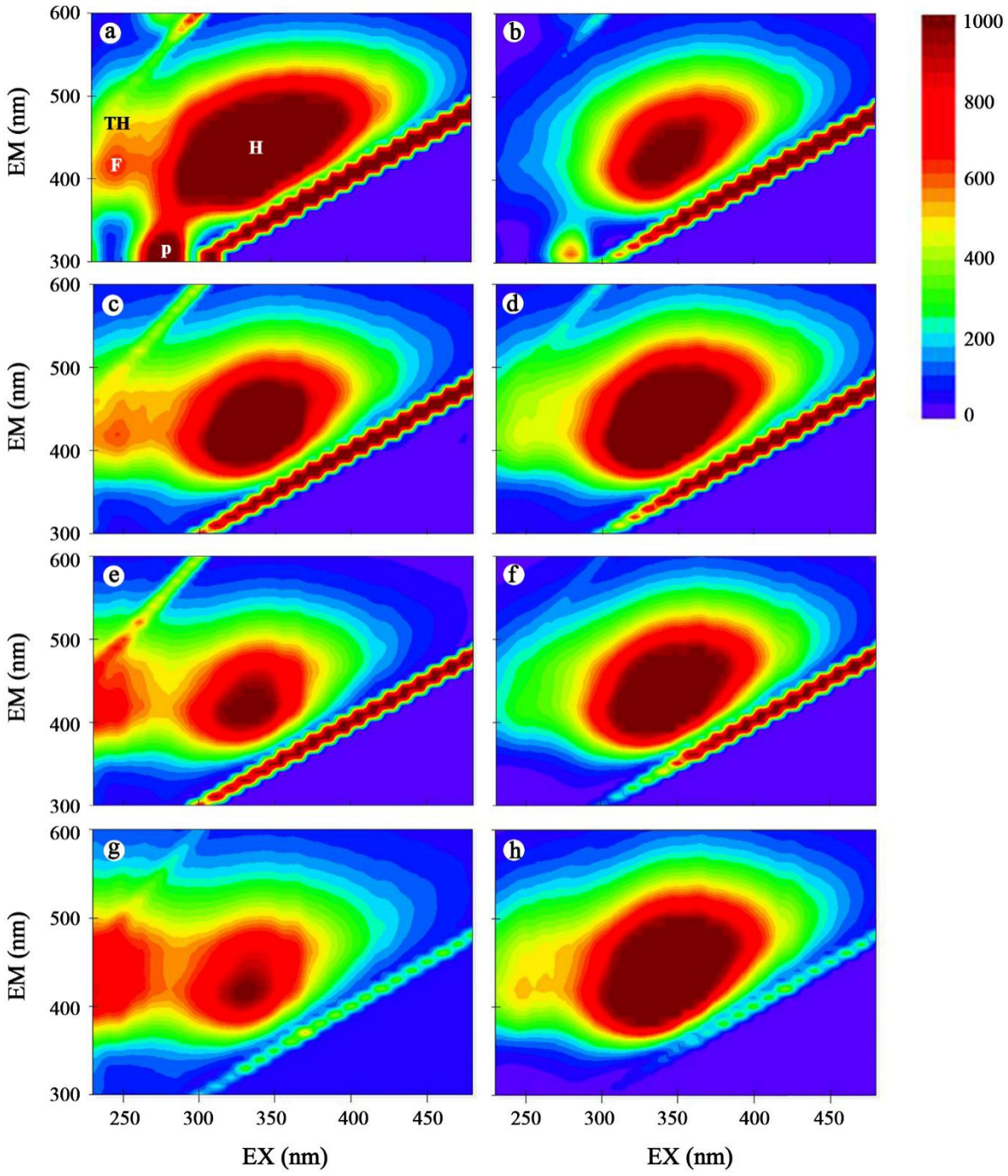

Figure S 6.3 EEM fluorescence spectra of DOC in soil porewater. Panels a, c, e and g show DOC spectra in sMFC-WM. Panels b, d, f, and h show DOC spectra in the control-WM. P is tryptohan-like, H ultraviolet C (UVC) humic acid-like, F is fulvic acid-like and TH is terrestrial humic acid-like.

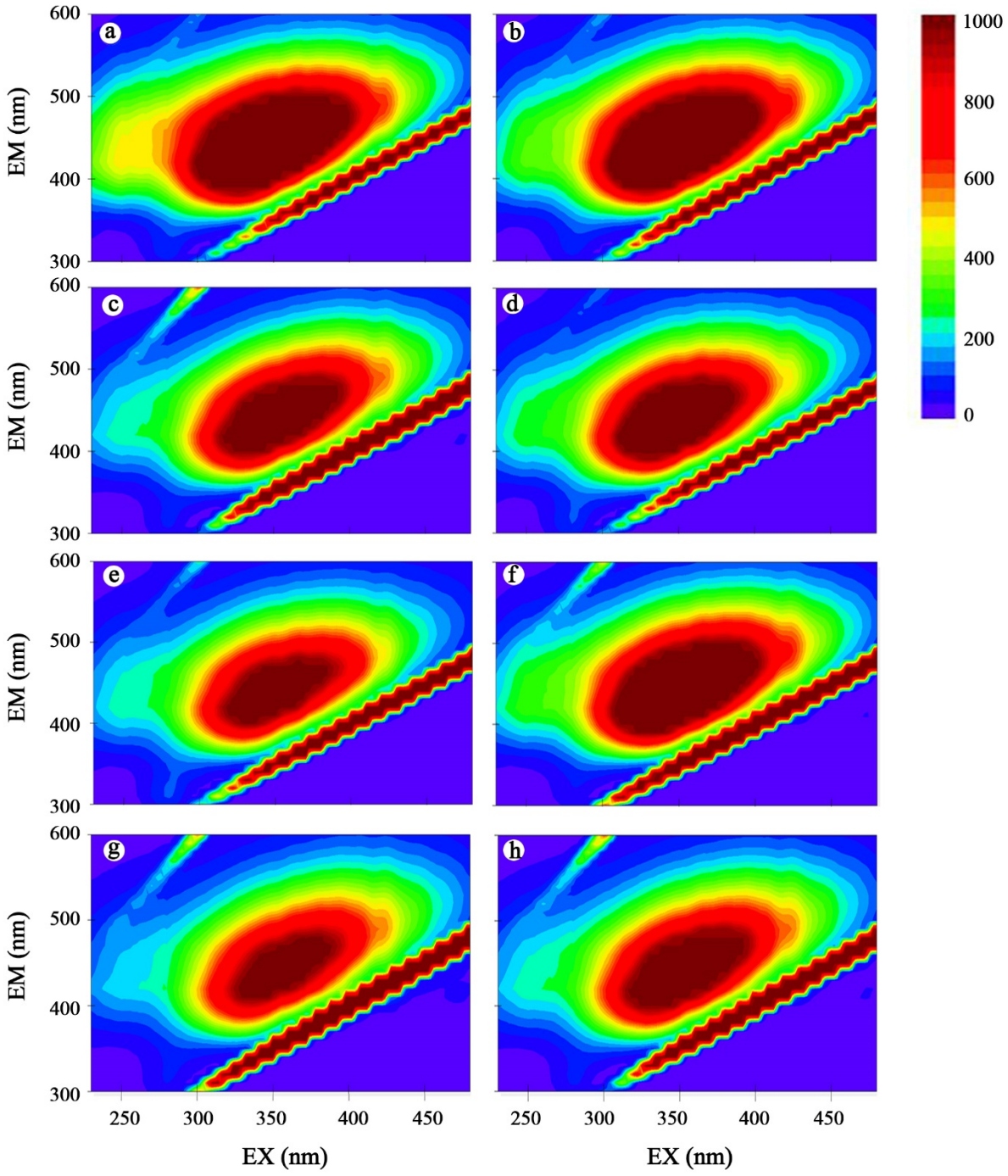

Figure S 6.4 EEM fluorescence spectra of DOC in soil porewater. Panels a, c, e and g show DOC spectra in sMFC. Panels b, d, f, and h show DOC spectra in the control.

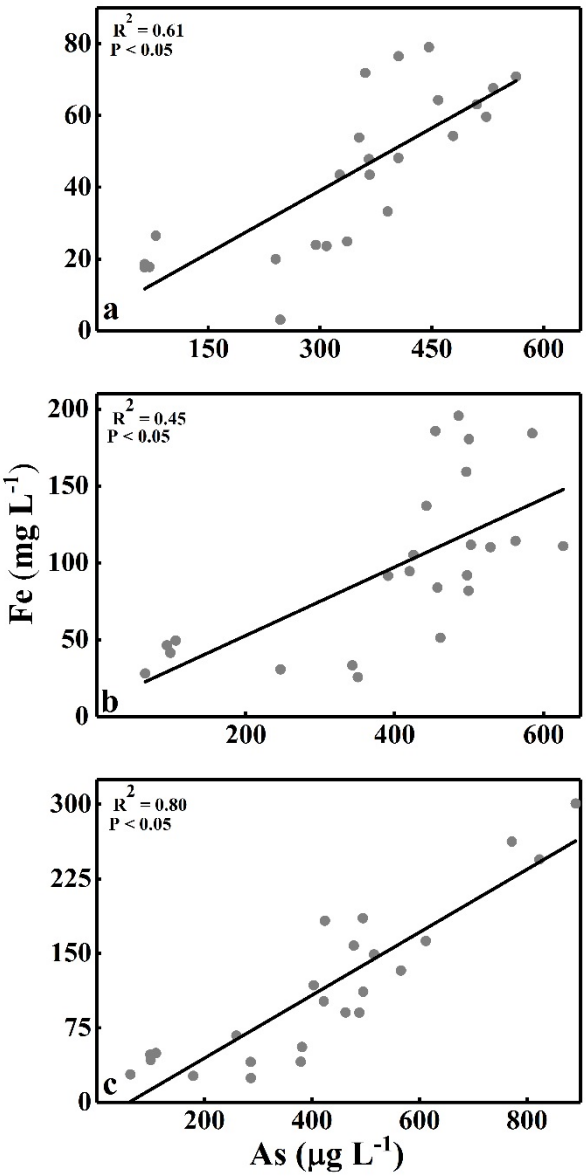

Figure S 6.5 Association between Fe and As release in the sMFC. Panels a, b and c represent the top, middle and bottom layers, respectively.

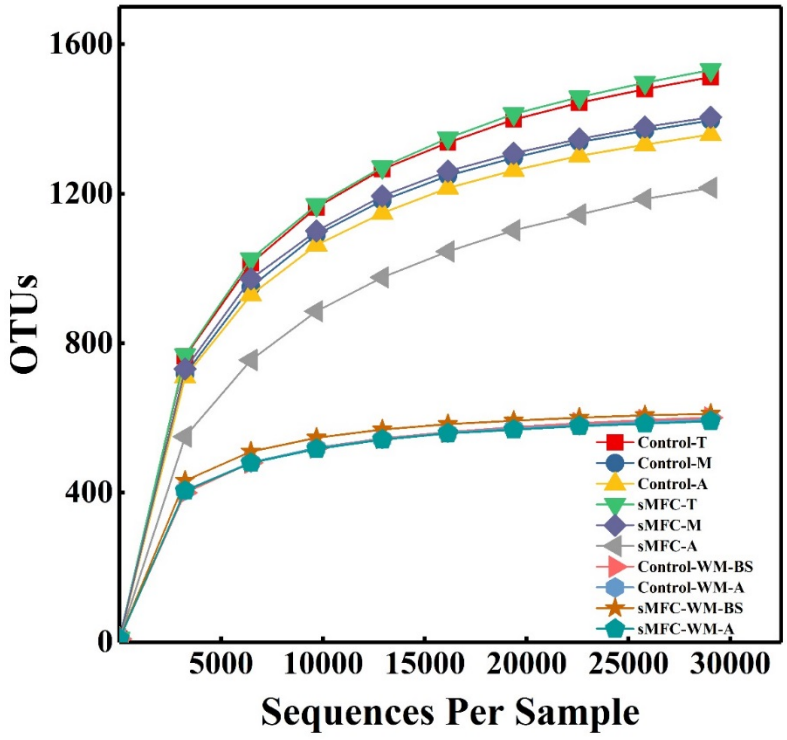

Figure S 6.6 Rarefaction curves showing the diversity of OTUs (similarity cut off of 97%). T, M, A and BS: represents samples collected from top layer, middle layer, anode vicinity and bulk soil respectively. The value represents the mean of four replicates.

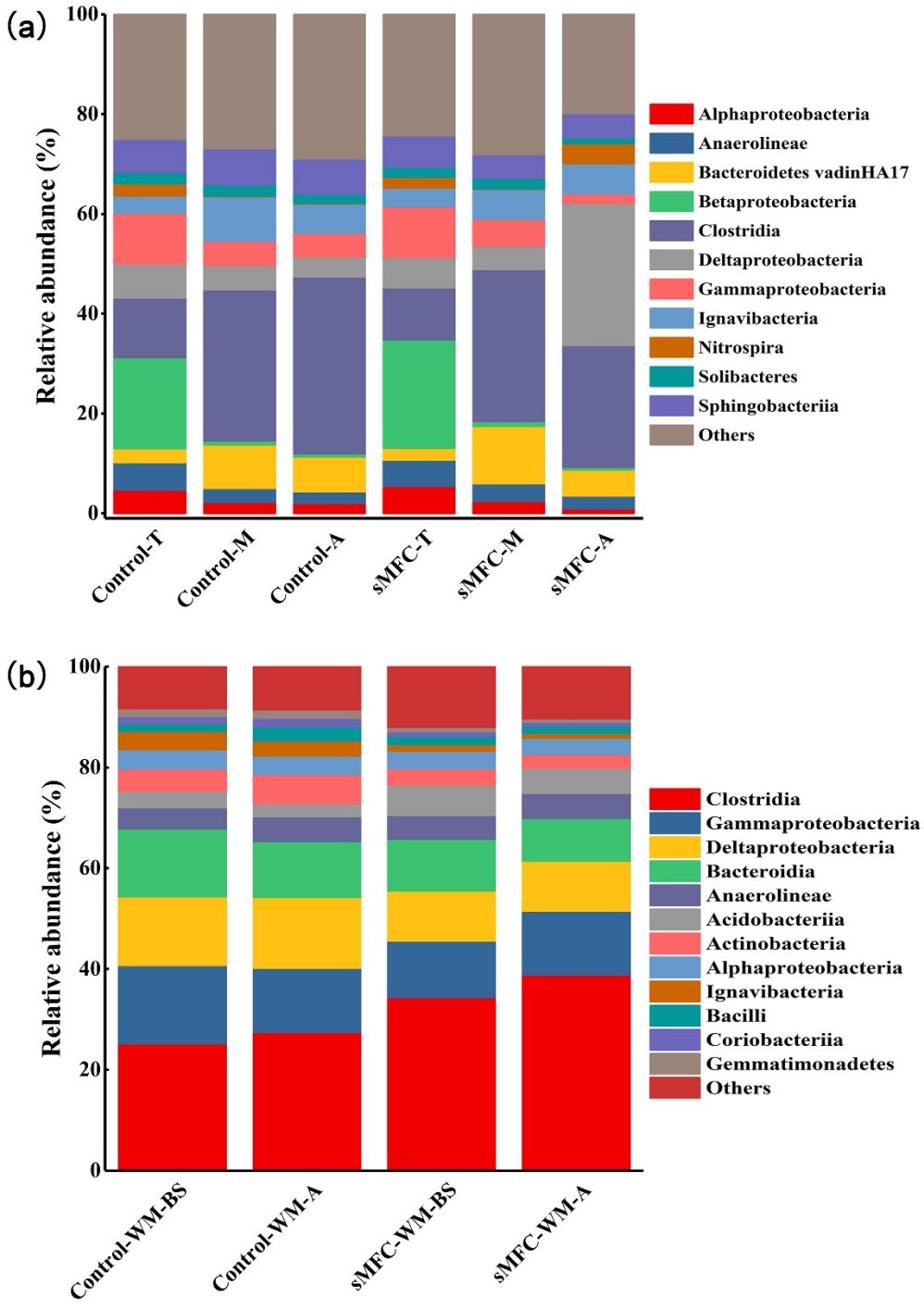

Figure S 6.7 Relative abundance of bacterial community composition at class level for the sMFC without (a) and with water management (b). T, M, A and BS: represents samples collected from top layer, middle layer, anode vicinity and bulk soil respectively. The value represents the mean of four replicates.

References

Caporaso, J.G., Kuczynski, J., Stombaugh, J., Bittinger, K., Bushman, F.D., Costello, E.K., Fierer, N., Pena, A.G., Goodrich, J.K., Gordon, J.I., 2010. QIIME allows analysis of high-throughput community sequencing data. Nat. Methods 7, 335-336.

Edgar, R.C., Haas, B.J., Clemente, J.C., Quince, C., Knight, R., 2011. UCHIME improves sensitivity and speed of chimera detection. Bioinformatics 27, 2194-2200.

Wang, Q., Garrity, G.M., Tiedje, J.M., Cole, J.R., 2007. Naïve Bayesian classifier for rapid assignment of rRNA sequences into the new bacterial taxonomy Appl. Environ. Microbiol. 73, 5261-5267.

Chapter 7 : The effect of the sMFC on the accumulation of arsenic in rice plant parts

7.1. Abstract

Rice (*Oryza sativa L.*) consumption is a major route of dietary exposure to arsenic (As) in humans. One main reason for the high accumulation of As in rice grain is the high bioavailability of As in porewater of flooded paddy soil. Recently, it has been shown that the application of soil microbial fuel cell (sMFC) can significantly reduce soil porewater As concentration, however, the effect of sMFC on As accumulation in rice is unknown. Hence, the aim of this study was to assess the effects of the sMFC in reducing As uptake in rice grown in As contaminated. Thus, a pot experiment was performed to investigate As distribution in rice tissues and the functional microbial communities in soil when the sMFC was installed. The As in the soil porewater and rice plant parts were analyzed by ICPMS. 16S rRNA sequencing and Quantitative PCR were used to examine the microbial community and to quantify the relative abundance of As resistance genes in the rhizosphere, respectively. The results suggested that the sMFC can simultaneously work as an electricity generator and As mitigator. The total As concentrations in the stems, leaves, husks, and rice grains were significantly decreased by 53.4%, 44.7%, 62.6%, and 67.9%, respectively in the plants with sMFC compared to the control. This decrease in As accumulation in the sMFC treatment may be explained by the decrease in the soil porewater dissolve organic matter content and abundance of As reducing gene (*arsC*). Moreover, known As reducing classes such as Clostridia, Bacilli and *Thermoleophilia* were significantly enhanced in the control treatment. Integrating the sMFC in rice paddy soil offers a promising way to mitigate As accumulation in rice tissue and reduce dietary As exposure, while simultaneously producing electricity.

7.2. Introduction

Rice (*Oryza sativa* L.), a staple food worldwide and is the major route of dietary exposure to arsenic (As) (Zhu et al. 2008). The health risk of As exposure through rice raises with increasing As level in paddy soils, which has been frequently reported in many countries (Patel et al., 2005; Zhu et al. 2008; Seyfferth, et al., 2014; Li et al. 2019). The As accumulation in rice grain is first determined by the bioavailability of As in paddy soil. Most of the As are fixed on the solid phase of iron (Fe) oxide in oxic soils, however, the release of As from the soil solid phase to the porewater accelerates when soils are flooded (Yamaguchi et al. 2011; Yamamura et al. 2018). This occurs because under these reducing condition, microorganisms able to reduce Fe oxide and arsenate (As(V)) thrive.

Iron and As reducing microbes transfer electrons from organic substrates to Fe oxide and As(V), respectively. The microbial reductive dissolution of Fe oxide results in the transformation of solid ferric (Fe(III)) minerals to dissolved ferrous (Fe(II)) ions and As liberation. Moreover, the direct reduction of absorbed As(V) from the surface of Fe oxide to arsenite (As(III)) also enhances the As bioavailability because As(III) is more mobile than As(V) (Qiao et al. 2017b; Takahashi et al. 2004). On the contrary, the excessive Fe(II) that is generated can react with microbially-derived sulfide and/or carbonate to form more stable secondary Fe minerals that can co-precipitate with As from the soil porewater (Burton et al. 2011; Hashimoto and Kanke 2018). However, As bioavailability is still relatively high in the anaerobic soil porewater, since As(III) is normally the dominant As species and has a lower tendency to precipitate with Fe minerals as compared to As(V) (Takahashi et al. 2004). Therefore, methods that are able to interfere with the microbial dissolution process of Fe oxides may be effective in reducing As bioavailability in flooded paddy soils.

Many studies have shown that the microbial reduction of Fe oxide and As(V) in flooded condition are impeded when chemical amendments, such as nitrates, metal-oxides and sulfates,

are added into the soil (Hu et al. 2007; Wang et al. 2019; Zhang et al. 2017). These studies suggested that the amendment can be used by soil microorganisms as a substitute final electron acceptor thereby limiting As(V) and Fe oxide reduction (Hu et al. 2007; Wang et al. 2019; Zhang et al. 2017). For example, in a previous study, Zhang et al. (2017) used nitrate to stimulate anaerobic oxidation of As(III) to As(V) and reduce As bioavailability in the paddy soil porewater. However, there are several disadvantages to such treatment because the oxidizing compound will eventually be consumed by the soil microorganisms, thus losing its function, and/or the compound have negative impacts on soil quality and plant growth (Liu et al. 2014; Sahrawat 2005). Recently, carbon electrodes of the soil microbial fuel cells (sMFC), which are inert in most environments, were found to be a stable sink of electrons and are able to slow down Fe oxide reduction and mitigate As risk in soils (Gustave et al. 2018a).

Plant sMFC, are special types of sMFC that can be used to convert solar energy to electricity. In plant sMFC, the electrogenic bacteria in the soil oxidizes organic compound and root exudates from the rhizosphere produce electricity (Kouzuma et al. 2014; Takanezawa et al., 2010, Schamphelaire et al. 2008). Plant sMFC have been tested for electricity production, however the sMFC power output was relatively low (Kaku et al. 2008; Schamphelaire et al. 2008; Khudzari et al., 2019). Subsequently, sMFC research has shifted towards environmental remediation (Chen et al. 2015; Gustave et al. 2018a; Gustave et al. 2018b). The sMFC have been shown to be a cost-effective way to reduce As concentration in soil porewater and simultaneously produce electricity in lab scale experiments (Gustave et al. 2018a). In the sMFC, the anode sustains the microbial degradation of dissolve organic carbon (DOC) by acting as an alternative electron acceptor, thereby limiting Fe and As reduction (Gustave et al. 2018a; Gustave et al. 2018b). This consequently results in less As being release into the paddy soil porewater which could possibly limit As uptake and translocation by rice plants (Gustave et al. 2018a). Moreover, it should be noted that the sMFC could also influence the behavior of redox

sensitive metals/ metalloids via electromigration and electroosmotic flow. Recently, sMFC have been used to generate energy that is needed to drive *in situ* electrokinetic remediation of the toxic metals without the addition of an external power source (Chen et al., 2015; Habibul et al., 2016a; Habibul et al., 2016b; Song et al., 2018). The current produced by the sMFC was used to accelerate the transfer of contaminants along with the pore fluid towards a charged electrode where it may be removed or treated. Nonetheless, as the dominant species of As in flooded paddy soils is As(III) and it is neutrally charged, the electromigration only has a minor influence on the soil porewater As(III). This phenomenon was confirmed in our earlier studies where we found electromigration had only minimal influence on As mobility (Gustave et al. 2018a; Gustave et al. 2018b). Our results showed sMFC's anode bacterial community's ability to out compete the As reducing bacteria in bulk soil for organic substrate was the dominating factor controlling As release into the soil porewater (Gustave et al. 2018a; Gustave et al. 2018b). However, to date, the effect of the anode on As and uptake in rice plants have not been reported.

Therefore, we proposed a hypothesis that the sMFC can be used to reduce As bioavailability and limit total As uptake by the rice plant. The sMFC will decrease DOC in the soil porewater which in turn will limit microbial Fe and As reduction. Thus, the major objective of this study were to investigate the effects of the sMFC on (i) the bacterial community and As transformation genes in the rhizosphere and to (ii) determine whether the sMFC can reduce total As accumulation in rice grown in As contaminated soils.

7.3. Materials and Methods

7.3.1. Paddy Soil Sample

The paddy soil (0-20cm) was collected from Shaoguan, Guandong Province (N25º6'38'', E113º 38'41''), PR China. The collected samples were air-dried and sieved to less than 2mm. The main physio-chemical properties of the soil were determined and are

presented in Table S1. The total carbon, As and Fe concentrations were measured to be 21.2±0.7 g/kg, 44.8±3.5 mgKg-1 and 38.3±1.2 g/kg, respectively (Table S 7.1).

7.3.2. Soil Microbial Fuel Cell Assembly

Eighteen sMFC were constructed from the paddy soil and were operated firstly in a plant cultivating room for 38 days and then transferred to an outdoor greenhouse until the end of the experiment. Of the eighteen sMFC, nine were control replicates, in which the anodes and cathodes were not connected to any resistor (open circuit). The remaining nine sMFC were treatment replicates and the anodes and cathodes were connected to 500Ω external resistors (close circuit). On day 110, all of the 500Ω external resistor were replaced with a 100Ω external resistor. All the sMFC were constructed according to our previously reported method (Gustave et al. 2018a) with few modifications. Briefly, 60 kg of homogenized soil was amended with basal fertilizers, NH_4NO_3 (120 mgN kg^{-1} soil) and K_2HPO_4 (30 mgP kg^{-1} soil and 75.7 mgK kg^{-1} soil). Then, 3kg of amended soil was used to construct the sMFC in the individual cylindrical polyvinylchloride pots (16 cm diameter × 30 cm depth) with a three valve ports. The valve ports were located adjacent to each anode. Circular carbon felts with geometric surface area of 850 cm^2 were used as anodes and a rectangular carbon felts with geometric surface area of 706.9 cm^2 was used as cathodes. A data logger (USB-7660B, ZTIC, China) was used to record the voltage (which was the difference in potential between the anode and the cathode) from day 0 to day 38. After day 38, a handheld Digital Multimeters (UNI-T UT71E) was used to record the voltage every 24 hours. We cease to use the automatic data logger on day 38 because the sMFCs were transported from a plant cultivation room to an outdoor greenhouse.

As depicted in Fig. 1, in each container, 2 cm depth of soil was added and then the bottom anode was placed on the surface of the soil layer. Then, 4 cm of the soil was used to bury the bottom anode. The middle anode was then placed on the surface of the soil layer and

buried with another 4 cm of soil before installing the top anode. The remaining soil sample was then be used to bury top anode. The anodes were cut into two pieces and were connected with a titanium wire. The two half anodes were placed 1 cm a part to leave space for the rice roots to grow. It should be noted that the three carbon felt used as the anode in each of the sMFCs were connected to each other and operated as a single anode with three layers, rather than three individual anodes. The cathode was vertically installed in the overlaying water in aerobic conditions. The water loss via evaporation and plant respiration during operation was routinely replenished with deionized water to maintain a constant water level of ca. 6 cm. However, prior to harvesting the rice, from day 110 to day 120, the sMFCs and controls were allowed to run dry.

7.3.3. Preparation of Rice Seedlings

Rice seeds of *Oryza sativa* (Yliangyou, YLY) were disinfected according to the method mentioned in study Chen et al. (2012) and then germinated on cleaned moist perlite. Prior to being transplanted into the sMFC the seedlings were grown in a non-contaminated (trace metal within the Chinese standard (GB15618-1995) specification for agricultural soils) soil in a plant cultivating room until the fourth leaf expanded. Then three uniform plantlets were transplanted into each sMFC. The rice plants were first grown in a plant cultivating room for 38 days in the sMFC at 25 °C during the day and night. The natural light was supplemented with led lights (1200 Lux) with photoperiod of 12h light/12 h dark. On June 8, 2018 the rice plants were moved to an outdoor greenhouse at ambient temperature and natural photoperiod.

7.3.4. Chemical Analysis

During the rice growing period, the soil porewater was collected every 10 days for the first 30 days and then collected every 20 days for remaining operational period using a custom-made rhizon sampler with a hollow fiber membrane (modified polyethersulfone, Motimo Membrane Technology Co., Ltd, Tianjin, China). The soil pH, soil redox potential (Eh) and

DOC were also measured. All of the analysis were conducted according to the methods descried in chapter 2.

7.3.5. Plant Samples Analysis

At the end of 120 days, the rice plants were harvested and washed with ultrapure water. The analyses were conducted according to the methods descried in chapter 2.

7.3.6. Microbial Community Analysis

At the end of the maturing stage, the anodes and rhizosphere soils were sampled from four randomly selected sMFCs and four controls for genomic DNA extraction. In each of the four treatment samples were taken from rhizosphere and the three individual anodes. The sample from the three anodes of one cell was combined to form one composite sample. Then the total DNA was extracted immediately after collection from 0.25g of each sample using a HiPure Soil DNA isolation Kit (Magen, China) according to the manufacturer's instructions. The extracted DNA quantity and quality were check by a Nanodrop® ND-1000 UV–vis spectrophotometer (NanoDrop Technologies, Wilmington, DE, USA). The V4-V5 region of the bacterial and archaea 16S rRNA genes were amplified using the forward primers 347F (5'-CCTACGGRRBGCASCAGKVRVGAAT-3') and reverse primers 802R (5'-GGACTACNVGGGTWTCTAATCC-3') (Li et al., 2017). Details for Illumina sequencing, experimental steps and data analyses are described in chapter 2.

7.3.7. Quantitative PCR (qPCR) of *arsC, aioA and arsM genes*

The abundances of *aioA, arsC* and *arsM* genes from the rice rhizosphere at the ending of the maturation stage was determined by quantitative real-time PCR (qPCR) performed on a real-time qPCR Instrument (LightCycler 480II, Switzerland). Details for qPCR, experimental steps and data analyses are described in chapter 2.

7.3.8. Nucleotide sequence accession number

The 16S rRNA-based high-throughput sequencing reads have been submitted to NCBI GeneBank database with accession number MK235250 - MK235990.

7.4. Results

7.4.1. Voltage generation

The average voltage from the sMFCs and controls over 120 days are showed in Fig. 7.1a. The voltage rapidly increased after connecting the 500Ω external. Afterwards, the voltage progress in an increasing direction until day 104. On day 110 the 500Ω external resistor was replaced with a 100Ω external resistor and the voltage dropped to around 63 mv. The control open voltage also increased without any lag time and was around 879 mV on day 120. As shown in Fig. 7.1b, the maximum power output was found to be 22.2 mW/m2 when the current was 2.42 mA.

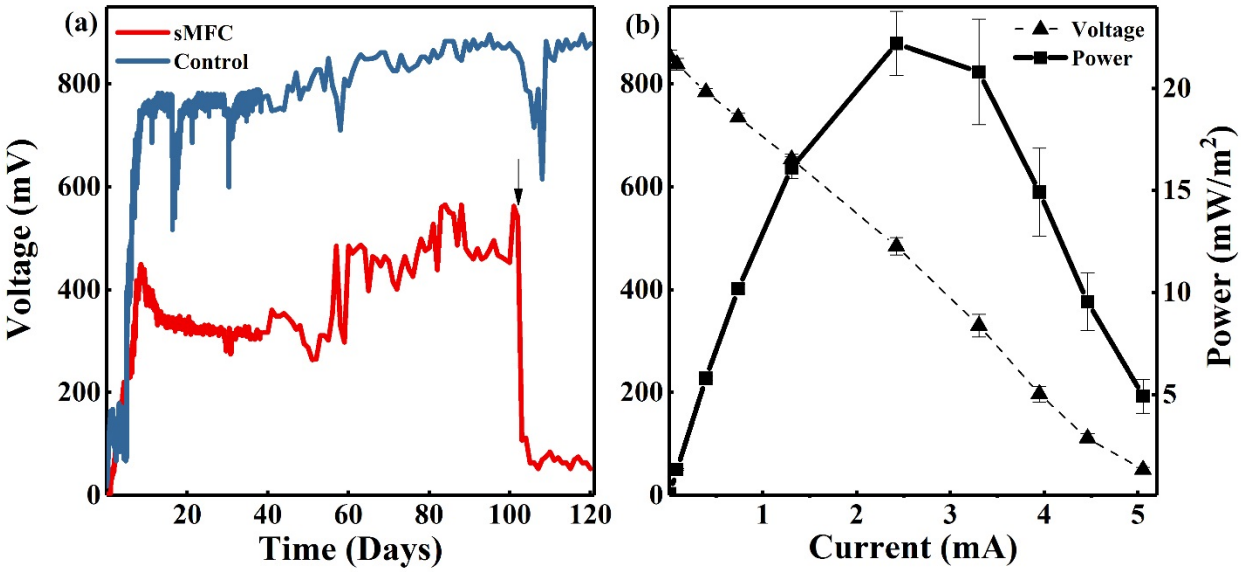

Figure 7.1 Voltage variation over time (a) and polarization curve (b). The arrow represent the time when the external resistor was changed to 100 Ω.

7.4.2. Effects of sMFC on soil pH, Eh, DOC and plant growth.

The pH was significantly ($p < 0.05$) lowered in the sMFC anode (7.42 ±0.06) vicinity compared to that of the control (8.16 ±0.8). However the pH in the sMFC rhizosphere (8.48 ±0.1) was higher than that of the control (8.03 ±0.1). In addition, the Eh in the sMFC rhizosphere soil was significantly ($p < 0.05$) higher than that of the control. The Eh in the sMFC was (84.4 ±10.6) and that of control was (-108.0 ±19.9).

The porewater DOC steadily decreased in all of the layers, regardless of treatment, from day 10 to 30, however on day 50 an increase in DOC was observed in the control (Fig.7 2a-c). This could have been due to DOC input from the rice roots. Nonetheless, DOC concentrations in the sMFC were consistently lower than that of the control in all layers. On day 110 the DOC concentration was 48.1%, 40.0% and 46.3% lower in the sMFC compared to the control (Fig. 7.2a-c). This indicates that the sMFC accelerated the degradation of DOC. Moreover, the sMFC influenced the plant height and tiller number. Average plant heights per pot were higher in the sMFC (92.3 ±0.9 cm/ pot) than that of the plants in the control (80.9 ±1.6 cm/ pot). Similarly the average tiller number were higher in the sMFC (36.2 ±1.6/ pot) compared to the control (28.2 ±1.6/ pot). As compared to control, both the plant heights and tiller number increased by 12.4% and 22.2% respectively.

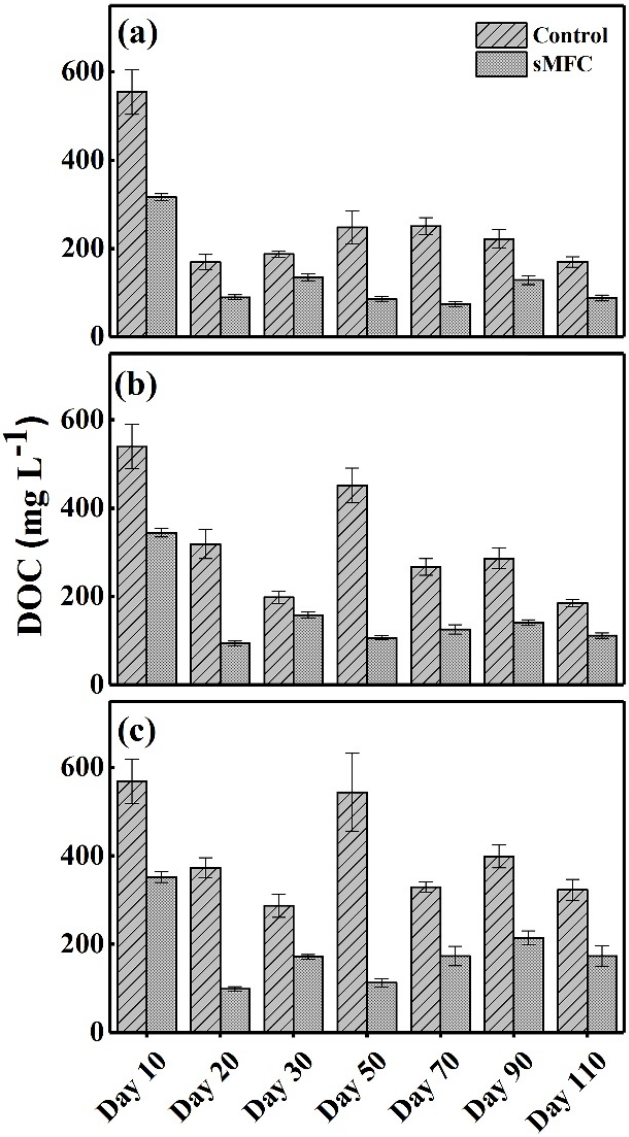

Figure 7.2 Variations in DOC in the sMFC and control treatment. Panels a, b and c show DOC concentrations in the top, middle and bottom layers, respectively.

7.4.3. Effect of sMFC on porewater As and Fe concentration

Figure 7.3a-f illustrates the soil porewater total As and Fe in the sMFC and control samples over the course of the 110 days of incubation. The porewater total As concentration was consistently lower in the sMFC than that of the control in all layers. On day 110 the total As concentrations were 25.2%, 41.8% and 39.1% lower in the sMFC top, middle and bottom layers respectively compared to the control (Fig. 7.3a-c). These results demonstrate that the sMFC limited the mobilization of As into the soil porewater. Furthermore, As(III) was the

predominate As species in the soil porewater on day 110 and accounted for more than 80% of the total soil porewater As in the control (Table S 7.2).

Moreover, a rapid increase in dissolved total Fe was observed on day 10, and then gradually declined in both the sMFC and the control. Similar to the porewater total As concentration, the total Fe concentrations were lower in the sMFC compared to the control in all layers on day 10 (Fig. 7.3d-f). However, with the increase in incubation time, the concentrations in the soil porewater total Fe became slightly higher in the sMFC compared to the control. Nonetheless it should be noted that the sMFC porewater also had higher concentration of Fe (III) than that of the control (Table S 7.2).

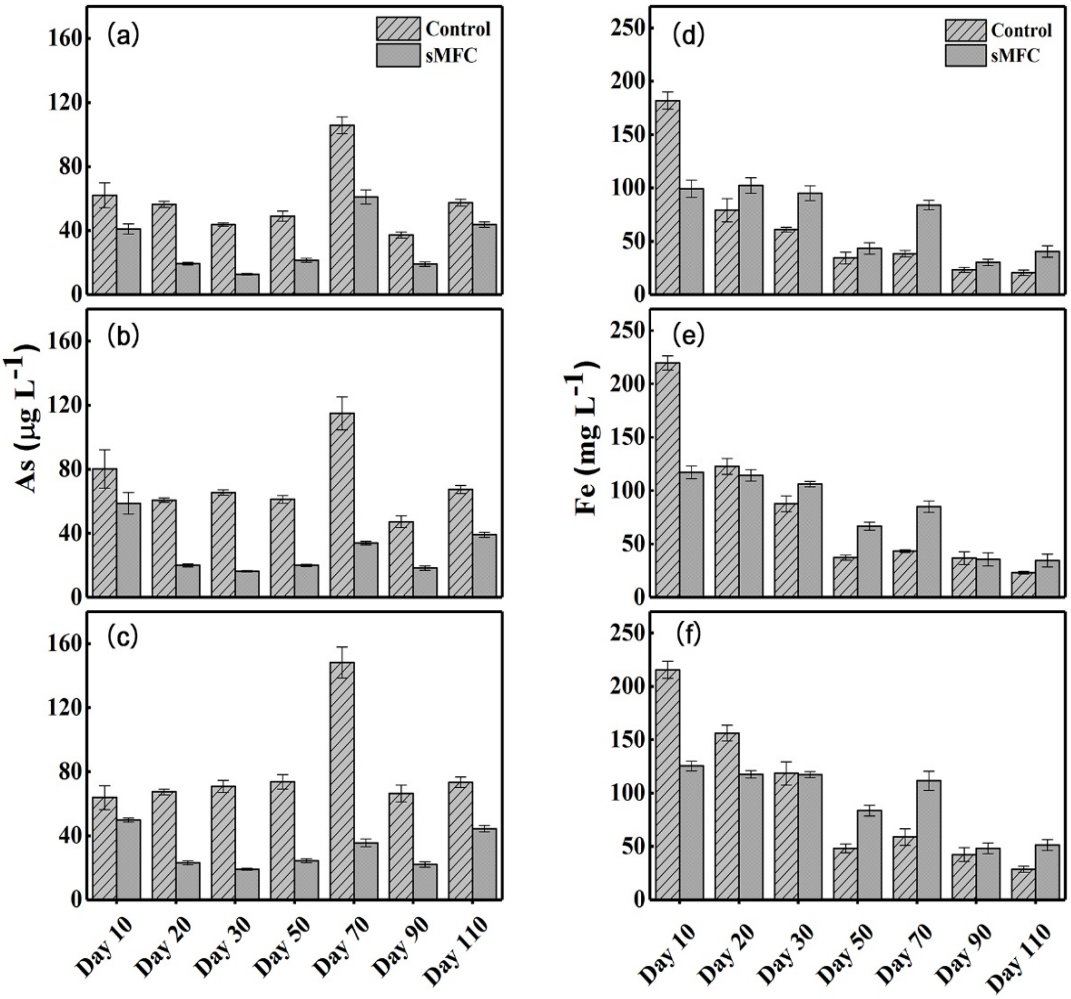

Figure 7.3 Variations in As and Fe concentration in the sMFC and control treatment. Panels a, b and c show As concentrations in the top, middle and bottom layers, respectively. Panels d, e and f show Fe concentrations in the top, middle and bottom layers, respectively.

7.4.4. Effects of sMFC on As accumulation in rice

The total As content in the roots, steams, husks and rice grains in the different treatments at the mature stage are given in Fig. 7.4.4. In general, regardless of the application of the sMFC, the distribution pattern of total As in the rice roots, stems, leaves, husks and grains follow the order of roots > leaves > stems > husks > grains. However, the total As content in the stems, leaves, husks and grains were lower in the rice plants grown in the soil with the sMFC compared with that of the control. This suggests that the sMFC can effectively impede the migration of As to

rice plants. In sMFC treatments, total As content in rice grains, husks, leaves and stems were reduced at the end of the mature stage (day 120) compared to the control. The total As content in rice grains, husks, leaves and stems were, 0.9, 1.2, 3.2 and 2.4 mg/kg, respectively in the control. Compared with control, the contents of total As in rice grains, husks, leaves and stems decreased by 53.4%, 44.7%, 62.6%, and 67.9%, respectively. Moreover, no significant differences were observed between the As concentration in the rice roots from the sMFC and those from the control although the total As concentration was higher in the rice roots from the sMFC. However, Fe concentration in the sMFC rice roots (13.1 ±1.2 g/kg) were higher than that of the control rice roots (11.1 ±0.4 g/kg). Nonetheless, it should be noted that Fe plaques were not separated from the rice roots in this study.

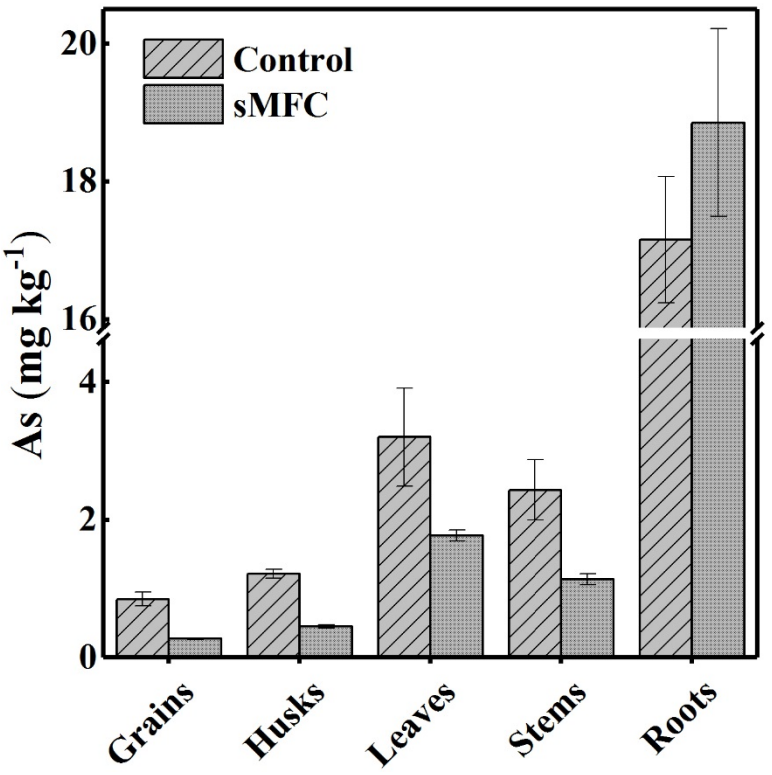

Figure 7.4 The concentration of As in the rice parts at maturation.

7.4.5. *arsC*, *aioA* and *arsM* genes abundance

Quantitative PCR assays were conducted to quantify absolute abundance of three As transformation genes in the rhizosphere from the sMFC and control samples (Fig. 7.5). The

results showed that the copy number of the *arsC*, *aioA* and *arsM* genes were significantly influenced by operating the sMFC. The abundance of the *arsC* gene that is responsible for the microbial transformation of As(V) to As(III) was significantly (p= 0.04) lower in the sMFC rhizosphere as compared to that of the controls rhizosphere. Furthermore *aioA* and *arsM* genes that are responsible for the microbial oxidation and methylation of As, respectively, were higher in the sMFC rhizosphere compared to that of the control. These results suggest that direct microbial reduction of As(V) to As(III) in the control could be responsible for the higher soil porewater total As. Moreover, these results also indicate that the transformation of As(III) to As(V) and the methylation of As could have played a role in the decrease of As mobility into the sMFC soil porewater.

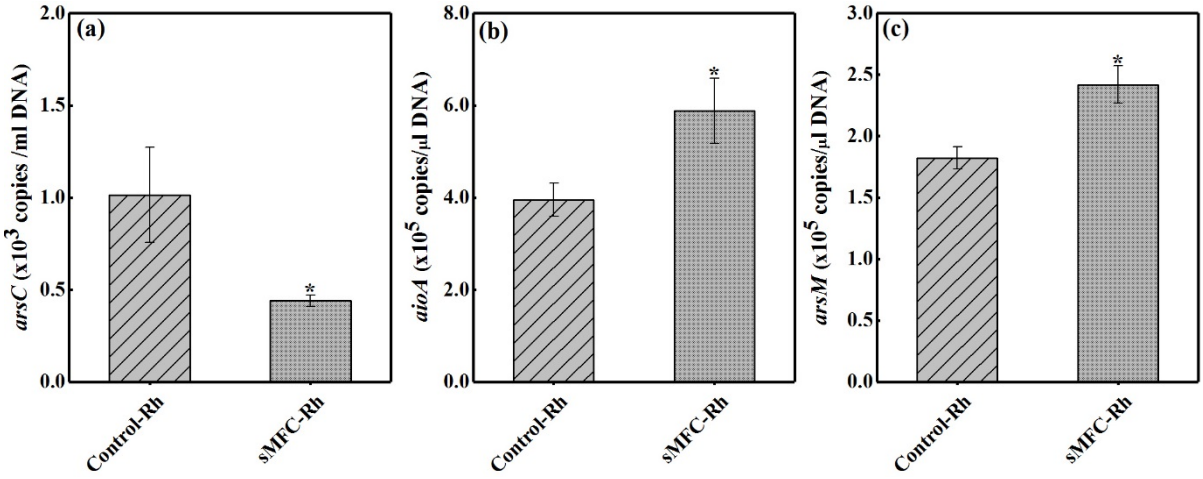

Figure 7.5 Absolute abundance of the (a) *arsC*, (b) *aioA* and (c) *arsM* genes in the sMFC and control rhizosphere soil at the end of the incubation period. The asterisk shows a statistically significant difference as compared with control ($p < 0.05$).

7.4.6. Functional bacterial community

The diversity of the bacterial community in both the anode vicinity and the rhizosphere were assessed by high-throughput sequencing of the 16S rRNA gene. In all of the samples the Good's coverage were above 99%, indicating that size of all the libraries were sufficient to

cover the bacterial communities (Table S 7.3). Based on the OTUs classified at 97% similarity, the sMFC had the highest richness compared to the control in both the anode vicinity and rhizosphere. Moreover, a higher diversity was observed in anode vicinity compared to the rhizosphere regardless of treatment. A similar trend was observed in the OTUs distribution, suggesting that the bacterial community in the anode vicinity were more diverse than that of the rhizosphere (Table S 7.3).

In addition, beta diversity and Anosim analysis were used to study the variances in the bacterial community between the sMFC and the control. The results showed that the sMFC bacterial community were significantly different compared to that of control. Principal Coordinates Analysis (PCoA)-PC1 vs PC2 (explaining 74.9%) showed that the sMFC significantly altered the bacterial community in the anode vicinity and rhizosphere soil compared to the control (Fig. 7.6). The bacterial community clustered into three main groups. Where samples from anode vicinity and rhizosphere of the sMFC formed two separate groups, while all the samples from the control comprised the third cluster. Moreover, Anosim analysis also supports the conclusion that bacterial community on the sMFC anode vicinity (p= 0.03) and the rhizosphere (p= 0.02) were significantly different from that of the control.

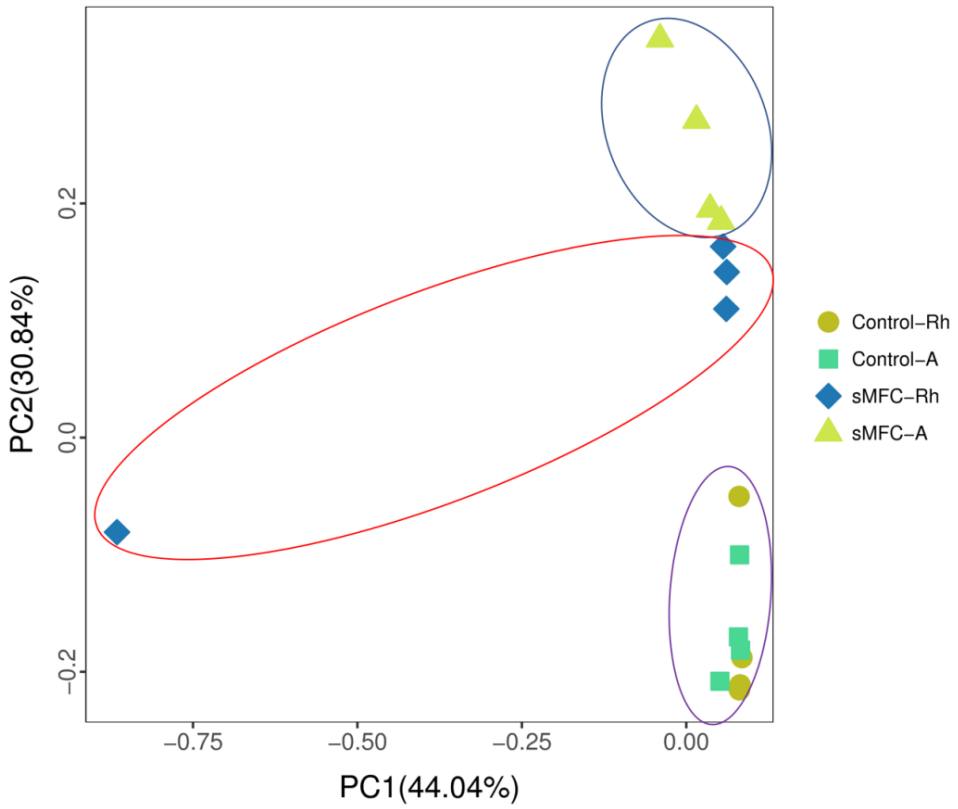

Figure 7.6 Principal Coordinates Analysis (PCoA) of the sMFC and controls bacterial community composition based on Bray-Curtis distance. The x- and y-axes are indicated by the first and second coordinates, respectively.

The composition of the microbial community in the sMFC and control were further investigated and classified into taxonomic groups. In all the treatments, *Alphaproteobacteria, Anaerolineae, Clostridia, Deltaproteobacteria, Gammaproteobacteria, Actinobacteria, Bacteroidia, Bacilli, Thermoleophilia* and *Chloroflexi* were the dominant classes and accounted for over 84% of the total OTUs (Fig. 7.7a). As expected *Deltaproteobacteria* (21.0% vs 6.2%), and *Actinobacteria* (10.4% vs 5.5%) dominated the anode vicinity of the sMFC, while *Alphaproteobacteria* (10.8% vs 15.6%), *Anaerolineae* (9.4% vs 15.6%), *Clostridia* (7.6% vs 15.9%) and *Bacilli* (4.3% vs 3.8%) were more abundant in the control anode vicinity. In the rhizosphere, *Deltaproteobacteria* (9.3% vs 4.7%), *Gammaproteobacteria* (14.1% vs 11.5%), *Actinobacteria* (15.4% vs 6.9%), and *Bacteroidia* (6.6% vs 3.5) were high in the sMFC

compared to the control. However, in the control rhizosphere *Alphaproteobacteria* (10.2% vs 17.4), *Anaerolineae* (8.9% vs 16.1), *Clostridia* (12.5% vs 13.3%), *Bacilli* (4.1% vs 5.0%) and *Thermoleophilia* (2.7% vs 4.3%) were more abundant.

At the genus level, *Geobacter* (1.4- 11.3%), *Anaerolinea* (1.5- 2.6%) and *Bacillus* (2.3-4.4%) were the most dominant groups in all of the samples. *Geobacter*, *Nocardiodes* and *Anaeromyxobacter* were significantly higher in the sMFC compared to the control in the anode vicinity (Fig. 7.7b). However, *Bacillus*, *Anaerolinea* and *Defluviicoccus* were significantly ($p < 0.05$) higher in the control compared to the sMFC in the rhizosphere.

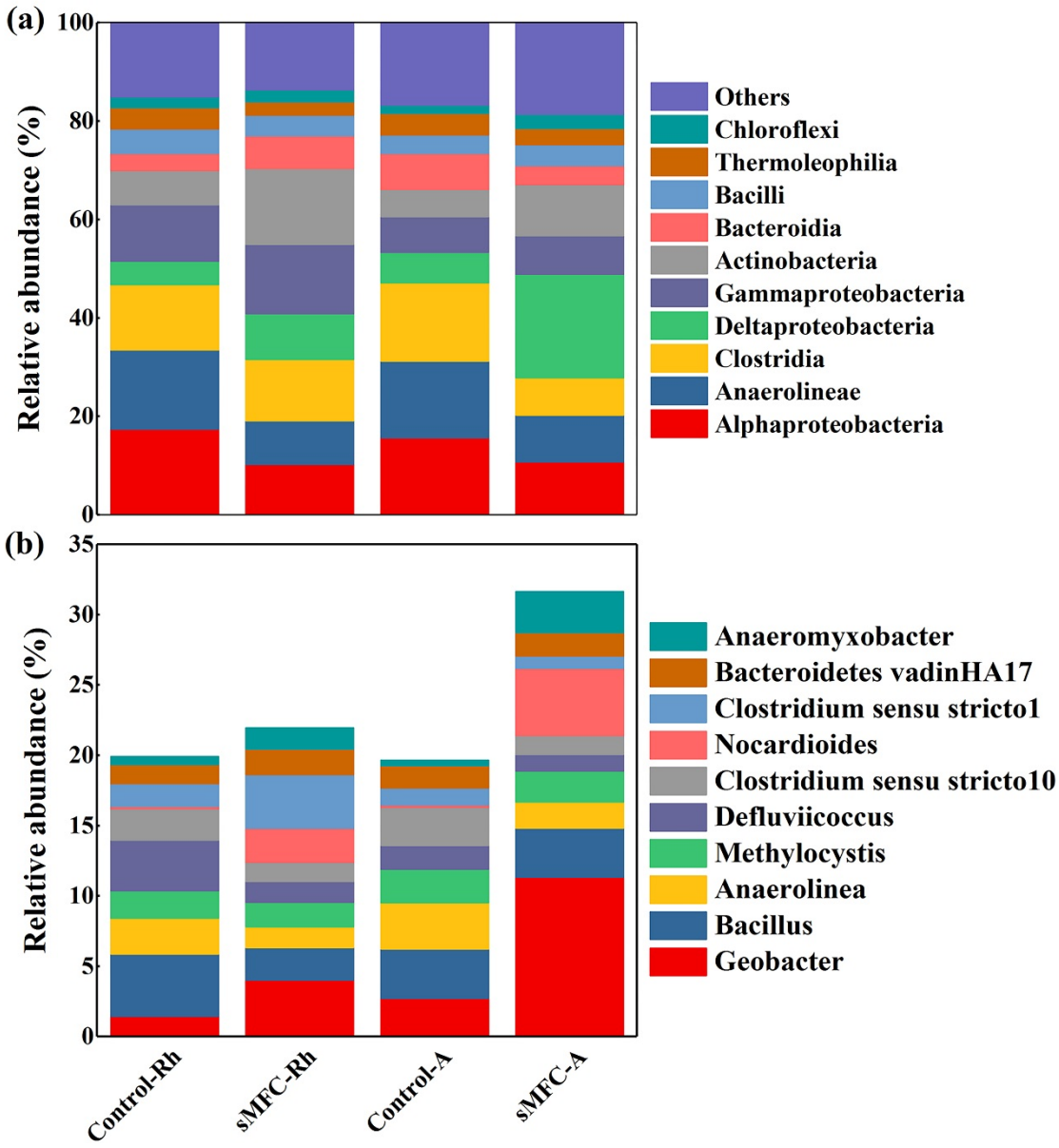

Figure 7.7 Relative abundance of bacterial community composition at class (a) and genus (b) levels. The relative abundance values represent the mean of four replicates.

7.5. Discussion

7.5.1. Voltage output

The high voltage generation without any lag time in the sMFC was likely due to the accumulation of electrogenic bacteria on the anode. Since, the start-up time is highly related to the biofilm attachment rate around anode (Song and Jiang 2018). The genera *Geobacter*, *Aneromyxobacter* and *Nocardioides* were significantly enhanced on the sMFC anodes

suggesting that they are able to respire the anode and contribute to the high voltage output. Previous studies have shown that these genera are able to transfer electrons outside of the cell membrane to respire solid mineral oxides (Gustave et al. 2018a; Qiao et al. 2017a). Moreover, the genera *Geobacter* and *Aneromyxobacter* are known electrogens and have been positively correlated to the sMFC performance (Kouzuma et al. 2014). The fluctuating voltage that was observed throughout the sMFC operation is characteristic of oxygen input from plant roots into the anode vicinity of the sMFC (Chen et al. 2012; Kouzuma et al. 2013; Liu et al. 2018). The plant roots accelerate the potentials near the anode because of oxygen loss from roots tip and this results in a decrease voltage due to a competition for electron between oxygen released from the roots and the anode (Kaku et al. 2008; Liu et al. 2018; Schamphelaire et al. 2008). The high power output of the cell was probably due to the ready available DOC from the plant roots and the development of a stable electrogenic community on the anodes (Schamphelaire et al. 2008).

7.5.2. The effect of the sMFC on the As and Fe mobility in the soil porewater

The anode of the sMFC is able to serve as an alternative electron acceptor for both As and Fe reducing bacteria (Gustave et al. 2018a). Thus, many known As and Fe reducers have been found to be enhanced in the vicinity of the anode and respire the anode of the sMFC thereby limiting the release of As and Fe (Gustave et al. 2018a; Wang et al. 2015; Wang et al. 2016). Recently, in a study investigating the effects of sMFC on As and Fe behaviors in paddy soil porewater, it was reported that the sMFC can reduce the soil porewater As and Fe by 53% and 35%, respectively (Gustave et al. 2018a). In the present study, our results demonstrated that the sMFC can significantly decrease As mobility in the rhizosphere which was consistent with the previous study results. Our results were also consistent with previous studies that observed As(III) as the dominant As speciation and very low concentration of DMA in the soil porewater after prolong flooding (Wang 2019 et al., Zhao et al., 2013). However, we observed an increase

in total Fe concentration in the sMFC as compared to the control after day 10. This suggest that up to day 10 Fe dissolution was responsible for the release of As, but after day 10 the release of As was independent of Fe release (Mirza et al. 2014; Zhang et al. 2018). The independent release of As has also been reported in other studies (Das et al. 2016; Mirza et al. 2014). The exact mechanism for the decoupling of As and Fe release is not well understood. However, previous studies have suggested that decoupling of As and Fe release occurred due to direct arsenic reduction and formation of secondary Fe minerals or the precipitation of Fe(II) on oxide surfaces. This may have occurred because it is thermodynamically more favorable for As(V) reduction to As(III) to happen before the reduction of secondary iron minerals such goethite and hematite to Fe(II) (Postma et al. 2010; Radloff et al. 2007).

The decoupling of As and Fe release in our study may have occurred as a results of direct As (V) reduction. Evidence from previous studies showed that some microbes are able to directly reduce As(V) from the surface of Fe oxides facilitating the release of As(III) (Das et al. 2016; Qiao et al. 2017a; Qiao et al. 2017b; Zhang et al., 2018). In the present study, sequences related to bacterial genera capable of direct As(V) reduction, such as *Clostridia*, *Bacilli* and *Thermoleophilia* were more abundant in the control samples. Moreover, the As reducing gene (*arsC*) was also significantly higher in the control (Villegas-Torres et al. 2011). These results coupled with the high concentration of immobilized As in the sMFC soil, led us to hypothesize that decoupling of As and Fe in our study may have been due to direct As reduction. Das et al., (2016) and Zhang et al., (2018) observed a similar phenomenon in their investigations on the decoupling of As and Fe in groundwater. In both studies, the authors concluded that direct As reduction was a major process leading to increase of As in the groundwater (Das et al., 2016; Zhang et al., 2018). Another reason for independent mobility of As could be due to the chemicals released by the rice roots to increase Fe bioavailability. The rice growth in the sMFC were much better than that of the control and previous studies have

shown that rice roots can secrete phytosiderophores to rhizosphere and chelate Fe(III) to enhance the bioavailability of Fe (Boonyaves et al. 2017). In our study, the concentration of dissolved Fe(III) was significantly higher ($p < 0.05$) in the sMFC compared to the treatment.

Furthermore, As immobilization by sMFC application could be explained by multi-mechanisms affiliated to the installation of sMFC, including the decrease of soil DOC, increase in soil Eh and the redistribution of the As reducing genes and bacterial community. The sMFC and the control treatments were constructed from the same paddy soil with 21.2±07 g/kg TOC (Table S1). Although we did not measure the DOC prior to day 10, we assume that the initial DOC concentrations were relatively the same in both sMFC and the control treatments. However, from day 10, the sMFC application significantly increased DOC mineralization from the soil porewater, which has been reported to decrease As release (Gustave et al. 2018a; Stuckey et al. 2015). Studies have shown that DOC is the main electron donor for the reduction and liberation of As (Jia et al. 2013; Stuckey et al. 2015). Hence, because the sMFC decrease DOC content in the soil porewater and DOC is the main electron donor this thereby could have led to a decrease in the rate of As reduction by As reducing and dissimilatory bacteria in the soil (Gustave et al. 2018a). Moreover, the increase in soil Eh also favor the decrease in soil porewater As. The direct reduction of As is more likely to occur under reducing condition rather oxidizing conditions (Takahashi et al. 2004; Yamaguchi et al. 2011).

Additionally, the sMFC significantly affected the abundance of functional genes and microbes that are involved in the As transformation. Microbes transform As by using different As transformation genes (Zhang et al. 2015). Studies have shown that the relative abundance and activity of these genes determine the bioavailability and speciation of As in the rice paddy soil (Jia et al. 2013; Qiao et al. 2017a; Zhang et al. 2015). Dissimilatory arsenic reduction is the main pathway that increase As mobility in paddy soil and is catalyzed by the respiratory *arrA* genes (Malasarn et al. 2004) and the detoxification *arsC* genes (Villegas-Torres et al.

2011) which transform As(V) to As(III). Conversely, As(III) oxidation by the *aioA* and *aioB* genes and As(III) methylation by the *arsM* genes favor As immobilization and vaporization in paddy soils respectively (Slyemi and Bonnefoy 2012; Yang et al. 2018).

In the sMFC the As reducing gene (*arsC*) was significantly suppressed in the rhizosphere. Thus, the decrease in the abundance of *arsC* gene and porewater total As suggests that the sMFC limited As(V) reduction. As(V) has a high tendency to co-precipitate from soil porewater with metal oxide as compared to As(III) which has a lower affinity for metal oxides (Yamaguchi et al. 2011). Moreover, the sMFC was also found to significantly increase the abundance of the As oxidizing (*aioA*) and methylation (*arsM*) genes. The *aioA* could have enhance the transformation of As(III) to As(V) which then favors the precipitation of As from the soil porewater (Jia et al. 2014; Slyemi and Bonnefoy 2012).

Furthermore, the increase of the classes *Clostridia*, *Bacilli* and *Thermoleophilia* may have also contributed to the release of As in the control soil porewater. Members of these classes have also been found to be associated with soils that have high As content (Das et al. 2016; Qiao et al. 2017a; Qiao et al. 2017b). Further analysis to the genus level shown a near two fold increase in the abundance of *Bacillus* related sequences in the control rhizosphere. The genus *Bacillus* has been shown to enhance As mobility in flooded paddy soils (Qiao et al. 2017a; Wang et al. 2017). However, it should be noted that *Geobacter* and *Anaeromyxobacter* (members of class *Deltaproteobacteria)* was significantly enhanced in the sMFC rhizosphere. Although both *Geobacter* and *Anaeromyxobacter* are known As reducers (Qiao et al. 2017a; Wang et al. 2017) the lower total As observed in the sMFC could be due to long distance electron transfer to the anode thus prevent As reduction (Lovley 2017). *Geobacter* can transfer electron to the anode via quinone-mediated electron shuttle and the use of nanowires (Reguera et al. 2005; Wu et al. 2018).

7.5.3. The sMFC significantly reduce total As accumulation in the rice grains

In this study, the uptake of As was determined to be highly dependent on As availability. Thus, with the decrease in total As concentration in soil porewater sMFC, total As accumulation in the rice leaves, stems, husks and rice grains were significantly decreased in the plants with the sMFC application. This occurred as the uptake of As is strongly dependent on the As bioavailability and speciation (Suriyagoda et al. 2018). As (III) is taken up through aquaporins in the rice plant roots and then enters the stele through the silicon- (Si) uptake pathway, while As(V) is taken up through the phosphate uptake system (Suriyagoda et al. 2018). In our study, As(III) was the dominant species and was more abundant in the control samples, hence higher As accumulation was observed in the rice grown in the control.

Moreover, higher As in the rice roots from sMFC suggest that the rice roots impede the translocation of As to other above ground plant tissues (Rahman et al. 2007). The rice roots are able to retain As and impede its translocation due the present of Fe plagues that form around the roots (Chen et al. 2005). The root Fe plaque was formed due to the oxidation of Fe(II) to Fe(III) by oxygen release from the roots surface. Ferric hydroxides is the main component of root plaques and has a high adsorption capacity for As from the soil porewater (Liu et al. 2005). However, the adsorption of As by the Fe(III) oxides is strongly affected by DOC concentration. The DOC in the soil may compete with As for adsorption sites thereby decreasing As adsorption and may enhance As release to the soil porewater (Williams et al. 2011). In our study, the rice roots in the sMFC had a thicker Fe plaque as was suggested by the higher Fe concentration and the DOC concentration in sMFC was significant lower than that of the control.

7.6. Conclusions

In this study the effect of the sMFC on the accumulation of As in the rice plants was investigated. The total As in the rice grains decreased by 53.4% in the sMFC compared to the

control and similar decreases were also observed in leaves, stems, husks and grains. The reason for the decrease in As in the rice tissue was due to the decrease in As bioavailability in the soil porewater. Furthermore, a maximum power output of 22.2 mW/m^2 was produced by the sMFC. These results demonstrate for the first time that the sMFC can be used to significantly reduce As accumulation in rice tissues and simultaneously generate electricity to power small devices. However it should be noted that the concentrations of As in the plant tissues were not standardized to the mass of the whole plants.

7.7. References

Boonyaves, K., Wu, T.Y., Gruissem, W., Bhullar, N.K., 2017. Enhanced grain iron levels in rice expressing an iron-regulated metal transporter, nicotianamine synthase, and ferritin gene cassette. Front. Plant. Sci. 8, 130.

Burton, E.D., Johnston, S.G., Bush, R.T., 2011. Microbial sulfidogenesis in ferrihydrite-rich environments: effects on iron mineralogy and arsenic mobility. Geochim. Cosmochim. Acta 75, 3072-3087.

Chen, Z., Huang, Y.C., Liang, J.H., Zhao, F., Zhu, Y.G., 2012. A novel sediment microbial fuel cell with a biocathode in the rice rhizosphere. Bioresour. Technol. 108, 55-59.

Chen, Z., Zhu, B.K., Jia, W.F., Liang, J.H., Sun, G.X., 2015. Can electrokinetic removal of metals from contaminated paddy soils be powered by microbial fuel cells? Environ. Techn. Innov.3, 63-67.

Chen, Z., Zhu, Y.G., Liu, W.J., Meharg, A.A., 2005. Direct evidence showing the effect of root surface iron plaque on arsenite and arsenate uptake into rice (Oryza sativa) roots. New Phyt. 165, 91-97.

Das, S., Liu, C.C., Jean, J.S., Lee, C.C., Yang, H.J., 2016. Effects of microbially induced transformations and shift in bacterial community on arsenic mobility in arsenic-rich deep aquifer sediments. J. Hazard. Mater. 310, 11-19.

Gustave, W., Yuan, Z.F., Sekar, R., Chang, H.C., Zhang, J., Wells, M., Ren, Y.X., Chen, Z., 2018a. Arsenic mitigation in paddy soils by using microbial fuel cells. Environ. Pollut. 238, 647-655.

Gustave, W., Yuan, Z.F., Sekar, R., Ren, Y.X., Chang, H.C., Liu, J.Y., Chen, Z., 2018b. The change in biotic and abiotic soil components influenced by paddy soil microbial fuel cells loaded with various resistances. J. Soils Sediments, 1-10.

Hashimoto, Y., Kanke, Y., 2018. Redox changes in speciation and solubility of arsenic in paddy soils as affected by sulfur concentrations. Environmental Pollution 238, 617-623.

Hu, Z.-Y., Zhu, Y.G., Li, M., Zhang, L.G., Cao, Z.H., Smith, F.A., 2007. Sulfur (S)-induced enhancement of iron plaque formation in the rhizosphere reduces arsenic accumulation in rice (Oryza sativa L.) seedlings. Environ. Pollut. 147, 387-393.

Jia, Y., Huang, H., Chen, Z., Zhu, Y.-G., 2014. Arsenic uptake by rice is influenced by microbe-mediated arsenic redox changes in the rhizosphere. Environ. Sci. Technol. 48, 1001-1007.

Jia, Y., Sun, G.-X., Huang, H., Zhu, Y.-G., 2013. Biogas slurry application elevated arsenic accumulation in rice plant through increased arsenic release and methylation in paddy soil. Plant and Soil 365, 387-396.

Kaku, N., Yonezawa, N., Kodama, Y., Watanabe, K., 2008. Plant/microbe cooperation for electricity generation in a rice paddy field. Appl. Microbiol. Biotechnol. 79, 43-49.

Kouzuma, A., Kaku, N., Watanabe, K., 2014. Microbial electricity generation in rice paddy fields: recent advances and perspectives in rhizosphere microbial fuel cells. Appl Microbiol. Biotechnol. 98, 9521-9526.

Kouzuma, A., Kasai, T., Nakagawa, G., Yamamuro, A., Abe, T., Watanabe, K., 2013. Comparative metagenomics of anode-associated microbiomes developed in rice paddy-field microbial fuel cells. PLoS One 8, e77443.

Li, B., Zhou, S., Wei, D., Long, J., Peng, L., Tie, B., Williams, P.N. and Lei, M., 2019. Mitigating arsenic accumulation in rice (Oryza sativa L.) from typical arsenic contaminated paddy soil of southern China using nanostructured α-MnO2: Pot experiment and field application. Sci. Total Environ., 650, pp.546-556.

Liu, B., Ji, M., Zhai, H., 2018. Anodic potentials, electricity generation and bacterial community as affected by plant roots in sediment microbial fuel cell: Effects of anode locations. Chemosphere.

Liu, W.-J., Zhu, Y.-G., Smith, F., 2005. Effects of iron and manganese plaques on arsenic uptake by rice seedlings (Oryza sativa L.) grown in solution culture supplied with arsenate and arsenite. Plant and Soil 277, 127-138.

Lovley, D.R., 2017. Electrically conductive pili: biological function and potential applications in electronics. Curr. Opin. Electrochem. 4, 190-198.

Lozupone, C., Knight, R., 2005. UniFrac: a new phylogenetic method for comparing microbial communities. Appl. Environ. Microbiol. 71, 8228-8235.

Malasarn, D., Saltikov, C., Campbell, K., Santini, J., Hering, J., Newman, D., 2004. arrA is a reliable marker for As (V) respiration. Science 306, 455-455.

Mirza, B.S., Muruganadam, S., Meng, X., Sorensen, D.L., Dupont, R.R., McLean, J.E., 2014. Arsenic (V) Reduction in Relation to Iron (III) Transformation and Molecular Characterization of the Structural and Functional Microbial Community in Sediments of a Northern Utah, Basin-Fill Aquifer. Appl. Environ. Microbiol. 00240-00214.

Postma, D., Jessen, S., Hue, N.T.M., Duc, M.T., Koch, C.B., Viet, P.H., Nhan, P.Q., Larsen, F., 2010. Mobilization of arsenic and iron from Red River floodplain sediments, Vietnam. Geochim. Cosmochim. Acta 74, 3367-3381.

Qiao, J.T., Li, X.M., Li, F.B., 2017a. Roles of different active metal-reducing bacteria in arsenic release from arsenic-contaminated paddy soil amended with biochar. J. Hazard. Mater. 344, 958-967.

Qiao, J., Li, X., Hu, M., Li, F., Young, L.Y., Sun, W., Huang, W., Cui, J., 2017b. Transcriptional activity of arsenic-reducing bacteria and genes regulated by lactate and

biochar during arsenic transformation in flooded paddy soil. Environ. Sci. Technol. 52, 61-70.

Quast, C., Pruesse, E., Yilmaz, P., Gerken, J., Schweer, T., Yarza, P., Peplies, J., Glöckner, F.O., 2012. The SILVA ribosomal RNA gene database project: improved data processing and web-based tools. Nucleic Acids Res. 41, D590-D596.

Radloff, K.A., Cheng, Z., Rahman, M.W., Ahmed, K.M., Mailloux, B.J., Juhl, A.R., Schlosser, P., van Geen, A., 2007. Mobilization of arsenic during one-year incubations of grey aquifer sands from Araihazar, Bangladesh. Environ. Sci. Technol. 41, 3639-3645.

Rahman, M.A., Hasegawa, H., Rahman, M.M., Rahman, M.A., Miah, M., 2007. Accumulation of arsenic in tissues of rice plant (Oryza sativa L.) and its distribution in fractions of rice grain. Chemosphere 69, 942-948.

Reguera, G., McCarthy, K.D., Mehta, T., Nicoll, J.S., Tuominen, M.T., Lovley, D.R., 2005. Extracellular electron transfer via microbial nanowires. Nature 435, 1098.

Schamphelaire, L.D., Bossche, L.V.d., Dang, H.S., Höfte, M., Boon, N., Rabaey, K., Verstraete, W., 2008. Microbial Fuel Cells Generating Electricity from Rhizodeposits of Rice Plants. Environ. Sci. Technol. 42, 3053-3058.

Slyemi, D., Bonnefoy, V., 2012. How prokaryotes deal with arsenic. Environ. Microbiol. Rep. 4, 571-586.

Song, N., Jiang, H.-L., 2018. Effects of initial sediment properties on start-up times for sediment microbial fuel cells. Int. J. Hydrog. Energy. 43, 10082-10093.

Stuckey, Jason W., Schaefer, Michael V., Kocar, Benjamin D., Benner, Shawn G., Fendorf, S., 2015. Arsenic release metabolically limited to permanently water-saturated soil in Mekong Delta. Nat. Geosci. 9, 70-76.

Suriyagoda, L.D., Dittert, K., Lambers, H., 2018. Mechanism of arsenic uptake, translocation and plant resistance to accumulate arsenic in rice grains. Agric. Ecosyst. Environ. 253, 23-37.

Takahashi, Y., Minamikawa, R., Hattori, K., Kurishima, K., Kihou, N., Yuita, K., 2004. Arsenic behavior in paddy fields during the cycle of flooded and non-flooded periods. Environ. Sci. Technol. 38, 1038-1044.

Villegas-Torres, M.F., Bedoya-Reina, O.C., Salazar, C., Vives-Florez, M.J., Dussan, J., 2011. Horizontal arsC gene transfer among microorganisms isolated from arsenic polluted soil. Int. Biodeterior. Biodegradation. 65, 147-152.

Wang, N., Chen, Z., Li, H.B., Su, J.Q., Zhao, F., Zhu, Y.G., 2015. Bacterial community composition at anodes of microbial fuel cells for paddy soils: the effects of soil properties. J. Soils and Sediments 15, 926-936.

Wang, X., Li, F., Yuan, C., Li, B., Liu, T., Liu, C., Du, Y., Liu, C., 2019. The translocation of antimony in soil-rice system with comparisons to arsenic: Alleviation of their accumulation in rice by simultaneous use of Fe (II) and NO3−. Sci. Total Environ. 650, 633-641.

Williams, P.N., Zhang, H., Davison, W., Meharg, A.A., Hossain, M., Norton, G.J., Brammer, H., Islam, M.R., 2011. Organic Matter□ Solid Phase Interactions Are Critical for Predicting Arsenic Release and Plant Uptake in Bangladesh Paddy Soils. Environ. Sci. Technol. 45, 6080-6087.

Wu, M., Xu, X., Lu, K., Li, X., 2018. Effects of the presence of nanoscale zero-valent iron on the degradation of polychlorinated biphenyls and total organic carbon by sediment microbial fuel cell. Sci. Total Environ. 656, 39-44.

Yamaguchi, N., Nakamura, T., Dong, D., Takahashi, Y., Amachi, S., Makino, T., 2011. Arsenic release from flooded paddy soils is influenced by speciation, Eh, pH, and iron dissolution. Chemosphere 83, 925-932.

Yamamura, S., Sudo, T., Watanabe, M., Tsuboi, S., Soda, S., Ike, M., Amachi, S., 2018. Effect of extracellular electron shuttles on arsenic-mobilizing activities in soil microbial communities. J. Hazard. Mater. 342, 571-578.

Yang, Y., Zhang, H., Yuan, H., Duan, G., Jin, D., Zhao, F., Zhu, Y., 2018. Microbe mediated arsenic release from iron minerals and arsenic methylation in rhizosphere controls arsenic fate in soil-rice system after straw incorporation. Environ. Pollut. 236, 598-608.

You, J., Wu, G., Ren, F., Chang, Q., Yu, B., Xue, Y., Mu, B., 2016. Microbial community dynamics in Baolige oilfield during MEOR treatment, revealed by Illumina MiSeq sequencing. Appl. Microbiol. Biotechnol. 100, 1469-1478.

Zhang, J., Ma, T., Yan, Y., Xie, X., Abass, O.K., Liu, C., Zhao, Z., Wang, Z., 2018. Effects of Fe-S-As coupled redox processes on arsenic mobilization in shallow aquifers of Datong Basin, northern China. Environ. Pollut. 237, 28-38.

Zhang, J., Zhao, S., Xu, Y., Zhou, W., Huang, K., Tang, Z., Zhao, F.-J., 2017. Nitrate stimulates anaerobic microbial arsenite oxidation in paddy soils. Environ. Sci. Technol. 51, 4377-4386.

Zhang, S.-Y., Zhao, F.-J., Sun, G.-X., Su, J.-Q., Yang, X.-R., Li, H., Zhu, Y.-G., 2015. Diversity and abundance of arsenic biotransformation genes in paddy soils from southern China. Environ. Sci. Technol. 49, 4138-4146.

Zhu, Y.-G., Sun, G.-X., Lei, M., Teng, M., Liu, Y.-X., Chen, N.-C., Wang, L.-H., Carey, A., Deacon, C., Raab, A., 2008. High percentage inorganic arsenic content of mining impacted and nonimpacted Chinese rice. Environ. Sci. Technol. 42, 5008-5013.

7.8. Supplementary data

The effect of the sMFC on the accumulation of arsenic in rice plant parts

Table S 7.1 Selected properties of the fresh soils.

Soils Texture	Fe(g/kg)	As (mg/kg)	TOC (g/kg)
Sandy loam	38.2±1.2	44.8±3.5	21.2±07

Notes: Fe, soil total iron, As, soil total arsenic, TOC, total organic carbon. The values represent the mean ±standard error of four replicate samples.

Table S 7.2 As and Fe speciation in the soil porewater on day 110.

Sample ID	As(III) (µg/L)	As(V) (µg/L)	Fe(II) (mg/L)	Fe(III) (mg/L)
sMFC-T	30.6±1.1	13.1±0.5	28.3±3.8	12.2±1.7
sMFC-M	30.1±1.2	9.0±0.4	24.4±4.3	10.2±1.9
sMFC-B	39.9±1.8	4.3±0.2	35.8±3.6	15.4±1.5
Control-T	45.9±1.7	11.5±0.4	18.2±2.3	2.4±0.2
Control-M	60.0±2.2	7.4±0.3	30.5±5.5	4.0±0.9
Control-B	66.1±3.0	7.3±0.3	25.4±2.7	4.0±0.9

Notes: T, M and A: represents samples collected from anode 1, anode 2 and anode 3 vicinity respectively. The values represent the mean ±standard error of nine replicate samples.

Table S 7.3 Similarity-based OTUs and species richness and diversity estimates.

Sample ID	OUTs	ACE	Chao1	Shannon index	Simpson	Good's Coverage (%)
sMFC-Rh	546±66	617±23.0	610±34.7	7.20±0.7	0.98±0	99.8±0
sMFC-A	616±4	645±4.7	657±5.7	7.65±0.1	0.99±0	99.8±0
Control-Rh	527±15	600±13.7	609±16.6	7.70±0.1	0.99±0	99.8±0
Control-A	584±13	611±14.3	619±16.5	7.78±0.1	0.99±0	99.8±0

Notes: OTUs, The operational taxonomic units were defined with 3% dissimilarity. Rh and A: represents samples collected from rhizosphere and anodes vicinity respectively.

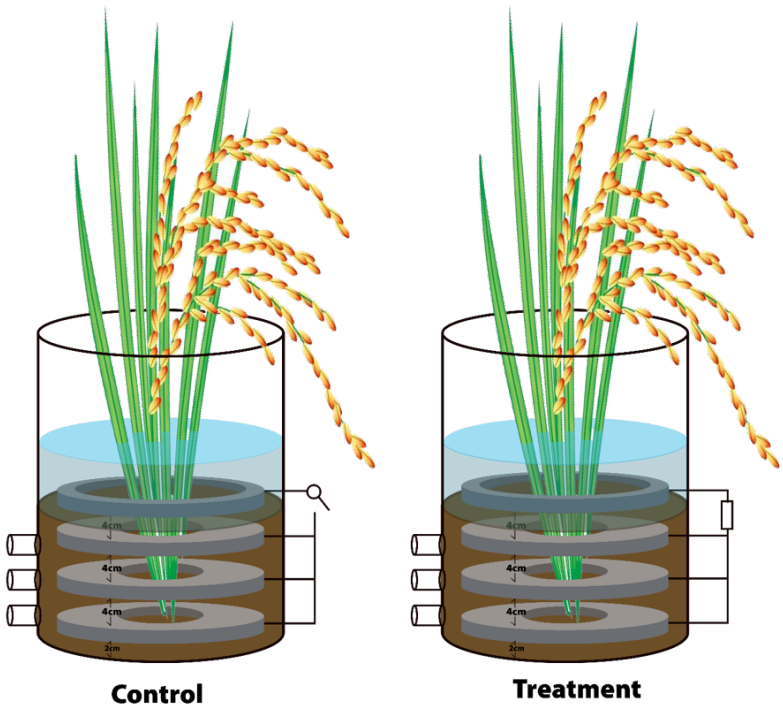

Figure S 7.1 Schematic diagram of soil microbial fuel cells

Chapter 8 : The effect of the sMFC on the accumulation of other trace heavy metal in rice plant parts

8.1. Abstract

The increase in toxic heavy metal pollutants in rice paddies threaten food safety and poses a serious health hazard. Therefore, there is an increasing need for low-cost remediation technology for decreasing the mobility and bioavailability of these trace metals. In this study, we showed that the application of the soil microbial fuel cell (sMFC) can greatly reduce the accumulation of Cd, Cu, Cr and Ni in the rice plant parts. In the sMFC treatment, the accumulation of Cd, Cu, Cr and Ni in rice grains were 35.1%, 32.8%, 56.9% and 21.3% lower, respectively, than the control. The reduction of these elements in the rice grain was due to their limited mobility into the soil porewater of the soils there were equipped with the sMFC. The restriction in Cd, Cu, Cr and Ni bioavailability was ascribed to the sMFC ability to immobilize trace metals through both biotic and abiotic means. The results suggest that the sMFC may be used as a promising technique to limit toxic trace metal bioavailability and translocation in the rice plants.

8.2. Introduction

Paddy fields are important ecosystems that provide more than half of the world's caloric intake (Zhu et al., 2008). However, an increasing amount of paddy soils are contaminated with heavy metals (Liu et al., 2016; Zeng et al., 2015; Zhao et al., 2014). Heavy metal contamination in rice paddy soil is of growing concern since these toxic metals has potential adverse effect on the food chain and subsequently public health (He et al., 2019; Mao et al., 2019). Cadmium (Cd), copper (Cu), nickel (Ni) and chromium (Cr) has all been shown to induce a variety of serious health effects and reduction in agricultural yield (Adrees et al., 2015; Liu et al., 2018b; Ramzani et al., 2016; Zhang et al., 2014). Cadmium, in particular has been associated with renal and lung failure (Järup and Åkesson, 2009; Zukowska and Biziuk, 2008), while Cu, Cr and Ni can affect a number of physiological processes in plant which results in the retardation of plant growth and yield (Adrees et al., 2015; Gardea-Torresdey et al., 2004; Liu et al., 2018b; Ramzani et al., 2016). Heavy metal pollutants, unlike organic pollutants are not biodegradable and tend to persist in the soil environment for long periods (Ahemad, 2012). However, the toxicity of these harmful metals are strongly dependent on their redox state and bioavailability for plant uptake (Violante et al., 2010). For example, Cr (VI) is a known carcinogen and is highly bioavailable in the soil. However, the reduce form Cr(III) is sparingly bioavailable and less toxic (Bhattacharyya et al., 2005). Hence, there is an urgent need to develop cost-effective techniques to limit the bioavailability and remediate toxic heavy metal pollutants in soil.

Numerous conventional soil cleaning technologies such as soil washing, electrokinetic extraction and soil excavation have many drawbacks such as the production of secondary pollutants (Liu et al., 2018c; Yao et al., 2012). Recently, soil microbial fuel cell (sMFC), which are a type of bioelectrochemical cells (Kaku et al., 2008; Schamphelaire et al., 2008) appears to be a promising technology that may be applied to either immobilize and/or the extract metal contaminates from the soil matrix (Chen et al., 2015; Gustave et al., 2018a; Gustave et al.,

2018b; Hong et al., 2010; Hong and Gu, 2009; Wu et al., 2018a). The sMFC employs the soil's anode respiring bacteria to convert chemical energy stored in the organic matter into electrical energy (Kaku et al., 2008; Schamphelaire et al., 2008). The anode of the sMFC serves as an electron acceptor and the electrons deposited onto the anode flow through a conductive material and a resistor to the cathode where they combine with protons and oxygen to form water. The two distant reactions that occurs in the sMFC anode and cathode chamber can greatly influence soil biotic and abiotic properties (Gustave et al., 2018b). For example, the sMFC can decrease the soil organic matter content, change the soil pH, and alters the soil functional microbial community (Hong et al., 2009; Touch et al., 2017).

Based on these characteristics the sMFC have been applied for soil remediation in a few studies recently (Abbas et al., 2017b; Chen et al., 2015; Wang et al., 2015; Zhang et al., 2012). The sMFC has been employed to limit the bioavailability of numerous redox sensitive heavy metals and metalloids such as arsenic (As), iron (Fe), uranium (U) and Cr (Gregory and Lovley, 2005; Li and Yu, 2015; Wang et al., 2015). Previous studies have demonstrated the ability of the sMFC to significantly reduce soil porewater As and Fe (Abbas et al., 2017a; Gustave et al., 2018a). Moreover, the sMFC has also been employed to significantly decrease Cr in the porewater (Habibul et al., 2016b). In addition to influencing redox sensitive metals that sMFC can also produce the energy that is needed to propel heavy metals out of the soil matrix (Chen et al., 2015; Gustave et al., 2018b; Habibul et al., 2016a). In a recent study the sMFC was used for the *in-situ* electrokinetic remediation of soil toxic heavy metals. It was observed that the sMFC can produce the energy required to remove 37% and 15.1% of lead (Pb) and zinc (Zn) from the soil after 100 days of operation (Song et al., 2018).

However, to the best of the authors' knowledge, no investigation has been made on the effect of the sMFC on heavy metal translocation in plants. Therefore, based on the above studies, we hypothesis that the sMFC can be potentially applied to directly or indirectly reduce

the bioavailability toxic trace metals in the soil porewater and subsequently limit their uptake by plant. Hence, in this study we investigated the application of the sMFC in reducing the accumulation of Cd, Cu, Cr and Ni in the rice plants parts.

8.3. Materials and Methods

8.3.1. Paddy Soil Sample

The paddy soil was sampled from a field located in Shaoguan, Guandong Province (N25.638. E113.3841). The total carbon, Cd, Cu, Cr and Ni concentrations were measured to be 21.2 ±0.7 g/kg, 3.4 ±0.3 mg/kg, 78.6 ±2.2 mg/kg, 177.7 ±8.5 mg/kg and 67.7 ±3.4 mg/kg.

8.3.2. Soil Microbial Fuel Cell Assembly

The sMFCs (18 reactors) were assembled in individual cylindrical polyvinylchloride pots (16 cm diameter × 30 cm depth) with three anodes and three sampling valve ports located adjacent to each anode. Each sampling valve port was equipped with a Rhizon soil moisture sampler. Circular carbon felts were cut into two halves and then the two halves were rejoined 1 cm apart with a titanium (Ti) wire were as the anodes. The total surface are of each anode were 850 cm^2. Rectangular shaped carbon felts (706.9 cm^2) was used as the cathodes. In each sMFC 3kg of soil that was previously amended with basal fertilizers (Khan et al., 2013) was added in each pot. Anode 1 of the sMFC was buried 2 cm above the bottom of the pot with 4cm of soil. Then anode 2 was added and buried with another 4 cm of soil. The remaining soil was used to bury anode 3 and the cathode was place vertically in the overlaying water. The soil layer between anode 3 and the cathode was 4 cm thick. Of the 18 sMFCs nine were connected to a 500Ω external resister (treatment) from day 0 to day 110 and then the 500Ω external resistor was replaced with a 100 Ω external resister until the end of the incubation period. The remaining reactors were not connected to any external resisters (control). It should be noted that all of the anodes in each individual sMFC reactors were connected together with Ti wire and operated as a single anode. The voltage between the anode and the cathode were recorded

using a data logger (USB-7660B, ZTIC, China) from day 0-38 and then a Digital Multimeters (UNI-T UT71E) was used to record the voltage every 24 hours until the end of the incubation period.

8.3.3. Preparation of Rice Seedlings

The rice seeds (*Oryza sativa* YLY) were disinfected with 30% H_2O_2 and were germinated on perlite until the 4-leaf stage. Then three uniformly geminated seedlings were the transplanting to each sMFCs reactor. The plants and reactors were firstly incubated in a plant cultivating room (25 °C and 12h light (1200 Lux) /12 h dark) for 38 days before being transferred to a greenhouse with natural day-night cycles and ambient temperature. The sMFC was allowed to dry prior to harvesting the rice plants.

8.3.4. Chemical Analysis

The soil porewater (5ml) was collected with a Rhizon soil moisture sampler under negative pressure using syringe. Prior to sampling, 100 µl of 2M hydrochloric acid was added in each syringe to acidify the sample and prevent precipitation. Soil pH and Eh were measured on the final sampling day. All of the analysis were conducted according to the methods descried in chapter 2.

8.3.5. Plant Samples Analysis

At the end of the grain maturity, sample of the grain, husk, leaves, stem and roots were collected. The plant parts were dried, grinded and digested following the technique in chapter 2. The total concentrations of Cd, Cu, Cr and Ni were determined by ICPMS.

8.3.6. Microbial Community Analysis

On the final incubation day soil samples were collected from the anodes vicinity and rhizosphere from four of the sMFC reactors. The anode soil samples from each individual sMFC were combined to form one composite (four composite anode samples in total). According to the manufacturer protocol, DNA was extracted from 0.25g of each sample using

a HiPure Soil DNA isolation Kit (Magen, China). The quality of the extracted DNA was assessed via gel electrophoresis (1% agarose) and the DNA quantity was determined by a Nanodrop ND-1000 UV–vis spectrophotometer (NanoDrop Technologies, Wilmington, DE, USA). The universal forward primer 347F (5'-CCTACGGRRBGCASCAGKVRVGAAT-3') and reverse primers 802R (5'-GGACTACNVGGGTWTCTAATCC-3') (Li et al., 2017b) with the incorporation of sequencing adapters were applied to amplified the V4-V5 region of the bacterial and archaea 16S rRNA genes. Illumina sequencing and the library preparations were outsourced to GENEWIZ, Inc., Suzhou, China. Details for Illumina sequencing, experimental steps and data analyses are described in Chapter 2.

8.3.7. Nucleotide sequence accession number

The 16S rRNA sequencing reads have been submitted to NCBI GeneBank database with accession number MK235250 - MK235990.

8.4. Results and Discussion

8.4.1. Current generation and power output

Figure 8.1 shows the average current variation in the sMFCs over the incubation period. The current increase rapidly from day 0 without any lag time and reached a maximum current output of ~1.20 mA during the course of the experiment. The rapid increase in the current output of the sMFC can be attributed to the establishment of the anode respiring bacteria on the anode and the abundance of organic matter in the soil porewater (Mohan et al., 2008; Rismani-Yazdi et al., 2011). The fluctuation observed in the current over time was probably caused by oxygen influx into the anode compartment from the rice roots (Liu et al., 2018a; Lu et al., 2015). Previous studies have reported that the oxygen lost from roots can negatively impact the current output of the sMFC since it creates oxic condition in the anode vicinity (Liu et al., 2018a; Lu et al., 2015).

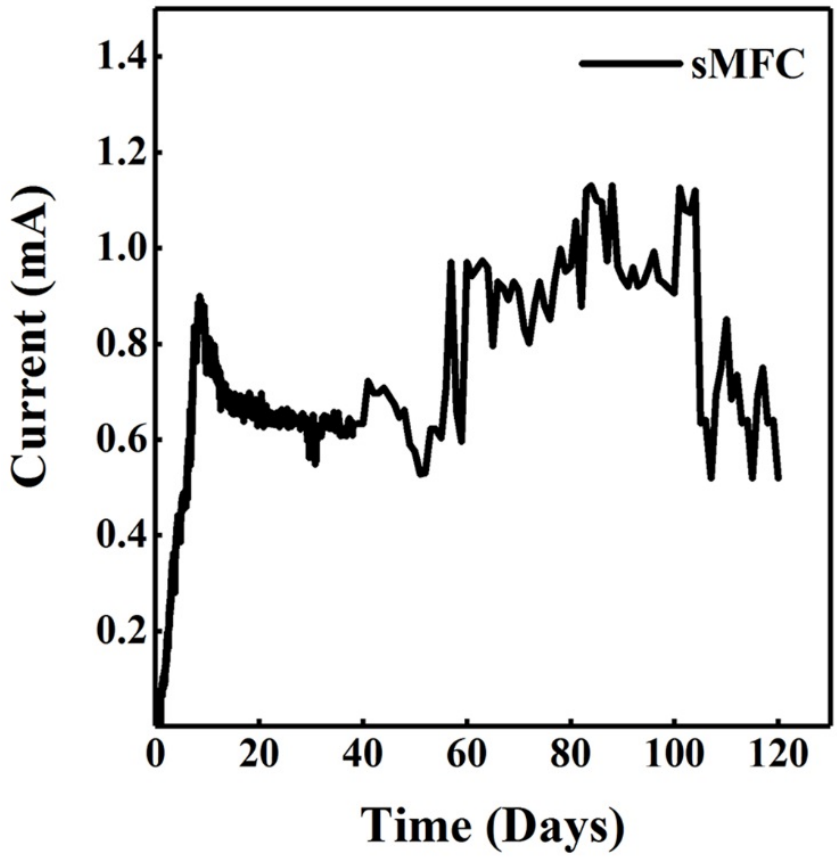

Figure 8.1 Current variation overtime.

The rapid decrease in the current that occurred on day 110 was due to replacement of the 500Ω with a 100Ω external resister. Studies have shown that the decrease of external resistance increase microbial metabolic breakdown rate of organic matter (Pitts et al., 2003; Yu et al., 2017) and this could have resulted in the decrease in current due to lack of electron donors in the anode vicinity. The maximum power density of the sMFC was 22.2 ±1.6 mW/m^2. The current and power density obtained here are comparable to the results obtained in the previously published works where the sMFC was used to alleviate soil of trace metal pollutants (Song et al., 2018; Habibul et al., 2016a).

8.4.2. Change is soil porewater metal concentrations

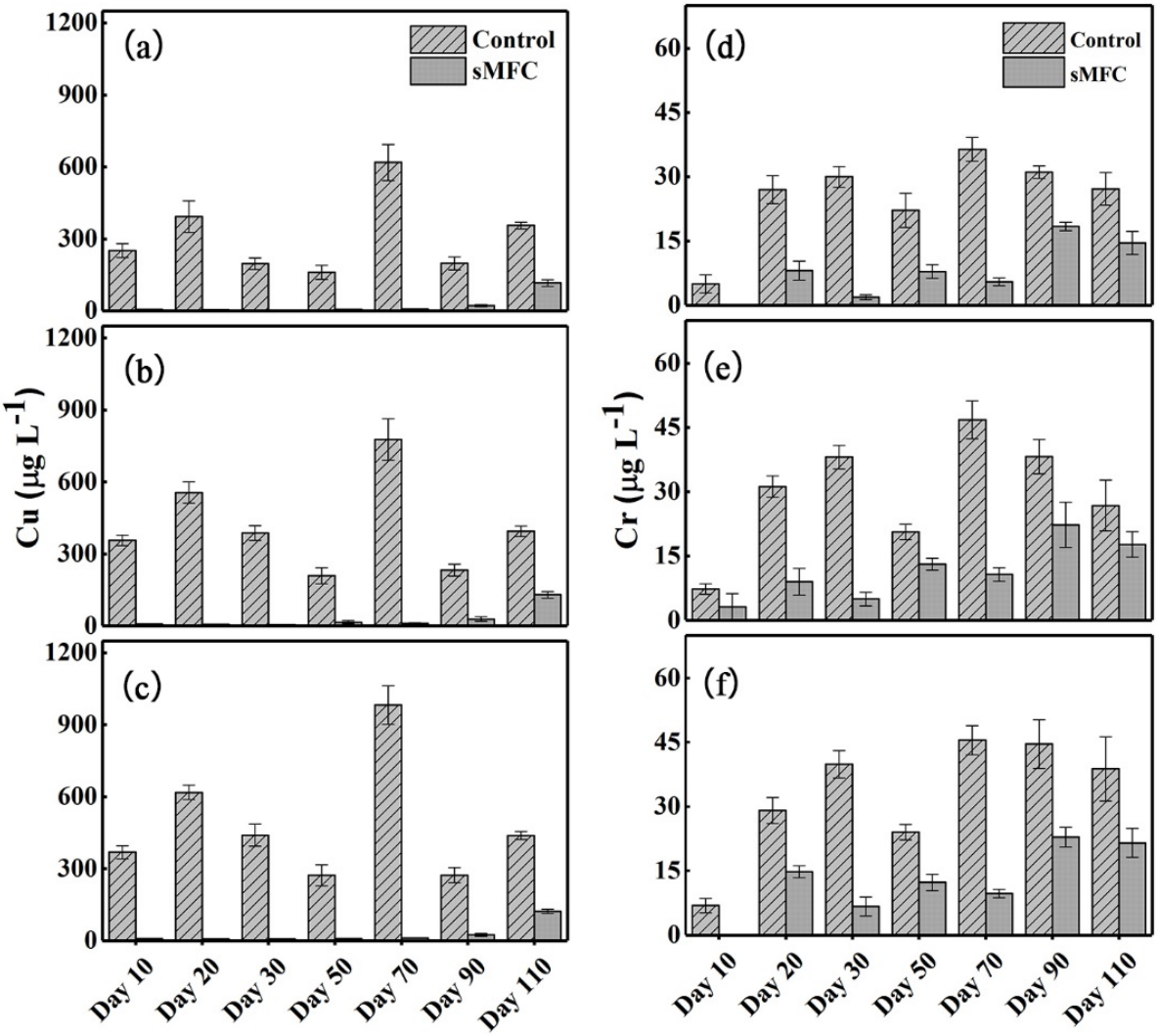

Figure 8.2 Variations in Cu and Cr concentration in the sMFC and control treatment. Panels a, b and c show Cu concentrations in the top, middle and bottom layers, respectively. Panels d, e and f show Cr concentrations in the top, middle and bottom layers, respectively.

The change in soil porewater Cu and Cr in the vicinity of the anode are shown in Fig. 8.2a-f. The trace metals were significantly affected by the sMFC operation. The concentrations of both Cu and Cr were lower in the sMFC compared to the control in all of the sampling points. On day 110 the concentration of Cu was 67.1-72.2% lower in the sMFC compared to the control and that of Cr was 41.4-46.7% less in the sMFC soil porewater. Similar to Cu and Cr, the Ni concentration in sMFC was also significantly reduced in the sMFC porewater compared to the

control (Fig. S 8.1). The concentration of Ni was 48.1-64.0% lower in the sMFC. Different from Cu, Cr and Ni, Cd was only detected in the sMFC and control porewater on day 10. However on day 10 the concentration of Cd in the sMFC porewater was 31.0-56.8% less than that of the control. The reason for the lack of Cd in the soil porewater after day 10 was due to the fact that Cd is not mobile under anaerobic conditions. Under sulfur reducing condition Cd tend to precipitate with the reduced sulfur to form CdS which has low solubility in water (Qiao et al., 2018).

The reduction in trace metals in the sMFC soil porewater can be achieved through both biotic and abiotic pathways. Previous studies have shown that the sMFC can produce an electric field that can drive the migration Cu ions from the bulk soil to the cathode area where the Cu ions may react with oxygen and precipitate as CuO and Cu_2O(Abbas et al., 2018; Wang et al., 2016; Wu et al., 2017). Furthermore, other studies has also shown that the anode respiring microbes' biofilm can absorb Cu ions (Li et al., 2017a). In our study the concentration of Cu was significantly reduce in the porewater of the sMFC, however the Cu concentration in the rhizosphere soil of the sMFC (61.4 ±1.6 mg/Kg) was higher than that of the control (58.8 ±1.9 mg/Kg). Moreover, the pH of the sMFC rhizosphere soil was (8.48±0.1) was higher than that of the control (8.03±0.1). The results obtained here suggest the electromigration and precipitation of Cu in the cathode region of the sMFC.

Furthermore, the sMFC enhance the relative abundance of some microbes that have been suggested to be involved in Cu removal. In our study the phyla *Proteobacteria*, *Firmicutes*, *Actinobacteria* and *Chroroflexi* accounted for more than 80% of the bacterial community (Fig. 8.3). The phylum *Actinobacteria* and *Acinobacteria* were observed in higher abundance in the sMFC compared to the control. Members of the phylum *Actinobacteria* and *Acinobacteria* have been shown to be Cu-resistant and capable of removing Cu. At the family level, *Geobacteraceae* (4.0-11.3% vs 1.4-2.7%) was more abundant in the sMFC (Bond D. R et al.,

2002) (Fig. S 8.2). *Geobacter* a member of the family *Geobacteraceae* has been reported to be involved in Cu removal via the interspecific synergism and conductive pili (Bond D. R et al., 2002; Wu et al., 2018b).

Similarly to the soil porewater Cu, the decrease in Cr and Ni bioavailability in the sMFC could be due to electromigration and microbial reduction. Under close circuit condition Cr(VI) can be electrokinetically driven to the cathode chamber of the sMFC and be reduced to Cr(III)(Chen et al., 2015; Habibul et al., 2016b). This may have contributed to the lower soil porewater Cr in the sMFC since Cr(VI) is more soluble than Cr(III) (Miller et al., 2016). Furthermore, the microbial reduction and abortion of Cr by the microbial community could have also contributed to the reduction of Cr in the sMFC porewater. Many studies have demonstrated that the use of microbes to reduce soluble Cr(VI) to relatively insoluble Cr(III) (Daulton et al., 2007; Liu et al., 2011; Miller et al., 2016). In the sMFC the phylum *Proteobacteria* (33.6-40.0%) was more abundant compared to the control (29.1-33.6%). A large proportion of iron-reducing microorganism belongs to the phylum *Proteobacteria* and iron-reducing microorganisms have been shown to direct or indirectly participate in Cr reduction (Liu et al., 2011; Miller et al., 2016). The iron-reducing bacterium *Shewanella oneidensis MR-1* belonging to the *Proteobacteria* clan has been demonstrated to direct reduce Cr(VI) to Cr(III)(Miller et al., 2016). Additionally, the anode respiring microbes can indirectly influence Cr solubility (Liu et al., 2011). The electron transferred to the anode by anode respiring bacteria can travel to the cathode and encourage Cr precipitation by changing the soil pH and/or direct Cr(VI) reduction (Liu et al., 2011). Analysis of the rhizosphere soil showed higher Cr in the sMFC (177.7 ±7.1 mg/Kg) than the control (129.2 ±6.4 mg/Kg). This results suggest the precipitation of Cr in the cathode chamber of the sMFC.

Analogous to Cu removal, Ni removal from the sMFC was probably due to the changes in soil chemistry and electromigration (Antoniadis et al., 2017; Rinklebe and Shaheen, 2017).

In our study, the concentration of Ni in the soil porewater may have decrease due to the electromigration and precipitation of Ni with hydroxides in the sMFC rhizosphere soil. In the sMFC rhizosphere soil both the pH and the Eh (84.4 ±10.6 vs -108 ±19.9) were significantly higher than that of the control and these conditions are favorable for Ni co-precipitation with solid hydroxides (Rinklebe et al., 2016; Moreira et al., 2008). In a previous study it was shown that under elevated Eh conditions, Ni mobility was significantly imped compared to the reducing conditions (Rinklebe et al., 2016). Furthermore, the increase in soil pH have also been reported to favor the precipitation of Ni with solid oxides (Moreira et al., 2008). Moreover, the sMFC anode biofilm could have also absorbed Ni from the soil porewater. Some studies have suggested the precipitation on and abortion of Ni by the anode and anode biofilm respectively (Giannis et al., 2010; Gustave et al., 2018b).

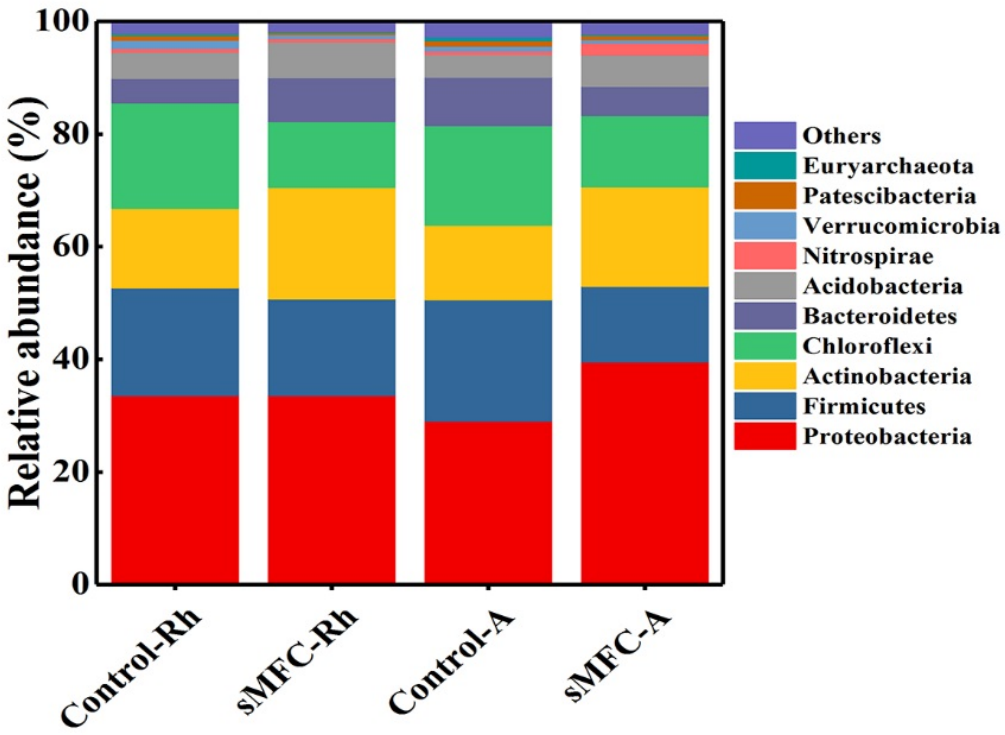

Figure 8.3 Relative abundance of bacterial community composition at the phylum level. The relative abundance values represent the mean of four replicates.

8.4.3. Decrease in Cd, Cu, Cr and Ni accumulation in rice plant tissue

In the present study the results suggest that applying the sMFC can significantly limited the translocation of toxic trace metals into the rice plants. In general, the order of Cd, Cu, Cr and Ni concentrations in the different plant parts followed the order: roots> stems> leaves> husks > grains (Fig. 8.4 a-d). The concertation of Cd, Cu, Cr and Ni were lowest in all the rice grains grown in the sMFC as compared to the control. The Cd, Cu, Cr and Ni concentrations were 35.1%, 32.8%, 56.9% and 21.3% lower, respectively, in the sMFC compared to the control. It is well known that plant roots uptake trace metals from the soil porewater (Antoniadis et al., 2017). Thus, the decrease in the Cd, Cu, Cr and Ni concertation in the sMFC rice grains could be attributed to the decrease of their bioavailability in the soil porewater. Although Cd was below the detection limit during the flooded period in both sMFC and the control, Cd was detected in the rice grains. The accumulation of Cd in rice grains have been shown to occur during the drying period prior to harvesting (Hu et al., 2013). In this study we dried the soil prior to harvest and it is believed that during that time the plants accumulated the Cd. However, the higher pH in the rhizosphere soil of the sMFC limited the Cd accumulation in the rice grains grown in the sMFC soil. Previous studies have shown that Cd solubility reduces with increasing soil pH (Houben et al., 2013; Qiao et al., 2018). The higher trace metal accumulation in the roots suggest that the trace metal translocation to above-ground parts from the roots was highly regulated. For example, Cr translocation from roots to above-ground plant parts have been shown to be significantly impede in the root vacuoles.

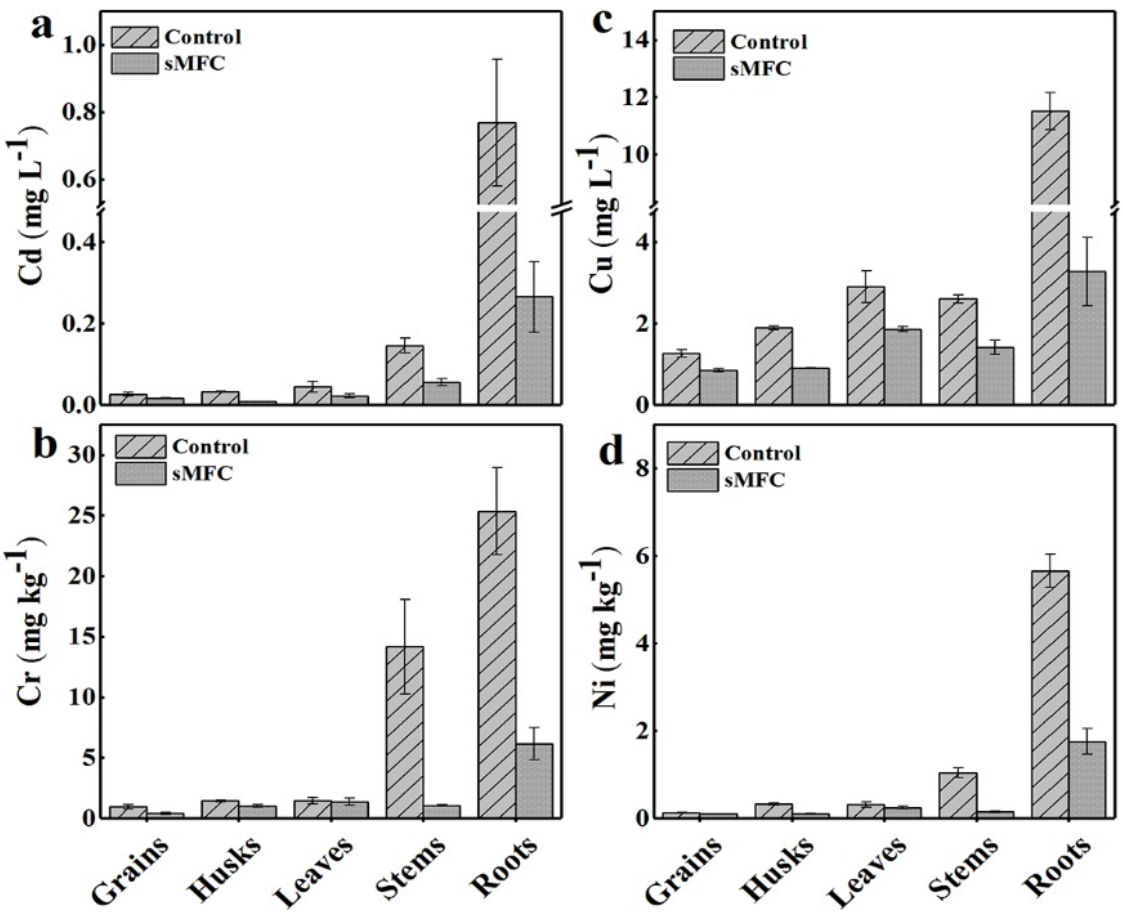

Figure 8.4 The concentrations of Cd (a), Cr (b), Cu (c) and Ni (d) in the rice parts at maturation.

8.5. Conclusions

The bioavailability of trace metals in soil can be limited by applying the sMFC. The sMFC employs both biotic and abiotic means to reduce the mobility of heavy metals into the soil porewater. In this study we showed that the sMFC can be used to significantly reduce the accumulation Cd, Cu, Cr and Ni the in rice grains while simultaneously producing electricity. The Cd, Cu, Cr and Ni concentrations were between 21.3-56.9% lower in the sMFC compared to the treatment. These results imply that the sMFC can be a promising technique to limit toxic trace metal bioavailability and translocation in rice plants. However is should be noted that the concentrations of Cd, Cu, Cr and Ni in the plant tissues were not standardized to the mass of the whole plants.

8.6. References

Abbas, S.Z., Rafatullah, M., Ismail, N., Nastro, R.A., 2017a. Enhanced bioremediation of toxic metals and harvesting electricity through sediment microbial fuel cell. Int. J. Energy Res. 41, 2345-2355.

Abbas, S.Z., Rafatullah, M., Ismail, N., Shakoori, F.R., 2018. Electrochemistry and microbiology of microbial fuel cells treating marine sediments polluted with heavy metals. Rsc Adv. 8, 18800-18813.

Abbas, S.Z., Rafatullah, M., Ismail, N., Syakir, M.I., 2017b. A review on sediment microbial fuel cells as a new source of sustainable energy and heavy metal remediation: mechanisms and future prospectiveInt. J. Energy Res. 41, 1242-1264.

Adrees, M., Ali, S., Rizwan, M., Ibrahim, M., Abbas, F., Farid, M., Zia-ur-Rehman, M., Irshad, M.K., Bharwana, S.A., 2015. The effect of excess copper on growth and physiology of important food crops: a review. Environ. Sci. Pollut. Res. 22, 8148-8162.

Ahemad, M., 2012. Implications of bacterial resistance against heavy metals in bioremediation: a review. J. Instit. . Integ. Omics App. Biotech. 3.

Antoniadis, V., Levizou, E., Shaheen, S.M., Yong, S.O., Sebastian, A., Baum, C., Prasad, M.N.V., Wenzel, W.W., Rinklebe, J., 2017. Trace elements in the soil-plant interface: Phytoavailability, translocation, and phytoremediation–A review. Earth-Sci. Rev. 171, 621-645.

Bhattacharyya, P., Chakraborty, A., Chakrabarti, K., Tripathy, S., Powell, M., 2005. Chromium uptake by rice and accumulation in soil amended with municipal solid waste compost. Chemosphere 60, 1481-1486.

Bond D. R, Holmes D. E, Tender L. M, R, L.D., 2002. Electrode reducing microorganisms that harvest energy from marine sediments. Science 295, 483–485.

Chen, Z., Zhu, B.-K., Jia, W.-F., Liang, J.-H., Sun, G.-X., 2015. Can electrokinetic removal of metals from contaminated paddy soils be powered by microbial fuel cells? Environ. Techn. Innov. 3, 63-67.

Daulton, T.L., Little, B.J., Jones-Meehan, J., Blom, D.A., Allard, L.F., 2007. Microbial reduction of chromium from the hexavalent to divalent state. Geochim. Cosmochim. Acta 71, 556-565.

Gardea-Torresdey, J., Peralta-Videa, J., Montes, M., De la Rosa, G., Corral-Diaz, B., 2004. Bioaccumulation of cadmium, chromium and copper by Convolvulus arvensis L.: impact on plant growth and uptake of nutritional elements. Bioresour. Technol. 92, 229-235.

Giannis, A., Pentari, D., Wang, J.Y., Gidarakos, E., 2010. Application of sequential extraction analysis to electrokinetic remediation of cadmium, nickel and zinc from contaminated soils. J. Hazard. Mater. 184, 547-554.

Gregory, K.B., Lovley, D.R., 2005. Remediation and recovery of uranium from contaminated subsurface environments with electrodes. Environ. Sci. Technol. 39, 8943-8947.

Gustave, W., Yuan, Z.-F., Sekar, R., Chang, H.-C., Zhang, J., Wells, M., Ren, Y.-X., Chen, Z., 2018a. Arsenic mitigation in paddy soils by using microbial fuel cells. Environ. Pollut. 238, 647-655.

Gustave, W., Yuan, Z.-F., Sekar, R., Ren, Y.-X., Chang, H.-C., Liu, J.-Y., Chen, Z., 2018b. The change in biotic and abiotic soil components influenced by paddy soil microbial fuel cells loaded with various resistances. J. Soils Sediments, 1-10.

Habibul, N., Hu, Y., Sheng, G.P., 2016a. Microbial fuel cell driving electrokinetic remediation of toxic metal contaminated soils. J. Hazard Mater. 318, 9-14.

Habibul, N., Hu, Y., Wang, Y.K., Chen, W., Yu, H.Q., Sheng, G.P., 2016b. Bioelectrochemical Chromium(VI) Removal in Plant-Microbial Fuel Cells. Environ. Sci. Technol. 50, 3882-3889.

He, M., Shen, H., Li, Z., Wang, L., Wang, F., Zhao, K., Liu, X., Wendroth, O., Xu, J., 2019. Ten-year regional monitoring of soil-rice grain contamination by heavy metals with implications for target remediation and food safety. Environ. Pollut. 244, 431-439.

Hong, S.W., Chang, I.S., Choi, Y.S., Kim, B.H., Chung, T.H., 2009. Responses from freshwater sediment during electricity generation using microbial fuel cells. Bioprocess Biosyst. Eng. 32, 389-395.

Hong, S.W., Kim, H.S., Chung, T.H., 2010. Alteration of sediment organic matter in sediment microbial fuel cells. Environ. Pollut. 158, 185-191.

Hong, Y., Gu, J., 2009. Bacterial anaerobic respiration and electron transfer relevant to the biotransformation of pollutants. Int. Biodeterior. Biodegradation. 63, 973-980.

Houben, D., Evrard, L., Sonnet, P., 2013. Mobility, bioavailability and pH-dependent leaching of cadmium, zinc and lead in a contaminated soil amended with biochar. Chemosphere 92, 1450-1457.

Hu, P., Huang, J., Ouyang, Y., Wu, L., Song, J., Wang, S., Li, Z., Han, C., Zhou, L., Huang, Y., 2013. Water management affects arsenic and cadmium accumulation in different rice cultivars. Environ. Geochem. Health 35, 767-778.

Järup, L., Åkesson, A., 2009. Current status of cadmium as an environmental health problem. Toxicol. Appl. Pharmacol. 238, 201-208.

Kaku, N., Yonezawa, N., Kodama, Y., Watanabe, K., 2008. Plant/microbe cooperation for electricity generation in a rice paddy field. Appl. Microbiol. Biotechnol. 79, 43-49.

Khan, S., Chao, C., Waqas, M., Arp, H.P.H., Zhu, Y.-G., 2013. Sewage sludge biochar influence upon rice (Oryza sativa L) yield, metal bioaccumulation and greenhouse gas emissions from acidic paddy soil. Environ. Sci. Technol. 47, 8624-8632.

Li, W., Yu, H., 2015. Stimulating sediment bioremediation with benthic microbial fuel cells. Biotechnol. Adv. 33, 1-12.

Li, X., Mu, S., Ren, Y., Wang, X., 2017a. Behavior of copper in membrane-less sediment microbial fuel cell. J. Renew. Sustain. Energy 9, 023103.

Li, Y., Hu, X., Yang, S., Zhou, J., Zhang, T., Qi, L., Sun, X., Fan, M., Xu, S., Cha, M., 2017b. Comparative Analysis of the Gut Microbiota Composition between Captive and Wild Forest Musk Deer. Front. Microbiol. 8, 1705.

Liu, B., Ji, M., Zhai, H., 2018a. Anodic potentials, electricity generation and bacterial community as affected by plant roots in sediment microbial fuel cell: Effects of anode locations. Chemosphere.

Liu, G., Wang, J., Zhang, E., Hou, J., Liu, X., 2016. Heavy metal speciation and risk assessment in dry land and paddy soils near mining areas at Southern China. Environ. Sci. Pollut. Res. Int. 23, 8709-8720.

Liu, J., Simms, M., Song, S., King, R.S., Cobb, G.P., 2018b. Physiological Effects of Copper Oxide Nanoparticles and Arsenic on the Growth and Life Cycle of Rice (Oryza sativa japonica 'Koshihikari'). Environ. Sci. Technol. 52, 13728-13737.

Liu, L., Li, W., Song, W., Guo, M., 2018c. Remediation techniques for heavy metal-contaminated soils: principles and applicability. Sci. Total Environ. 633, 206-219.

Liu, L., Yuan, Y., Li, F.-b., Feng, C.-h., 2011. In-situ Cr (VI) reduction with electrogenerated hydrogen peroxide driven by iron-reducing bacteria. Bioresour. Technol. 102, 2468-2473.

Lu, L., Xing, D., Ren, Z.J., 2015. Microbial community structure accompanied with electricity production in a constructed wetland plant microbial fuel cell. Bioresour. Technol. 195, 115-121.

Mao, C., Song, Y., Chen, L., Ji, J., Li, J., Yuan, X., Yang, Z., Ayoko, G.A., Frost, R.L., Theiss, F., 2019. Human health risks of heavy metals in paddy rice based on transfer characteristics of heavy metals from soil to rice. Catena 175, 339-348.

Miller, R.B., Giai, C., Iannuzzi, M., Monty, C.N., Senko, J.M., 2016. Microbial reduction of Cr (VI) in the presence of chromate conversion coating constituents. Biodegrad. J. 20, 174-182.

Mohan, S.V., Mohanakrishna, G., Reddy, B.P., Saravanan, R., Sarma, P., 2008. Bioelectricity generation from chemical wastewater treatment in mediatorless (anode) microbial fuel cell (MFC) using selectively enriched hydrogen producing mixed culture under acidophilic microenvironment. Biochem. Eng. J. 39, 121-130.

Moreira, C.S., Casagrande, J.C., Alleoni, L.R.F., de Camargo, O.A., Berton, R.S., 2008. Nickel adsorption in two Oxisols and an Alfisol as affected by pH, nature of the electrolyte, and ionic strength of soil solution. J. Soils and Sediments 8, 442-451.

Pitts, K., Dobbin, P.S., Reyesramirez, F., Thomson, A.J., Richardson, D.J., Seward, H.E., 2003. Characterization of the Shewanella oneidensis MR-1 Decaheme Cytochrome MtrA expression in *Escherichia Coli* confers the ability to reduce soluble Fe(III) chelates. J. Biol. Chem. 278, 27758-27765.

Qiao, J.T., Liu, T.X., Wang, X.Q., Li, F.B., Lv, Y.H., Cui, J.H., Zeng, X.D., Yuan, Y.Z., Liu, C.P., 2018. Simultaneous alleviation of cadmium and arsenic accumulation in rice by applying zero-valent iron and biochar to contaminated paddy soils. Chemosphere 195, 260-271.

Ramzani, P.M.A., Iqbal, M., Kausar, S., Ali, S., Rizwan, M., Virk, Z.A., 2016. Effect of different amendments on rice (Oryza sativa L.) growth, yield, nutrient uptake and grain quality in Ni-contaminated soil. Environ. Sci. Pollut. R. 23, 18585-18595.

Rinklebe, J., Antić-Mladenović, S., Frohne, T., Stärk, H.-J., Tomić, Z., Ličina, V., 2016. Nickel in a serpentine-enriched Fluvisol: redox affected dynamics and binding forms. Geoderma 263, 203-214.

Rinklebe, J., Shaheen, S.M., 2017. Redox chemistry of nickel in soils and sediments: A review. Chemosphere 179, 265-278.

Rismani-Yazdi, H., Christy, A.D., Carver, S.M., Yu, Z., Dehority, B.A., Tuovinen, O.H., 2011. Effect of external resistance on bacterial diversity and metabolism in cellulose-fed microbial fuel cells. Bioresour Technol. 102, 278-283.

Schamphelaire, L.D., Bossche, L.V.d., Dang, H.S., Höfte, M., Boon, N., Rabaey, K., Verstraete, W., 2008. Microbial Fuel Cells Generating Electricity from Rhizodeposits of Rice Plants. Environ. Sci. Technol. 42, 3053-3058.

Song, T.S., Zhang, J., Hou, S., Wang, H., Zhang, D., Li, S., Xie, J., 2018. In situ electrokinetic remediation of toxic metal-contaminated soil driven by solid phase microbial fuel cells with a wheat straw addition. J. Chem. Technol. Biotechnol. 93, 2860-2867.

Touch, N., Hibino, T., Morimoto, Y., Kinjo, N., 2017. Relaxing the formation of hypoxic bottom water with sediment microbial fuel cells. Environ.Tech.1-25.

Violante, A., Cozzolino, V., Perelomov, L., Caporale, A., Pigna, M., 2010. Mobility and bioavailability of heavy metals and metalloids in soil environments. J. Soil Sci. Plant Nutr. 10, 268-292.

Wang, C., Deng, H., Zhao, F., 2015. The Remediation of Chromium (VI)-Contaminated Soils Using Microbial Fuel Cells. Soil Sediment Contam. 25, 1-12.

Wang, H., Song, H., Yu, R., Cao, X., Fang, Z., Li, X., 2016. New process for copper migration by bioelectricity generation in soil microbial fuel cells. Environ. Sci. Pollut. Res. Int. 23, 13147-13154.

Wu, M., Xu, X., Zhao, Q., Wang, Z., 2017. Simultaneous removal of heavy metals and biodegradation of organic matter with sediment microbial fuel cells. Rsc Advances 7, 53433-53438.

Wu, Y., Jing, X., Gao, C., Huang, Q., Cai, P., 2018a. Recent advances in microbial electrochemical system for soil bioremediation. Chemosphere.

Wu, Y., Zhao, X., Jin, M., Li, Y., Li, S., Kong, F., Nan, J., Wang, A., 2018b. Copper removal and microbial community analysis in single-chamber microbial fuel cell. Bioresour. Technol. 253, 372-377.

Yang, Y., Zhang, H., Yuan, H., Duan, G., Jin, D., Zhao, F., Zhu, Y., 2018. Microbe mediated arsenic release from iron minerals and arsenic methylation in rhizosphere controls arsenic fate in soil-rice system after straw incorporation. Environ. Pollut. 236, 598-608.

Yao, Z., Li, J., Xie, H., Yu, C., 2012. Review on Remediation Technologies of Soil Contaminated by Heavy Metals. Procedia Environ. Sci. 16, 722-729.

You, J., Wu, G., Ren, F., Chang, Q., Yu, B., Xue, Y., Mu, B., 2016. Microbial community dynamics in Baolige oilfield during MEOR treatment, revealed by Illumina MiSeq sequencing. Appl. Microbiol. Biotechnol. 100, 1469-1478.

Yu, B., Tian, J., Feng, L., 2017. Remediation of PAH polluted soils using a soil microbial fuel cell: Influence of electrode interval and role of microbial community. J. Hazard. Mater. 336, 110.

Zeng, F., Wei, W., Li, M., Huang, R., Yang, F., Duan, Y., 2015. Heavy metal contamination in rice-producing soils of Hunan province, China and potential health risks. Int. J. Environ. Res. Public Health. 12, 15584-15593.

Zhang, C.P., Shan-Shan, C., Guang-Li, L., ZHANG, R.-D., Jian, X., 2012. Characterization of strain Pseudomonas sp. Q1 in microbial fuel cell for treatment of quinoline-contaminated water. Pedosphere 22, 528-535.

Zhang, W.L., Du, Y., Zhai, M.M., Shang, Q., 2014. Cadmium exposure and its health effects: A 19-year follow-up study of a polluted area in China. Sci. Total Environ. 470, 224-228.

Zhao, F.J., Ma, Y., Zhu, Y.G., Tang, Z., McGrath, S.P. 2014. Soil contamination in China: current status and mitigation strategies. Environ. Techn. 49, 750-759.

Zhu, Y., Williams, P., Meharg, A.A., 2008. Exposure to inorganic arsenic from rice: a global health issue? Environ. Pollut. 154, 169-171.

Zukowska, J., Biziuk, M., 2008. Methodological evaluation of method for dietary heavy metal intake. J. Food Sci. 73, R21-29.

8.7. Supplementary data

The effect of the sMFC on the accumulation of other trace heavy metal in rice plant parts

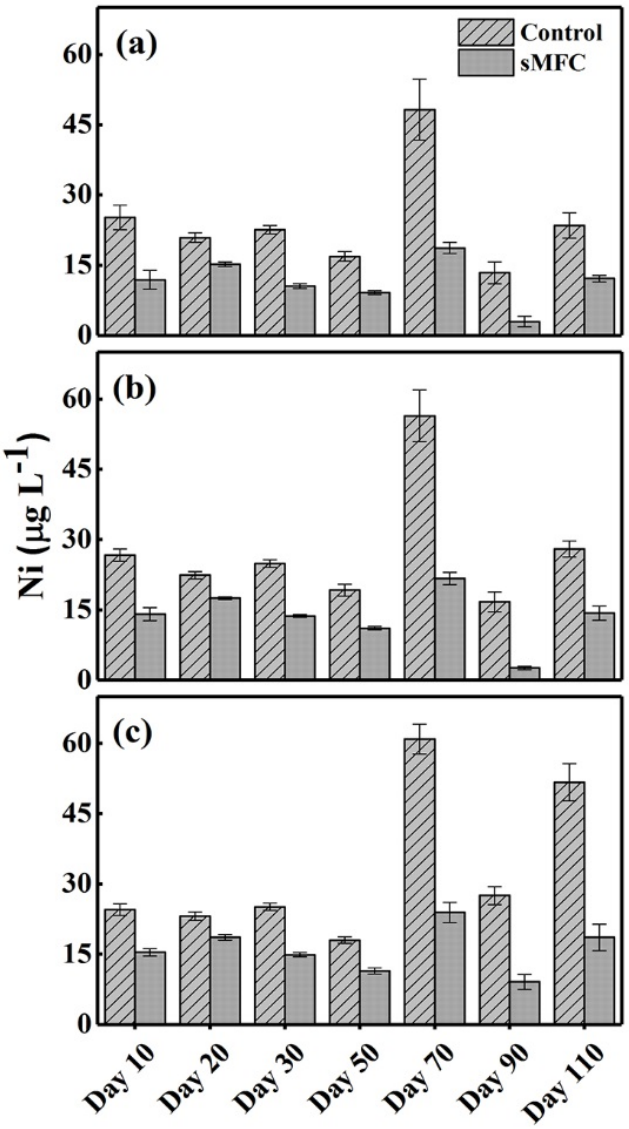

Figure S 8.1 Variations in Ni concentration in the sMFC and control treatment. Panels a, b and c show Ni concentrations in the top, middle and bottom layers, respectively.

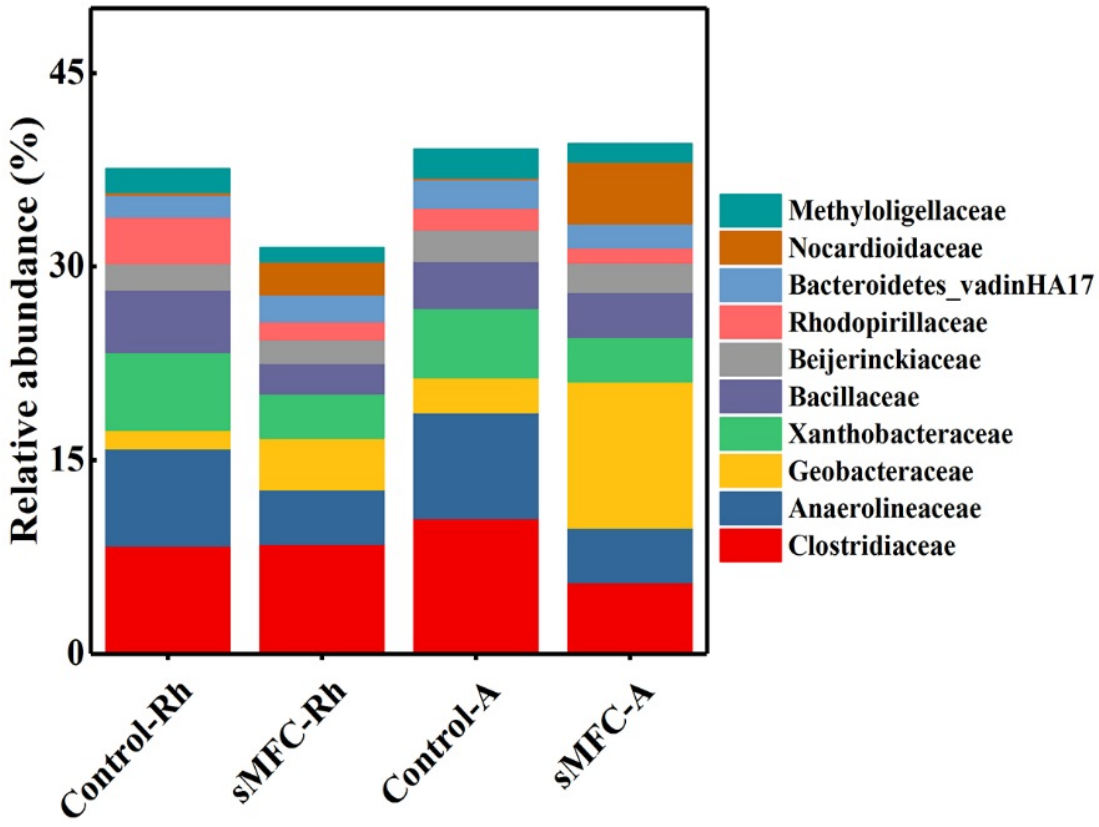

Figure S 8.2 Relative abundance of bacterial community composition at the phylum level. The relative abundance values represent the mean of four replicates.

Chapter 9 : General Discussion, Conclusions and Future Directions

9.1. General Discussion and Conclusions

In this thesis, the influence of the sMFC anode on the paddy soil components and its possible application for trace metal alleviation in rice grains were explored. We showed that the sMFC can significantly influence both the biotic and abiotic components of paddy soils. We also showed that the sMFC could potentially be used as a mitigation strategy to limit trace heavy metals and metalloids mobility in paddy soil, which consequently reduces their accumulation in the rice grains.

Operating the sMFC has been shown to greatly influence the soil microbial community that developed on the anode and the surrounding soil (Lu et al., 2014; Yu et al., 2017; Zhao et al., 2016). In addition to affecting the soil microbial community, the sMFC can also alter the soil physiochemical properties such as Eh, pH and organic matter content (Hong et al., 2009; Touch et al., 2017). These changes in soil properties can play a vital role in the behavior of soil trace metal components. For example, the speciation, bioavailability and toxicity of arsenic is strongly dependent on the soil's pH, Eh and the functional microbial community (Charlatchka and Cambier, 2000; Qiao et al., 2017; Yamaguchi et al., 2011). Although it is well known that the sMFC anode can significantly alter these soil properties, the extent in which the anode influence extends remains unclear (Hong et al., 2009; Hong et al., 2010; Kouzuma et al., 2014; Lu et al., 2014). In chapters 3 and 4, we investigated the influence of the anode on the soil biotic and abiotic components along the soil profile. We also examined the influence of the relic DNA generated from operating the sMFC on the culture independent estimates of the microbial community. Additionally, the influence of the applied external resistor on the soil properties were also studied. The results revealed that the sMFC's anode can influence the

microbial community structure of the bulk soil profile centimeters away and the relic DNA have minimum influence on the culture independent community. Furthermore, in chapter 4 we also illustrated that applying lower external resistance can selectively enhance the anode respiring bacterial community relative abundance and increase the organic matter removal efficiencies while decreasing metal concentration in the soil porewater.

The results obtained in chapters 3 and 4 coincide with the existing literature and offers possible explanation to some of the answered questions. Numerous studies have reported that the relic DNA present in the samples can negatively influence the culture independent estimates of the microbial community (Carini et al., 2016; Dellanno and Corinaldesi, 2004; Morrissey et al., 2015). Others however reported that relic DNA does not significantly obscure the results and lead to misrepresentation (Lennon et al., 2018). Moreover, very few studies have investigated the effect of relic DNA in MFCs (Cerrillo et al., 2017; Dessì et al., 2018) and prior to our study none have investigated relic DNA influence on the sMFC community. In the studies investigating the effect of relic DNA in well buffered double chamber MFCs and MECs the results suggest that the relic DNA hamper the true microbial community structure (Cerrillo et al., 2017; Dessì et al., 2018). However, in our study our results coincide with that of Lennon et al. (2018) suggesting that the relic DNA had minimal influence on the sMFC microbial community estimates. A possible explanation for this was that the microbial community sampled in our sMFC was at a state of equilibrium. Meaning that the rate of cell death and the rate of relic DNA removal was at a steady state (Lennon et al., 2018).

In addition to the influence of relic DNA we also provided insight on the extent in which the sMFC anode can influence the soil microbial community composition. In accordance with Lu et al. (2014), the operation of the sMFC can alter the microbial community at the anode and the bulk soil. However, we provided a more detail insight on why this phenomenon occurs (chapter 3). Our results suggest that the change in the sMFC microbial community was due to

both cathodic and anodic reactions. The reactions occurring at both the anode and cathode can alter the sMFC's soil's pH, Eh, nutrients and organic matter bioavailability which are known determinants of the microbial community structure (Dunaj et al., 2012; Wang et al., 2015; Yuan et al., 2018). In the sMFC the pH near the cathode increases while the pH near the anode significantly decreases. Moreover, operating the sMFC enhances the metabolic actives of electrogens, giving them a competitive edge over other microbial groups such as methanogens (Jung and Regan, 2011; Kouzuma et al., 2014).

Expanding on the results obtained in chapter 3 and of the existing literature (Rismani-Yazdi et al., 2011; Song et al., 2010; Torres et al., 2009), in chapter 4 we showed that tuning the electrode potential by changing the external resistor can significantly influence both the soil biotic and abiotic components of sMFC. Similar to the results obtained in previous studies, changing the external resistor significantly influenced the sMFC performance and the organic matter removal efficiency (Cao et al., 2015; Song et al., 2010). The sMFC equipped with lower external resistor produced higher currents and have higher organic matter removal efficiency than that of those with higher external resistors. This increase in sMFC performance was ascribed to the lower internal resistance observed in the sMFC with smaller external resistors which was consistent with previous studies result (Cao et al., 2015; Song et al., 2010). As a consequence, the high currents in the sMFC with low external resistors also had higher organic matter removal efficiency. This was due to the fact that lower external resistance increase the metabolic activity of anaerobic bacteria by simulating the release enzyme and altering the permeability of anaerobe cell membranes (Pitts et al., 2003; Yu et al., 2017). Different from the previously literature we reported for the first time that changing the external resistance can be used to selectively enhance the relative abundance of electrogenic bacteria in the soil medium. Our result agrees with those obtained from double chamber MFCs (Jung and Regan, 2011; Torres et al., 2009). Furthermore, our results also showed that operating the sMFC also

affected the behavior of the soil porewater iron, arsenic and nickel. Our data also indicated a positive correlation between dissolve iron, arsenic and organic matter.

Therefore in chapters 5 and 6 we focused on the effect of the sMFC anode on the behavior of iron and arsenic mobility into the soil porewater under low and high organic matter paddy soil conditions. In chapter 5 the results showed that the sMFC is able to limit the release of arsenic in to the soil porewater by creating a substrate competition between the bacterial community in the anode vicinity and those in the bulk soil. However, as shown in chapter 6, if the soil organic matter contain is high, the sMFC enhances the reduction of iron and increase the mobility of arsenic into the soil porewater. Nonetheless, this risk is reversible by combining the sMFC with wet-dry cycles. The sMFC combined with wet-dry cycle enhances the mineralizing of organic matter and limits the release of arsenic into the soil porewater (chapter 6). Based on the results obtained in chapters 3-6, we concluded that the sMFC influences was able to limit the release of arsenic by creating a substrate competition between the microbes in the anode vicinity and those in the bulk soil. When soils were equipped with sMFC the dissolved organic matter degradation rate increases and the composition of dissolved organic matter changes to become less humic acid-like. This results in less electron donors and shuttles being available to bacteria in the bulk soil to reduce iron oxide and liberates the arsenic that is coprecipitated with iron oxide into the soil pore water. In addition to preventing iron reduction, the sMFC microbial community can also enhance the oxidation of ferrous iron to ferric iron as a result of changes in soil redox potential (Touch et al., 2017; Wang et al., 2015; Yang et al., 2016).

According to the results obtained in chapters 5 and 6 we showed in chapters 7 and 8 that the application of the sMFC can be extended to reduce the accumulation of trace heavy metals in the rice plant parts. In both of these chapters the sMFC was found to be a promising way to mitigate trace heavy metals and metalloids accumulation in rice tissue and reduce their

dietary exposure, while simultaneously producing electricity. The concentration of arsenic in the rice grains were 68% lower in the sMFC treatment compared to that of the control (chapter 7). Moreover, the rice grown in the sMFC also contained 35.1%, 32.8%, 56.9% and 21.3% less cadmium, cupper, chromium and nickel, respectively in the compered to the control (chapter 8). These results were comparable to those obtained when iron and other metal oxides as sorbents or as an oxidants were employed (Duan et al., 2016; Li et al., 2019; Qiao et al., 2018; Suda and Makino, 2016).

However, the sMFC differs from these other technologies, since the sMFC's anode can serve as an inert and stable sink of electrons. The application of chemical amendments, such as nitrates, metal-oxides and sulfates, although can impeded the release of toxic heavy metals, has many several disadvantages. These amendments only can served for a short period of time, they can lead to the production of secondary pollutants and are not always effective. For example, many studies have shown that the addition of iron and the increase of root iron plaque can increase or have no significant effects on arsenic uptake (Rahman et al., 2013; Syu et al., 2013). It was speculated that this may have occurred because iron can upregulate the phosphate transporters which enhance the uptake of arsenic (Ward et al., 2008) and root iron plaques are less effective in trapping As(III) (Chen et al., 2005). Moreover, although the application of sulfur may limit arsenic mobility in porewater and the translocation of arsenic within rice (Hu et al., 2007), some studies have reported that the application of sulfur (gypsum) to arsenic contaminated soil had limited potential for minimizing arsenic uptake by rice plants (Boye et al., 2017; Chen et al., 2014). These results suggest that even though an amendment can decrease soil porewater arsenic, there are still some instances where their application, in the presence of plants, were ineffective or promote the arsenic uptake.

In the present PhD thesis the effect of the sMFC anode on the soil trace element behavior was studied. Similarly the application of the sMFC as a mitigation technology was

also explored. The results presented in this work show for the first time that operating the sMFC can significantly influence the behavior of paddy soil trace elements and the microbial community along the soil profile. We also showed for the first time that the sMFC can be used as a promising technique to limit toxic trace metal bioavailability and their translocation in the rice plants while simultaneously producing electricity. The data presented here might contribute to the knowledge available on using the BES as a soil heavy metal remediation technology.

9.2. Future Directions

In this thesis we have demonstrated the use of the sMFC for the *in-situ* remediation of both redox and non-redox sensitive toxic heavy metals from soil in lab based experiments, however data from field application of this technique was not collected. Thus, the future research on using sMFC for soil heavy metal remediation should be focused on moving this technology from the lab to field application. However, before the transfer of this technology to field application technical questions such as the following need to be fully address;

1. Which sMFC configuration would be most suitable for maximum area of influence, sMFC performance and field application?
2. Given that soil is complex and the effect of the sMFC on soil heavy metals maybe influence by soil property, can the sMFC be combined with other remediation techniques to improve its efficiency?

To overcome the above challenges associated with the field application of the sMFC, we are proposing the use of “inserting sMFC” with air cathodes. Inserting sMFC will offer some solutions to the challenges linked with laying two pieces of carbon felts as electrode into the wetland. Moreover, the inserting sMFC can also improve the sMFC performance by reducing internal resistance, since the inserting sMFC will eliminate the large spaces between

the two electrodes. Lastly the inserting sMFC will also increase the radius of simulation by the sMFC because it will be inserted vertical into the soil.

In the case of soil with high organic matter content the sMFC can be combine with hematite and goethite which can be used to improve organic matter mineralization and soil conductivity. Moreover, the sMFC can be combine with phytoremediation remediation. Plants that are known to be hyper metal accumulated can be added in the sMFC to improve the removal efficiency of metals from the soil porewater. Therefore in the future, more attention should be paid to the above to facilitate the transfer of the sMFC to field.

9.3. References

Boye, K., Lezama-Pacheco, J., Fendorf, S., 2017. Relevance of Reactive Fe: S Ratios for Sulfur Impacts on Arsenic Uptake by Rice. Channels 8, 11.

Cao, X., Song, H.L., Yu, C.Y., Li, X.N., 2015. Simultaneous degradation of toxic refractory organic pesticide and bioelectricity generation using a soil microbial fuel cell. Bioresour. Technol. 189, 87-93.

Carini, P., Marsden, P.J., Leff, J.W., Morgan, E.E., Strickland, M.S., Fierer, N., 2016. Relic DNA is abundant in soil and obscures estimates of soil microbial diversity. Nat. Microbiol. 2, 16242.

Cerrillo, M., Viñas, M., Bonmatí, A., 2017. Unravelling the active microbial community in a thermophilic anaerobic digester-microbial electrolysis cell coupled system under different conditions. Water Res. 110, 192-201.

Charlatchka, R., Cambier, P., 2000. Influence of reducing conditions on solubility of trace metals in contaminated soils. Water Air Soil Pollut. 118, 143-168.

Chen, X.P., Zhou, J., Lei, Y., He, C., Liu, X., Chen, Z., Bao, P., 2014. The fate of arsenic in contaminated paddy soil with gypsum and ferrihydrite amendments. Int. J. Environ. Pollut. 56, 48-62.

Chen, Z., Zhu, Y.G., Liu, W.J., Meharg, A.A., 2005. Direct evidence showing the effect of root surface iron plaque on arsenite and arsenate uptake into rice (Oryza sativa) roots. New Phytol. 165, 91-97.

Dellanno, A., Corinaldesi, C., 2004. Degradation and Turnover of Extracellular DNA in Marine Sediments: Ecological and Methodological Considerations. Appl. Environ. Microbiol. 70, 4384-4386.

Dessì, P., Porca, E., Haavisto, J., Lakaniemi, A.-M., Collins, G., Lens, P.N., 2018. Composition and role of the attached and planktonic microbial communities in mesophilic and thermophilic xylose-fed microbial fuel cells. Rsc Advances 8, 3069-3080.

Duan, G., Zhang, H., Shen, Y., Li, G., Wang, H., Cheng, W., 2016. Mitigation Of Heavy Metal Accumulation In Rice Grain With Silicon In Animal Manure Fertilized Field. Environ. Eng. Manag. J.15.

Dunaj, S.J., Vallino, J.J., Hines, M.E., Gay, M., Kobyljanec, C., Rooney-Varga, J.N., 2012. Relationships between soil organic matter, nutrients, bacterial community structure, and the performance of microbial fuel cells. Environ. Sci. Technol. 46, 1914-1922.

Hong, S.W., Chang, I.S., Choi, Y.S., Kim, B.H., Chung, T.H., 2009. Responses from freshwater sediment during electricity generation using microbial fuel cells. Bioprocess Biosyst. Eng. 32, 389-395.

Hong, S.W., Kim, H.S., Chung, T.H., 2010. Alteration of sediment organic matter in sediment microbial fuel cells. Environ. Pollut. 158, 185-191.

Hu, Z.Y., Zhu, Y.G., Li, M., Zhang, L.G., Cao, Z.H., Smith, F.A., 2007. Sulfur (S)-induced enhancement of iron plaque formation in the rhizosphere reduces arsenic accumulation in rice (Oryza sativa L.) seedlings. Environ. Pollut. 147, 387-393.

Jung, S., Regan, J.M., 2011. Influence of External Resistance on Electrogenesis, Methanogenesis, and Anode Prokaryotic Communities in Microbial Fuel Cells. Appl. Environ. Microbiol. 77, 564-571.

Kouzuma, A., Kaku, N., Watanabe, K., 2014. Microbial electricity generation in rice paddy fields: recent advances and perspectives in rhizosphere microbial fuel cells. Appl. Microbiol. Biotechnol. 98, 9521-9526.

Lennon, J., Muscarella, M., Placella, S., Lehmkuhl, B., 2018. How, When, and Where Relic DNA Affects Microbial Diversity. Mbio 9, e00637-00618.

Li, B., Zhou, S., Wei, D., Long, J., Peng, L., Tie, B., Williams, P.N., Lei, M.J, 2019. Mitigating arsenic accumulation in rice (Oryza sativa L.) from typical arsenic contaminated paddy soil of southern China using nanostructured α-MnO2: Pot experiment and field application. Sci. Total Environ. 650, 546-556.

Lu, L., Huggins, T., Jin, S., Zuo, Y., Ren, Z.J., 2014. Microbial metabolism and community structure in response to bioelectrochemically enhanced remediation of petroleum hydrocarbon-contaminated soil. Environ. Sci. Technol. 48, 4021.

Morrissey, E.M., Mchugh, T.A., Preteska, L., Hayer, M., Dijkstra, P., Hungate, B.A., Schwartz, E., 2015. Dynamics of extracellular DNA decomposition and bacterial community composition in soil. Soil Biol. Biochem. 86, 42-49.

Pitts, K., Dobbin, P.S., Reyesramirez, F., Thomson, A.J., Richardson, D.J., Seward, H.E., 2003. Characterization of the Shewanella oneidensis MR-1 Decaheme Cytochrome MtrA expression in Escherichia Coli confers the ability to reduce soluble Fe(III) chelates. J. Biol. Chem. 278, 27758-27765.

Qiao, J. T., Li, X.M., Li, F.B., 2017. Roles of different active metal-reducing bacteria in arsenic release from arsenic-contaminated paddy soil amended with biochar. J. Hazard. Mater. 344, 958-967.

Qiao, J.T., Liu, T.X., Wang, X.Q., Li, F.B., Lv, Y.H., Cui, J.H., Zeng, X.D., Yuan, Y.Z., Liu, C.P., 2018. Simultaneous alleviation of cadmium and arsenic accumulation in rice by applying zero-valent iron and biochar to contaminated paddy soils. Chemosphere 195, 260-271.

Rahman, M.A., Hasegawa, H., Rahman, M.M., Maki, T., Lim, R.P., 2013. Effect of Iron (Fe 2+) Concentration in Soil on Arsenic Uptake in Rice Plant (Oryza sativa L.) when Grown with Arsenate [As (V)] and Dimethylarsinate (DMA). Water Air Soil Pollut. 224, 1623.

Rismani-Yazdi, H., Christy, A.D., Carver, S.M., Yu, Z., Dehority, B.A., Tuovinen, O.H., 2011. Effect of external resistance on bacterial diversity and metabolism in cellulose-fed microbial fuel cells. Bioresour. Technol. 102, 278-283.

Song TS, Yan ZS, Zhao ZW, Jiang HL. 2010. Removal of organic matter in freshwater sediment by microbial fuel cells at various external resistances. J. Chem. Technol. Biotechnol. 85(11), 1489-1493

Suda, A., Makino, T., 2016. Functional effects of manganese and iron oxides on the dynamics of trace elements in soils with a special focus on arsenic and cadmium: a review. Geoderma 270, 68-75.

Syu, C.H., Jiang, P.Y., Huang, H.H., Chen, W.T., Lin, T.H., Lee, D.Y., 2013. Arsenic sequestration in iron plaque and its effect on As uptake by rice plants grown in paddy soils with high contents of As, iron oxides, and organic matter. Soil Sci. Plant Nutr. 59, 463-471.

Torres, C.I., Krajmalnikbrown, R., Parameswaran, P., Marcus, A.K., Wanger, G., Gorby, Y.A., Rittmann, B.E., 2009. Selecting Anode-Respiring Bacteria Based on Anode Potential: Phylogenetic, Electrochemical, and Microscopic Characterization. Environ. Sci. Technol. 43, 9519-9524.

Touch, N., Hibino, T., Morimoto, Y., Kinjo, N., 2017. Relaxing the formation of hypoxic bottom water with sediment microbial fuel cells. Environ. Technol., 1-25.

Wang, N., Chen, Z., Li, H.B., Su, J.Q., Zhao, F., Zhu, Y.G., 2015. Bacterial community composition at anodes of microbial fuel cells for paddy soils: the effects of soil properties. J. Soils Sediments 15, 926-936.

Ward, J.T., Lahner, B., Yakubova, E., Salt, D.E., Raghothama, K.G., 2008. The effect of iron on the primary root elongation of Arabidopsis during phosphate deficiency. Plant Physiol. 147, 1181-1191.

Yamaguchi, N., Nakamura, T., Dong, D., Takahashi, Y., Amachi, S., Makino, T., 2011. Arsenic release from flooded paddy soils is influenced by speciation, Eh, pH, and iron dissolution. Chemosphere 83, 925-932.

Yang, Q., Zhao, H., Zhao, N., Ni, J., Gu, X., 2016. Enhanced phosphorus flux from overlying water to sediment in a bioelectrochemical system. Bioresource Technology 216, 182.

Yu, B., Tian, J., Feng, L., 2017. Remediation of PAH polluted soils using a soil microbial fuel cell: Influence of electrode interval and role of microbial communityJ. Hazard. Mater. 336, 110.

Yuan, H.Y., Liu, P.P., Wang, N., Li, X.-M., Zhu, Y.G., Khan, S.T., Alkhedhairy, A.A., Sun, G.X., 2018. The influence of soil properties and geographical distance on the bacterial community compositions of paddy soils enriched on SMFC anodes. J. Soils Sediments 18, 517-525.

Zhao, Q., Li, R., Ji, M., Ren, Z.J., 2016. Organic content influences sediment microbial fuel cell performance and community structure. Bioresour. Technol. 220, 549-556.